

THE ROLE OF AMPK IN NEUROMUSCULAR HEALTH AND DISEASE

THE ROLE OF AMPK IN NEUROMUSCULAR HEALTH AND DISEASE

By SEAN Y. NG, B.Sc., MSc.

A Thesis Submitted to the School of Graduate Studies in Partial Fulfilment of the
Requirements for the Degree Doctor of Philosophy

DOCTOR OF PHILOSOPHY (2023)
Kinesiology

McMaster University
Hamilton, Ontario

TITLE: The role of AMPK in neuromuscular health and disease

AUTHOR: Sean Y. Ng
Hon. B.Sc (McMaster University)
MSc. (McMaster University)

SUPERVISOR: Vladimir Ljubcic, Ph.D.

NUMBER OF PAGES: xviii, 201

LAY ABSTRACT

The neuromuscular junction (NMJ) plays a vital role in maintaining muscle function and countering aging and neuromuscular disorders. This thesis investigated the role of AMP-activated protein kinase (AMPK) in neuromuscular biology during conditions of health and disease. We conducted various experiments involving genetic modifications, drug treatments, and exercise. First, we determined that AMPK is necessary to maintain the NMJ during aging. Stimulation of AMPK with a potent activator, MK-8722 (MK), led to elevated NMJ-related gene expression. We then shifted our focus to the most prevalent neuromuscular disorder, Duchenne Muscular Dystrophy (DMD). Our results showed that MK activated AMPK in dystrophic mice, prompting us to further investigate the long-term effects of daily treatment in a pre-clinical DMD model. Repeated MK treatment significantly improved neuromuscular function and reduced the symptoms of DMD. Together, our comprehensive investigation demonstrates the critical role of AMPK in shaping neuromuscular plasticity during healthy and diseased conditions.

ABSTRACT

The neuromuscular junction (NMJ) exhibits an extraordinary capacity for adaptation and plasticity throughout an individual's lifespan. This remarkable adaptability assumes a central role in safeguarding optimal neuromuscular function and counteracting neurodegenerative processes commonly associated with aging and prevalent neuromuscular disorders. The plasticity of the NMJ is under the influence of its cellular constituents, including the α -motoneuron and the innervated muscle fiber. Among the diverse array of regulatory molecules, AMP-activated protein kinase (AMPK) plays a pivotal role in governing the phenotype of these cellular components, thereby potentially contributing to synaptic modifications. To explore the regulatory role of AMPK on the NMJ phenotype, we undertook a comprehensive investigation encompassing transgenic, pharmacologic, and physiologic manipulations of this kinase. In Study 1, we investigated the significance of skeletal muscle AMPK during aging, revealing its necessity in preserving NMJ integrity. Moreover, we observed that pharmacological and physiological activation of AMPK result in an enhanced synaptic gene profile in young animals, suggesting its role in NMJ modulation. Building upon these insights, we validate the stimulatory effects of a pan-AMPK activator, MK-8722 (MK), in the context of a prevalent neuromuscular disorder, Duchenne Muscular Dystrophy (DMD). Our investigations demonstrated that MK effectively evoked AMPK activation and downstream signaling in dystrophic muscle, providing the experimental foundations our third study. Here, we assess of the chronic effects of daily MK treatment in a pre-clinical DMD model and revealed significant improvements in mitochondrial health, neuromuscular function, and a reduction

in muscle fibrosis and fatigue. Taken together, these findings support a critical role of AMPK in neuromuscular plasticity and highlight the kinase as a promising therapeutic target for muscular dystrophy.

ACKNOWLEDGEMENTS

To Dr. Vladimir Ljubicic - Looking back, it is hard to imagine what led you to take me on as a student with my limited expertise at the time. I am grateful for this opportunity, in addition to the many others that you have provided me over the past 8 years. Truly, my future endeavors would not be possible without your guidance within and beyond the laboratory. Thank you for taking a chance with me.

To Drs. Thomas Hawke and Gregory Steinberg - Thank you for your time serving on this supervisory committee. Your collective insight, guidance, and continued support have been integral throughout my Ph.D.

To Drs. Sophie Joannis, Joshua Nederveen, James McKendry, Changhyun Lim, and Nathan Hodson - Thank you for being the guiding postdoctoral fellows who were always willing to share your research expertise and career advice. Thank you for always lending a scientific ear, fueling my caffeine addiction with impromptu coffee meetings, and providing invaluable life advice. I greatly appreciate your friendship and mentorship throughout grad school.

To Derek, Alex, Tiffany, Andrew, Steph, and the rest of the INBL - Thank you for your diligence in the lab, keeping the weekly lab cleanups on schedule, and, more importantly, always being available for spontaneous java or an Aperol spritz.

To Jamo, Khang, Chang, Giulia, Nathan, Brad, and Jem - Thank you for being part of the Beddoe experience and supporting me throughout this academic endeavour.

Thank you to Todd Prior and Linda May for your help and expertise in the lab. The laboratory would not operate without your daily contributions. To the rest of the EMRG colleagues, thank you for providing an amazing working environment that has given rise to many current and future collaborations.

To Carlita Velastegui - Thank you for being my one constant throughout this journey so far. I hope that I can continue doing the same for you.

To Mimi and Albert Ng - This life would not be possible without everything you have done for me. Thank you for your sacrifices and the opportunities that you have provided me. I dedicate this thesis to you both.

SECTION	TABLE OF CONTENTS	<u>PAGE</u>
TITLE PAGE		
DESCRIPTIVE NOTE		ii
LAY ABSTRACT		iii
ABSTRACT		iv
ACKNOWLEDGEMENTS		vi
TABLE OF CONTENTS		vii
LIST OF FIGURES AND TABLES		ix
LIST OF ABBREVIATIONS		xiii
DECLARATION OF ACADEMIC ACHEIVEMENT		xvi
CHAPTER 1: INTRODUCTION		1
1.1 Overview of neuromuscular junction biology		2
1.1.1 Development, maintenance and remodelling of the NMJ during health and disease		2
1.1.2 Molecular regulators of the neuromuscular synapse		4
1.2 AMPK biology		7
1.2.1 Structure and expression of AMPK		7
1.2.2 Regulation of AMPK		9
1.2.3 Functions of AMPK		12
1.2.4 Evidence for the role of AMPK on NMJ		16
1.3 DMD overview		19
1.3.1 Cellular and molecular pathways affected by AMPK relevant to DMD		22
1.3.2 Current landscape of AMPK agonists for the treatment of DMD		25
1.4 Objectives and Hypotheses		27
1.5 References		31

CHAPTER 2: The neurotrophic factor AMP-activated protein kinase regulates neuromuscular junction plasticity	42
CHAPTER 3: Acute, next-generation AMPK activation initiates a disease-resistant gene expression program in dystrophic skeletal muscle	84
CHAPTER 4: Orally bioavailable pan-AMPK activator MK-8722 attenuates the dystrophic phenotype in D2.mdx animals	101
CHAPTER 5: INTEGRATED DISCUSSION	148
5.1 Introduction	149
5.2 AMPK as a nexus signaling molecule affecting the NMJ	150
5.2.1 Regulatory impact of AMPK on cellular pathways relevant to the NMJ	150
5.2.2 Influence of AMPK on cell-specific alterations and implications for the neuromuscular synapse	152
5.3 Proposed AMPK-mediated mechanisms affecting synapse formation and stability	154
5.3.1 AMPK drives favourable mitochondrial adaptations in preclinical models of DMD	158
5.3.2 AMPK controls autophagic signaling in DMD muscle	160
5.3.3 AMPK targets muscle fibrosis and regeneration in dystrophic animals	161
5.4 Future considerations for AMPK activators	163
5.5 Limitations and future directions	166
5.6 Summary and main contributions of thesis	168
5.7 References	170
APPENDIX A: Copyright Permissions	178
AA.1 Creative Common Attribution License 4.0 (Chapter 1)	179
AA.2 John Wiley and Son License (Chapter 3)	186
APPENDIX B: Additional Data	192
AB.1 Chronic adaptations in response to repeated O304 treatment in D2.mdx animals	193
APPENDIX C: Other Contributions	199

LIST OF FIGURES AND TABLES

FIGURES:

	<u>PAGE</u>
CHAPTER 1: INTRODUCTION	1
Figure 1. Regulation of AMPK in skeletal muscle	11
Figure 2. Regulation of mitochondria biology, autophagy, and the fibrosis gene program by AMPK	14
CHAPTER 2: The neurotrophic factor AMP-activated protein kinase regulates neuromuscular junction plasticity	42
Figure 1. AMP-activated protein kinase (AMPK) $\beta 1\beta 2$ skeletal muscle-specific knockout (mKO) mice exhibit perturbed downstream signaling and characteristics of a prematurely aged neuromuscular junction (NMJ) gene expression profile	76
Figure 2. AMPK regulates NMJ morphology during aging	78
Figure 3. Targeted pharmacological AMPK stimulation elicits synaptic gene expression	79
Figure 4. AMPK activation promotes accumulation of pAMPK ^{Thr172} and PGC-1 α at the NMJ and in fundamental myonuclei.	80
Figure 5. AMPK activation in skeletal muscle induces AChR clustering	81
Figure 6. Exercise-evokes AMPK stimulation and downstream <i>Ppargc1α</i> and <i>Dok7</i> expression in mouse and human skeletal muscle	82
CHAPTER 3: Acute, next-generation AMPK activation initiates a disease-resistant gene expression program in dystrophic skeletal muscle	84
Figure 1. MK-8722 (MK) elicits AMP-activated protein kinase (AMPK) activity in dystrophic skeletal muscles	90
Figure 2. Acute MK-induced AMPK activation drives the myonuclear accumulation of peroxisome proliferator-activated receptor γ coactivator-1 α (PGC-1 α) in a fiber type-specific manner and evokes a slower, more oxidative gene program in dystrophic muscle	91

Figure 3. Acute MK-dosing enhances utrophin protein expression in dystrophic skeletal muscle	93
Figure 4. The effects of MK on autophagy signaling pathways in mdx muscle	95
Figure 5. Effects of acute MK-evoked AMPK stimulation on myogenic regulatory factor expression and satellite cell biology in dystrophic muscle	96
CHAPTER 4: Orally bioavailable pan-AMPK activator MK-8722 attenuates the dystrophic phenotype in D2.mdx animals	101
Figure 1: In vivo muscle function metrics in D2.mdx animals treated with MK-8722 (MK)	139
Figure 2. Ex vivo muscle function metrics in D2.mdx animals treated with MK	140
Figure 3. Enhanced utrophin expression in dystrophic skeletal muscle with MK treatment	141
Figure 4. MK treatment and physical activity increases mitochondrial respiration and content in skeletal muscle of D2.mdx animals	143
Figure 5. Effects of repeated MK treatment on skeletal muscle fibrosis in D2.mdx animals	144
Supplementary Figure 1: The effects of a MK dosing on AMP-activated protein kinase signaling in dystrophic skeletal muscle	145
CHAPTER 5: DISCUSSION	148
Figure 1. The role of AMPK in regulating the NMJ niche.	154
Figure 2. Proposed muscle mechanism of AMPK-mediated NMJ plasticity	155
Figure 3. Acute responses and chronic adaptations from MK dosing in dystrophic animals.	159

ADDITIONAL DATA: Chronic effects of O304 treatment in D2.mdx animals	192
Figure AB1: The effects of a O304 dosing on AMP-activated protein kinase (AMPK) signaling in skeletal muscle of D2.mdx animals.	194
Figure AB2: The impact of repetitive O304 treatment on muscle function and morphology in D2.mdx animals.	196
Figure AB3: Effects of repeated O304 treatment on skeletal muscle fibrosis in D2.mdx animals.	197
Figure AB4. The impact of chronic O304 dosing effects on mitochondrial respiration and content.	198

TABLES:

	<u>PAGE</u>
CHAPTER 1: INTRODUCTION	1
Table 1: Small molecule AMPK agonist in DMD skeletal muscle	26
CHAPTER 4: Orally bioavailable pan-AMPK activator MK-8722 attenuates the dystrophic phenotype in D2.mdx animals	101
Table 1: Effects of chronic MK-8722 (MK), exercise (EX), or MK and Ex on tissue morphology in D2.mdx mice	146
Table 2: Effects of chronic MK, EX, or MK + Ex on cardiac morphology	146
Table 3: Effects of chronic MK, EX, or MK + Ex on cardiac function	147
Table 4: Effects of chronic MK, EX, or MK + Ex on mitral valve function	147
Table 5: Effects of chronic MK, EX, or MK + Ex on EDL muscle twitch kinetics	147

LIST OF ABBREVIATIONS

α BTX	α -Bungarotoxin
ACC	Acetyl-CoA Carboxylase
ACh	Acetylcholine
AChR	Acetylcholine Receptor
AChEst	Acetylcholinesterase
ZMP	AICAR Monophosphate
ADaM	Allosteric Drug And Metabolite
AMPK	AMP-Activated Protein Kinase
ALS	Amyotrophic Lateral Sclerosis
ATG7	Autophagy-Related Gene 7
ERK	Extracellular Signal-Regulated Kinase
CAMKII	Calcium/Calmodulin-Dependent Protein Kinase Kinase 2
CLEAR	Coordinated Lysosomal Expression And Regulation
Dok7	Docking Protein 7
DMD	Duchenne Muscular Dystrophy
DRP1	Dynamin-Related Protein 1
DAPC	Dystrophin-Associated Protein Complex
ETS	E26 Transformation-Specific
EC	Eccentric Contraction
EPP	Endplate Potential
ETA	Epitrochleoanconeus
EDL	Extensor Digitorum Longus
ECM	Extracellular Matrix
FAP	Fibroblast Growth Factor Binding Protein 1
FGFBP1	Fibroadipogenic Progenitors
FNIP1	Folliculin-Interacting Protein 1
FS	Fractional Shortening
GABP	Ga-Binding Protein
GAST	Gastrocnemius
HDAC	Histone Deacetylase 5
KO	Knockout
TA	Tibialis Anterior
TGF- β	Latent Transforming Growth Factor Beta
TGF- β R	Latent Transforming Growth Factor Beta Receptor
LV	Left Ventricular

LKB1	Liver Kinase B1
LRP4	Low-Density Lipoprotein Receptor-Related Protein 4
mTORC1	Mammalian Target of Rapamycin Complex 1
+dF/dt	Maximum Rates of Twitch Force Production
-dF/dt	Maximum Rates of Twitch Force Relaxation
MET	Metformin
LC3	Microtubule-Associated Protein 1 Light Chain 3
FIS1	Mitochondrial Fission 1
MFF	Mitochondrial Fission Factor
TFAM	Mitochondrial Transcription Factor A
MK	MK-8722
SMAD	Mothers Against Decapentaplegic
MuRF1	Muscle Ring Finger 1
MuSC	Muscle Stem Cells
MuSK	Muscle-Specific Kinase
mKO	Muscle-Specific Knock Out
NFM	Neurofilament M
NMDs	Neuromuscular Disorders
NMJ	Neuromuscular Junction
NuGEMs	Nuclear Genes Encoding Mitochondrial Proteins
NRF1/2	Nuclear Respiratory Factors 1 And 2
PGC-1 α	Peroxisome Proliferator-Activated Receptor γ Coactivator-1 α
PDGFR	Platelet-Derived Growth Factor Receptor
PKA	Protein Kinase A
PP	Protein Phosphatases
ROS	Reactive Oxygen Species
rapsyn	Receptor-Associated Protein of the Synapse
RESV	Resveratrol
S6	Ribosomal Protein S6
p62	Sequestosome 1
SIRT1	Sirtuin 1
SV2	Synaptic Vesicle 2
TBC1D1	Tbc1 Domain Family Member 1
TPT	Time To Peak Tension
TFEB	Transcription Factor Eb

TRI	Triceps
TSC	Tuberous Sclerosis Protein
ULK1	Unc-51-Like Autophagy Kinase 1
Veh	Vehicle
WT	Wild-Type
α MN	α -Motoneuron
β DG	β -Dystroglycan
γ SG	γ -Sarcoglycan

PREFACE:

DECLARATION OF ACADEMIC ACHEIVEMENT

FORMAT AND ORANIZATION OF THESIS

This thesis is prepared in the “sandwich” format as outlined in the School of Graduate Studies Guide for the Preparation of Theses. It includes a general introduction, three original research papers prepared in journal article format, and a general discussion. The candidate is the first author on manuscripts 1, 2, and 3. At the time of thesis preparation Chapter 3 was published in peer-reviewed journals.

CONTRIBUTION TO PAPERS WITH MULTIPLE AUTHORSHIPS

Chapter 1: Literature review (certain sections)

Neuromuscular Junction and DMD Sections (Sections 1.1, and 1.3)

Ng, S. Y., & Ljubicic, V. (2020). Recent insights into neuromuscular junction biology in Duchenne muscular dystrophy: Impacts, challenges, and opportunities. *EBioMedicine*, 61, 103032.

Mitochondrial biology in DMD Section (Section 1.2)

Mikhail, A. I., Ng, S. Y., Mattina, S. R., & Ljubicic, V. (2023). AMPK is mitochondrial medicine for neuromuscular disorders. *Trends in Molecular Medicine*, 29(7), 512–529.

Contributions:

SYN wrote sections and generated the figures for the review articles that are included in this thesis. All authors edited and approved the final version of the manuscript.

Chapter 2:

Ng, S. Y., Mikhail, A. I., Mattina, S. R., Mohammed, S. A., Khan, S. K., Desjardins, E.M., Lim, C., Phillips, S.M., Steinberg, G.R., Ljubicic, V. (2023). The neurotrophic factor AMP-activated protein kinase regulates neuromuscular junction plasticity. *Submitted to Science Signaling*.

Contribution:

SYN and VL conceived and designed the research. SYN conducted formal analysis. SYN, AIM, SRM, SAM, SKK, and CL acquired and analyzed the data during investigation. SYN interpreted the data. SYN and VL drafted and edited the manuscript.

Chapter 3:

Ng, S. Y., Mikhail, A. I., Mattina, S. R., Manta, A., Diffey, I. J., & Ljubicic, V. (2023). Acute, next-generation AMPK activation initiates a disease-resistant gene expression program in dystrophic skeletal muscle. *The FASEB Journal*, 37(5), e22863.

Contribution:

SYN and VL conceived and designed the research; SYN, AIM, SRM, AM, and IJD acquired and analyzed the data; and SYN and VL interpreted the data. SYN and VL drafted and edited the manuscript. All authors approved the final manuscript.

Chapter 4:

Ng, S. Y., Osbourne, A. K., Mikhail, A. I., Rebalka, I.A., Hamstra, S. I., Mattina, S. R., Khan, S. K., Yap B.V., Fajardo, V.A., Steinberg, G.R., Hawke, T.J., & Ljubicic, V. Orally bioavailable pan-AMPK activator MK-8722 attenuates the dystrophic phenotype in D2.mdx animals. *In preparation*.

Contribution:

SYN and VL conceived and designed the research. SYN and AKO performed animals experiments. SYN and AIM performed high-resolution respirometry experiments. IAR performed ex vivo force stimulation experiments. SIH performed echocardiography experiments and analyses. SYN, AKO, AIM, IAR, SIH, SRM, SRK, and BVY contributed to the data collection and image analysis. SYN and VL interpreted the data. SYN and VL drafted and edited the manuscript.

CHAPTER 1:
INTRODUCTION

1.1 Overview of neuromuscular junction biology

The NMJ is an electrochemical signalling apparatus that lies at the interface between an α -motoneuron (α MN) and the skeletal muscle cells that it innervates. It is comprised of an α MN nerve terminal, the endplate region of a muscle fibre, and perisynaptic Schwann cells that envelop the synapse (1–4). Depolarization of the α MN terminal prompts the presynaptic exocytosis of acetylcholine (ACh)-containing vesicles. ACh from a single vesicle (i.e., quantal content) diffuses into the synaptic cleft and binds to ACh receptors (AChR) to evoke an endplate potential (EPP) at the postsynapse. In the healthy condition, the EPP is almost always sufficient to surpass the threshold required for depolarization of the sarcolemma, which then causes a muscle action potential to ensue and leads to the contraction of all myofibers innervated by the α MN. The amplitude by which the EPP surpasses the depolarization threshold is known as the “safety factor”, and disruption to the morphology and/or function of the NMJ will lower this safety factor below depolarization threshold leading to transmission failure, muscle weakness and dysfunction (5).

1.1.1 Development, maintenance and remodelling of the NMJ during health and disease

The development and maturation of the NMJ is well characterized in rodents (1, 3, 6). As early as embryonic day (E) 9.5, myofibers develop with broadly dispersed AChRs that subsequently accumulate to the central region of the fibre, a process known as pre-patterning. Shortly after at E11-12, motor axons are directed towards this central, pre-patterned domain (7). The axons first branch, then extend to appose these AChRs to form

nascent NMJs (3). These newly formed, oval-like plaques are innervated by multiple nerve terminals that compete with each other in an activity-based manner to seize territory within an AChR cluster. Polyinnervation of AChR clusters is eliminated by approximately 14 days post-birth (P), when a dominant presynaptic terminal has been established (1). Subsequently, these more mature synapses adopt a perforated, pretzel-like morphology.

The degeneration of the NMJ can arise from alterations affecting either the motor neuron or the myofiber components. Notably, sarcopenia, the progressive decline of skeletal muscle observed with aging, is linked to morphological and functional changes at the presynaptic, synaptic, and postsynaptic compartments of the NMJ (2, 8–10). Specifically, in aged individuals, the postsynapse exhibits reduced expression of AChRs, which are typically arranged in a fragmented pattern, alongside a loss of synaptic folds. Moreover, there is a decrease in synaptic alignment between the pre- and postsynaptic compartments, leading to reduced areas of active neurotransmission. As aging advances, the synaptic connection is lost, prompting neighboring axons to undergo axonal sprouting to reinnervate the denervated NMJ (3, 8, 11). Similarly, various NMDs are characterized by dysmorphic synapses and pathological dysfunction arising from complications at the presynaptic, synaptic, or postsynaptic levels. For instance, congenital myasthenic syndromes encompass a diverse group of genetic disorders, distinguished by their primary defects at the presynaptic, synaptic, or postsynaptic components. Likewise, NMDs such as amyotrophic lateral sclerosis or spinal muscular atrophy exhibit synapse-specific alterations leading to defective maturation and remodeling of the NMJ (12, 13). NMDs

caused by muscle-specific mutations, including muscular dystrophies, can also exert a retrograde influence on the NMJ, impairing synaptic function (3, 14).

1.1.2 Molecular regulators of the neuromuscular synapse

The maturation and stability of the NMJ is governed by multiple proteins including the canonical agrin/low-density lipoprotein receptor-related protein 4 (LRP4)/muscle-specific kinase (MuSK) signalling axis, downstream targets docking protein 7 (Dok7), and receptor-associated protein of the synapse (rapsyn), as well as additional synaptic gene regulators such as GA-binding protein (GABP; also known as nuclear respiratory factor 2, or NRF-2), peroxisome proliferator-activated receptor γ coactivator-1 α (PGC-1 α) and mammalian target of rapamycin complex 1 (mTORC1). Other proteins, such as utrophin and protein kinase A (PKA) also modulate the stability and therefore function of the NMJ. Additionally, many additional signalling pathways have been identified that play a role in synapse specialization, including neuregulin/ErbB, Wnt/ β -catenin, and Hippo/Yes-associated protein signalling cascades (15).

Agrin was identified as the first neurotrophic factor to regulate NMJ biology (3, 7). The proteoglycan governs the expression and localization of AChRs and is therefore critical for the postnatal development, as well as plasticity, of the NMJ. The importance of this molecule is demonstrated by rodents lacking agrin which form unstable and dispersed organization AChR clusters along the myofibers, resembling an arrangement that is observed during development or denervation (3, 6, 16). Additionally, recombinant agrin treatment of denervated muscles eliminates ectopic AChR cluster formation, further demonstrating the importance of this neural factor (6, 15). Agrin exerts its effects by

initiating the LRP4/MuSK signalling cascade, which is essential for its downstream control of AChR expression. For instance, the agrin/LRP4/MuSK interaction promotes the expression of several synaptic proteins that encourage AChR transcription, stabilization, and turnover. These effector molecules include rapsyn, Dok7, Abl tyrosine kinase, geranylgeranyltransferase, Rho GTPases, and P21-activated kinase 1 (3, 6). Notably, Dok7 and rapsyn are indispensable for the maintenance of the postsynaptic apparatus (3). Additional evidence for the importance of the agrin/LRP4/MuSK signalling axis is demonstrated by LRP4 and MuSK knockdown and knockout (KO) studies (2, 3, 7). For example, LRP4 KO mice exhibit perinatal lethality due to severe impairments in NMJ postsynaptic endplate formation (17). Thus, the agrin/LRP4/MuSK cascade serves as the regulatory centrepiece for the maturation and remodelling of the NMJ.

The links between agrin/LRP4/MuSK and synaptic gene expression are still being identified. Established players include transcription factors that are part of the E26 transformation-specific (Ets) family of proteins, including GABP α/β and Ets variant 5 (Erm) (2). These factors are also regulated at the synapse by mitogen activated protein kinase pathways, including c-Jun N-terminal kinases and extracellular signal-regulated kinase (ERK) signalling (15). An abundance of subsynaptic genes contain a common, conserved sequence in their promoters known as the N-box motif (CCGGAA). Here, in subsynaptic myonuclei (also known as fundamental myonuclei), Ets transcription factors bind and facilitate the transcription of synaptic genes, including AChR subunits (*Chrn δ* and *Chrn ϵ*), acetylcholinesterase (*AChEst*), *Musk*, *Rapsn*, and utrophin (*Utrn*). Although Ets factors are dispensable for synapse formation (18–20), these proteins play a remarkable

role in NMJ remodelling. For example, rodents lacking GABP α/β exhibit impaired postsynaptic development as a result of attenuated agrin signalling and reduced subsynaptic gene transcription (18, 19). Furthermore, Hippenmeyer and colleagues demonstrate severe impairments in NMJ plasticity and function in animals lacking Erm (20). This evidence underscores the importance of Ets transcription factors, specifically GABP α/β and Erm, in regulating the NMJ gene expression program and synaptic function.

The transcriptional coactivator PGC-1 α is another important modulator of the NMJ (10, 21, 22). PGC-1 α is regulated through several post-translational modifications that are mediated by upstream molecules such as adenosine monophosphate-activated protein kinase (AMPK), which is critical protein that governs neuromuscular system biology.(21) Mechanistic links have been elegantly established between PGC-1 α and synaptic gene regulation via GABP α/β /N-box signalling (23, 24). Further evidence for the role of PGC-1 α in the NMJ gene program can be observed *in vivo* (25–28). For instance, in addition to demonstrating slower, and more oxidative muscle characteristics such as mitochondrial biogenesis and type 1 and 2a myosin heavy chain expression, mice overexpressing PGC-1 α specifically in skeletal muscle exhibit a strong postsynaptic gene expression signature, as well as a type 1 α MN phenotype (27, 29). Interestingly, the latter alteration indicates that the transcriptional coactivator mediates a retrograde signalling network from myofibers to their innervating α MN. Elaborating on this phenomenon, Mills and colleagues showed in cell culture experiments that a PGC-1 α isoform directs axon recruitment and NMJ formation through the release of the myokine, neurturin (30).

Numerous lines of evidence have established mTORC1 as a crucial regulator of NMJ morphology and function (31–34). To investigate the impact of mTORC1 activity on NMJ, researchers have employed constitutive or inducible models of Raptor muscle-specific KO, which results in reduced mTORC1 activity. Initial investigations by Bentzinger et al. demonstrated that muscle-specific absence of mTORC1 activity leads to severe myopathy preceding the onset of neuromuscular changes (34). Building upon this work, subsequent studies employing the inducible mTORC1 model revealed denervation and fragmentation of NMJs following 1 or 7 months of transgenic and pharmacological mTORC1 depletion (33). Moreover, situations characterized by chronic mTOR activation, such as in tuberous sclerosis protein (TSC) mKO animal models or during aging, also exhibit dysmorphic and dysfunctional NMJs (31). The regulatory role of mTOR at the NMJ likely involves multiple mechanisms, including translation, autophagy, and transcription (32). Evidence supports the presence of downstream targets of mTOR, such as ribosomal protein S6 (S6) and eukaryotic translation initiation factor 4 (eIF4E) (31, 37), within the synaptic space, further implicating these pathways in mediating the effects of mTORC1 at the NMJ. Thus, interventions that modulate PGC-1 α and/or mTORC1 in skeletal muscle, like exercise for example, may evoke adaptive plasticity throughout the peripheral neuromuscular system. This warrants further research into the therapeutic potential of these proteins and the upstream regulatory kinases.

1.2 AMPK biology

1.2.1 Structure and expression of AMPK

AMPK is a heterotrimeric molecule that is comprised of an α , β , and γ subunit. The α subunit contains an α -KD, α -AID, and α -CTD domain structure. The α -KD region possesses an activation loop where phosphorylation of Thr¹⁷² occurs and facilitates the catalytic function of AMPK. The latter α -AID and α -CTD regions serve as components part of a regulatory module, which also extends to a β -CTR region and the entire γ subunit. The regulation of AMPK also occurs through the β subunit through the carbohydrate binding module, essential for the binding of glycogen and small molecule activators that bind to the allosteric drug and metabolite (ADaM) binding pocket. Lastly, the γ subunit contains four potential ligand-binding sites for adenosine-containing metabolites such as AMP, ADP, or ATP. Here, the competitive binding of AMP occurs in select CBS sites (CBS3 and CBS4), to ultimately provide the unique cellular sensing capabilities of AMPK.

Each subunit of AMPK possesses several isoforms (α 1, α 2, β 1, β 2, γ 1, γ 2, γ 3) and can be arranged into 12 possible trimeric combinations. Although AMPK is expressed in all eukaryotic cells, certain compositions exist in a cell-type-specific manner. For example, rodent and human skeletal muscle exclusively express α 2 β 2 γ 1, α 2 β 2 γ 3, α 2 β 1 γ 1, α 1 β 2 γ 1, and α 1 β 1 γ compositions (38, 39), whereas α MNs typically express α 2 β 2 γ 2 complexes (40). The expression pattern of AMPK also varies within certain cell phenotypes. Slow-twitch oxidative muscles typically lack the γ 3 isoform, whereas the faster, more glycolytic muscles present the isoform in an α 2 β 2 γ 3 composition. Interestingly, these unique

heterotrimer compositions also display a distinct response to physical activity in human skeletal muscle, with $\alpha 2\beta 2\gamma 1$ and $\alpha 1\beta 2\gamma 1$ becoming more active during prolonged exercise.

The spatial organization of AMPK is intricately governed by its functional role and its associations with specific cellular organelles. Skeletal muscle AMPK possesses a nuclear localization signal on the α subunit and permits nuclear localization of the kinase in response to physiological stressors like exercise (41–43). Recent advancements in the field have further corroborated these findings through the implementation of genetically encoded fluorescent biosensors of AMPK, enabling researchers to gain a precise understanding of kinase-to-organelle interactions (44). For example, Schmitt and colleagues revealed that the pharmacological activation of AMPK resulted in distinct cellular compartmentalization of AMPK. The complete purpose underlying AMPK's nuclear localization remains an area of ongoing investigation, necessitating a deeper exploration to unravel the intricate molecular mechanisms at play. A plausible hypothesis arises, suggesting that AMPK might exert transcriptional regulation through this particular mechanism, considering its capacity to target various transcription factors (43, 45).

1.2.2 Regulation of AMPK

The activity of AMPK is controlled by several hormonal and metabolic signals that impart post-translational changes on the kinase to stimulate its function (38, 45, 46). The primary phosphorylation site occurs at the α subunit, Thr¹⁷², and is responsible for mediating covalent activation, typically mediated by upstream signaling kinases, liver kinase B1 (LKB1) and calcium/calmodulin-dependent protein kinase kinase 2 (CAMKII). The resulting covalent activation leads to a significant increase in the kinase's activity (100-

fold rise), often quantified as with immunoblotting. As a primary cellular energy sensor, the canonical regulatory mechanism of AMPK is caused by the binding of AMP and the ensuing molecular events: 1) allosteric activation of the kinase, 2) promotion of Thr¹⁷² phosphorylation, and 3) inhibition of Thr¹⁷² dephosphorylation. Specifically, when AMP is bound to the γ subunit the kinase becomes undergoes allosteric activation and binds the regulatory and catalytic module together to prevent dephosphorylation. It is important to note that this allosteric effect results in the conformational that enhances the activity of AMPK by 10-fold, resulting in the immense capacity to stimulate the kinase up to 1000-fold with covalent and allosteric mechanism (Figure 1). Non-canonical regulation of AMPK encompasses a variety of intricate processes, including molecular signaling cascades mediated by CAMKII or transforming growth factor- β -activated kinase 1, as well as instances of lysosomal and mitochondrial damage (45). Moreover, the activation of AMPK can be induced by specific metabolites, such as glucose, glycogen, and fatty acids, which interact with the AMPK-ADaM binding site.

Physiological interventions which deplete cellular energy, such as physical activity or fasting, induce AMPK activation through its canonical regulatory mechanism. Several pharmacological agents that indirectly activate AMPK also function by elevating the AMP/ADP:ATP ratio (46–48). Predominate AMPK activators in the field include the anti-diabetic drug, metformin (MET), that inhibits mitochondrial complex I and causes a reduction in cellular respiration and ATP production (49, 50). MET primary functions in the liver and provides limited AMPK induction in other tissues, including skeletal muscle. Alternative metformin-like compounds, such as R419, have been successful in stimulating

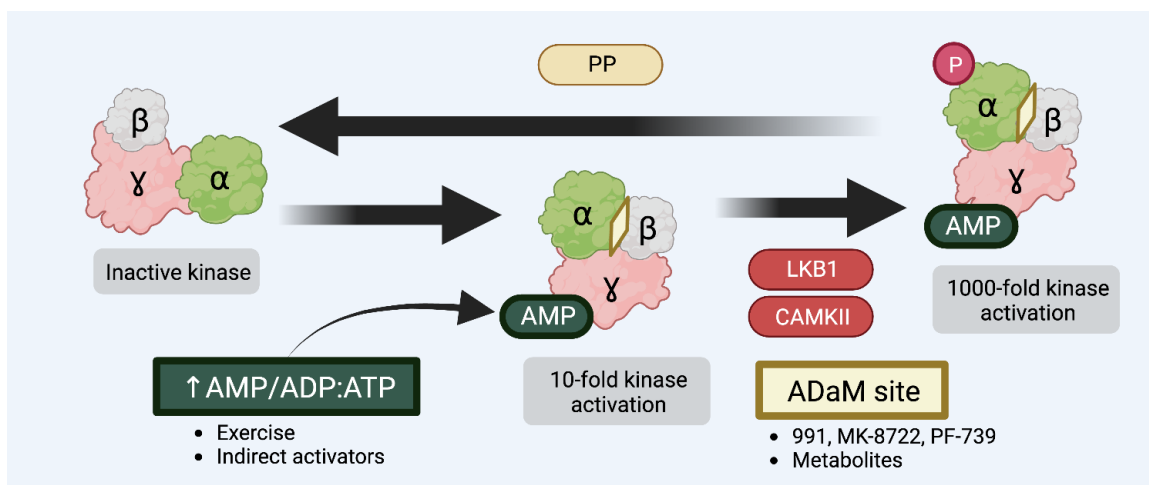


Fig. 1. Regulation of AMPK in skeletal muscle. When AMPK is devoid of AMP, the kinase adopts a structure that leaves the α Thr¹⁷² phosphorylation site accessible. Energy consumption leads to increases in AMP and ADP in skeletal muscle. AMP or ADP binds to the γ subunit of AMPK, causing a conformational change that stimulates the kinase up to 10-fold. This conformational change encourages Thr172 phosphorylation via upstream kinases, liver kinase B 1 (LKB1), or calcium–calmodulin-dependent protein kinase II (CAMKII) and prevents dephosphorylation. The combination of these mechanisms can lead to a >1000-fold increase in kinase activation. Following energy repletion, AMPK is converted back to its inactive form by protein phosphatases (PP). Notably, allosteric activation of AMPK can also occur through the allosteric drug and metabolite (ADaM) site. Several direct AMPK activators, including 991, MK-8722, and PF-739, can bind to this pocket to facilitate AMPK activation. The red circle with a “P” denotes phosphorylation, whereas the yellow diamond between the α and β subunits indicates the ADaM. the Adapted from (38, 46)

AMPK activation and blood glucose lowering in skeletal muscle (51), but have failed to translate to clinical trials due to adverse lactic acidosis events. Common indirect AMPK agonists include resveratrol (RESV), a plant-derived compound that inhibits mitochondrial function, phosphodiesterase, and activation of the SIRT1/AMPK signalling axis.

Several AMPK activators directly bind and activate AMPK induce conformational change on the AMPK complex to engage the kinase in a state that is resilient to dephosphorylation (39, 46). For instance, AICAR is a widely employed AMPK activator, that functions as an adenosine analog, AICAR monophosphate (ZMP). ZMP, akin to AMP, exerts its effects through binding to the γ subunit of AMPK, thereby inducing the activation

of this kinase. Notably, the action of AICAR extends beyond AMPK, as it can also activate other AMP-dependent enzymes, rendering it a non-specific agent targeting AMPK (52). In contrast, alternative AMPK activators such as A-769662 or PF-249 specifically bind to the ADaM binding pocket, thereby eliciting selective activation in AMPK complexes containing the β 1 subunit (46). These distinctive attributes have fostered investigations into the possibility of cell-specific targeting of AMPK, particularly in cell types where the predominant expression of AMPK β 1 is lacking, such as skeletal muscle. Notably, a number of these allosteric agonists, including PXL770 and O304, have gone through clinical trials and demonstrated promising results in metabolic diseases [NCT03763877, (53–55)].

Recent advancements have resulted in the identification of potent pan-AMPK activators capable of effectively stimulating AMPK across all 12 potential compositions (56–58). These compounds facilitate targeted and robust AMPK activation including cell types that predominantly comprising β 2-containing AMPK complexes, such as skeletal muscle and neurons. Indeed, several of these agonists have demonstrated a potent ability to enhance AMPK and regulate downstream physiological events in a favorable manner (57–61). However, it has been reported that the systemic nature of these AMPK activators can also lead to undesired effects on the heart, including cardiac hypertrophy and glycogen accumulation (57, 58). Therefore, careful consideration of the duration and potency of these systemic AMPK activators should be considered to mitigate adverse effects.

1.2.3 Functions of AMPK

AMPK assumes a central role in preserving cellular homeostasis by orchestrating a diverse array of cellular processes via the phosphorylation of numerous substrates (45, 62,

63). This extensive repertoire of phosphorylation targets plays a crucial role in governing cellular functions, including macronutrient metabolism, mitochondrial dynamics, autophagy, and cell immunology. It is worth noting that AMPK exhibits the ability to translocate within cellular compartments, thereby contributing to its pleiotropic functions. For instance, AMPK has been observed to translocate to the nucleus, where it exerts control over several transcription factors, coactivators, and deacetylases to evoke acute transcriptional regulation on many genes which may endow cellular and molecular adaptations (43).

The precise mechanism through which AMPK contributes to mitochondrial biogenesis involves its direct interaction with key transcription factors, such as transcription factor EB (TFEB) and PGC-1 α (Figure 2A). This interaction leads to the nuclear translocation and subsequent transcriptional control of nuclear respiratory factors 1 and 2 (NRF1/2), which, in turn, promote the expression of nuclear-encoded mitochondrial proteins (7). Recent research has shed light on the significance of folliculin-interacting protein 1 (FNIP1) in the process of mitochondrial biogenesis. Several laboratories have reported an association between heightened AMPK activity and increased transcriptional actions of PGC-1 α , leading to a slow and oxidative muscle phenotype (8). The precise mechanism of this relation was revealed, where AMPK targets FNIP1 to mediate PGC-1 α - and TFEB-mediated mitochondrial biogenesis (64). Beyond its role in biogenesis, AMPK also plays a role in regulating the dynamic morphology and motility of the mitochondrial reticulum (15). Specifically, AMPK-mediated phosphorylation of mitochondrial fission

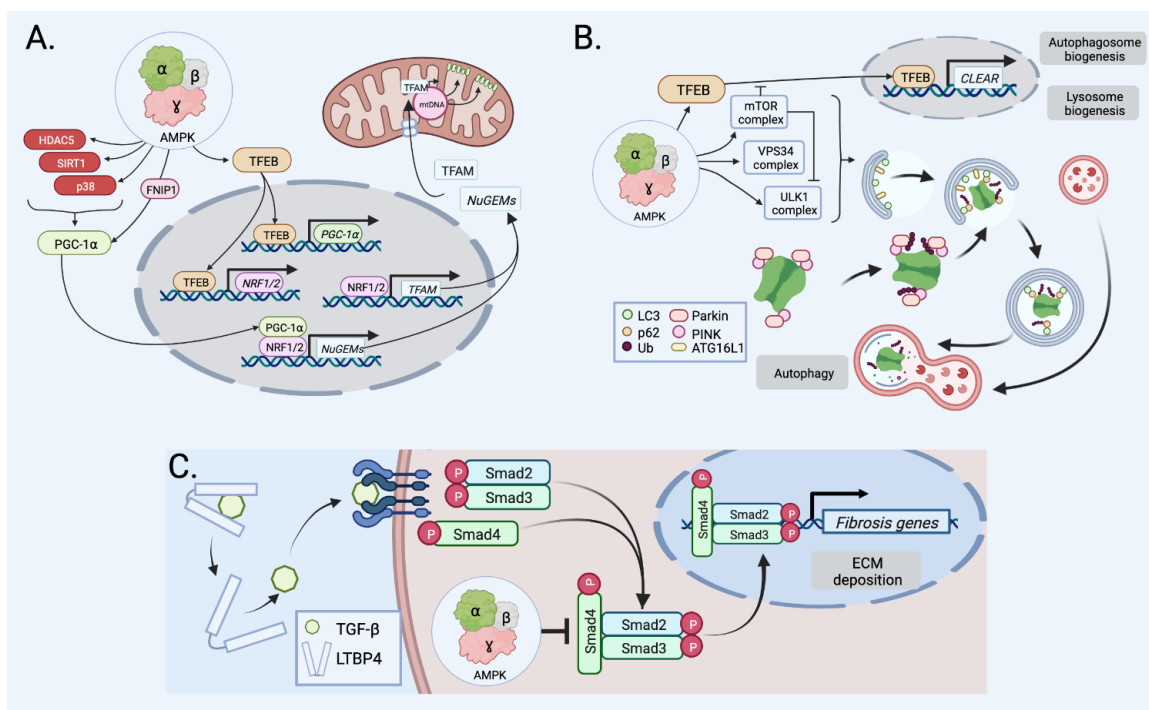


Fig. 2. Regulation of mitochondria biology, autophagy, and the fibrosis gene program by AMPK. AMPK is a pleiotropic molecule that targets hundreds of downstream targets and thus regulates several cellular pathways, including mitochondrial biogenesis, autophagy, and fibrosis. **(A)** AMPK targets its downstream effectors histone deacetylase 5 (HDAC5), sirtuin 1 (SIRT1), p38 mitogen-activated protein kinase (p38), folliculin-interacting protein 1 (FNIP1), as well as the master regulator of mitochondrial biogenesis, peroxisome proliferator-activated receptor γ coactivator-1 α (PGC-1 α). These signals converge to upregulate the transcription of nuclear genes encoding mitochondrial proteins (NuGEMs) and mitochondrial transcription factor A (TFAM), which collectively expands the mitochondrial reticulum. **(B)** AMPK activates unc-51-like autophagy kinase 1 (ULK1) as well as several other autophagy-related protein complexes, which together initiate the autophagy program. Following protein ubiquitin (Ub) tagging, proteins are engulfed by autophagosomes and degraded. AMPK also influences TFEB activity to augment the transcription of coordinated lysosomal expression and regulation (CLEAR) genes, the core machinery for autophagosome and lysosomal biogenesis. **(C)** Latent transforming growth factor beta (TGF- β) can be bound by latent transforming growth factor beta binding protein 4 (LTBP4) to regulate the pro-fibrotic signaling. Upon dissociation, TGF- β can become cleaved into its active form and induce cellular signaling through receptor binding. This leads to a mothers against decapentaplegic (SMAD) signaling cascade that results in the nuclear translation and induction of fibrosis-related genes. Notably, AMPK has been shown to inhibit the phosphorylation of SMAD and reduce downstream fibrotic signaling pathways. Adapted from (65, 66)

factor (MFF) results in the recruitment of dynamin-related protein 1 (DRP1) to mitochondria, where it binds to its receptors MFF and mitochondrial fission 1 (FIS1) on the outer mitochondrial membrane. This influence of AMPK on mitochondria dynamics favors a pro-fission state, contributing to the regulation of mitochondrial shape and movement.

AMPK serves as a central regulatory molecule controlling the process of autophagy (2) (Figure 2B). One of its key roles in this context is driving autophagy through the phosphorylation of unc-51-like autophagy-activating kinase 1 (ULK1) at Ser⁵⁵⁵, which induces ULK1 activity and leads to the upregulation of downstream autophagy-related machinery (Figure 2B). This phosphorylation event is a crucial step necessary for the subsequent assembly of the autophagosome (6, 12). Interestingly, autophagy is also regulated by the mTORC1 complex, which directly phosphorylates ULK1 at Ser⁷⁵⁷, thereby highlighting an additional regulatory interaction between AMPK, mTOR, and ULK1 (67). Notably, in the absence of AMPK, these events are significantly impaired, underscoring the essential role of AMPK in autophagic processes. Furthermore, AMPK exerts its influence on autophagy by targeting TFEB, an important upstream regulator of genes involved in autophagy and lysosomal function (13). Through its interactions with TFEB, AMPK contributes to the transcriptional control of genes related to autophagy and lysosome biogenesis, emphasizing its regulatory involvement in these cellular processes.

The involvement of AMPK in regeneration and repair processes is noteworthy due to its wide-ranging impact on cell growth and inflammation. Extensive research, including AMPK loss-of-function and rescue studies, has revealed compelling evidence for the importance of AMPK in satellite cells (or muscle stem cells; MuSC) during optimal regeneration in skeletal muscle (42, 43). Specifically, investigations focusing on MuSC lacking AMPK α have demonstrated increased self-renewal capabilities, although they display impaired myogenic capacity when transplanted *in vivo*. These findings underscore the indispensable role of AMPK in guiding MuSC behavior and optimal skeletal muscle

regeneration. Moreover, AMPK α 1 in macrophages has been identified as a crucial factor in orchestrating the resolution of inflammation during skeletal muscle regeneration, both in cases of acute and chronic damage (68, 69). Notably, the specific deletion of AMPK α 1 in macrophages leads to a defect in macrophage skewing, hindering the transition from the damage-associated phenotype to the restorative macrophage phenotype (48, 70). Perturbations in AMPK-latent transforming growth factor β binding protein 4 (LTBP4)-transforming growth factor β (TGF- β) signaling have been identified as a modulating pathway in this regulatory process (69) (Figure 2C). In summary, the diverse functions of AMPK in cell biology make it a key player in modulating phenotypic processes. Leveraging the pleiotropic effects of AMPK may continue to open current avenues for therapeutic interventions in various neuromuscular conditions where these processes are dysregulated. The specifics of these conditions will be later elaborated in *Section 1.3.1*.

1.2.4 Evidence for the role of AMPK on NMJ

The NMJ, comprising the α MN and the innervated muscle, is a crucial cellular signaling apparatus, and modifications to this complex structure can derive from either compartment. Transgenic deletion of AMPK expression specifically in neuronal cells results in notable morphological abnormalities and impaired mitochondrial features (71, 72). Moreover, animal models with skeletal muscle AMPK deficiencies exhibit severe exercise intolerance and a mild myopathy (67, 73–75), while transgenic models with constitutively active AMPK (AMPK γ 3-R225Q) demonstrate an enhanced oxidative phenotype in their skeletal muscles (76). Additionally, pharmacological activation of AMPK has been reported to augment mitochondrial content and respiration in skeletal

muscle (77, 78) and neurons (71). More recently, it has been demonstrated that repeated administration of orally bioactive AMPK agonists, such as PF-739 and MK-8722, can replicate these beneficial characteristics in skeletal muscles, a phenotype that is more resilient to disease (56, 58). Further support for the involvement of AMPK at the neuromuscular synapse comes from the work of Samuel and colleagues (79), who revealed that AMPK signaling plays a regulatory role in synaptic plasticity. In their study, the authors observed that the aging-induced remodeling of retinal synapses was associated with a natural decline in AMPK activity, and this age-related effect could be reversed through genetic or pharmacological activation of AMPK. Moreover, synapses deficient in AMPK exhibited characteristics similar to those observed in the retinal synapses of their aged wild-type controls, thus highlighting the significant role of AMPK in synaptic plasticity. Several AMPK-regulated processes have also been associated with NMJ dysfunction. Implications can be made from observations in aging or NMDs where these cellular processes naturally decline. These processes and their relevance to the neuromuscular synapse are briefly described below.

Mitochondrial dysfunction is a significant cellular process regulated by AMPK. The neuromuscular junction contains mitochondria within both the pre- and postsynaptic regions, highlighting their crucial role in supporting the synapse's neurotransmission function (80). Recent investigations by Li and colleagues have demonstrated that synaptic activity induces AMPK activation, leading to enhanced mitochondrial motility and facilitation of presynaptic metabolism (81). The importance of mitochondria at the neuromuscular junction is further underscored by age-related changes characterized by

declines in mitochondrial function preceding NMJ dysfunction (82). Additionally, adult-onset NMDs, such as DMD, ALS, or DM1, present comparable features of mitochondrial and NMJ impairments (65). These observations collectively emphasize the essential interplay between AMPK-regulated mitochondrial processes and their profound impact on the integrity of the neuromuscular system.

At the motor endplate, precise accumulation of synaptic proteins relies on a tightly regulated turnover, governed by a delicate balance between synthesis and degradation processes (9). The degradation of AChRs involves selective autophagy mechanisms, wherein the E3 ubiquitin ligase muscle ring finger 1 (MuRF1), the cargo protein sequestosome 1 (p62), and endophilin B, play pivotal roles (83, 84). Following denervation, there is a notable increase in autophagy-dependent AChR degradation, accompanied by a marked up-regulation of AChR synthesis, resulting in significant elevations in AChR turnover (85–87). The presence of AChRs within endocytic vesicles in the synaptic region further supports the active flux of autophagy at the neuromuscular junction (88). Pharmacological inhibition of autophagy has also been demonstrated to induce mTORC1-dependent blockade of autophagy, preventing postsynaptic degradation (89). Conversely, the targeted muscle-specific deletion of autophagy-related gene 7 (*Atg7*) leads to impaired autophagy, muscle fiber denervation, and synapse fragmentation (90). This genetic manipulation is associated with elevated AChR turnover, implying compensatory incorporation of new AChRs (87). To support this, certain NMJ transcripts (*Musk*, *Lrp4*, *Chrna1*) are upregulated as part of a denervation response in aged muscle. A similar

observation on this transcriptional alteration can be made across several NMDs which exhibit autophagy complications (91).

Muscle regeneration plays a crucial role in the maintenance of the NMJ. Adult MuSCs have been identified as indispensable contributors to myofiber nuclei and are essential for muscle regeneration (9, 92, 93). Their significance in NMJ regeneration is exemplified by both acute and chronic injury models in healthy and dystrophic conditions (14, 94, 95). Acute injury in mdx animals, a commonly used model for dystrophic muscle, exacerbates this NMJ defect, leading to greater fragmentation and loss of NMJ function (95, 97). In dystrophic muscle, characterized by continuous muscle degeneration and regeneration, impaired NMJ morphology and neurotransmission have been observed (14, 96). Furthermore, the depletion of satellite cells results in deficits in NMJ reinnervation, postsynaptic morphology, and a loss of postsynaptic myonuclei, highlighting the role of satellite cells in NMJ regeneration (94). This observation is also evident in aged tissue, where impairments in MuSC manifest (93, 98). Additionally, the loss of satellite cells has been linked to accelerated age-related NMJ degeneration, while an increase in satellite cells is associated with attenuated NMJ deterioration (99). These findings collectively emphasize the critical role of muscle regeneration, particularly involving satellite cells, in the maintenance and preservation of the neuromuscular junction.

1.3 DMD overview

DMD is the most common congenital NMD affecting approximately 1 in 6,000 live male births (100, 101). The economic burden associated with DMD is significant for patients (\$23,000-\$54,000 USD) and their families (\$58,000-\$71,000 USD) all over the

world (102). Natural history studies demonstrate that boys with DMD experience progressive proximal muscle weakness and wasting at approximately 2-5 years of age, which is also accompanied by a delay in motor milestone achievements (101, 103). This gradual loss in limb function typically necessitates ambulatory supports by early adolescence. Other clinical hallmarks that manifest in these patients include the accumulation of intramuscular fatty and fibrotic tissue resulting in excessive enlargement (i.e., pseudohypertrophy), particularly of the gastrocnemius muscle, as well as a positive Gowers' sign that presents as a predictable difficulty rising from a lying supine position. Respiratory and/or cardiac failure claim most DMD patients in their third or fourth decades.

DMD is caused by mutations in the *DMD* gene and the subsequent absence of its dystrophin protein product. Without dystrophin, its eponymous oligomeric structure termed the dystrophin-associated protein complex (DAPC) cannot be formed (21, 103). Highly localized along the sarcolemma, the DAPC is a critical signalling apparatus between the extracellular matrix and intracellular cytoskeleton that serves to maintain the structural integrity of muscle cells. The lack of dystrophin, and by extension the DAPC, ultimately lead to repetitive cycles of degeneration/regeneration, chronic inflammation, and muscle atrophy (101, 104, 105). While dystrophin is certainly important, other members of the DAPC also play critical roles in health and disease. Although often overlooked when discussing the devastating effects of DAPC deficiency, NMJ structure and function are remarkably impacted in muscular dystrophies, DMD in particular (95, 97, 106–116). Veritably, the biology of dystrophic NMJs is significantly compromised in several pre-clinical models, which strongly suggests that this phenomenon contributes to the muscle

wasting and weakness apparent in DMD patients. This is not surprising considering the critically important role of the NMJ in regulating skeletal muscle phenotype and contractile activity (117).

There is currently no effective treatment for DMD (118). Symptomatic patients are prescribed glucocorticoids as a standard of care, which attenuates the decline in muscle strength and function while also delaying the onset of catastrophic respiratory and cardiac dysfunction (101, 119). However, long-term corticosteroid usage results in detrimental side effects such as abnormal behaviour and weight gain. Vamorolone (ReveraGen BioPharma) and Edaslonexent (Catabasis Pharmaceuticals), two anti-inflammatory medications currently in the latter phases of clinical trials, provide similar therapeutic effects of glucocorticoids without the adverse off-target effects (119). Other emerging therapies include exon-skipping compounds, such as Amondys 45, Exondys 51 and Vyondys 53 (Sarepta Therapeutics), as well as the nonsense mutation suppressor, Translarna (PTC Therapeutics), which have been approved by the U.S. Food and Drug Administration and European Medicines Agency, respectively. However, these therapeutic strategies are not without their limitations. For example, Vyondys 53 might be effective only for those who have a *DMD* mutation that is germane to the skipping of exon 53, which represents approximately 8% of all DMD patients (120). Moreover, premature termination codon readthrough capability could successfully address disease-causing mutations in a maximum of 15% of boys with DMD (121). A common shortcoming of these genetic therapies is the restoration of a truncated and less functional dystrophin, which will ultimately translate, in a best case scenario, to a milder, Becker-like dystrophic phenotype (122). Thus, there is a

critical, unmet clinical need to identify effective curative approaches that apply to all DMD patients.

1.3.1 Cellular and molecular pathways affected by AMPK relevant to DMD

The mitochondrial morphological and functional adaptations in dystrophin-deficient human skeletal muscle have been extensively investigated and well-documented. It is widely recognized that mitochondrial biogenesis is impaired in DMD skeletal muscle, as evidenced by reduced mitochondrial enzyme activity, diminished expression of ETC complexes, and a decline in respiratory capacity observed in dystrophic animals and DMD patients (65). Dystrophic muscle exhibits an overabundance of damaged mitochondria and impaired mitophagy (123). Several investigations have also reported a reduction in the expression of autophagy and mitophagy-related components in skeletal muscle biopsies obtained from individuals with DMD (124, 125). Notably, the evaluation of isolated mitochondria from mdx muscle tissue and primary DMD patient muscle cells has revealed lower levels of Parkin and BNIP3 compared to healthy controls, collectively indicating compromised mitophagy flux (125). The collective presence of numerous poor-quality mitochondria resulting from impaired mitochondrial degradation is considered to contribute to the exacerbation of mitochondrial respiratory distress in DMD. This is further supported by the observation of simplified mitochondrial ultrastructure in both DMD patients and animals. This characteristic is attributed to the relative disparities in the expression of mitochondrial fusion and fission genes in DMD muscle, collectively indicating a skewed mitochondrial dynamics towards a fragmented phenotype in dystrophic skeletal muscle.

Autophagy impairment has been observed in the skeletal muscles of patients with DMD as well as in various preclinical models of dystrophy. Notably, dystrophic muscles exhibit a substantial reduction in the lipidated microtubule-associated protein 1 light chain 3 (LC3), which serves as a prevalent marker of autophagy induction in these contexts (126, 127). This compromised autophagic processing has been attributed to the hyperactivation of mTOR, which coincides with the dystrophic phenotype (126, 128, 129). Recent research have demonstrated that this pathological decline involves impairments in lysosomal clearance mechanisms (130). Supporting this notion, TFEB, a crucial regulator for lysosomal biogenesis, has been found to be reduced in the muscles of mdx animals, reinforcing the connection between autophagy dysfunction and lysosomal activity in DMD (130). Additionally, studies have reported impairments in organelle-specific autophagy, such as mitophagy, in mdx animals. Remarkably, this defect can be ameliorated using metabolite activators of mitophagy, such as urolithin A (125). Likewise, autophagy targeted at AChR in dystrophic muscle has also been found to be reduced in mdx models (83, 84, 96). Given the accumulating evidence of autophagy dysregulation in DMD, there is growing interest in exploring autophagy as a promising therapeutic avenue for this condition. By understanding and potentially modulating autophagy mechanisms, novel treatment strategies could be developed to address the underlying pathophysiology of DMD and improve the prognosis for affected individuals.

Fibrosis, another prominent hallmark of DMD, is characterized by the excessive or dysregulated deposition of extracellular matrix ECM components (131). The intricate orchestration of these processes involves a concerted interplay among resident immune

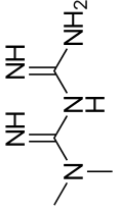
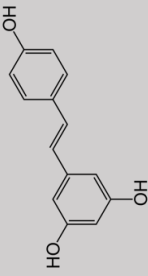
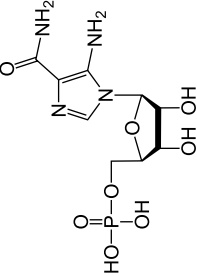
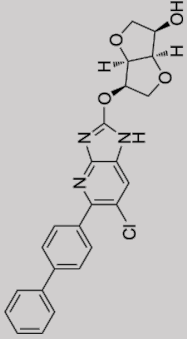
cells, MuSC, fibroadipogenic progenitors (FAP), and other cellular constituents within the regenerative niche. At the core of fibrosis promotion lies the profibrogenic factor, TGF- β , which remains in a latent state until activated in response to tissue damage or growth stimuli (132). Upon activation, active TGF- β binds to its corresponding receptor, TGF- β R, initiating a cascade of events that stimulate fibroblasts to synthesize ECM proteins, including collagen and fibronectin. This cellular response is mediated through the activin-receptor-like kinase 5 pathway, leading to the phosphorylation of SMAD2/3 and the formation of the respective signaling complex (133, 134). In the context of DMD, dystrophic muscle typically expresses elevated levels of TGF- β , resulting in hyperactive fibrosis signaling and subsequent excessive deposition of ECM components. This dysregulated fibrotic response further contributes to the pathological progression of DMD, underscoring the significance of TGF- β -mediated fibrosis in the disease pathogenesis (131, 133). recently, several genetic modifiers have been discovered in patients with DMD, and some of these modifiers are involved in the regulation of fibrosis through the TGF- β signaling pathway. For instance, specific variants of *LTBP4* have been linked to elevated fibrosis in DMD patients, resulting in a more severe onset of dystrophy (135, 136). Similarly, in animal models of dystrophy, such as mdx mice, the introduction of a genetic background carrying a polymorphism on the *LTBP4* gene leads to hyperactive TGF- β signaling and increased fibrosis, mirroring the phenotype observed in DMD patients with elevated fibrosis levels.

1.3.2 Current landscape of AMPK agonists for the treatment of DMD

The chronic induction of AMPK activity in skeletal muscle holds considerable promise as a therapeutic strategy for DMD, as it targets the AMPK-targeted pathways that include the activation of slow oxidative myofibers, corrective autophagic signaling, regulation of myofiber regeneration, and suppression of profibrotic pathways. These collective effects play a vital role in mitigating the dystrophic phenotype (21), and importantly, they are applicable to all DMD patients. Exposure to pharmacological AMPK activators, such as AICAR, MET, and RESV, has been shown to shift skeletal muscle towards a slower, more oxidative profile, resulting in enhanced resistance to the DMD myopathy (Table 1). Metformin, a widely prescribed indirect AMPK activator, has demonstrated improvements in skeletal muscle function and strength in dystrophic mice. Moreover, a 16-week concurrent treatment of DMD patients with metformin and l-arginine (NCT02516085) resulted in increased expression of skeletal muscle electron transport chain (ETC) proteins and improvements in motor function (137). However, the extent to which metformin contributes to this mitochondrial response independently of AMPK activation remains uncertain. Resveratrol (RESV), can also stimulate PGC-1 α activity and cytochrome c oxidase mRNA expression in the skeletal muscle of mdx mice (138–140). Notably, RESV has been reported to improve certain aspects of motor function in dystrophic boys (141).

Despite the promising advances, the translational impact of pharmacological AMPK activation for mitigating the dystrophic pathology in the DMD clinic has faced hindrances due to off-target adverse effects, such as lactic acidosis and hepatomegaly (142),

Table 1: Small molecule AMPK agonists in DMD skeletal muscle

Compound	Structure	Mechanism of action	Adaptations	Ref.
Metformin		Indirect activator, Complex I inhibition	Preclinical: ↑ muscle function, ↑ sarcolemma integrity ↓ muscle damage, ↑ neurotransmission, ↑ slow oxidative program. Clinical: ↑ Motor function, ↑ Mitochondrial content Similar muscle force production	(143–145) (137)
Resveratrol		Indirect activator, SIRT1 activator, ATP synthase inhibitor	Preclinical: ↑ fatigue resistance, ↓ muscle damage, ↓ ECM deposition, ↑ slow oxidative program, ↑ Mitochondria-related gene expression. Clinical: ↑ Motor function	(26, 138–140) (141)
AICAR		Direct activator, ZMP analog	Preclinical: ↑ muscle function, ↓ muscle damage, ↓ ECM deposition, ↑ Mitochondria content, ↓ dysmorphic mitochondria, ↑ slow oxidative program, ↑ Utrophin A expression	(69, 77, 146–148)
MK-8722 (Merck)		Direct activator, ADaM binding	Preclinical: ↑ AMPK activation ↑ downstream mitochondrial signaling ↑ downstream autophagy signaling	Study 2; (59)

AMPK, AMP-activated protein kinase; SIRT1, sirtuin 1; CSA, cross sectional area; ZMP, 5-aminoimidazole-4-carboxamide ribonucleotide; ECM, extracellular matrix; ADaM, allosteric drug and metabolite. Adapted from reference (46, 149).

or limited potency in attenuating the disease phenotype in DMD muscle (77, 137, 138, 141). The emergence of direct allosteric AMPK activators has brought new possibilities, with several small molecules demonstrating high levels of kinase activation in pre-clinical models of metabolic conditions (56–58). Moreover, some of these compounds have been successfully validated and well-tolerated in metabolic disease patient cohorts. However, their evaluation in the context of muscular dystrophy remains pending. Further investigation into these new generation AMPK compounds may expand the applicability of clinically relevant AMPK activators and potentially offer a broader range of treatment options for all DMD mutations.

1.4 Objectives and Hypotheses

The overall purpose of this dissertation is to investigate the role of AMPK in neuromuscular biology. Utilizing three distinct, but complementary experimental designs, we have tested the hypothesis that AMPK is important for maintaining and remodelling the peripheral neuromuscular system in healthy and pathological conditions. The objective of the first study was to ascertain whether AMPK assumes a requisite role in the sustenance and plasticity of the NMJ. We postulated that the activity and expression of skeletal AMPK is important the preservation and adaptive alterations of the NMJ. To this end, we utilized *in vivo*, *in vitro*, and *in silico* models to examine the activity and functional significance of AMPK and its interplay with NMJ biology. In the subsequent study, our focus shifted to investigating the acute effects of pharmacological AMPK activation on skeletal muscle intracellular signalling and gene expression germane to DMD. Here, we treated mdx mice with a single dose of MK, thereby enabling the assessment of determine the downstream

signalling events on the slow, oxidative gene program, autophagy, and MuSC biology. This study served as foundation for the following study, which aimed to evaluate the chronic adaptations induced by the AMPK activator in the more clinically relevant D2.mdx mice model. To this end, a comprehensive evaluation encompassing an array of in vivo muscle function tests, ex vivo electrical muscle force stimulation, and echocardiography was conducted, while concurrently exploring MK-induced cellular responses impacting mitochondrial biology and muscle fibrosis in these dystrophic animals

Study 1: The neurotrophic factor AMP-activated protein kinase regulates neuromuscular junction plasticity

Our principal aim was to shed light on the regulatory function of AMPK in the context of the NMJ. It is worth noting that a parallel correlation exists between the activity of skeletal muscle AMPK and the overall neuromuscular health, both in the context of aging and various NMDs, including DMD. Moreover, the involvement of AMPK in sustaining the NMJ's structural integrity can be inferred from multiple investigations, wherein downstream AMPK substrates, such as PGC-1 α and mTORC1, have been implicated in critical roles (23, 31). AMPK exhibits potential as a neurotrophic factor capable of instigating neuromuscular synapse remodeling. The physiological and pharmacological studies that induce AMPK activity endow favorable neuromuscular adaptations in otherwise degenerative conditions such as aging or muscular dystrophy (77, 79, 150–151). Nevertheless, despite the wealth of evidence amassed from these diverse studies, the precise role of skeletal muscle AMPK in both the maintenance and plasticity of the NMJ

remains indeterminate. As such, we formulated the hypothesis that AMPK would occupy a central position in maintaining the NMJ phenotype across the entire lifespan. Furthermore, we posited that stimulating the kinase would augment synaptic processes, thus facilitating the essential remodeling of the NMJ.

Study 2: Acute, next-generation AMPK activation initiates a disease-resistant gene expression program in dystrophic skeletal muscle

Several studies have revealed benefits associated with AMPK induction, alongside a comprehensive elucidation of the cellular and molecular mechanisms underlying these adaptations, both in experimental models of muscular dystrophy and in patients afflicted with DMD. However, the clinical feasibility of these first-generation AMPK agonists remains constrained due to their adverse off-target effects or insufficient potency in ameliorating the dystrophic phenotype. These limitations likely stem from the reliance on indirect mechanisms for stimulating AMPK. In response to these challenges, we administered MK, a direct and potent pan-AMPK activator, to dystrophic mdx animals. We postulated that the dosing of MK would indeed trigger AMPK activation in dystrophic muscle, thereby prompting consequential downstream signaling events, notably pertaining to mitochondrial biogenesis, autophagy, and muscle regeneration.

Study 3: Orally bioavailable pan-AMPK activator MK-8722 attenuates the dystrophic phenotype in D2.mdx animals

In Study 3, we investigated the therapeutic efficacy of recurrent MK treatment in dystrophic animal. The outcomes from Study 2 confirmed the agonistic impact of MK in dystrophic muscle, concomitantly stimulating several crucial disease-mitigating signaling pathways (59). However, it is important to note that these acute responses merely offer insight into immediate effects and do not necessarily provide a comprehensive understanding of the chronic adaptations that may arise from the repetitive administration of MK. Furthermore, prior research has reported cardiac hypertrophy, resulting from AMPK activation due to chronic MK exposure (57, 58). Given these potentially ambivalent adaptations, we subjected dystrophic animals to a daily treatment regimen of MK for a duration of 7 weeks. Our hypothesis postulated that, on balance, MK would augment muscle function in the treated animals and mitigate the dystrophic phenotype. Furthermore, we suspected that these MK-induced adaptations would primarily be attributed to canonical AMPK-mediated processes, entailing enhancements in mitochondrial function, autophagy correction, and reductions in muscle fibrosis.

1.5 References

1. Darabid,H., Perez-Gonzalez,A.P. and Robitaille,R. (2014) Neuromuscular synaptogenesis: coordinating partners with multiple functions. *Nat. Publ. Gr.*, **15**, 703.
2. Tintignac,L.A., Brenner,H.R. and Rüegg,M.A. (2015) Mechanisms regulating neuromuscular junction development and function and causes of muscle wasting. *Physiol. Rev.*, **95**, 809–852.
3. Li,L., Xiong,W.-C. and Mei,L. (2018) Neuromuscular Junction Formation, Aging, and Disorders. *Annu. Rev. Physiol*, **80**, 159–188.
4. Rudolf,R., Khan,M.M. and Witzemann,V. (2019) Motor Endplate—Anatomical, Functional, and Molecular Concepts in the Historical Perspective. *Cells*, **8**, 387.
5. Wood,S.J. and R. Slater,C. (2001) Safety factor at the neuromuscular junction. *Prog. Neurobiol.*, **64**, 393–429.
6. Wu,H., Xiong,W.C. and Mei,L. (2010) To build a synapse: Signaling pathways in neuromuscular junction assembly. *Development*, **137**, 1017–1033.
7. Burden,S.J., Huijbers,M.G. and Remedio,L. (2018) Fundamental molecules and mechanisms for forming and maintaining neuromuscular synapses. *Int. J. Mol. Sci.*, **19**, 1–19.
8. Aare,S., Spendiff,S., Vuda,M., Elkrief,D., Perez,A., Wu,Q., Mayaki,D., Hussain,S.N.A., Hettwer,S. and Hepple,R.T. (2016) Failed reinnervation in aging skeletal muscle. *Skelet. Muscle*, **6**.
9. Liu,W. and Chakkalakal,J. V The Composition , Development , and Regeneration of Neuromuscular Junctions 1st ed. Elsevier Inc.
10. Taetzsch,T. and Valdez,G. (2018) NMJ maintenance and repair in aging. *Curr. Opin. Physiol.*, **4**, 57–64.
11. Hepple,R.T. and Rice,C.L. (2016) Innervation and neuromuscular control in ageing skeletal muscle. *J. Physiol.*, **594**, 1965–1978.
12. Martineau,É., Di Polo,A., Velde,C. Vande and Robitaille,R. (2018) Dynamic neuromuscular remodeling precedes motor-unit loss in a mouse model of ALS. *Elife*, **7**, 1–19.
13. Boido,M. and Vercelli,A. (2016) Neuromuscular Junctions as Key Contributors and Therapeutic Targets in Spinal Muscular Atrophy. *Front. Neuroanat.*, **10**, 1–10.
14. Ng,S.Y. and Ljubovic,V. (2020) Recent insights into neuromuscular junction biology in Duchenne muscular dystrophy: Impacts, challenges, and opportunities. *EBioMedicine*, **61**, 103032.
15. Belotti,E. and Schaeffer,L. (2020) Regulation of Gene expression at the neuromuscular Junction. *Neurosci. Lett.*, **735**, 135163.
16. Guarino,S.R., Canciani,A. and Forneris,F. (2020) Dissecting the Extracellular Complexity of Neuromuscular Junction Organizers. *Front. Mol. Biosci.*, **6**.
17. Weatherbee,S.D., Anderson,K. V. and Niswander,L.A. (2006) LDL-receptor-related protein 4 is crucial for formation of the neuromuscular junction. *Development*, **133**, 4993–5000.
18. Briguët,A. and Rüegg,M.A. (2000) The Ets transcription factor GABP is required for postsynaptic differentiation in vivo. *J. Neurosci.*, **20**, 5989–5996.
19. Jaworski,A., Smith,C.L. and Burden,S.J. (2007) GA-Binding Protein Is Dispensable

- for Neuromuscular Synapse Formation and Synapse-Specific Gene Expression. *Mol. Cell. Biol.*, **27**, 5040–5046.
20. Hippenmeyer,S., Huber,R.M., Ladle,D.R., Murphy,K. and Arber,S. (2007) ETS Transcription Factor Erm Controls Subsynaptic Gene Expression in Skeletal Muscles. *Neuron*, **55**, 726–740.
 21. Dial,A.G., Ng,S.Y., Manta,A. and Ljubicic,V. (2018) The Role of AMPK in Neuromuscular Biology and Disease. *Trends Endocrinol. Metab.*, **29**, 300–312.
 22. Kupr,B. and Handschin,C. (2015) Complex Coordination of Cell Plasticity by a PGC-1 α -controlled Transcriptional Network in Skeletal Muscle. *Front. Physiol.*, **6**, 325.
 23. Handschin,C., Kobayashi,Y.M., Chin,S., Seale,P., Campbell,K.P. and Spiegelman,B.M. (2007) PGC-1 α regulates the neuromuscular junction program and ameliorates Duchenne muscular dystrophy. *Genes Dev.*, **21**, 770–783.
 24. Angus,L.M., Chakkalakal,J. V., Méjat,A., Eibl,J.K., Bélanger,G., Megeney,L.A., Chin,E.R., Schaeffer,L., Michel,R.N. and Jasmin,B.J. (2005) Calcineurin-NFAT signaling, together with GABP and peroxisome PGC-1 α , drives utrophin gene expression at the neuromuscular junction. *Am. J. Physiol. - Cell Physiol.*, **289**, C908–C917.
 25. Khan,M.M., Lustrino,D., Silveira,W.A., Wild,F., Straka,T., Issop,Y., O’Connor,E., Cox,D., Reischl,M., Marquardt,T., *et al.* (2016) Sympathetic innervation controls homeostasis of neuromuscular junctions in health and disease. *Proc. Natl. Acad. Sci. U. S. A.*, **113**, 746–750.
 26. Hollinger,K., Gardan-Salmon,D., Santana,C., Rice,D., Snella,E. and Selsby,J.T. (2013) Rescue of dystrophic skeletal muscle by PGC-1 α involves restored expression of dystrophin-associated protein complex components and satellite cell signaling. *Am. J. Physiol. - Regul. Integr. Comp. Physiol.*, **305**, 13–23.
 27. Chakkalakal,J. V., Nishimune,H., Ruas,J.L., Spiegelman,B.M. and Sanes,J.R. (2010) Retrograde influence of muscle fibers on their innervation revealed by a novel marker for slow motoneurons. *Development*, **137**, 3489–3499.
 28. Chan,M.C., Rowe,G.C., Raghuram,S., Patten,I.S., Farrell,C. and Arany,Z. (2014) Post-natal induction of PGC-1 α protects against severe muscle dystrophy independently of utrophin. *Skelet. Muscle*, **4**.
 29. Arnold,A.S., Gill,J., Christe,M., Ruiz,R., McGuirk,S., St-Pierre,J., Tabares,L. and Handschin,C. (2014) Morphological and functional remodelling of the neuromuscular junction by skeletal muscle PGC-1 α . *Nat. Commun.*, **5**.
 30. Mills,R., Taylor-Weiner,H., Correia,J.C., Agudelo,L.Z., Allodi,I., Kolonelou,C., Martinez-Redondo,V., Ferreira,D.M.S., Nichterwitz,S., Comley,L.H., *et al.* (2018) Neurturin is a PGC-1 α -controlled myokine that promotes motor neuron recruitment and neuromuscular junction formation. *Mol. Metab.*, **7**, 12–22.
 31. Ham,D.J., Börsch,A., Lin,S., Thürkauf,M., Weihrauch,M., Reinhard,J.R., Delezie,J., Battilana,F., Wang,X., Kaiser,M.S., *et al.* (2020) The neuromuscular junction is a focal point of mTORC1 signaling in sarcopenia. *Nat. Commun.*, **11**, 1–21.
 32. Castets,P., Rion,N., Théodore,M., Falcetta,D., Lin,S., Reischl,M., Wild,F., Guérard,L., Eickhorst,C., Brockhoff,M., *et al.* (2019) mTORC1 and PKB/Akt control the muscle response to denervation by regulating autophagy and HDAC4. *Nat.*

- Commun.*, **10**, 1–16.
33. Baraldo,M., Geremia,A., Pirazzini,M., Nogara,L., Solagna,F., Türk,C., Nolte,H., Romanello,V., Megighian,A., Boncompagni,S., *et al.* (2020) Skeletal muscle mTORC1 regulates neuromuscular junction stability. *J. Cachexia. Sarcopenia Muscle*, **11**, 208–225.
 34. Bentzinger,C., Romanino,K., Cloë tta,D., Lin,S., Mascarenhas,J.B., Oliveri,F., Xia,J., Casanova,E., line Costa,C.F., Brink,M., *et al.* Cell Metabolism Skeletal Muscle-Specific Ablation of raptor, but Not of rictor, Causes Metabolic Changes and Results in Muscle Dystrophy. *Cell Metab.*, **8**, 411–424.
 37. Sigrist,S.J., Thiel,P.R., Reiff,D.F., Lachance,P.E.D., Lasko,P. and Schuster,C.M. (2000) Postsynaptic translation affects the efficacy and morphology of neuromuscular junctions. *Nat. 2000 4056790*, **405**, 1062–1065.
 38. Kjøbsted,R., Hingst,J.R., Fentz,J., Foretz,M., Sanz,M.-N., Pehmøller,C., Shum,M., Marette,A., Mounier,R., Treebak,J.T., *et al.* (2018) AMPK in skeletal muscle function and metabolism. *FASEB J.*, **32**, 1741–1777.
 39. Olivier,S., Foretz,M. and Viollet,B. (2018) Promise and challenges for direct small molecule AMPK activators. 10.1016/j.bcp.2018.01.049.
 40. Alkaslasi,M.R., Piccus,Z.E., Hareendran,S., Silberberg,H., Chen,L., Zhang,Y., Petros,T.J. and Le Pichon,C.E. Single nucleus RNA-sequencing defines unexpected diversity of cholinergic neuron types in the adult mouse spinal cord. 10.1038/s41467-021-22691-2.
 41. Kodiha,M., Ho-Wo-Cheong,D. and Stochaj,U. (2011) Pharmacological AMP-kinase activators have compartment-specific effects on cell physiology. *Am. J. Physiol. - Cell Physiol.*, **301**, 1307–1315.
 42. McGee,S.L., Howlett,K.F., Starkie,R.L., Cameron-Smith,D., Kemp,B.E. and Hargreaves,M. (2003) Exercise Increases Nuclear AMPK α 2 in Human Skeletal Muscle. *Diabetes*, **52**, 926–928.
 43. Trefts,E. and Shaw,R.J. (2021) AMPK: restoring metabolic homeostasis over space and time. *Mol. Cell*, **81**, 3677–3690.
 44. Schmitt,D.L., Curtis,S.D., Lyons,A.C., Zhang,J., Chen,M., He,C.Y., Mehta,S., Shaw,R.J. and Zhang,J. (2022) Spatial regulation of AMPK signaling revealed by a sensitive kinase activity reporter. *Nat. Commun. 2022 131*, **13**, 1–12.
 45. Steinberg,G.R. and Hardie,D.G. (2022) New insights into activation and function of the AMPK. *Nat. Rev. Mol. Cell Biol. 2022 244*, **24**, 255–272.
 46. Steinberg,G.R. and Carling,D. (2019) AMP-activated protein kinase: the current landscape for drug development. *Nat. Rev. Drug Discov.*, 10.1038/s41573-019-0019-2.
 47. Mounier,R., Théret,M., Lantier,L., Foretz,M. and Viollet,B. (2015) Expanding roles for AMPK in skeletal muscle plasticity. *Trends Endocrinol. Metab.*, **26**, 275–286.
 48. Mounier,R., Theret,M., Arnold,L., Cuvellier,S., Bultot,L., Goransson,O., Sanz,N., Ferry,A., Sakamoto,K., Foretz,M., *et al.* (2013) AMPK α 1 regulates macrophage skewing at the time of resolution of inflammation during skeletal muscle regeneration. *Cell Metab.*, **18**, 251–264.
 49. Foretz,M., Guigas,B. and Viollet,B. (2023) Metformin: update on mechanisms of

- action and repurposing potential. *Nat. Rev. Endocrinol.* 2023 198, **19**, 460–476.
50. Rena,G., Pearson,E.R. and Sakamoto,K. (2013) Molecular mechanism of action of metformin: old or new insights? *Diabetologia*, **56**, 1898–1906.
 51. Marcinko,K., Bujak,A.L., Lally,J.S.V., Ford,R.J., Wong,T.H., Smith,B.K., Kemp,B.E., Jenkins,Y., Li,W., Kinsella,T.M., *et al.* (2015) The AMPK activator R419 improves exercise capacity and skeletal muscle insulin sensitivity in obese mice. *Mol. Metab.*, **4**, 643–651.
 52. Hasenour,C.M., Ridley,D.E., Hughey,C.C., James,F.D., Donahue,E.P., Shearer,J., Viollet,B., Foretz,M. and Wasserman,D.H. (2014) 5-Aminoimidazole-4-carboxamide-1- β -D-ribofuranoside (AICAR) effect on glucose production, but not energy metabolism, is independent of hepatic AMPK in vivo. *J. Biol. Chem.*, **289**, 5950–5959.
 53. Cusi,K., Alkhoury,N., Harrison,S.A., Fouquieray,P., Moller,D.E., Hallakou-Bozec,S., Bolze,S., Grouin,J.M., Jeannin Megnien,S., Dubourg,J., *et al.* (2021) Efficacy and safety of PXL770, a direct AMP kinase activator, for the treatment of non-alcoholic fatty liver disease (STAMP-NAFLD): a randomised, double-blind, placebo-controlled, phase 2a study. *Lancet Gastroenterol. Hepatol.*, **6**, 889–902.
 54. Fouquieray,P., Bolze,S., Dubourg,J., Gluais-Dagorn,P., Moller,D.E., Correspondence,K.C., Hallakou-Bozec,S., Theurey,P., Grouin,J.-M., Mence Chevalier,C., *et al.* (2021) Pharmacodynamic effects of direct AMP kinase activation in humans with insulin resistance and non-alcoholic fatty liver disease: A phase 1b study. *Cell Reports Med.*, **2**, 100474.
 55. Steneberg,P., Lindahl,E., Dahl,U., Lidh,E., Straseviciene,J., Backlund,F., Kjellkvist,E., Berggren,E., Lundberg,I., Bergqvist,I., *et al.* (2018) PAN-AMPK activator O304 improves glucose homeostasis and microvascular perfusion in mice and type 2 diabetes patients. *JCI Insight*, **3**.
 56. Cokorinos,E.C., Delmore,J., Reyes,A.R., Albuquerque,B., Kjøbsted,R., Jørgensen,N.O., Tran,J.L., Jatkar,A., Cialdea,K., Esquejo,R.M., *et al.* (2017) Activation of Skeletal Muscle AMPK Promotes Glucose Disposal and Glucose Lowering in Non-human Primates and Mice. *Cell Metab.*, **25**, 1147-1159.e10.
 57. Muise,E.S., Guan,H.-P., Liu,J., Nawrocki,A.R., Yang,X., Wang,C., Rodríguez,C.G., Zhou,D., Gorski,J.N., Kurtz,M.M., *et al.* (2019) Pharmacological AMPK activation induces transcriptional responses congruent to exercise in skeletal and cardiac muscle, adipose tissues and liver. *PLoS One*, **14**, e0211568.
 58. Myers,R.W., Guan,H.-P., Ehrhart,J., Petrov,A., Prahalada,S., Tozzo,E., Yang,X., Kurtz,M.M., Trujillo,M., Gonzalez Trotter,D., *et al.* (2017) Systemic pan-AMPK activator MK-8722 improves glucose homeostasis but induces cardiac hypertrophy. *Science*, **357**, 507–511.
 59. Ng,S.Y., Mikhail,A.I., Mattina,S.R., Manta,A., Diffey,I.J. and Ljubicic,V. (2023) Acute, next-generation AMPK activation initiates a disease-resistant gene expression program in dystrophic skeletal muscle. *FASEB J*, **37**, e22863.
 60. Rhein,P., Desjardins,E.M., Rong,P., Ahwazi,D., Bonhoure,N., Stolte,J., Santos,M.D., Ovens,A.J., Ehrlich,A.M., Sanchez Garcia,J.L., *et al.* (2021) Compound- and fiber type-selective requirement of AMPK γ 3 for insulin-independent glucose uptake in

- skeletal muscle. *Mol. Metab.*, **51**.
61. Zhang,J., Muise,E.S., Han,S., Kutchukian,P.S., Costet,P., Zhu,Y., Kan,Y., Zhou,H., Shah,V., Huang,Y., *et al.* (2020) Molecular Profiling Reveals a Common Metabolic Signature of Tissue Fibrosis. *Cell Reports Med.*, **1**, 100056.
 62. Hoffman,N.J., Parker,B.L., Chaudhuri,R., Fisher-Wellman,K.H., Kleinert,M., Humphrey,S.J., Yang,P., Holliday,M., Trefely,S., Fazakerley,D.J., *et al.* (2015) Global Phosphoproteomic Analysis of Human Skeletal Muscle Reveals a Network of Exercise-Regulated Kinases and AMPK Substrates. *Cell Metab.*, **22**, 922–935.
 63. Blazev,R., Carl,C.S., Ng,Y.-K., Molendijk,J., Voldstedlund,C.T., Zhao,Y., Xiao,D., Kueh,A.J., Miotto,P.M., Haynes,V.R., *et al.* (2022) Phosphoproteomics of three exercise modalities identifies canonical signaling and C18ORF25 as an AMPK substrate regulating skeletal muscle function. *Cell Metab.*, 10.1016/J.CMET.2022.07.003.
 64. Malik,N., Ferreira,B.I., Hollstein,P.E., Curtis,S.D., Trefts,E., Weiser Novak,S., Yu,J., Gilson,R., Hellberg,K., Fang,L., *et al.* (2023) Induction of lysosomal and mitochondrial biogenesis by AMPK phosphorylation of FNIP1. *Science*, **380**, eabj5559.
 65. Mikhail,A.I., Ng,S.Y., Mattina,S.R. and Ljubicic,V. (2023) AMPK is mitochondrial medicine for neuromuscular disorders. *Trends Mol. Med.*, **29**(7), 512–529.
 66. Dial,A.G., Rooprai,P., Lally,J.S., Bujak,A.L., Steinberg,G.R. and Ljubicic,V. (2018) The role of AMP-activated protein kinase in the expression of the dystrophin-associated protein complex in skeletal muscle. *FASEB J.*, **32**, 2950–2965.
 67. Bujak,A.L., Crane,J.D., Lally,J.S., Ford,R.J., Kang,S.J., Rebalka,I.A., Green,A.E., Kemp,B.E., Hawke,T.J., Schertzer,J.D., *et al.* (2015) AMPK activation of muscle autophagy prevents fasting-induced hypoglycemia and myopathy during aging. *Cell Metab.*, **21**, 883–890.
 69. Juban,G., Saclier,M., Yacoub-Youssef,H., Kernou,A., Arnold,L., Boisson,C., Ben Larbi,S., Magnan,M., Cuvellier,S., Th eret,M., *et al.* (2018) AMPK Activation Regulates LTBP4-Dependent TGF- 1 Secretion by Pro-inflammatory Macrophages and Controls Fibrosis in Duchenne Muscular Dystrophy. *Cell Rep.*, **25**, 2163-2176.e6.
 70. Varga,T., Mounier,R., Gogolak,P., Poliska,S., Chazaud,B. and Nagy,L. (2013) Tissue LyC6- macrophages are generated in the absence of circulating LyC6- monocytes and Nur77 in a model of muscle regeneration. *J. Immunol.*, **191**, 5695–5701.
 71. Dasgupta,B. and Milbrandt,J. (2007) Resveratrol stimulates AMP kinase activity in neurons. *Proc. Natl. Acad. Sci. U. S. A.*, **104**, 7217–7222.
 72. Dasgupta,B. and Milbrandt,J. Article AMP-Activated Protein Kinase Phosphorylates Retinoblastoma Protein to Control Mammalian Brain Development. *Dev. Cell*, **16**, 256–270.
 73. Bujak,A.L., E Bl umer,R.M., Marcinko,K., Fullerton,M.D., Kemp,B.E. and Steinberg,G.R. (2014) Reduced skeletal muscle AMPK and mitochondrial markers do not promote age-induced insulin resistance. *J Appl Physiol*, **117**, 171–179.
 74. Thomas,M.M., Wang,D.C., D’Souza,D.M., Krause,M.P., Layne,A.S., Criswell,D.S., O’Neill,H.M., Connor,M.K., Anderson,J.E., Kemp,B.E., *et al.* (2014) Muscle-specific AMPK  1 2-null mice display a myopathy due to loss of capillary density in

- nonpostural muscles. *FASEB J.*, **28**, 2098–2107.
75. O’Neill,H.M., Maarbjerg,S.J., Crane,J.D., Jeppesen,J., Jorgensen,S.B., Schertzer,J.D., Shyroka,O., Kiens,B., van Denderen,B.J., Tarnopolsky,M.A., *et al.* (2011) AMP-activated protein kinase (AMPK) 1 2 muscle null mice reveal an essential role for AMPK in maintaining mitochondrial content and glucose uptake during exercise. *Proc. Natl. Acad. Sci.*, **108**, 16092–16097.
 76. Garcia-Roves,P.M., Osler,M.E., Holmström,M.H. and Zierath,J.R. (2008) Gain-of-function R225Q mutation in AMP-activated protein kinase gamma3 subunit increases mitochondrial biogenesis in glycolytic skeletal muscle. *J. Biol. Chem.*, **283**, 35724–34.
 77. Ljubcic,V., Miura,P., Burt,M., Boudreault,L., Khogali,S., Lunde,J.A., Renaud,J.M. and Jasmin,B.J. (2011) Chronic AMPK activation evokes the slow, oxidative myogenic program and triggers beneficial adaptations in mdx mouse skeletal muscle. *Hum. Mol. Genet.*, **20**, 3478–3493.
 78. Thomson,D.M., Herway,S.T., Fillmore,N., Kim,H., Brown,J.D., Barrow,J.R. and Winder,W.W. (2007) AMP-activated protein kinase phosphorylates transcription factors of the CREB family. *J. Appl. Physiol.*, **104**, 429–438.
 79. Samuel,M.A., Emanuela Voinescu,P., Lilley,B.N., de Cabo,R., Foretz,M., Viollet,B., Pawlyk,B., Sandberg,M.A., Vavvas,D.G. and Sanes,J.R. (2014) LKB1 and AMPK regulate synaptic remodeling in old age. *Nat. Publ. Gr.*, **17**.
 80. Hepple,R.T. and Rice,C.L. (2016) Innervation and neuromuscular control in ageing skeletal muscle. *J. Physiol.*, **594**, 1965–1978.
 81. Li,S., Xiong,G., Huang,N. and Sheng,Z. (2020) The cross-talk of energy sensing and mitochondrial anchoring sustains synaptic efficacy by maintaining presynaptic metabolism. *Nat. Metab.*, **2**.
 82. Spendiff,S., Vuda,M., Gouspillou,G., Aare,S., Perez,A., Morais,J.A., Jagoe,R.T., Filion,M.E., Glicksman,R., Kapchinsky,S., *et al.* (2016) Denervation drives mitochondrial dysfunction in skeletal muscle of octogenarians. *J. Physiol.*, **594**, 7361–7379.
 83. Rudolf,R., Khan,M.M., Lustrino,D., Labeit,S., Kettelhut,Í.C. and Navegantes,L.C.C. (2013) Alterations of cAMP-dependent signaling in dystrophic skeletal muscle. *Front. Physiol.*, **4**, 290.
 84. Rudolf,R., Khan,M.M., Labeit,S. and Deschenes,M.R. (2014) Degeneration of neuromuscular junction in age and dystrophy. *Front. Aging Neurosci.*, **6**, 99.
 85. Akaaboune,M., Culican,S.M., Turney,S.G. and Lichtman,J.W. (1999) Rapid and reversible effects of activity on acetylcholine receptor density at the neuromuscular junction in vivo. *Science (80-)*, **286**, 503–507.
 86. Bruneau,E.G. and Akaaboune,M. (2006) The dynamics of recycled acetylcholine receptors at the neuromuscular junction in vivo. *Development*, **133**, 4485–4493.
 87. Strack,S., Khan,M.M., Wild,F., Rall,A. and Rudolf,R. (2015) Turnover of acetylcholine receptors at the endplate revisited: novel insights into nerve-dependent behavior. *J. Muscle Res. Cell Motil.*, **36**, 517–524.
 88. Khan,M.M., Strack,S., Wild,F., Hanashima,A., Gasch,A., Brohm,K., Reischl,M., Carnio,S., Labeit,D., Sandri,M., *et al.* (2014) Role of autophagy, SQSTM1,

- SH3GLB1, and TRIM63 in the turnover of nicotinic acetylcholine receptors. *Autophagy*, **10**, 123–136.
89. Machado,J., Silveira,W.A., Gonçalves,D.A., Schavinski,A.Z., Khan,M.M., Zanon,N.M., Diaz,M.B., Rudolf,R., Kettelhut,I.C. and Navegantes,L.C. (2019) α -Calcitonin gene-related peptide inhibits autophagy and calpain systems and maintains the stability of neuromuscular junction in denervated muscles. *Mol. Metab.*, **28**, 91.
 90. Carnio,S., LoVerso,F., Baraibar,M.A., Longa,E., Khan,M.M., Maffei,M., Reischl,M., Canepari,M., Loeffler,S., Kern,H., *et al.* (2014) Autophagy Impairment in Muscle Induces Neuromuscular Junction Degeneration and Precocious Aging. *Cell Rep.*, **8**, 1509–1521.
 91. Sandri,M., Barberi,• L, Bijlsma,• A Y, Blaauw,• B, Dyar,K.A., Milan,• G, Mammucari,• C, Meskers,• C G M, Pallafacchina,• G, Paoli,• A, *et al.* (2013) Signalling pathways regulating muscle mass in ageing skeletal muscle. The role of the IGF1-Akt-mTOR-FoxO pathway. *Biogerontology*, **14**, 303–323.
 92. Chakkalakal,J. V., Jones,K.M., Basson,M.A. and Brack,A.S. (2012) The aged niche disrupts muscle stem cell quiescence. *Nat. 2012 4907420*, **490**, 355–360.
 93. Relaix,F. and Zammit,P.S. (2012) Satellite cells are essential for skeletal muscle regeneration: the cell on the edge returns centre stage. *Development*, **139**, 2845–2856.
 94. Liu,W., Wei-LaPierre,L., Klose,A., Dirksen,R.T. and Chakkalakal,J. V (2015) Inducible depletion of adult skeletal muscle stem cells impairs the regeneration of neuromuscular junctions. *Elife*, **4**.
 95. Pratt,S.J.P., Shah,S.B., Ward,C.W., Inacio,M.P., Stains,J.P. and Lovering,R.M. (2013) Effects of in vivo injury on the neuromuscular junction in healthy and dystrophic muscles. *J. Physiol.*, **591**, 559–570.
 96. Haddix,S.G., Lee,Y. il, Kornegay,J.N. and Thompson,W.J. (2018) Cycles of myofiber degeneration and regeneration lead to remodeling of the neuromuscular junction in two mammalian models of Duchenne muscular dystrophy. *PLoS One*, **13**, e0205926.
 97. Pratt,S.J.P., Shah,S.B., Ward,C.W., Kerr,J.P., Stains,J.P. and Lovering,R.M. (2014) Recovery of altered neuromuscular junction morphology and muscle function in mdx mice after injury. *Cell. Mol. Life Sci.*, **72**, 153–164.
 98. Chakkalakal,J. V, Jones,K.M., Basson,M.A. and Brack,A.S. (2012) The aged niche disrupts muscle stem cell quiescence. 10.1038/nature11438.
 99. Liu,W., Klose,A., Forman,S., Paris,N.D., Wei-LaPierre,L., Cortés-Lopéz,M., Tan,A., Flaherty,M., Miura,P., Dirksen,R.T., *et al.* (2017) Loss of adult skeletal muscle stem cells drives age-related neuromuscular junction degeneration. *Elife*, **6**.
 100. Emery,A.E.H. (1991) Population frequencies of inherited neuromuscular diseases-A world survey. *Neuromuscul. Disord.*, **1**, 19–29.
 101. Birnkrant,D.J., Bushby,K., Bann,C.M., Apkon,S.D., Blackwell,A., Brumbaugh,D., Case,L.E., Clemens,P.R., Hadjiyannakis,S., Pandya,S., *et al.* (2018) Diagnosis and management of Duchenne muscular dystrophy, part 1: diagnosis, and neuromuscular, rehabilitation, endocrine, and gastrointestinal and nutritional management. *Lancet Neurol.*, **17**, 251–267.
 102. Landfeldt,E., Lindgren,P., Bell,C.F., Schmitt,C., Guglieri,M., Straub,V.,

- Lochmüller,H. and Bushby,K. (2014) The burden of Duchenne muscular dystrophy An international, cross-sectional study.
103. Guiraud,S., Aartsma-Rus,A., Vieira,N.M., Davies,K.E., van Ommen,G.-J.B. and Kunkel,L.M. (2015) The Pathogenesis and Therapy of Muscular Dystrophies. *Annu. Rev. Genomics Hum. Genet.*, **16**, 281–308.
 104. Guiraud,S. and Davies,K.E. (2017) Pharmacological advances for treatment in Duchenne muscular dystrophy. *Curr. Opin. Pharmacol.*, **34**, 36–48.
 105. Allen,D.G., Whitehead,N.P. and Froehner,S.C. (2015) Absence of dystrophin disrupts skeletal muscle signaling: Roles of Ca²⁺, reactive oxygen species, and nitric oxide in the development of muscular dystrophy. *Physiol. Rev.*, **96**, 253–305.
 106. Panayiotopoulos,C.P., Scarpalezos,S. and Papapetropoulos,T. (1974) Electrophysiological estimation of motor units in Duchenne muscular dystrophy. *J. Neurol. Sci.*, **23**, 89–98.
 107. Sakakibara,H., Engel,A.G. and Lambert,E.H. (1977) Duchenne dystrophy: Ultrastructural localization of the acetylcholine receptor and intracellular microelectrode studies of neuromuscular transmission. *Neurology*, **27**, 741–745.
 108. Minatel,E., Santo Neto,H. and Marques,M.J. (2003) Acetylcholine receptor distribution and synapse elimination at the developing neuromuscular junction of mdx mice. *Muscle and Nerve*, **28**, 561–569.
 109. Pilgram,G.S.K., Potikanond,S., Baines,R.A., Fradkin,L.G. and Noordermeer,J.N. (2010) The roles of the dystrophin-associated glycoprotein complex at the synapse. *Mol. Neurobiol.*, **41**, 1–21.
 110. Banks,G.B., Chamberlain,J.S. and Froehner,S.C. (2009) Truncated dystrophins can influence neuromuscular synapse structure. *Mol. Cell. Neurosci.*, **40**, 433–441.
 111. Nagel,A., Lehmann-Horn,F. and Engel,A.G. (1990) Neuromuscular transmission in the mdx mouse. *Muscle Nerve*, **13**, 742–749.
 112. Lyons,P.R. and Slater,C.R. (1991) Structure and function of the neuromuscular junction in young adult mdx mice.
 113. Kong,J. and Anderson,J.E. (1999) Dystrophin is required for organizing large acetylcholine receptor aggregates. *Brain Res.*, **839**, 298–304.
 114. Pratt,S.J.P., Valencia,A.P., Le,G.K., Shah,S.B. and Lovering,R.M. (2015) Pre- and postsynaptic changes in the neuromuscular junction in dystrophic mice. *Front. Physiol.*, **6**, 252.
 115. Jerusalem,F., Engel,A.G. and Gomez,M.R. (1974) Duchenne dystrophy: II. Morphometric study of motor end-plate fine structure. *Brain*, **97**, 123–130.
 116. Harriman,D.G.F. (1976) A comparison of the fine structure of motor end-plates in duchenne dystrophy and in human neurogenic diseases. *J. Neurol. Sci.*, **28**, 233–247.
 117. Sanes,J.R. and Yamagata,M. (2009) Many paths to synaptic specificity. *Annu. Rev. Cell Dev. Biol.*, **25**, 161–195.
 118. Verhaart,I.E.C. and Aartsma-Rus,A. (2019) Therapeutic developments for Duchenne muscular dystrophy. *Nat. Rev. Neurol.*, **15**, 373–386.
 119. Hoffman,E.P. (2019) Pharmacotherapy of Duchenne Muscular Dystrophy. In *Handb Exp Pharmacol.* pp. 25–37.
 120. Frank,D.E., Schnell,F.J., Akana,C., El-Husayni,S.H., Desjardins,C.A., Morgan,J.,

- Charleston, J.S., Sardone, V., Domingos, J., Dickson, G., *et al.* (2020) Increased dystrophin production with golodirsen in patients with Duchenne muscular dystrophy. *Neurology*, **94**, e2270–e2282.
121. Haas, M., Vlcek, V., Balabanov, P., Salmonson, T., Bakchine, S., Markey, G., Weise, M., Schlosser-Weber, G., Brohmann, H., Yerro, C.P., *et al.* (2015) European medicines agency review of ataluren for the treatment of ambulant patients aged 5 years and older with Duchenne muscular dystrophy resulting from a nonsense mutation in the dystrophin gene. *Neuromuscul. Disord.*, **25**, 5–13.
122. Asher, D.R., Thapa, K., Dharia, S.D., Khan, N., Potter, R.A., Rodino-Klapac, L.R. and Mendell, J.R. (2020) Clinical development on the frontier: gene therapy for duchenne muscular dystrophy. *Expert Opin. Biol. Ther.*, **20**, 263–274.
123. Dubinin, M. V., Talanov, E.Y., Tenkov, K.S., Starinets, V.S., Mikheeva, I.B., Sharapov, M.G. and Belosludtsev, K.N. (2020) Duchenne muscular dystrophy is associated with the inhibition of calcium uniport in mitochondria and an increased sensitivity of the organelles to the calcium-induced permeability transition. *Biochim. Biophys. Acta - Mol. Basis Dis.*, **1866**, 165674.
124. Hardee, J.P., Caldow, M.K., Chan, A.S., Plenderleith, S.K., Trieu, J., Koopman, R. and Lynch, G.S. Dystrophin deficiency disrupts muscle clock expression and mitochondrial quality 1 control in mdx mice Corresponding Author.
125. Luan, P., Amico, D.D., Andreux, P.A., Laurila, P.P., Wohlwend, M., Li, H., Lima, T.I., Place, N., Rinsch, C., Zanou, N., *et al.* (2021) Urolithin A improves muscle function by inducing mitophagy in muscular dystrophy. *Sci. Transl. Med.*, **13**, 319.
126. De Palma, C., Morisi, F., Cheli, S., Pambianco, S., Cappello, V., Vezzoli, M., Rovere-Querini, P., Moggio, M., Ripolone, M., Francolini, M., *et al.* (2012) Autophagy as a new therapeutic target in Duchenne muscular dystrophy. *Cell Death Dis.*, **5**, e1363.
127. Bibee, K.P., Cheng, Y.J., Ching, J.K., Marsh, J.N., Li, A.J., Keeling, R.M., Connolly, A.M., Golumbek, P.T., Myerson, J.W., Hu, G., *et al.* (2014) Rapamycin nanoparticles target defective autophagy in muscular dystrophy to enhance both strength and cardiac function. *FASEB J.*, **28**, 2047–2061.
128. Sebori, R., Kuno, A., Hosoda, R., Hayashi, T. and Horio, Y. (2018) Resveratrol decreases oxidative stress by restoring mitophagy and improves the pathophysiology of dystrophin-deficient MDX mice. *Oxid. Med. Cell. Longev.*, **2018**.
129. De Palma, C., Morisi, F., Cheli, S., Pambianco, S., Cappello, V., Vezzoli, M., Rovere-Querini, P., Moggio, M., Ripolone, M., Francolini, M., *et al.* (2014) Autophagy as a new therapeutic target in Duchenne muscular dystrophy. *Cell Death Dis.*, **5**, e1363.
130. Spaulding, H.R., Kelly, E.M., Quindry, J.C., Sheffield, J.B., Hudson, M.B. and Selsby, J.T. (2018) Autophagic dysfunction and autophagosome escape in the mdx mus musculus model of Duchenne muscular dystrophy. *Acta Physiol.*, **222**, e12944.
131. Kharraz, Y., Guerra, J., Pessina, P., Serrano, A.L. and Muñoz-Cánoves, P. (2014) Understanding the process of fibrosis in Duchenne muscular dystrophy. *Biomed Res. Int.*, **2014**.
132. Bowen, T., Jenkins, R.H. and Fraser, D.J. (2013) MicroRNAs, transforming growth factor beta-1, and tissue fibrosis. *J. Pathol.*, **229**, 274–285.
133. Wynn, T.A. (2007) Common and unique mechanisms regulate fibrosis in various

- fibroproliferative diseases. *J. Clin. Invest.*, **117**, 524–529.
134. Samarakoon,R., Dobberfuhr,A.D., Cooley,C., Overstreet,J.M., Patel,S., Goldschmeding,R., Meldrum,K.K. and Higgins,P.J. (2013) Induction of renal fibrotic genes by TGF- β 1 requires EGFR activation, p53 and reactive oxygen species. *Cell. Signal.*, **25**, 2198–2209.
135. Flanigan,K.M., Ceco,E., Lamar,K.M., Kaminoh,Y., Dunn,D.M., Mendell,J.R., King,W.M., Pestronk,A., Florence,J.M., Mathews,K.D., *et al.* (2013) LTBP4 genotype predicts age of ambulatory loss in duchenne muscular dystrophy. *Ann. Neurol.*, **73**, 481–488.
136. Bello,L., Kesari,A., Gordish-Dressman,H., Cnaan,A., Morgenroth,L.P., Punetha,J., Duong,T., Henricson,E.K., Pegoraro,E., McDonald,C.M., *et al.* (2015) Genetic modifiers of ambulation in the cooperative international Neuromuscular research group Duchenne natural history study. *Ann. Neurol.*, **77**, 684–696.
137. Hafner,P., Bonati,U., Klein,A., Rubino,D., Gocheva,V., Schmidt,S., Schroeder,J., Bernert,G., Laugel,V., Steinlin,M., *et al.* (2019) Effect of Combination l-Citrulline and Metformin Treatment on Motor Function in Patients With Duchenne Muscular Dystrophy: A Randomized Clinical Trial. *JAMA Netw. open*, **2**, e1914171.
138. Gordon,B.S., Delgado-Diaz,D.C., Carson,J., Fayad,R., Wilson,L.B. and Kostek,M.C. (2013) Resveratrol improves muscle function but not oxidative capacity in young mdx mice. *Clin. Nutr.*, **32**, 104–111.
139. Ljubicic,V., Burt,M., Lunde,J.A. and Jasmin,B.J. (2014) Resveratrol induces expression of the slow, oxidative phenotype in mdx mouse muscle together with enhanced activity of the SIRT1-PGC-1 axis. *AJP Cell Physiol.*, **307**, C66–C82.
140. Yusuke S. Hori, Atsushi Kuno, Ryusuke Hosoda, Masaya Tanno, Tetsuji Miura, Kazuaki Shimamoto, and Y.H. (2011) Resveratrol Ameliorates Muscular Pathology in the Dystrophic mdx Mouse, a Model for Duchenne Muscular Dystrophy. *Clin. Nutr.*, **338**, 784–794.
141. Kawamura,K., Fukumura,S., Nikaido,K., Tachi,N., Kozuka,N., Seino,T., Hatakeyama,K., Mori,M., Ito,Y.M., Takami,A., *et al.* (2020) Resveratrol improves motor function in patients with muscular dystrophies: an open-label, single-arm, phase IIa study. *Sci. Reports 2020 101*, **10**, 1–11.
142. Goodyear,L.J. (2008) The exercise pill - Too good to be true? *N. Engl. J. Med.*, **359**, 1842–1844.
143. Ljubicic,V. and Jasmin,B.J. (2015) Metformin increases peroxisome proliferator-activated receptor γ Co-activator-1 α and utrophin a expression in dystrophic skeletal muscle. *Muscle Nerve*, **52**, 139–142.
144. Angebault,C., Panel,M., Lacôte,M., Rieusset,J., Lacampagne,A. and Fauconnier,J. (2021) Metformin Reverses the Enhanced Myocardial SR/ER–Mitochondria Interaction and Impaired Complex I-Driven Respiration in Dystrophin-Deficient Mice. *Front. Cell Dev. Biol.*, **8**, 609493.
145. Dong,X., Hui,T., Chen,J., Yu,Z., Ren,D., Zou,S., Wang,S., Fei,E., Jiao,H. and Lai,X. (2021) Metformin Increases Sarcolemma Integrity and Ameliorates Neuromuscular Deficits in a Murine Model of Duchenne Muscular Dystrophy. *Front. Physiol.*, **0**, 606.
146. Ljubicic,V., Khogali,S., Renaud,J.-M. and Jasmin,B.J. (2012) Chronic AMPK

- stimulation attenuates adaptive signaling in dystrophic skeletal muscle. *AJP Cell Physiol.*, **302**, C110–C121.
147. Al-Rewashdy,H., Ljubicic,V., Lin,W., Renaud,J.M. and Jasmin,B.J. (2015) Utrophin A is essential in mediating the functional adaptations of mdx mouse muscle following chronic AMPK activation. *Hum. Mol. Genet.*, **24**, 1243–1255.
148. Péladeau,C., Ahmed,A., Amirouche,A., Crawford Parks,T.E., Bronicki,L.M., Ljubicic,V., Renaud,J.M. and Jasmin,B.J. (2016) Combinatorial therapeutic activation with heparin and AICAR stimulates additive effects on utrophin A expression in dystrophic muscles. *Hum. Mol. Genet.*, **25**, 24–43.
149. Ljubicic,V., Burt,M. and Jasmin,B.J. (2014) The therapeutic potential of skeletal muscle plasticity in Duchenne muscular dystrophy: Phenotypic modifiers as pharmacologic targets. *FASEB J.*, **28**, 548–568.
150. Valdez,G., Tapia,J.C., Kang,H., Clemenson,G.D., Gage,F.H., Lichtman,J.W. and Sanes,J.R. (2010) Attenuation of age-related changes in mouse neuromuscular synapses by caloric restriction and exercise. *Proc. Natl. Acad. Sci. U. S. A.*, **107**, 14863–14868.
151. Stockinger,J., Maxwell,N., Shapiro,D., DeCabo,R. and Valdez,G. (2017) Caloric Restriction Mimetics Slow Aging of Neuromuscular Synapses and Muscle Fibers. *J. Gerontol. A. Biol. Sci. Med. Sci.*, **73**, 21–28.

CHAPTER 2:

**The neurotrophic factor AMP-activated protein kinase regulates neuromuscular
junction plasticity**

Submitted to *Science Signaling*

Title: The neurotrophic factor AMP-activated protein kinase regulates neuromuscular junction plasticity

Authors: Sean Y Ng¹, Andrew I Mikhail¹, Stephanie R Mattina¹, Salah A Mohammed¹, Shahzeb K Khan¹, Eric M Desjardins^{2,3,4}, Changhyun Lim¹, Stuart M Phillips¹, Gregory R Steinberg^{2,3,4}, Vladimir Ljubcic^{1*}

Affiliations:

¹Department of Kinesiology, McMaster University, 1280 Main St. W., Hamilton, ON, Canada L8S 4L8.

²Centre for Metabolism, Obesity and Diabetes Research, McMaster University, 1280 Main St. W., Hamilton, ON, Canada L8N 3Z5.

³Division of Endocrinology and Metabolism, Department of Medicine, McMaster University, 1280 Main St. W., Hamilton, ON, Canada L8N 3Z5.

⁴ Department of Biochemistry and Biomedical Sciences, McMaster University, 1280 Main St. W., Hamilton, ON, Canada L8N 3Z5.

*Corresponding author. Email: ljubicic@mcmaster.ca

Abstract:

AMP-activated protein kinase (AMPK) is a critical regulator of cell metabolism and phenotype, and therefore is considered a key molecule in several chronic conditions affecting the neuromuscular system, including aging, neurodegenerative diseases, and neuromuscular disorders (NMDs). Although AMPK is a well-established modulator of skeletal muscle plasticity, the role of the enzyme in the maintenance and plasticity of the neuromuscular junction (NMJ) is undefined. Our data reveal that young mice null for AMPK in skeletal muscle exhibited an aged NMJ gene signature and morphology akin to those observed in old, wild-type animals. In complementary *in vivo* studies, we demonstrate that acute, pharmacological stimulation of AMPK promoted its accumulation at the motor endplate and in fundamental myonuclei, as well as that of the downstream substrate peroxisome proliferator-activated receptor γ coactivator-1 α (PGC-1 α), which together preceded the induction of NMJ-related transcripts. Moreover, this small molecule-

mediated, targeted AMPK activation enhanced myotube acetylcholine receptor (AChR) clustering on par with levels observed with agrin or Wnt dosing, further indicating that AMPK exerts neurotrophic effects at the endplate. Finally, a single bout of exercise-induced AMPK stimulation in mouse skeletal muscle evoked a broad transcriptional response in NMJ-related genes that was consistent with data from muscle biopsies in human participant studies employing a variety of exercise modalities, which included identifying *Dok7* as a novel and conserved downstream target of AMPK. Collectively, these results uncover neurotrophic effects of AMPK at the neuromuscular synapse that may be leveraged for the maintenance and remodeling of the NMJ in health and disease.

INTRODUCTION

AMPK is a heterotrimeric protein comprised of a catalytic α , scaffolding β , and regulatory γ subunit. Each subunit has various isoforms (i.e., $\alpha 1$, $\alpha 2$, $\beta 1$, $\beta 2$, $\gamma 1$, $\gamma 2$, and $\gamma 3$) that result in twelve possible enzyme formations that are selectively expressed in different cell types (1–3). For example, in murine skeletal muscle the most prevalent AMPK composition is $\alpha 2\beta 2\gamma 1$, whereas in human muscle, $\alpha 2\beta 2\gamma 3$ is most common (3). Mice with skeletal muscle-specific knock out (mKO) of AMPK are typically characterized by a myopathy of mild-to-moderate severity (3–7), whereas genetic AMPK gain-of-function mice demonstrate elevated muscle mitochondrial abundance and enhanced exercise capacity (8, 9), which altogether highlight the nexus function of this kinase in regulating skeletal muscle plasticity. AMPK is simulated by increases in the AMP/ADP:ATP ratio, such as occurs during exercise (10). AMP binding to the γ subunit

allosterically activates the enzyme, while the presence of AMP/ADP elevates threonine (Thr)¹⁷² phosphorylation of the catalytic α subunit and prevents dephosphorylation by phosphatases (10). Marking of Thr¹⁷² can further be enhanced by upstream kinases in skeletal muscle. Pharmacological AMPK activators induce the enzyme via a variety of mechanisms. For instance, metformin indirectly activates AMPK by increasing the AMP/ADP:ATP ratio and the 5-aminoimidazole-4-carboxamide-1- β -D-ribofuranoside (AICAR) metabolite ZMP acts as an AMP analog. More recently discovered small molecule agonists like A769662, 991, MK-8722 (MK), and PXL770 are allosteric activators that directly bind to AMPK and elicit highly specific and potent stimulation of the kinase (2, 11). Genetic, physiological, and pharmacological approaches have provided valuable insights into the biological functions and clinical significance of AMPK.

The NMJ is an electrochemical signaling apparatus between an α MN and the skeletal muscle fibers it innervates with the primary function of stimulating muscle contraction (12–14). The NMJ undergoes cyclic periods of phenotypic maintenance and plasticity throughout the lifespan, for instance during development (12), damage, repair and regeneration (15, 16), as well as amid increased muscle use (i.e., exercise) and disuse, and advance aging (12, 14, 15). Neurotrophic factors such as agrin (Agr) and Wnt assist in coordinating the expression, localization, and activity of synaptic machinery required to remodel the NMJ in health and disease (12, 17). Given the considerable influence of AMPK on the determination, maintenance, and adaptability of skeletal muscle biology, we and others have postulated that its regulatory role extends to the NMJ (14, 18, 19). Indeed, mice with ablated downstream targets of AMPK, such as mammalian target of rapamycin

(mTOR) and PGC-1 α , exhibit dysmorphic NMJs and dysregulated synaptic gene expression (20–22). Further support is highlighted in recent work demonstrating pharmacological or transgenic modulation of mTOR and PGC-1 α and their beneficial effects on neuromuscular synapse function and morphology in aging and disease (22–25). Notably, neurotrophic effects of AMPK are also implied by studies that employ pharmacological activators, such as metformin or AICAR, which enhance the morphology and function of synapses in aged animals (14, 19, 26–28), as well as preserve α MN function and survival in pre-clinical models of neurodegenerative diseases (29–31). However, despite the collective evidence from these elegant studies, the role of skeletal muscle AMPK in the maintenance and plasticity of the NMJ is undefined. Hence, we utilized a multifaceted methodology encompassing genetic, physiological, and pharmacological approaches to determine the impact of AMPK on the neuromuscular synapse. Our findings reveal a novel neurotrophic function of AMPK specifically at the NMJ.

RESULTS

Muscle-specific *AMPK β 1 β 2*^{-/-} KO (mKO) mice exhibit perturbed downstream signaling and characteristics of a prematurely aged NMJ

We employed wild-type (WT) mice aged 3-, 12-, and 22 months (mo), along with 3- and 12mo mKO littermates to investigate the influence of skeletal muscle-specific AMPK deletion on NMJ biology (Fig. 1A). To confirm the absence of AMPK activity in the skeletal muscle of mKO animals, immunoblotting experiments were performed with tibialis anterior (TA) muscles to reveal threonine 172 (Thr¹⁷²)-phosphorylated AMPK

(pAMPK^{Thr172}). pAMPK^{Thr172} expression and AMPK phospho-status (i.e., the phosphorylated form of the protein relative to its total amount within the same sample) were markedly reduced in the mKO animals when compared to their WT littermates (Fig 1B). Similar to previous reports (32), a significant age-associated reduction (-50%) in AMPK phospho-status was observed in the TA muscles of 22 mo WT animals when compared to their younger 3 mo controls (Fig. 1B, 1C).

Several studies have identified that AMPK substrates PGC-1 α and mTOR regulate NMJ biology (21, 33, 34). Given this, we sought to evaluate the effect of age and skeletal muscle AMPK deletion on the activity of these NMJ-modifying molecules. Despite 40-50% lower PGC-1 α content in the TA muscles of 22mo WT mice as compared to younger animals, there was not a statistically significant difference in PGC-1 α levels across age (Fig. 1D, 1E). mKO mice exhibited 35% lower PGC-1 α expression versus their age-matched WT controls. Notably, PGC-1 α protein levels were similar between 3 mo mKO, 12 mo mKO, and 22 mo WT animals. Phospho-status of mTOR (mTOR^{Ser2448}), as well as its downstream effector kinase S6 (S6^{Ser235/236} and S6^{Ser240/244}), were significantly altered with age (Fig. 1D, 1F-1H). Specifically, mTOR^{Ser2448} phospho-status was 180-390% higher ($P < 0.05$) in 12 mo WT and mKO animals relative to 3 mo groups. mTOR^{Ser2448} phospho-status was similar ($P > 0.05$) between 22 mo WT mice and both 3 mo cohorts. Generally, S6^{Ser235/236} and S6^{Ser240/244} phospho-status were significantly higher in muscles from older mice, and mKO animals exhibited reduced ($P < 0.05$) levels when compared to their WT littermates.

We next surveyed the transcript levels of several critical regulators of NMJ structure and function in whole TA muscles from WT and mKO animals. Similar to previous work (22), 22 mo WT mice exhibited significantly greater (+150-260%) AChR subunit $\alpha 1$ (*Chrna1*) and γ (*Chrng*) mRNA levels relative to the 3 mo WT mice, whereas AChR β subunit (*Chrnbb*) gene expression was 80% lower ($P < 0.05$) in the old mice (Fig. 1I). *Chrna1*, *Chrnbb*, and *Chrnb* levels were similar ($P > 0.05$) between WT and mKO animals at 3 and 12 mo. The fetal isoform of AChR, *Chrng*, was significantly higher (+4.8-fold) in the muscles of 12 mo mKO animals relative to their age-matched, WT controls and comparable ($P > 0.05$) to the 22 mo WT group. Agrin (*Agrn*), low-density lipoprotein receptor-related (*Lrp4*), receptor-associated protein of the synapse (*Rapsn*), docking protein 7 (*Dok7*), ETS variant transcription factor 5 (*Etv5*), and utrophin (*Utrn*) mRNA expression were 70-95% lower ($P < 0.05$) in the 22 mo WT mice relative to their younger controls (Fig. 1J). Additionally, GA-binding protein α (GABP; *Gabpa*) was affected by age, where muscles from 12 mo WT mice expressed +200% more ($P < 0.05$) *Gabpa* transcript content when compared to the 3 mo WT group. *Agrn*, *Rapsn*, *Dok7*, PGC-1 α (*Ppargc1a*), and fibroblast growth factor binding protein 1 (*Fgfbp1*) transcript levels were significantly lower (-20-35%) in the mKO animals when compared to their age-matched WT group, while muscle-specific kinase (*Musk*) and *Lrp4* gene expression were similar ($P > 0.05$) between genotypes. *Gabpa* content was 3.2-fold higher ($P < 0.05$) in 3 mo mKO relative to their age-matched controls and comparable ($P > 0.05$) to 12- and 22 mo WT animals.

Some indicators of denervation in the form of prevalent small angular muscle fibers and reduced muscle force production have been previously reported in mKO animals (4). Thus, to further investigate this phenomenon we assessed fiber type grouping, which is another accepted characteristic of muscle fiber denervation/reinnervation. Soleus (SOL) muscles from 12 mo mKO mice exhibited a 2.1-fold greater ($P < 0.05$) occurrence of myofiber type clustering relative to their age-matched WT group (Fig. 1K, 1L). Notably, the SOL muscles of 12 mo mKO animals demonstrated similar ($P > 0.05$) fiber type groupings when compared to the SOL muscles of 22 mo WT mice.

AMPK regulates NMJ morphology during aging

To further examine the influence of AMPK on NMJ biology, we next evaluated NMJ morphology in the fast, glycolytic extensor digitorum longus (EDL) muscle and the slower, more oxidative SOL muscle of WT and mKO animals (Fig. 2A, 2B). Neurofilament M (NFM) and synaptic vesicle 2 (SV2) were used for labeling presynaptic components, while α -bungarotoxin (α BTX) stained AChRs to reveal postsynaptic morphology. As expected, we observed a significantly higher prevalence of fragmented and ectopic synaptic endplates in the EDL and SOL muscles of 22 mo WT animals compared to their younger counterparts (Fig. 2A-2D). On balance, the number of fragmented and ectopic NMJs were greater ($P < 0.05$) in EDL and SOL muscles of mKO mice relative to their age-matched WT controls. Further, these metrics in 12 mo mKO mice were either similar ($P > 0.05$) to or significantly higher than 22 mo WT animals.

We continued our evaluation of NMJ morphology by investigating presynaptic components in all experimental groups. A significantly greater (+40%) degree of axon

blebbing was observed in the EDL muscles from 22 mo WT animals relative to the 3 mo WT group (Fig. 2B, 2E). Additionally, axon sprouting occurred more (+30%) in the SOL muscles of 12- and 22 mo WT mice as compared to their younger WT controls (Fig. 2B, 2F). AMPK deficient SOL muscles from 3 mo mKO animals demonstrated a trending 40% increase ($P = 0.06$) in the number of blebbing axons when compared to their WT counterparts. Sprouting axons were 30% lower ($P < 0.05$) in 12 mo mKO SOL muscles when compared to the 12 mo WT group.

Targeted pharmacological AMPK stimulation elicits synaptic gene expression

Ensuing experiments to further elucidate the role of AMPK at the NMJ contrasted the aging and mKO models with one that pharmacologically stimulates the kinase. Here, we administered a single dose of the orally bioavailable, direct AMPK activator, MK (5 mpk), via oral gavage to WT animals. Mice were euthanized 3- (MK 3hr) or 6 hours (MK 6hr) post-treatment, while a cohort of age-matched WT animals were treated with the vehicle (Veh) solution to serve as a control group (Fig. 3A). AMPK^{Thr172} phospho-status was 135% higher ($P < 0.05$) in the triceps (TRI) muscles of the MK 3hr group compared to the Veh group (Fig. 3B, 3C). This significant increase in phosphorylation was maintained in the MK 6hr cohort. The phospho-status of AMPK substrates acetyl-CoA carboxylase (ACC^{Ser212}) and unc-51-like autophagy activating kinase (ULK1^{Ser555}) were also significantly greater (+25-100%) in the MK 6hr group. NMJ gene expression analyses revealed that *Chrng* and *Fgfbp1* mRNAs were rapidly decreased ($P < 0.05$) by 35-50% in the TRI muscles of MK 3hr animals relative to their Veh controls, while other NMJ-related

genes, such as *Musk*, *Rapsn*, *Dok7*, and *Ppargcal* were significantly higher (+35-105%) in the MK 6hr group compared to Veh-treated mice (Fig. 3D, 3E).

AMPK and its downstream target PGC-1 α regulate transcription and thus can be found within the myonuclear compartment (21, 35–37). Therefore, we evaluated the presence of myonuclear AMPK and PGC-1 α in the gastrocnemius (GAST) muscles of Veh- and MK-treated animals within the broader context of NMJ gene expression. The MK 3hr group demonstrated 30-40% elevations ($P < 0.05$) in nuclear pAMPK^{Thr172}, total AMPK, and PGC-1 α levels relative to their Veh-treated counterparts (Fig. 3F, 3G).

AMPK activation promotes accumulation of pAMPK^{Thr172} and PGC-1 α at the NMJ and in fundamental myonuclei

Subsynaptic myonuclei, also known as fundamental nuclei, are specialized gene transcription sites for NMJ-related mRNAs (16, 38). We postulated that AMPK-mediated transcriptional control of NMJ genes is associated with AMPK and PGC-1 α localization at the neuromuscular synapse. To evaluate this, we employed an immunofluorescence-based strategy to identify postsynaptic protein expression (39–41). First, we observed postsynaptic enrichment of pAMPK^{Thr172} in EDL muscles of Veh- and MK-treated animals (Fig. 4A-C). pAMPK^{Thr172} expression at the synapse was 2.1-3.0-fold higher ($P < 0.05$) in the MK 3hr and MK 6hr groups relative to their Veh controls (Fig. 4A, 4D). Moreover, pAMPK^{Thr172} within subsynaptic myonuclei was also significantly greater (+1.6-fold) in the MK 6hr mice compared to Veh treated animals (Fig. 4A, 4F). Next, the data revealed that PGC-1 α shared a similar expression pattern to pAMPK^{Thr172} in response to MK treatment (Fig. 4F-H). Specifically, synaptic PGC-1 α expression was ~1.3-fold higher (P

< 0.05) in the MK 3hr and MK 6hr cohorts relative to their Veh-treated counterparts (Fig. 4I). PGC-1 α levels in fundamental myonuclei were also significantly greater (1.9-fold) in the MK 6hr group compared to Veh-treated animals (Fig. 4J).

AMPK activation in skeletal muscle induces AChR clustering

To further characterize the role of skeletal muscle AMPK on NMJ biology, we assessed whether pharmacological AMPK activation elicits AChR clustering (Fig. 5A). C2C12 myotubes were treated with Veh or MK (2.5-10 μ M), or with neurotrophic factors agrin (0.4 μ M), or Wnt11 (Wnt; 0.1 μ M) for 24hrs. MK-treated cells demonstrated significant increases (+60-225%) in the phospho-status of AMPK-targeted substrates ACC^{Ser212}, ULK1^{Ser555}, and Ser⁷⁰⁰-phosphorylated TBC1 domain family member 1 (TBC1D1^{Ser700}) (Fig. 5B, 5C). These indices of AMPK activity were similar ($P > 0.05$) between the Veh-, agrin-, and Wnt-treated conditions. A 35-40% higher ($P < 0.05$) number of AChR clusters were observed in the 2.5 and 5 μ M MK-treated cells when compared to Veh-treated myotubes (Fig. 5D-F). As expected, AChR cluster counts were significantly higher in the agrin and Wnt-treated myotubes relative to Veh conditions.

Exercise-evokes AMPK stimulation and downstream *Pparg1 α* and *Dok7* expression in mouse and human skeletal muscle

Next, we utilized a single bout of exercise to physiologically stimulate AMPK and evaluated the transcriptional responses of NMJ-related genes. TRI muscles were analyzed immediately following (Ex 0hr) or 3 hrs (Ex 3hr) post-aerobic-type treadmill running exercise (Fig. 6A). We observed rapid and significant increases (+30-160%) of AMPK^{Thr172}, ACC^{Ser212}, and ULK1^{Ser555} phospho-status in the exercise groups when

compared to their sedentary (Sed) controls (Fig. 6B, 6C). NMJ gene analyses revealed a transient 25% increase ($P < 0.05$) in *Chrna1* mRNA expression in the TRI muscles of Ex 0hr animals relative to their Sed counterparts (Fig. 6D). *Agrn*, *Lrp4*, and *Fgfbp1* transcript levels were significantly reduced (-25-30%) in the Ex 3hr group compared to Sed, whereas *Musk* and *Dok7* transcript content was 80-100% higher ($P < 0.05$) after exercise (Fig. 6E). Additionally, a trending 35% increase ($P = 0.06$) of *Utrn* mRNA was detected 3 hrs post-exercise. Lastly, *Ppargc1a* mRNA expression was significantly induced in the Ex 0hr and Ex 3hr groups relative to the Sed mice.

Finally, we examined NMJ-specific transcriptional changes in human skeletal muscle caused by exercise, an established physiological activator of AMPK in the neuromuscular system (14, 42). MetaMEx (v.3.2208) extracted skeletal muscle transcriptomic data from 39 aerobic, 23 resistance, and 9 high intensity interval (HIIT) acute exercise experiments, which were comprised of a total of 575 participants across all studies. Within our panel of NMJ-related genes, we anticipated that *PPARGCIA* would be an exercise-inducible transcript (43), and therefore could serve as a positive control for our analysis. Indeed, using MetaMEx we found that *PPARGCIA* gene expression was robustly stimulated by exercise in human skeletal muscle (Fig. 6F). We also identified *DOK7* as a novel exercise responsive gene in human muscle. MetaMEx exercise timecourse analyses displayed a 1.85-fold increase in *DOK7* expression 2-3hr post-exercise compared to the sedentary, control timepoint (data not shown). This significant elevation in *DOK7* was sustained at the 4-6hr timepoint and returned to resting levels 48hrs following exercise. Furthermore, subgroup analyses based on exercise type indicated that *DOK7* was 1.5-fold

greater (Fig. 6G) in response to aerobic exercise and 1.60-fold higher (Fig. 6H) after acute resistance exercise as compared to resting conditions. Meta-analysis of HIIT studies did not reveal an overall significant effect on *DOK7*, despite demonstrating a significant +1.4-2.4 log fold change (LogFC) versus control among in 6/9 studies examined (Fig. 6I).

DISCUSSION

In the current study we used a comprehensive, combinatory physiological, genetic, pharmacological gain- and loss-of-function approach to further elucidate the role of AMPK in the maintenance and plasticity of the NMJ. The data show that adult AMPK mKO mice exhibit an NMJ gene expression profile and phenotype comparable to old animals where skeletal muscle AMPK activity naturally declines. Our findings also demonstrate that acute, targeted pharmacological AMPK stimulation elicited myonuclear accumulation of the kinase and its proximal substrate PGC-1 α that preceded the transcriptional induction of synaptic genes. In fact, a single dose of MK resulted in rapid AMPK and PGC-1 α localization to the NMJ and specifically within fundamental myonuclei, which strongly suggests AMPK-PGC-1 α pathway-mediated synaptic regulation. Furthermore, AMPK activation via MK enhanced myotube AChR clustering on par with levels observed using agrin and Wnt, indicating that AMPK exerts neurotrophic effects at the endplate. Finally, a single bout of aerobic-type exercise-induced AMPK stimulation in mouse skeletal muscle evoked a broad transcriptional response in NMJ-related genes, including augmented *Ppargcal* and *Dok7*, which was consistent with data from muscle biopsies in human participant studies employing a variety of exercise modalities. Our in vivo, in vitro, and in

silico findings altogether provide robust evidence for a novel regulatory role of AMPK in the maintenance and remodeling of the NMJ.

AMPK-regulated processes such as autophagy, mitochondrial turnover, and inflammation, have been implicated in contributing to age-associated NMJ dysfunction (14, 44–46). Given that the transgenic ablation of skeletal muscle AMPK significantly impacts these cellular pathways (5, 6, 47, 48), and that AMPK activity is reduced in old age (32), it was reasonable to speculate that AMPK mKO mice would present with a synaptic phenotype of accelerated aging. Our study provides experimental evidence, in conjunction with previous work, to support this hypothesis. First, we confirm that the deletion of skeletal muscle AMPK lowers PGC-1 α expression as previously shown (7), as well as decreases mTOR activity, indicated by reduced pS6^{Ser235/236} and pS6^{Ser240/244} levels. These outcomes are meaningful because PGC-1 α and mTOR regulate NMJ biology throughout the lifespan (21, 22, 33, 49). Second, the absence of skeletal muscle AMPK in adult mice resulted in a NMJ transcriptional profile similar to that observed in aged WT animals (50). Third, the increased prevalence of fiber type grouping in adult mKO mice, as well as the previously described presence of small angular and necrotic myofibers in these animals (51), suggest denervation/reinnervation cycling characteristic of advanced aging (52). Fourth, adult AMPK mKO animals displayed postsynaptic dysmorphia, a common feature of old mice (12). Lastly, AMPK mKO mice exhibited diminished muscle force production that implicates impaired neurotransmission at the NMJ, analogous to the senescent condition (12). Together, these data from models of genetic and physiological skeletal muscle AMPK reduction strongly imply that the kinase is required for optimal maintenance

of NMJ biology. NMDs such as amyotrophic lateral sclerosis, spinal muscular atrophy, and muscular dystrophies, which manifest synaptic dysfunction that in some respects recapitulate the effects of aging (16, 53, 54), also show aberrations in AMPK activity (18, 55). Future work should investigate whether enhancing AMPK function in these conditions normalizes NMJ gene expression and phenotype.

Acute AMPK stimulation in skeletal muscle drives gene programs involved in several metabolic pathways (10, 43, 56). In the current study, we reveal that AMPK-mediated transcriptional regulation extends to the NMJ. Specifically, the data demonstrate that synaptic gene expression, including *Musk*, *Dok7*, and *Ppargcal*, was significantly elevated in response to pharmacological AMPK activation. These MK-induced NMJ transcripts are regulated by an N-box promoter motif that is controlled by a PGC-1 α /GABP complex (21). Given the well-documented link between AMPK and PGC-1 α in skeletal muscle (10, 57), it is plausible that the induction of synaptic genes occurs through an AMPK/PGC-1 α /GABP signalling cascade. To support this assertion, we also detected a rapid rise of MK-evoked postsynaptic pAMPK^{Thr172} and PGC-1 α , as well as a coincident accumulation of these molecules in fundamental nuclei, which preceded the elevation in NMJ gene expression. AMPK and PGC-1 α nuclear localization have been previously described (35, 36, 58), although non-specific myonuclei were surveyed and mRNA analyses were not conducted in these studies. The current project did not interrogate additional AMPK-inducible signaling pathways that are related to neuromuscular plasticity, such as Hippo/Yes-associated protein or Wnt/ β -catenin cascades. As such,

continued investigation downstream of AMPK may reveal new mechanisms by which the kinase coordinates the neuromuscular synapse.

Physiological interventions capable of activating AMPK, such as exercise or caloric restriction, effectively remodel the neuromuscular synapse (14, 22, 26, 27). Furthermore, in animals with fragmented NMJs due to aging (14, 19, 26–28), dystrophy (16, 59), or neurodegenerative disorders (29–31), chronic pharmacological AMPK stimulation preserves both synaptic morphology and function. However, these studies did not account experimentally for the contributions of AMPK-independent effects at the neuromuscular synapse. Here, we treated cultured muscle cells with MK to model targeted skeletal muscle-specific AMPK gain-of-function and investigate the role of the kinase at the motor endplate. Our findings indicate that AMPK induces AChR clustering in C2C12 cells to a comparable extent as the canonical neurotrophic factors agrin and Wnt. Prior *in vitro* studies have demonstrated that indirect AMPK activators like metformin and resveratrol do not exert any influence on AChR clustering (27). This discrepancy with our data may be attributed to the superior magnitude and specificity of AMPK stimulation achieved with MK in comparison to other compounds (60, 61). Additionally, we observed that agrin and Wnt did not elicit AMPK phosphorylation or activity, suggesting that their neurotrophic effects are AMPK-independent. These findings imply that AMPK agonists may exhibit additive or synergistic effects in conjunction with other NMJ-targeted approaches to evoke synapse remodeling.

Using an alternative, *in vivo* physiological approach, our study further strengthened the connection between AMPK and the NMJ by uncovering an exercise-associated NMJ

transcriptional program in murine skeletal muscle, with some genes upregulated (e.g., *Chrna1*, *Musk*, *Dok7*, *Ppargc1a*) and others downregulated (e.g., *Agrn*, *Lrp4*, *Fgfbbp1*) subsequent to AMPK activation. These results call back to the acute effects of MK where AMPK activation also largely preceded the changes in NMJ-related transcripts. Altogether, these data are consistent with a paper by Muise et al. that showed a similar gene expression response in rodent muscle upon a single bout of physical activity or MK (56), including a coincident upregulation of *Dok7* and *Ppargc1a*. To extend this investigation into humans, we conducted a meta-analysis using MetaMEx (v. 3.2208), surveying 71 acute exercise-induced skeletal muscle transcriptomic databases (43). Here, we confirmed upregulation of *DOK7* and *PPARGCIA* in human skeletal muscle by aerobic and resistance exercise, while other transcripts in our NMJ gene panel remained unchanged. Methodological limitations to acknowledge using this strategy include the lack of NMJs due to biopsy sampling location and therefore contain a dearth of synapse-specific transcripts, as well as the lower NMJ-to-muscle size ratio compared to mice (62), possibly resulting in underestimated motor endplate gene expression. Furthermore, although it is reasonable to assume that skeletal muscle AMPK was stimulated following these exercise stimuli, only one study (GSE86931; 42) provided information regarding its activity (43). Popov and colleagues demonstrated immediate AMPK activation and a subsequent rise in *DOK7* and *PPARGCIA* expression in the vastus lateralis muscles of aerobically exercised men (63). Altogether, these data indicate that upregulation of *DOK7* occurs with AMPK stimulation and is conserved across species, including humans. *Dok7* protein possesses several AMPK phosphorylation motifs around Thr²¹⁴, Thr³⁸³, and Thr⁴⁰⁶ (64), with the latter two mediating

agrin/Lrp4/Musk-induced phosphorylation of Dok7 (36). The significance of this lies in the implication that AMPK possesses dual mechanisms for regulating Dok7, whereby the kinase upregulates Dok7 mRNA levels, as well as posttranslationally modifies the protein to yet unknown effect. Furthermore, Dok7 is implicated as a therapeutic target for several neurodegenerative conditions, including aging (65), and NMDs (66–69), many of which are positively influenced by physiological and pharmacological AMPK agonism (16, 18). Further investigation of the relationship between AMPK and Dok7 may unveil novel regulatory mechanisms exerted by the kinase on the NMJ.

In summary, using a comprehensive experimental strategy we demonstrate neurotrophic effects of AMPK at the NMJ. The influence of the kinase is mediated, at least in part, via PGC-1 α , an established regulator of the neuromuscular synapse. Furthermore, we identify the NMJ adaptor protein Dok7 as a target of AMPK, but additional work is necessary to define mechanisms involved and functional significance. Altogether, this report provides strong evidence of a novel role for AMPK that may be leveraged for the maintenance and remodeling of the NMJ in health and disease.

MATERIALS AND METHODS

Animal experiments

Mice were cared for according to the Canadian Council on Animal Care guidelines in the McMaster University Central Animal Facility. All animal experiments were approved under Animal Utilization Protocol #22-07-26 in the primary investigator's laboratory.

The generation and genotyping of *AMPK β 1 β 2^{-/-}* animals were previously described (7). Male and female mKO mice were aged to 3 and 12 mo. Sex- and age-matched WT littermates served as control groups, while 22 mo WT animals were employed as a cohort of advanced aging. Animals were euthanized via cervical dislocation and their tissues were rapidly dissected. Muscle samples were prepared using different preservation methods based on the intended experimental procedures: flash-freezing, embedding in optimum cutting temperature (OCT) compound, or processing for whole-mount immunofluorescence. All frozen muscles were stored in -80°C until analysis.

2 mo WT mice (Jackson Laboratory, 000666) were orally gavaged with MK (5 mpk, Merck) or a Veh solution (0.25% methylcellulose, 5% polysorbate 80, and 0.02% sodium lauryl sulfate). Animals were euthanized via cervical dislocation 3- and 6-hrs post gavage. TRI muscles were immediately flash frozen in liquid nitrogen while EDL muscles were embedded in OCT compound, cooled in isopentane.

A separate cohort of 2 mo WT mice were acclimatized to a motorized rodent treadmill (Exer-3/6, Columbus Instruments). Animals were then randomized into a sedentary or exercised group. Exercised mice performed a single bout of treadmill running at 15 m/min for 90 mins as previously described (70). Immediately following exercise or 3 hrs post-exercise, TRI muscles were rapidly collected and flash frozen in liquid nitrogen.

Skeletal muscle protein extraction and fractionation

Muscle tissue or cell extracts were processed for immunoblotting as previously described (41). In brief, samples were suspended in RIPA buffer (Sigma-Aldrich, R0278) supplemented with Complete Mini Protease Inhibitor Cocktail (Sigma-Aldrich,

05892970001) and PhosSTOP Phosphatase Inhibitor Cocktail (Sigma-Aldrich, 4906845001). Muscle preparations were then mechanically homogenized with TissueLyser (Qiagen) and sonication (Branson Ultrasonics Sonifier, Thermo Fisher Scientific, SFX150). Cell debris was removed with centrifugation at 14,000g and the remaining supernatants were collected and processed for further analysis. When nuclear fractionation was required, skeletal muscles were mechanically lysed in STM buffer (250 mM Sucrose, 50 mM Tris-HCl pH 7.4, 5 mM MgCl₂, protease and phosphatase inhibitor cocktails) with scissors and a Teflon pestle as previously described (71). Prepared samples were then centrifuged at 800g and the resultant pellet (nuclear compartment) was washed twice and then resuspended in NET buffer (20 mM HEPES pH 7.9, 1.5 mM MgCl₂, 0.5 M NaCl, 0.2 mM EDTA, 20% glycerol, 1% Triton-X-100, protease and phosphatase inhibitors), sonicated, and centrifuged at 9,000g for 30 mins. The remaining myonuclei-enriched supernatant was then collected.

Immunoblotting

All protein samples were tested with a bicinchoninic assay (Thermo Fisher Scientific, PI23225) to determine protein concentrations. Muscle homogenates were then diluted to equal concentrations (2 µg/µl) mixed with 4x loading buffer and ddH₂O. 10-20 µg of prepared sample was loaded into 4-15% gradient polyacrylamide gels and electrophoresed. Subsequently, proteins were transferred onto a nitrocellulose membrane and then stained with Ponceau S (Sigma-Aldrich, P7170) to ensure even loading amounts. Membranes were then blocked with a 5% bovine serum albumin (BSA) solution followed by overnight incubation with a diluted primary antibody at 4°C with mild agitation. We

used the following antibodies at a 1:1,000 dilution in 5% BSA solution: pAMPK^{Thr172} (Cell Signaling, 2535S), Ser²⁴⁴⁸-phosphorylated mTOR (Cell Signaling, 2971), mTOR (Cell Signaling, 2972), Ser^{235/236}-phosphorylated S6 (Cell Signaling, 2211), Ser^{240/244}-phosphorylated S6 (Cell Signaling, 2215), S6 (Cell Signaling, 2217), PGC-1 α (EMD Millipore, AB3242), Ser²¹²-phosphorylated ACC (Cell Signaling, 3661S), ACC (Cell Signaling, 3676S), Ser⁵⁵⁵-phosphorylated ULK1 (Cell Signaling, 5869S), ULK1 (Cell Signaling, 8054S), Ser⁷⁰⁰-phosphorylated TBC1D1 (Cell signaling, 6929), TBC1D1 (Cell Signaling, 4629), Histone H3 (Abcam, ab18521) and GAPDH (Thermo Fisher Scientific, PA1-987). On the following day, membranes were washed and incubated with the appropriate horseradish peroxidase linked secondaries (1:10,000, Cell Signaling, 7074S/7076S). Blots were then washed with TBST and visualized with enhanced chemiluminescence on the ChemiDoc MP Imaging System (Bio-Rad Laboratories). Densitometry analysis was performed using Image Lab (Bio-Rad Laboratories). All blots were normalized to the ponceau and standardized to a pooled control on each gel.

Gene expression analysis

TRIzol reagent (Thermo Fisher Scientific, 15596018) was used to homogenize all skeletal muscle samples in Lysing D matrix tubes (MP Biomedicals, 6913-050) with the FastPrep-24 Tissue and Cell Homogenizer (MP Biomedicals). Samples were then mixed with chloroform, shaken vigorously, and then centrifuged at 12,000g as per manufacturer's instruction. The total RNA Omega Bio-Tek kit (VWR International, R6834-02) was used to purify the upper aqueous layer containing RNA. Concentration and purity of the RNA was determined using the NanoDrop 1000 Spectrophotometer (Thermo Fisher Scientific).

RNA samples were diluted and then reverse-transcribed into cDNA using a high-capacity cDNA reverse transcription kit (Thermo Fisher Scientific, 4368814) according to the instructions provided by the manufacturer.

All qPCR assays were run with 2 µg of cDNA in triplicate reactions containing GoTaq qPCR Master Mix (Promega, A6002). Data were analysed using the comparative CT method (72). Ribosomal protein S11 (*Rps11*) was used as the normalizing gene for rodent experiments since it did not differ between all experimental groups (data not shown). qPCR primers (Sigma-Aldrich) used were as follows: *Rps11*: F – CGTGACGAACATGAAGATGC, R – GCACATTGAA TCGCACAGTC; *Pparg1a*: F – AGTGGTGTAGCGACCAAT, R – GGGCAATCCGTCTTCATCCA; *Utrn*: F - CCGGAGCTAAACACCACTGT, R - ATTCAGCTGAGCGAGCATGT; *Gabpa*: F - TTCTTTCAGCAGCATCCTCTCCAC, R - ACAGCCTTCAATAGTCCCGTCCAG; *Etv5*: F - TCAAGCAGGAATACCATGACCC, R - GGCAGTTAGGCACTTCTGAGTC; *Chrna1*: F - TCCCTTCGAYGAGCAGAACT, R - GGGCAGCAGGAGTAGAACAC; *Chrn b*: F - CATCATCGCTCACCCAC, R - ACGGTCCACAACCATGGC; *Chrne*: F - GCTGTGTGGATGCTGTGAAC; R - GCTGCCCAAAAACAGACATT; *Chrng*: F - ACGAAGGCCTGTGGATATTG; R - ACAGAGATGGAGCAGGAGGA; *Ag rn*: F - CCTCAACTTGGACACGAAGCT; R - AGGCCGATGCCACAGA; *Musk*: F - CCACACTGCGTGGAATGAGC; R - CTCTGCAAATGGGCATGGGG; *Lrp4*: F - GGCAAAAAGCAGGAACTTGT; R - TCTACCCAGTGGCCAGAACT; *Rapsn*: F - GTGCCATGGAGTGTTGTGAG; R - CGGTTTCCGATCTCAGTCAT; *Dok7*: F -

GGTACTGGGCTGGAGTC; R - TCGGACGATGCAGTCAAACA; *Fgfbp1*: F -
ACACTCACAGAAAGGTGTCCA; R - CTGAGAACGCCTGAGTAGCC.

Immunolabelling of whole-mount muscles

Immunohistochemical labeling of the pre- and postsynaptic components was performed as previously described (73). In brief, EDL and SOL muscles were carefully dissected in oxygenated Ringer's Solution (110mM NaCl, 5mM KCl, 1 MgCl₂, 25mM NaHCO₃, 2mM CaCl₂, 11mM glucose, 0.3mM glutamic acid, 0.4mM glutamine, 5mM BES (N,N-Bis(2-hydroxyethyl)-2-aminoethanesulfonic acid sodium salt, 0.036mM choline chloride, and 4.34 x 10⁻⁷mM cocarboxylase) and pinned in a Sylgard coated 10 mm Petri dish. Whole muscles were then fixed with 4% PFA for 10 mins at room temperature and then permeabilized in cold methanol at -20°C for 6 mins. Muscles were then incubated with 10% normal donkey serum in PBS containing 0.1% Triton X-100 for 60 mins at room temperature. NFM (1:2,000, Rockland Immunochemicals, 212-901-D84) and SV2 (1:2,000, DSHB, SV2-c) were labeled overnight at 4°C. On the following day, muscles were washed and then incubated with the appropriate fluorescent-conjugated secondary antibodies (1:500, Jackson ImmunoResearch Laboratories, 703-585-155) for 60 mins. AChRs were labeled with Alexa-488-conjugated- α -bungarotoxin (1:500, Invitrogen, B-13422) for 60 mins. All antibody incubations were performed in PBS containing 0.1% Triton X-100 and 2% normal donkey serum at room temperature. Samples were then mounted in Prolong Gold antifade reagent (Invitrogen, P366930). All NMJ images were captured with a 60x Plan Apochromat 1.4 NA oil immersion objective (Nikon Instruments), Nikon C2⁺ confocal microscopy unit (Nikon Instruments), and a Nikon LU-N4 laser system

(Nikon Instruments). For the qualitative analyses, 15-20 ‘en face’ NMJs were imaged and assessed for canonical aging features such as fragmentation, ectopic formation, axonal blebbing, and sprouting axons, as previously described (75, 76).

Immunofluorescence muscle fiber typing

Skeletal muscle fiber types were determined as previously described (74). Briefly, SOL muscles embedded in OCT compound were cut into 10 μm thick sections at -20°C on a cryostat (Leica Biosystems), collected on Superfrost Plus Gold slides (Thermo Fisher Scientific, 22-035813), and stored at -80°C until the day of staining. Slides were blocked with 10% goat serum in 1% BSA for 60 mins at room temperature. Sections were then incubated with a primary antibody cocktail containing 10% goat serum, myosin heavy chain I (MHCI, 1:50, DSHB, BA-F8), MHCIIa (1:600, DSHB, SC-71), MHCIIb (1:100, DSHB, BF-F3) and laminin (1:500, Sigma-Aldrich, L0663) for 120 mins. Following multiple washes with PBS, a secondary antibody cocktail (Alexa Fluor 350 IgG_{2b}, Invitrogen, A-21140; Alexa Fluor 488 IgG₁, Invitrogen, A-21121; Alexa Fluor 555 IgM, Invitrogen, A-21426; 647-conjugated anti-rat, 1:500, Jackson ImmunoResearch, 112-605-167) was applied for 60 mins. After washing, the slides were air dried and mounted with Prolong Gold (Thermo Fisher Scientific, P366930). Immunolabelled muscle sections were captured with a 20x Plan Fluor 0.5 NA objective (Nikon Instruments) and a widefield photometric camera (Accu-Scope). To reveal muscle fiber typing, the entire muscle section was scanned. Muscle fiber type grouping was then classified as a myofiber that was surrounded by neighbouring fibers of the same MHC expression.

Subcellular localization of synaptic proteins

To evaluate the synaptic localization of pAMPK^{Thr172} and PGC-1 α , EDL muscles embedded in OCT compound were cut into 10 μ m thick sections at -20°C. Duplicate muscle sections were collected on a Superfrost Plus Gold slides, and then stored in -80°C. On the day of staining, muscle sections were fixed with 4% PFA for 10 mins at room temperature, washed with PBST, and then blocked with 10% normal goat serum in PBST for 60 mins. Sections were then stained with an antibody cocktail comprised of laminin (1:500, Sigma-Aldrich, L0663) and pAMPK^{Thr172} (1:250, Cell Signaling, 2535S) or laminin (1:500, Sigma-Aldrich, L0663) and PGC-1 α (1:100, EMD Millipore, AB3242). Following multiple washes with PBST, muscle sections were incubated with a secondary antibody cocktail (Alexa Fluor 594 anti rabbit, 1:500, Invitrogen, A-11037; 647-conjugated anti-rat, 1:500, Jackson ImmunoResearch, 112-605-167). After washing, Alexa-488-conjugated- α -bungarotoxin (1:500, Invitrogen, B-13422) was applied for 60 mins at room temperature to reveal AChRs. DAPI (1:10,000, Invitrogen, D9542) was then applied to the muscle sections. Slides were then air dried and mounted with Prolong Gold (Thermo Fisher Scientific, P366930).

To appropriately assess the localization of pAMPK^{Thr172} and PGC-1 α at the NMJ and in fundamental nuclei, prepared samples were imaged under a 60x oil objective (Nikon Instruments) and a Z-stack image was generated for each synapse. Within a Z-stack image, a single slice was selected to represent a NMJ and its surrounding subsynaptic nuclei. A series of thresholding was then applied to create a mask to represent the synaptic regions, all nuclei, and subsynaptic myonuclei. Following this, processed images were then screened by a blinded investigator to exclude non-synaptic nuclei. Mean intensity of the

protein of interest was determined in the synaptic region, as well as within fundamental myonuclei.

AChR clustering experiment

Commercially available C2C12 cells (American Tissue Culture Collection, CRL-1772: lot# 70044015) were seeded and grown on a 0.1% gelatin 6-well plates with growth media (10% FBS, Invitrogen, 12483020; DMEM, Invitrogen, 11995065). Following confluence, cells were differentiated with media comprised of 98% DMEM and 2% Horse Serum (Invitrogen, 16050122). Following 4 days of differentiation, myotubes were incubated for 24 hrs with or without MK (2.5-10 μ g/ml, Merck), recombinant Agr protein (0.4 μ g/ml, R&D Systems, 6624-AG-050), or Wnt protein (10 ng/ml, R&D systems, catalog no. 6179-WN/CF). Cells were then collected for Western blotting and AChR clustering analyses.

C2C12 cells cultured for AChR clustering experiments were differentiated on coverslips. Following MK, Agr, or Wnt treatment, myotubes were washed twice with PBS and fixed with 4% PFA for 10 mins. Cells were then washed in PBS, immersed in 0.25% Triton-X for 5 mins, then blocked with 10% normal goat serum. Next, cells were incubated in embryonic myosin heavy chain (eMHC, 1:250, DHSB, BF-G6) for 120 mins, washed in PBS and then incubated with Alexa 594 anti-mouse (1:500, Invitrogen, A11005). After washing, 488-conjugated α BTX (1:500, Invitrogen, B-13422) was applied for 60 mins. Coverslips were then washed with PBS, air dried, and then mounted on slides with Prolong Gold (Thermo Fisher Scientific, P366930). Immunolabelled myotube images were captured with a 20x Plan Fluor 0.5 NA objective (Nikon Instruments). To quantify AChR

clusters, a minimum of four regions of interest were imaged from each coverslip. To calculate the area of positive stained AChRs, a binary threshold was applied by a blinded investigator. The resultant thresholding layer was used to calculate the number of total AChR clusters (objects with a min ferret diameter greater than 4 μ M).

MetaMEx analysis

The study utilized the publicly accessible Meta-analyses program, MetaMEx (version 3.2208, <https://metamex.eu/>), to investigate exercise-induced effects on NMJ gene expression in human skeletal muscle (43). We excluded data from participants with metabolic, neurological, or cardiovascular diseases. To examine the exercise timecourse response on NMJ-related genes, we searched for *CHRNA1*, *CHRNA2*, *CHRNE*, *CHRNA3*, *AGRN*, *LRP4*, *MUSK*, *RAPSN*, *DOK7*, *PPARGC1A*, *GABPA*, *ETV5*, and *UTRN*. Gene logFC (Ex vs. control) and significance values for each transcript were extracted and presented as a heat map.

Statistical analysis

One-way ANOVA and Tukey post-hoc tests were conducted to examine age-related differences among WT animals. Two-way ANOVA and Tukey post-hoc tests were employed to investigate statistical differences between genotypes. Unpaired t-tests were utilized to compare the means between the 12 mo mKO and 22 mo WT groups. One-way ANOVA and Tukey post-hoc tests were conducted to interrogate effects of MK and exercise among WT animals, as well as to examine the effects of MK in cultured myotubes. Statistical analyses for MetaMEx-related data are previously described (<https://metamex.eu/>).

References and Notes:

1. Mounier,R., Théret,M., Lantier,L., Foretz,M. and Viollet,B. (2015) Expanding roles for AMPK in skeletal muscle plasticity. *Trends Endocrinol. Metab.*, **26**, 275–286.
2. Steinberg,G.R. and Hardie,D.G. (2022) New insights into activation and function of the AMPK. *Nat. Rev. Mol. Cell Biol.* 2022 244, **24**, 255–272.
3. Kjøbsted,R., Hingst,J.R., Fentz,J., Foretz,M., Sanz,M.-N., Pehmøller,C., Shum,M., Marette,A., Mounier,R., Treebak,J.T., *et al.* (2018) AMPK in skeletal muscle function and metabolism. *FASEB J.*, **32**, 1741–1777.
4. Thomas,M.M., Wang,D.C., D’Souza,D.M., Krause,M.P., Layne,A.S., Criswell,D.S., O’Neill,H.M., Connor,M.K., Anderson,J.E., Kemp,B.E., *et al.* (2014) Muscle-specific AMPK β 1 β 2-null mice display a myopathy due to loss of capillary density in nonpostural muscles. *FASEB J.*, **28**, 2098–2107.
5. Bujak,A.L., E Blümer,R.M., Marcinko,K., Fullerton,M.D., Kemp,B.E. and Steinberg,G.R. (2014) Reduced skeletal muscle AMPK and mitochondrial markers do not promote age-induced insulin resistance. *J Appl Physiol*, **117**, 171–179.
6. Bujak,A.L., Crane,J.D., Lally,J.S., Ford,R.J., Kang,S.J., Rebalka,I.A., Green,A.E., Kemp,B.E., Hawke,T.J., Schertzer,J.D., *et al.* (2015) AMPK activation of muscle autophagy prevents fasting-induced hypoglycemia and myopathy during aging. *Cell Metab.*, **21**, 883–890.
7. O’Neill,H.M., Maarbjerg,S.J., Crane,J.D., Jeppesen,J., Jorgensen,S.B., Schertzer,J.D., Shyroka,O., Kiens,B., van Denderen,B.J., Tarnopolsky,M.A., *et al.* (2011) AMP-activated protein kinase (AMPK) 1 2 muscle null mice reveal an essential role for AMPK in maintaining mitochondrial content and glucose uptake during exercise. *Proc. Natl. Acad. Sci.*, **108**, 16092–16097.
8. Röckl,K.S.C., Hirshman,M.F., Brandauer,J., Fujii,N., Witters,L.A. and Goodyear,L.J. (2007) Skeletal muscle adaptation to exercise training: AMP-activated protein kinase mediates muscle fiber type shift. *Diabetes*, **56**, 2062–2069.
9. Garcia-Roves,P.M., Osler,M.E., Holmström,M.H. and Zierath,J.R. (2008) Gain-of-function R225Q mutation in AMP-activated protein kinase gamma3 subunit increases mitochondrial biogenesis in glycolytic skeletal muscle. *J. Biol. Chem.*, **283**, 35724–34.
10. Kjøbsted,R., Hingst,J.R., Fentz,J., Foretz,M., Sanz,M.N., Pehmøller,C., Shum,M., Marette,A., Mounier,R., Treebak,J.T., *et al.* (2018) AMPK in skeletal muscle function and metabolism. *FASEB J.*, **32**, 1741–1777.
11. Steinberg,G.R. and Carling,D. (2019) AMP-activated protein kinase: the current landscape for drug development. *Nat. Rev. Drug Discov.*, 10.1038/s41573-019-0019-2.
12. Li,L., Xiong,W.-C. and Mei,L. (2018) Neuromuscular Junction Formation, Aging, and Disorders. *Annu. Rev. Physiol.*, **80**, 159–188.

13. Tintignac,L.A., Brenner,H.R. and Rüegg,M.A. (2015) Mechanisms regulating neuromuscular junction development and function and causes of muscle wasting. *Physiol. Rev.*, **95**, 809–852.
14. Taetzsch,T. and Valdez,G. (2018) NMJ maintenance and repair in aging. *Curr. Opin. Physiol.*, **4**, 57–64.
15. Rudolf,R., Khan,M.M., Labeit,S. and Deschenes,M.R. (2014) Degeneration of neuromuscular junction in age and dystrophy. *Front. Aging Neurosci.*, **6**, 99.
16. Ng,S.Y. and Ljubicic,V. (2020) Recent insights into neuromuscular junction biology in Duchenne muscular dystrophy: Impacts, challenges, and opportunities. *EBioMedicine*, **61**, 103032.
17. Darabid,H., Perez-Gonzalez,A.P. and Robitaille,R. (2014) Neuromuscular synaptogenesis: coordinating partners with multiple functions. *Nat. Publ. Gr.*, **15**, 703.
18. Dial,A.G., Ng,S.Y., Manta,A. and Ljubicic,V. (2018) The Role of AMPK in Neuromuscular Biology and Disease. *Trends Endocrinol. Metab.*, **29**, 300–312.
19. Samuel,M.A., Emanuela Voinescu,P., Lilley,B.N., de Cabo,R., Foretz,M., Viollet,B., Pawlyk,B., Sandberg,M.A., Vavvas,D.G. and Sanes,J.R. (2014) LKB1 and AMPK regulate synaptic remodeling in old age. *Nat. Publ. Gr.*, **17**.
20. Baraldo,M., Geremia,A., Pirazzini,M., Nogara,L., Solagna,F., Türk,C., Nolte,H., Romanello,V., Megighian,A., Boncompagni,S., *et al.* (2020) Skeletal muscle mTORC1 regulates neuromuscular junction stability. *J. Cachexia. Sarcopenia Muscle*, **11**, 208–225.
21. Handschin,C., Kobayashi,Y.M., Chin,S., Seale,P., Campbell,K.P. and Spiegelman,B.M. (2007) PGC-1 α regulates the neuromuscular junction program and ameliorates Duchenne muscular dystrophy. *Genes Dev.*, **21**, 770–783.
22. Ham,D.J., Börsch,A., Lin,S., Thürkauf,M., Weihrauch,M., Reinhard,J.R., Delezie,J., Battilana,F., Wang,X., Kaiser,M.S., *et al.* (2020) The neuromuscular junction is a focal point of mTORC1 signaling in sarcopenia. *Nat. Commun.*, **11**, 1–21.
23. Castets,P., Rion,N., Théodore,M., Falcetta,D., Lin,S., Reischl,M., Wild,F., Guérard,L., Eickhorst,C., Brockhoff,M., *et al.* (2019) mTORC1 and PKB/Akt control the muscle response to denervation by regulating autophagy and HDAC4. *Nat. Commun.*, **10**, 1–16.
24. Mills,R., Taylor-Weiner,H., Correia,J.C., Agudelo,L.Z., Allodi,I., Kolonelou,C., Martinez-Redondo,V., Ferreira,D.M.S., Nichterwitz,S., Comley,L.H., *et al.* (2018) Neurturin is a PGC-1 α 1-controlled myokine that promotes motor neuron recruitment and neuromuscular junction formation. *Mol. Metab.*, **7**, 12–22.
25. Castets,P., Ham,D.J. and Rüegg,M.A. (2020) The TOR Pathway at the Neuromuscular Junction: More Than a Metabolic Player? *Front. Mol. Neurosci.*, **13**, 162.
26. Valdez,G., Tapia,J.C., Kang,H., Clemenson,G.D., Gage,F.H., Lichtman,J.W. and

- Sanes, J.R. (2010) Attenuation of age-related changes in mouse neuromuscular synapses by caloric restriction and exercise. *Proc. Natl. Acad. Sci. U. S. A.*, **107**, 14863–14868.
27. Stockinger, J., Maxwell, N., Shapiro, D., DeCabo, R. and Valdez, G. (2017) Caloric Restriction Mimetics Slow Aging of Neuromuscular Synapses and Muscle Fibers. *J. Gerontol. A. Biol. Sci. Med. Sci.*, **73**, 21–28.
28. Andonian, M.H. and Fahim, M.A. (1988) Endurance exercise alters the morphology of fast- and slow-twitch rat neuromuscular junctions. *Int. J. Sports Med.*, **9**, 218–223.
29. Coughlan, K.S., Mitchem, M.R., Hogg, M.C. and Prehn, J.H.M. (2015) ‘Preconditioning’ with latrepirdine, an adenosine 5’-monophosphate-activated protein kinase activator, delays amyotrophic lateral sclerosis progression in SOD1G93A mice. *Neurobiol. Aging*, **36**, 1140–1150.
30. Mancuso, R., del Valle, J., Modol, L., Martinez, A., Granado-Serrano, A.B., Ramirez-Núñez, O., Pallás, M., Portero-Otin, M., Osta, R. and Navarro, X. (2014) Resveratrol Improves Motoneuron Function and Extends Survival in SOD1G93A ALS Mice. *Neurotherapeutics*, **11**, 419–432.
31. Cerveró, C., Montull, N., Tarabal, O., Piedrafita, L., Esquerda, J.E. and Calderó, J. (2016) Chronic Treatment with the AMPK Agonist AICAR Prevents Skeletal Muscle Pathology but Fails to Improve Clinical Outcome in a Mouse Model of Severe Spinal Muscular Atrophy. *Neurotherapeutics*, **13**, 198–216.
32. Salminen, A., Kaarniranta, K. and Kauppinen, A. (2016) Age-related changes in AMPK activation: Role for AMPK phosphatases and inhibitory phosphorylation by upstream signaling pathways. *Ageing Res. Rev.*, **28**, 15–26.
33. Arnold, A.S., Gill, J., Christie, M., Ruiz, R., McGuirk, S., St-Pierre, J., Tabares, L. and Handschin, C. (2014) Morphological and functional remodelling of the neuromuscular junction by skeletal muscle PGC-1 α . *Nat. Commun.*, **5**.
34. Mills, R., Taylor-Weiner, H., Correia, J.C., Agudelo, L.Z., Allodi, I., Kolonelou, C., Martinez-Redondo, V., Ferreira, D.M.S., Nichterwitz, S., Comley, L.H., *et al.* (2018) Neurturin is a PGC-1 α 1-controlled myokine that promotes motor neuron recruitment and neuromuscular junction formation. *Mol. Metab.*, **7**, 12–22.
35. Schmitt, D.L., Curtis, S.D., Lyons, A.C., Zhang, J., Chen, M., He, C.Y., Mehta, S., Shaw, R.J. and Zhang, J. (2022) Spatial regulation of AMPK signaling revealed by a sensitive kinase activity reporter. *Nat. Commun.* 2022 131, **13**, 1–12.
36. Trefts, E. and Shaw, R.J. (2021) AMPK: restoring metabolic homeostasis over space and time. *Mol. Cell*, **81**, 3677–3690.
37. Kodiha, M., Ho-Wo-Cheong, D. and Stochaj, U. (2011) Pharmacological AMP-kinase activators have compartment-specific effects on cell physiology. *Am. J. Physiol. - Cell Physiol.*, **301**, 1307–1315.
38. Belotti, E. and Schaeffer, L. (2020) Regulation of Gene expression at the

- neuromuscular Junction. *Neurosci. Lett.*, **735**, 135163.
39. Osseni,A., Ravel-Chapuis,A., Thomas,J.-L., Gache,V., Schaeffer,L. and Jasmin,B.J. (2020) HDAC6 regulates microtubule stability and clustering of AChRs at neuromuscular junctions. *J. Cell Biol.*, **219**.
 40. Shapiro,D., Massopust,R., Taetzsch,T. and Valdez,G. (2022) Argonaute 2 is lost from neuromuscular junctions affected with amyotrophic lateral sclerosis in SOD1G93A mice. *Sci. Reports 2022 121*, **12**, 1–14.
 41. Ng,S.Y., Mikhail,A.I., Mattina,S.R., Manta,A., Diffey,I.J. and Ljubicic,V. (2023) Acute, next-generation AMPK activation initiates a disease-resistant gene expression program in dystrophic skeletal muscle. *FASEB J*, **37**, e22863.
 42. Egan,B. and Zierath,J.R. (2013) Exercise metabolism and the molecular regulation of skeletal muscle adaptation. *Cell Metab.*, **17**, 162–184.
 43. Pillon,N.J., Gabriel,B.M., Dollet,L., Smith,J.A.B., Sardón Puig,L., Botella,J., Bishop,D.J., Krook,A. and Zierath,J.R. (2020) Transcriptomic profiling of skeletal muscle adaptations to exercise and inactivity. *Nat. Commun. 2020 111*, **11**, 1–15.
 44. Carnio,S., LoVerso,F., Baraibar,M.A., Longa,E., Khan,M.M., Maffei,M., Reischl,M., Canepari,M., Loeffler,S., Kern,H., *et al.* (2014) Autophagy Impairment in Muscle Induces Neuromuscular Junction Degeneration and Precocious Aging. *Cell Rep.*, **8**, 1509–1521.
 45. Gonzalez-Freire,M., de Cabo,R., Studenski,S.A. and Ferrucci,L. (2014) The neuromuscular junction: Aging at the crossroad between nerves and muscle. *Front. Aging Neurosci.*, **6**, 208.
 46. Aare,S., Spendiff,S., Vuda,M., Elkrief,D., Perez,A., Wu,Q., Mayaki,D., Hussain,S.N.A., Hettwer,S. and Hepple,R.T. (2016) Failed reinnervation in aging skeletal muscle. *Skelet. Muscle*, **6**, 1–13.
 47. Dial,A.G., Rooprai,P., Lally,J.S., Bujak,A.L., Steinberg,G.R. and Ljubicic,V. (2018) The role of AMP-activated protein kinase in the expression of the dystrophin-associated protein complex in skeletal muscle. *FASEB J.*, **32**, 2950–2965.
 48. Mounier,R., Théret,M., Arnold,L., Cuvellier,S., Bultot,L., Göransson,O., Sanz,N., Ferry,A., Sakamoto,K., Foretz,M., *et al.* (2013) AMPK α 1 regulates macrophage skewing at the time of resolution of inflammation during skeletal muscle regeneration. *Cell Metab.*, **18**, 251–264.
 49. Baraldo,M., Geremia,A., Pirazzini,M., Nogara,L., Solagna,F., Türk,C., Nolte,H., Romanello,V., Megighian,A., Boncompagni,S., *et al.* (2020) Skeletal muscle mTORC1 regulates neuromuscular junction stability. *J. Cachexia. Sarcopenia Muscle*, **11**, 208–225.
 50. Aare,S., Spendiff,S., Vuda,M., Elkrief,D., Perez,A., Wu,Q., Mayaki,D., Hussain,S.N.A., Hettwer,S. and Hepple,R.T. (2016) Failed reinnervation in aging skeletal muscle. *Skelet. Muscle*, **6**.

51. Thomas,M.M., Wang,D.C., D’Souza,D.M., Krause,M.P., Layne,A.S., Criswell,D.S., O’Neill,H.M., Connor,M.K., Anderson,J.E., Kemp,B.E., *et al.* (2014) Muscle-specific AMPK β 1 β 2-null mice display a myopathy due to loss of capillary density in nonpostural muscles. *FASEB J.*, **28**, 2098–2107.
52. Hepple,R.T. and Rice,C.L. (2016) Innervation and neuromuscular control in ageing skeletal muscle. *J. Physiol.*, **594**, 1965–1978.
53. Mateos-Aierdi,A.J., Goicoechea,M., Aiastui,A., Torrón,R.F., Garcia-Puga,M., Matheu,A. and de Munain,A.L. (2015) Muscle wasting in myotonic dystrophies: A model of premature aging. *Front. Aging Neurosci.*, **7**, 125.
54. Stangl,M.K., Böcker,W., Chubanov,V., Ferrari,U., Fischereder,M., Gudermann,T., Hesse,E., Meinke,P., Reincke,M., Reisch,N., *et al.* (2019) Sarcopenia - Endocrinological and Neurological Aspects. *Exp. Clin. Endocrinol. Diabetes*, **127**, 8–22.
55. Mikhail,A.I., Ng,S.Y., Mattina,S.R. and Ljubicic,V. (2023) AMPK is mitochondrial medicine for neuromuscular disorders. *Trends Mol. Med.*, **In press**.
56. Muise,E.S., Guan,H.-P., Liu,J., Nawrocki,A.R., Yang,X., Wang,C., Rodríguez,C.G., Zhou,D., Gorski,J.N., Kurtz,M.M., *et al.* (2019) Pharmacological AMPK activation induces transcriptional responses congruent to exercise in skeletal and cardiac muscle, adipose tissues and liver. *PLoS One*, **14**, e0211568.
57. Jäger,S.S., Handschin,C.C., St-Pierre,J.J. and Spiegelman,B.M.B.M. (2007) AMP-activated protein kinase (AMPK) action in skeletal muscle via direct phosphorylation of PGC-1alpha. *Pnas*, **104**, 12017–12022.
58. Little,J.P., Safdar,A., Cermak,N., Tarnopolsky,M.A. and Gibala,M.J. (2010) Acute endurance exercise increases the nuclear abundance of PGC-1alpha in trained human skeletal muscle. *Am. J. Physiol. Regul. Integr. Comp. Physiol.*, **298**, R912-7.
59. Dong,X., Hui,T., Chen,J., Yu,Z., Ren,D., Zou,S., Wang,S., Fei,E., Jiao,H. and Lai,X. (2021) Metformin Increases Sarcolemma Integrity and Ameliorates Neuromuscular Deficits in a Murine Model of Duchenne Muscular Dystrophy. *Front. Physiol.*, **0**, 606.
60. Myers,R.W., Guan,H.-P., Ehrhart,J., Petrov,A., Prahallada,S., Tozzo,E., Yang,X., Kurtz,M.M., Trujillo,M., Gonzalez Trotter,D., *et al.* (2017) Systemic pan-AMPK activator MK-8722 improves glucose homeostasis but induces cardiac hypertrophy. *Science*, **357**, 507–511.
61. Feng,D., Biftu,T., Romero,F.A., Kekec,A., Dropinski,J., Kassick,A., Xu,S., Kurtz,M.M., Gollapudi,A., Shao,Q., *et al.* (2017) Discovery of MK-8722: A Systemic, Direct Pan-Activator of AMP-Activated Protein Kinase. 10.1021/acsmchemlett.7b00417.
62. Boehm,I., Alhindi,A., Leite,A.S., Logie,C., Gibbs,A., Murray,O., Farrukh,R., Pirie,R., Proudfoot,C., Clutton,R., *et al.* (2020) Comparative anatomy of the mammalian neuromuscular junction. *J. Anat.*, **237**, 827–836.

63. Popov,D. V., Lysenko,E.A., Vepkhvadze,T.F., Kurochkina,N.S., Maknovskii,P.A. and Vinogradova,O.L. (2015) Promoter-specific regulation of PPARGC1A gene expression in human skeletal muscle. *J. Mol. Endocrinol.*, **55**, 159–168.
64. Hoffman,N.J., Parker,B.L., Chaudhuri,R., Fisher-Wellman,K.H., Kleinert,M., Humphrey,S.J., Yang,P., Holliday,M., Trefely,S., Fazakerley,D.J., *et al.* (2015) Global Phosphoproteomic Analysis of Human Skeletal Muscle Reveals a Network of Exercise-Regulated Kinases and AMPK Substrates. *Cell Metab.*, **22**, 922–935.
65. Ueta,R., Sugita,S., Minegishi,Y., Shimotoyodome,A., Ota,N., Ogiso,N., Eguchi,T. and Yamanashi,Y. (2020) DOK7 Gene Therapy Enhances Neuromuscular Junction Innervation and Motor Function in Aged Mice. *iScience*, **23**.
66. Oury,J., Zhang,W., Leloup,N., Koide,A., Corrado,A.D., Ketavarapu,G., Hattori,T., Koide,S. and Burden,S.J. (2021) Mechanism of disease and therapeutic rescue of Dok7 congenital myasthenia. *Nat. 2021 5957867*, **595**, 404–408.
67. Arimura,S., Okada,T., Tezuka,T., Chiyo,T., Kasahara,Y., Yoshimura,T., Motomura,M., Yoshida,N., Beeson,D., Takeda,S., *et al.* (2014) DOK7 gene therapy benefits mouse models of diseases characterized by defects in the neuromuscular junction. *Science (80-.)*, **345**, 1505–1508.
68. Kaifer,K.A., Villalón,E., Smith,C.E., Simon,M.E., Marquez,J., Hopkins,A.E., Morcos,T.I. and Lorson,C.L. (2020) AAV9-DOK7 gene therapy reduces disease severity in Smn2B⁻ SMA model mice. *Biochem. Biophys. Res. Commun.*, **530**, 107–114.
69. Trajanovska,S., Ban,J., Huang,J., Gregorevic,P., Morsch,M., Allen,D.G. and Phillips,W.D. (2019) Muscle specific kinase protects dystrophic mdx mouse muscles from eccentric contraction-induced loss of force-producing capacity. *J. Physiol.*, **597**, 4831–4850.
70. vanLieshout,T.L., Stouth,D.W., Tajik,T. and Ljubicic,V. (2017) Exercise-induced Protein Arginine Methyltransferase Expression in Skeletal Muscle.
71. Dimauro,I., Pearson,T., Caporossi,D. and Jackson,M.J. (2012) A simple protocol for the subcellular fractionation of skeletal muscle cells and tissue. *BMC Res. Notes*, **5**, 1–5.
72. Schmittgen,T.D. and Livak,K.J. (2008) Analyzing real-time PCR data by the comparative CT method. *Nat. Protoc.*, **3**, 1101–1108.
73. vanLieshout,T.L., Stouth,D.W., Hartel,N.G., Vasam,G., Ng,S.Y., Webb,E.K., Rebalka,I.A., Mikhail,A.I., Graham,N.A., Menzies,K.J., *et al.* (2022) The CARM1 transcriptome and arginine methylproteome mediate skeletal muscle integrative biology. *Mol. Metab.*, **64**, 101555.
74. Bloemberg,D. and Quadriatero,J. (2012) Rapid determination of myosin heavy chain expression in rat, mouse, and human skeletal muscle using multicolor immunofluorescence analysis. *PLoS One*, **7**.

75. Arbour,D., Tremblay,E., Martineau,E., Julien,J.-P. and Robitaille,R. (2015) Early and Persistent Abnormal Decoding by Glial Cells at the Neuromuscular Junction in an ALS Model. *J. Neurosci.*, **35**, 688–706.
76. Tremblay,E., Martineau,É. and Robitaille,R. (2017) Opposite synaptic alterations at the neuromuscular junction in an ALS mouse model: When motor units matter. *J. Neurosci.*, **37**, 8901–8918.

Acknowledgments:

The authors thank Dr. Richard Robitaille and Joanne Vallée for their technical assistance on muscle dissections and NMJ immunolabeling. We would also like to thank Linda May for her expertise in cell culture. We also extend our appreciation to Todd Prior and the rest of the Integrative Neuromuscular Biology Laboratory and the Exercise Metabolism Research Group.

Funding:

Canadian Institutes of Health Research (CIHR) Project Grant #408289 (VL)
Muscular Dystrophy Canada Translational Seed Science Grant #681362 (VL)
CIHR Tier 2 Canada Research Chair Grant #232338 (VL)
Ontario Ministry of Economic Development, Job Creation and Trade Early Researcher Grant #ER17-13-087 (VL)
CIHR Fellowship (CL)
CIHR Vanier Scholarship (EMD)
Natural Sciences and Engineering Research Council of Canada Scholarship (SYN, SRM)
Ontario Graduate Scholarship (AIM)

Figures:

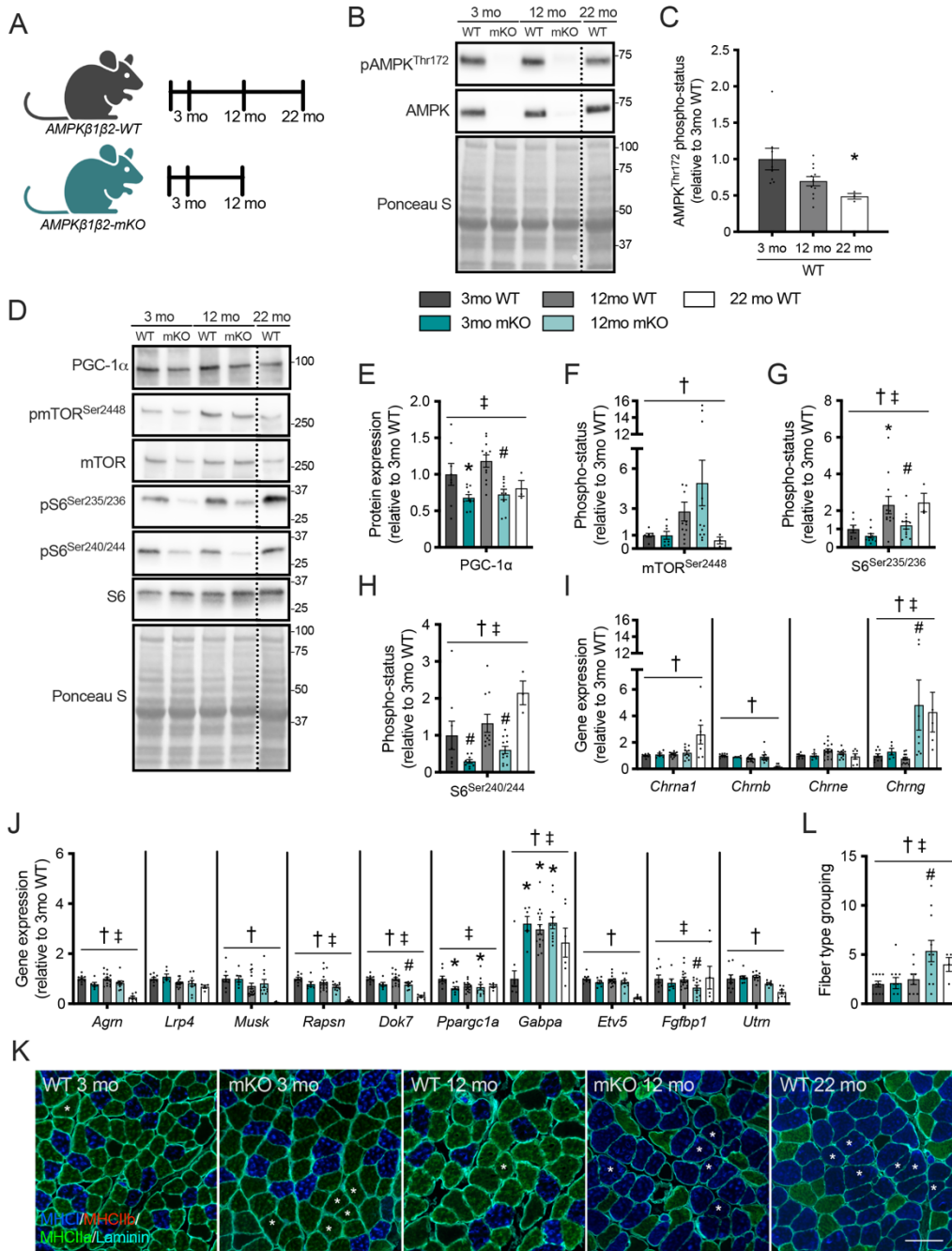


Fig. 1. AMP-activated protein kinase (AMPK) β 1 β 2 skeletal muscle-specific knockout (mKO) mice exhibit perturbed downstream signaling and characteristics of a prematurely aged neuromuscular junction (NMJ) gene expression profile. (A) 3-, 12-, and 22-month (mo)-old wild-type (WT) animals and 3- and 12 mo mKO mice were examined. (B) Representative Western blots of threonine¹⁷²-phosphorylated AMPK (pAMPK^{Thr172}) and AMPK protein in the tibialis anterior (TA) muscles of 3- and 12 mo WT and mKO animals and 22 mo WT mice. Ponceau S staining is shown below to indicate loading between samples. Protein ladder markers at right of blots are expressed as kDa. (C) Graphical summary of AMPK phospho-status

(i.e., the phosphorylated form of the protein relative to its total amount within the same sample) in 3-, 12-, and 22 mo WT animals. **(D)** Representative Western blots of peroxisome proliferator-activated receptor γ coactivator-1 α (PGC-1 α), Ser²⁴⁴⁸-phosphorylated mammalian target of rapamycin (pmTOR^{Ser2448}), mTOR, Ser^{235/236}-phosphorylated S6 (pS6^{Ser235/236}), Ser^{240/244}-phosphorylated S6 (pS6^{Ser240/244}), and S6 protein, in the TA muscles of 3- and 12 mo WT and mKO animals and 22 mo WT mice. Graphical summaries of PGC-1 α **(E)**, as well as mTOR **(F)** and S6 **(G, H)** phospho-status in TA muscles of all experimental groups. **(I)** Graphical summaries of acetylcholine receptor (AChR) subunit α (*Chrn1*), β (*Chrn2*), ϵ (*Chrne*), and γ (*Chrng*) transcript levels in TA muscles. **(J)** Summaries of NMJ-related gene expression, including agrin (*Agri*), low-density lipoprotein receptor-related protein 4 (*Lrp4*), muscle-specific kinase (*Musk*), 43 kDa receptor-associated protein of the synapse (*Rapsn*), docking protein 7 (*Dok7*), PGC-1 α (*Ppargc1a*), GABA-binding protein α (*Gabpa*), ETS variant transcription factor 5 (*Etv5*), fibroblast growth factor binding protein 1 (*Fgfbp1*), and utrophin (*Utrn*) in TA muscles. All protein and mRNA data are shown relative to the 3 mo WT group. **(K)** Representative immunofluorescence (IF) images of myosin heavy chain (MHC) expression in soleus (SOL) muscles. MHC I, MHC IIa, and MHC IIb, are shown in blue, green and red, respectively, while laminin (cyan) demarks the sarcolemma. Asterisks indicate myofiber type grouping (i.e., a muscle fiber surrounded by neighboring fibers with the same fiber type). The scale bar represents 100 μ M. **(L)** Graphical summary of myofiber type grouping in SOL muscles of mice in all experimental groups. All graphical summaries display individual data points and group means (bars) with standard error of the means (SEM). n = 8 animals per group whereas n = 3 - 4 animals in the 22 mo WT group. *, P < 0.05 vs. 3 mo WT; #, P < 0.05 vs. 12 mo WT; †, P < 0.05 main effect of age; ‡, P < 0.05 main effect of genotype.

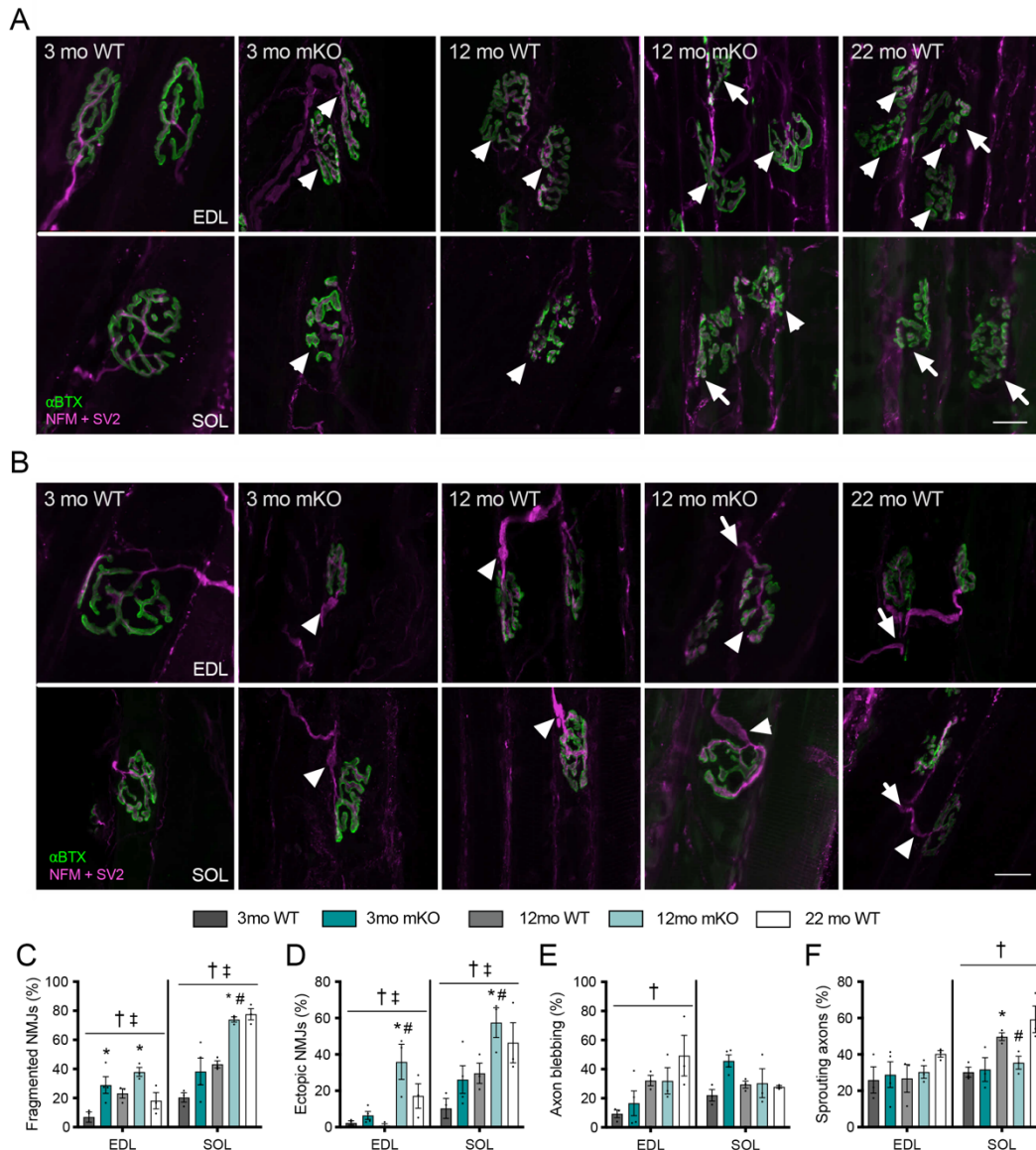


Fig. 2. AMPK regulates NMJ morphology during aging. (A, B) Typical confocal IF images of NMJs in extensor digitorum longus (EDL) and SOL muscles of 3-, 12-, and 22 mo WT animals, as well as 3- and 12 mo mKO mice. Magenta neurofilament M (NFM) and synaptic vesicle 2 (SV2) stains denote NMJ presynaptic architecture, while green α -bungarotoxin (α BTX) marks the postsynaptic compartment. Scale bars represent 20 μ m. The top panels (A) demonstrate abnormal postsynaptic characteristics in EDL and SOL muscles, where the arrows and arrowheads indicate ectopic and fragmented NMJs, respectively. The bottom rows (B) show presynaptic axon sprouting and blebbing as depicted by arrows and arrowheads, respectively. Graphical summaries of the percentage of fragmented (C), and ectopic NMJs (D), as well as axonal blebbing (E) and sprouting (F) in EDL and SOL muscles from WT and mKO mice. The dotted line in the graphical summaries represent the mean value of the 22 mo WT group. All graphical summaries display individual data points and group means (bars) with SEM. $n = 3 - 4$ animals per group. †, $P < 0.05$ main effect of age; ‡, $P < 0.05$ main effect of genotype; *, $P < 0.05$ vs. 3 mo WT; #, $P < 0.05$ vs. mKO 3 mo.

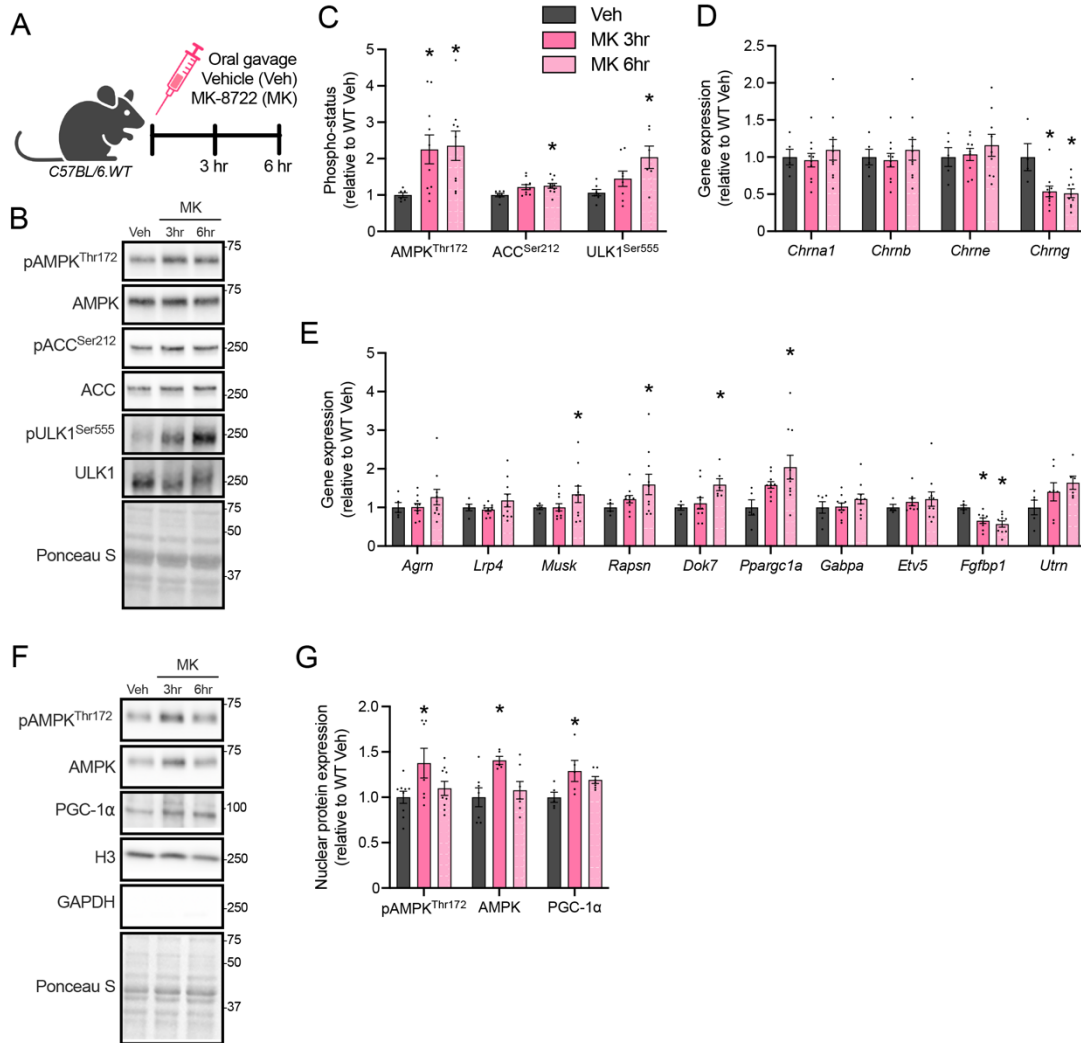


Fig. 3. Targeted pharmacological AMPK stimulation elicits synaptic gene expression. (A) 2 mo WT animals were orally gavaged a single dose of vehicle (Veh) or MK-8722 (MK; 10 mpk). Veh-treated mice were euthanized 3 hours post-gavage, whereas MK-treated animals were euthanized 3 hours (MK 3hr), or 6 hours (MK 6hr) post-administration. (B) Representative Western blots of pAMPK^{Thr172}, AMPK, Ser²¹²-phosphorylated acetyl-CoA carboxylase (pACC^{Ser212}), ACC, Ser⁵⁵⁵-phosphorylated unc-51-like autophagy activating kinase (pULK1^{Ser555}), and ULK1 in triceps (TRI) muscles of Veh- or MK-treated animals. Ponceau S staining is shown below to indicate equal loading between samples. Protein ladder markers at right are expressed as kDa. (C) Graphical summaries of AMPK, ACC, and ULK1 phospho-status. (D) Summaries of *Chrna1*, *Chrn b*, *Chrne*, and *Chrng* transcript levels in TRI muscles from Veh- or MK-treated mice. (E) Graphical summaries of NMJ-related genes including *Agrp*, *Lrp4*, *Musk*, *Rapsn*, *Dok7*, *Ppargc1a*, *Gabpa*, *Etv5*, *Fgfbp1* and *Utrn* in TRI muscle from the three experimental groups. (F) Representative Western blots of nuclear pAMPK^{Thr172}, AMPK, PGC-1α, as well as histone H3 (H3) and glyceraldehyde 3-phosphate dehydrogenase (GAPDH), from the gastrocnemius muscles of Veh- or MK-treated animals. (G) Graphical summaries of myonuclear pAMPK^{Thr172}, AMPK, and PGC-1α protein content. Protein and mRNA data are expressed relative to the WT Veh group. All graphical summaries display individual data points and group means (bars) with SEM. n = 6 - 8 animals per group. *, P < 0.05 vs. WT Veh.

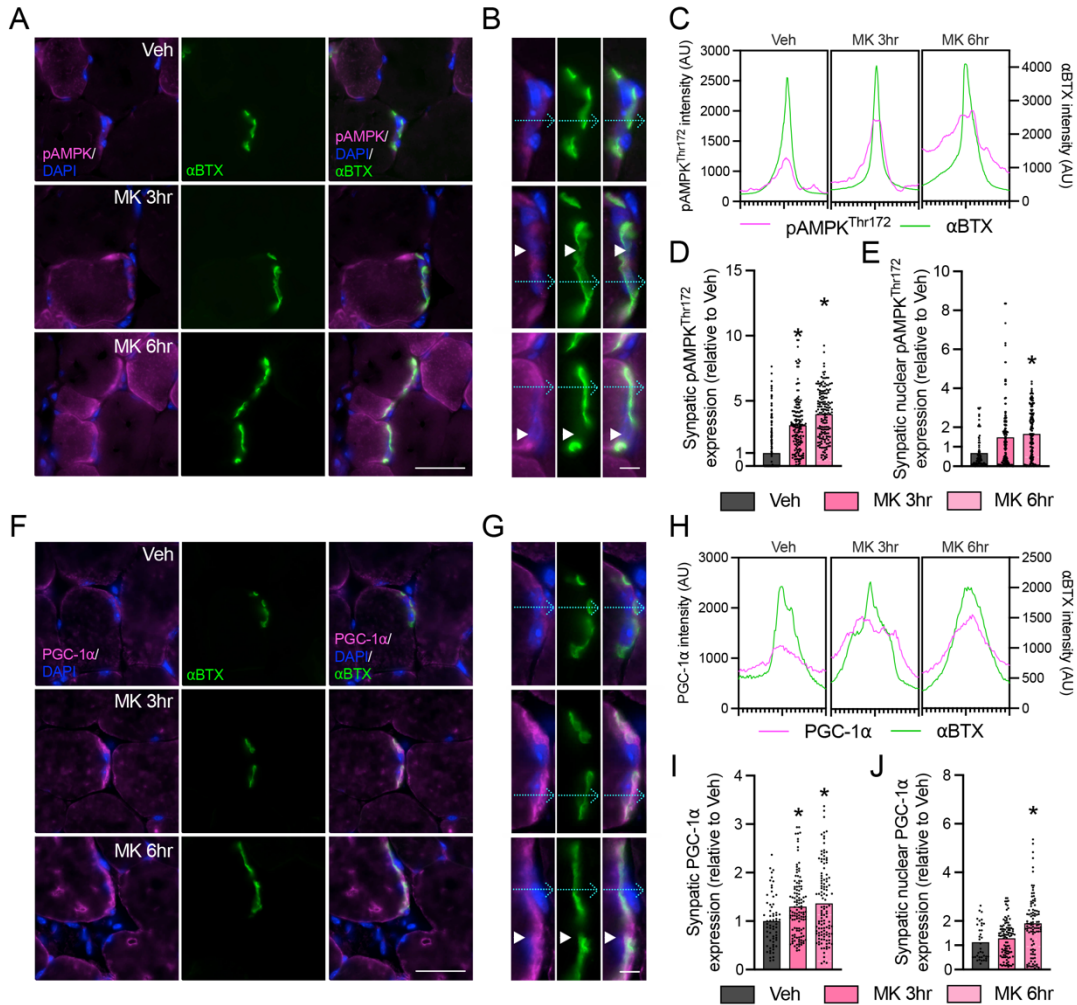


Fig. 4. AMPK activation promotes accumulation of pAMPK^{Thr172} and PGC-1α at the NMJ and in fundamental myonuclei. (A) Typical IF images of pAMPK^{Thr172} (magenta), αBTX (green), and 4',6-diamidino-2-phenylindole (DAPI; blue) in EDL muscles of Veh, MK 3hr, and MK 6hr groups. αBTX and DAPI denote the postsynaptic region and myonuclei, respectively. (B) Magnified images of each synapse in (A) demonstrate the overlay of pAMPK^{Thr172} with αBTX. The white arrowheads indicate pAMPK^{Thr172}-positive myonuclei within the postsynaptic compartment. (C) Fluorescent intensity markers (dotted cyan arrows) intersect pAMPK^{Thr172} localized at the synapse in panels (A) and are plotted as a function of distance. Graphical summaries of synaptic pAMPK^{Thr172} expression (D) and subsynaptic myonuclear pAMPK^{Thr172} accumulation (E). (F) Typical IF images of PGC-1α (magenta), αBTX, and DAPI in the EDL muscles of Veh, MK 3hr, and MK 6hr groups. (G) Magnified images of each synapse in (F) demonstrate PGC-1α expression at the neuromuscular synapse. The white arrowheads in (G) indicates a PGC-1α-positive myonucleus within the postsynaptic compartment. (H) Fluorescent intensity markers (dotted cyan arrows) intersect PGC-1α localized at the synapse and are plotted as a function of distance. Graphical summary of synaptic PGC-1α expression (I) and subsynaptic myonuclear PGC-1α accumulation (J). Data in the graphical summaries are shown relative to the Veh group. Scale bars in A and F represent 20 μm, whereas scale bars in B and G represent 5 μm. n = 8-10 animals per experimental group. For confocal microscopy analysis the points represent individual synapses from 6 experimental replicates per group. *, P < 0.05 vs. WT Veh.

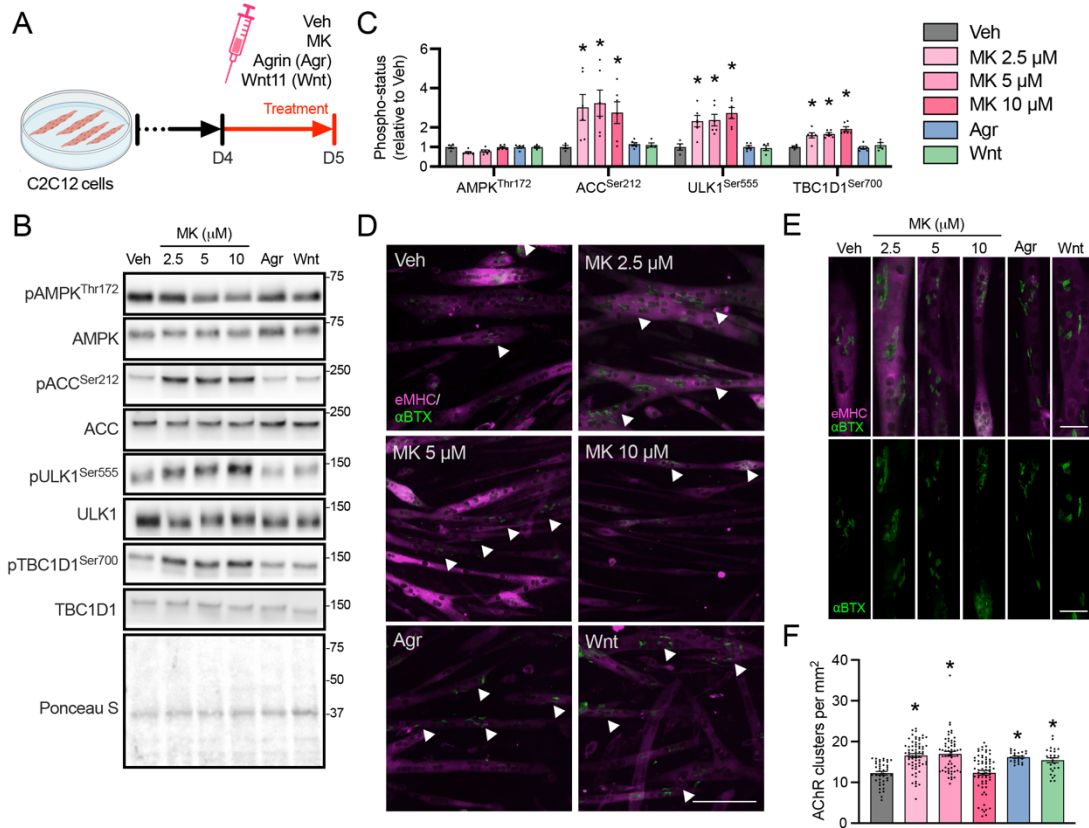


Fig. 5. AMPK activation in skeletal muscle induces AChR clustering. (A) Following four days of differentiation (D4) C2C12 myotubes were treated with Veh, MK (2.5 μM, 5 μM, 10 μM), agrin (Agr, 0.4 μM/mL), or Wnt11 (Wnt, 0.1 μM/mL) for 24 hrs. Treated myotubes were then collected at D5 for immunoblotting and IF experiments. (B) Typical Western blots of pAMPK^{Thr172}, AMPK, pACC^{Ser212}, ACC, pULK1^{Ser555}, ULK1, Ser⁷⁰⁰-phosphorylated TBC1 domain family member 1 (pTBC1D1^{Ser700}), and TBC1D1 in all experimental groups. Ponceau S staining is shown below to indicate equal loading between samples. Protein ladder markers at right are expressed as kDa. (C) Graphical summaries of AMPK, ACC, ULK1, and TBC1D1 phospho-status. (D) Typical IF images of Veh-, MK-, Agr-, and Wnt-treated C2C12 myotubes at D5. Embryonic myosin heavy chain (eMHC; magenta) denotes myotubes, while αBTX staining (green) indicates AChRs. White arrowheads point to areas enriched with AChRs. (E) Magnified images depict AChR localization in single myotubes from each experimental condition. The scale bars represent 125 μm and 50 μm in the low and high magnification panels, respectively. (F) Graphical summary of AChR density [i.e., the number of AChR clusters per field of view (mm²)] in Veh-, MK-, Agr-, and Wnt-treated C2C12 myotubes. Protein data are expressed relative to the WT Veh group. All graphical summaries display individual data points and group means (bars) with SEM. n = 4 - 5 per independent experiment. For immunofluorescent microscopy analysis points represent individual micrographs from 4 experimental replicates per group. *, P < 0.05 vs. Veh.

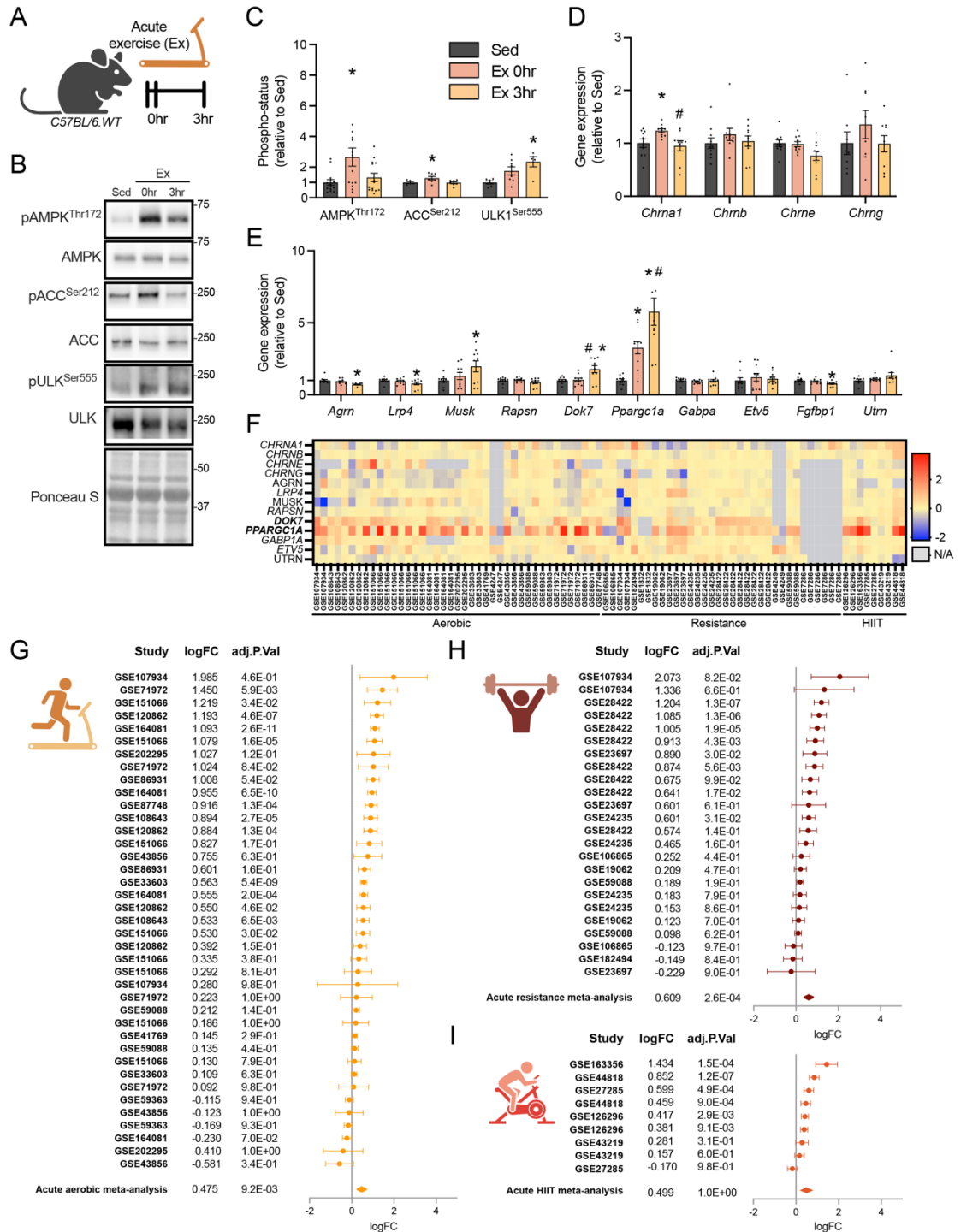


Fig. 6. Exercise evokes AMPK stimulation and downstream Ppargc1 α and Dok7 expression in mouse and human skeletal muscle. (A) 2 mo WT animals performed a single bout of aerobic-type exercise and were euthanized immediately after (Ex 0hr) or 3 hrs post-exercise (Ex 3hr). Sedentary WT (Sed) mice served as controls. (B) Representative Western blots of pAMPK^{Thr172}, AMPK, pACC^{Ser212}, ACC, pULK1^{Ser555}, and ULK1 in TRI muscles from mice in the Ex and Sed groups. Ponceau S staining is shown below to indicate

equal loading between samples. Protein ladder markers at right are expressed as kDa. **(C)** Graphical summaries of AMPK, ACC, and ULK1 phospho-status. Graphical summaries of *Chrna1*, *Chrnb*, *Chrne*, and *Chrng* **(D)** transcript levels, as well as NMJ-related genes *Aggrn*, *Lrp4*, *Musk*, *Rapsn*, *Dok7*, *Ppargc1a*, *Gabpa*, *Etv5*, *Utrn*, and *Fgfbp1* **(E)** in TRI muscles of Sed and Ex animals. Protein and mRNA data are expressed relative to the Sed group. All graphical summaries display individual data points and group means (bars) with SEM. n = 6 - 8 animals per group. *, P < 0.05 vs. WT Sed; #, P < 0.05 vs Ex 0hr. **(F)** Heat map summary of publicly available transcriptomic data sets showing differential expression of NMJ-related genes in human skeletal muscle after a single bout of aerobic-, resistance-, and high-intensity interval training (HIIT)-type exercise. Bolded genes are significantly different [adjusted P values (adj.P.Val) < 0.05] from their control condition. Data are expressed as log fold-change (logFC) relative to the control condition. Forest plots of individual logFC and adj.P.Val, as well as meta-analysis scores, for skeletal muscle *DOK7* expression in studies evaluating acute aerobic **(G)**, resistance **(H)**, and HIIT **(I)** exercise responses in human participants.

CHAPTER 3:

Acute, next-generation AMPK activation initiates a disease-resistant gene expression program in dystrophic skeletal muscle.

Published in *The FASEB J* 2023, 37(5): e22863.

Published under the Creative Commons Attribution License 4.0

Acute, next-generation AMPK activation initiates a disease-resistant gene expression program in dystrophic skeletal muscle

Sean Y. Ng | Andrew I. Mikhail | Stephanie R. Mattina | Alexander Manta | Ian J. Diffey | Vladimir Ljubcic 

Department of Kinesiology, McMaster University, Hamilton, Ontario, Canada

Correspondence

Vladimir Ljubcic, Department of Kinesiology, McMaster University, Hamilton, ON L8S 4L8, Canada.
Email: ljubicic@mcmaster.ca

Funding information

Canada Research Chairs (Chaires de recherche du Canada), Grant/Award Number: 232338; Gouvernement du Canada | Canadian Institutes of Health Research (IRSC), Grant/Award Number: 408289; Muscular Dystrophy Canada (DYSTROPHIE MUSCULAIRE CANADA), Grant/Award Number: 681362; Ontario Ministry of Economic Development, Job Creation and Trade (MDECEC), Grant/Award Number: ER17 -13 -087

Abstract

Duchenne muscular dystrophy (DMD) is a life-limiting neuromuscular disorder characterized by muscle weakness and wasting. Previous proof-of-concept studies demonstrate that the dystrophic phenotype can be mitigated with the pharmacological stimulation of AMP-activated protein kinase (AMPK). However, first-generation AMPK activators have failed to translate from bench to bedside due to either their lack of potency or toxic, off-target effects. The identification of safe and efficacious molecules that stimulate AMPK in dystrophic muscle is of particular importance as it may broaden the therapeutic landscape for DMD patients regardless of their specific dystrophin mutation. Here, we demonstrate that a single dose of the next generation, orally-bioactive AMPK agonist MK-8722 (MK) to mdx mice evoked skeletal muscle AMPK and extensive downstream stimulation within 12 h post-treatment. Specifically, MK elicited a gene expression profile indicative of a more disease-resistant slow, oxidative phenotype including increased peroxisome proliferator-activated receptor γ coactivator-1 α activity and utrophin levels. In addition, we observed augmented autophagy signaling downstream of AMPK, as well as elevations in critical autophagic genes such as *Map1lc3* and *Sqstm1* subsequent to the myonuclear accumulation of the master regulator of the autophagy gene program, transcription factor EB. Lastly, we show that pharmacological AMPK stimulation normalizes the expression of myogenic regulatory factors and amends activated muscle stem cell content in mdx muscle. Our results indicate that AMPK activation via MK enhances

Abbreviations: ACC, acetyl-CoA carboxylase; AICAR, 5-aminoimidazole-4-carboxamide ribonucleoside; AMPK, AMP-activated protein kinase; BNIP3, BCL2 Interacting Protein 3; DIA, diaphragm; DMD, Duchenne muscular dystrophy; EDL, extensor digitorum longus; Gabra1, gamma-aminobutyric acid receptor-associated protein-like 1; GAPDH, glyceraldehyde 3-phosphate dehydrogenase; GAST, gastrocnemius; H3, histone H3; LC3, microtubule-associated protein 1A/1B-light chain 3; MK, MK-8722; MuSC, muscle stem cell; MyoD, myoblast determination protein 1; MyoG, myogenin; NMJ, neuromuscular junction; NRF-1, nuclear respiratory factor 1; NRF-2, nuclear respiratory factor 2; P62, sequestosome-1; Pax7, paired box 7; PGC-1 α , peroxisome proliferator-activated receptor γ coactivator-1 α ; RPS11, ribosomal protein S11; SOL, soleus; TA, tibialis anterior; TFEB, transcription factor EB; ULK1, Unc-51-like autophagy activating kinase; WT, wild-type.

This is an open access article under the terms of the [Creative Commons Attribution-NonCommercial License](https://creativecommons.org/licenses/by/4.0/), which permits use, distribution and reproduction in any medium, provided the original work is properly cited and is not used for commercial purposes.

© 2023 The Authors. *The FASEB Journal* published by Wiley Periodicals LLC on behalf of Federation of American Societies for Experimental Biology.

disease-mitigating mechanisms in dystrophic muscle and prefaces further investigation on the chronic effects of novel small molecule AMPK agonists.

KEYWORDS

autophagy, muscular dystrophy, myogenic regulatory factors, PGC-1 α , utrophin

1 | INTRODUCTION

Duchenne muscular dystrophy (DMD) is the most common, life-limiting congenital neuromuscular disorder, affecting every 1 in 3600–6000 newborn boys.^{1,2} Mutations in the DMD gene result in the absence of the structural protein dystrophin and lead to dismantling of its larger, eponymous oligomeric complex that is normally expressed along the length of the sarcolemma. Dystrophin deficiency causes progressive muscle wasting and weakness in DMD patients usually beginning at age 2–5, which lead to respiratory and cardiac complications that precipitate death by age 20–30.² There is no cure for DMD, however, tremendous research efforts have led to the recent clinical approval of several dystrophin-dependent exon-skipping-based therapies that aim to introduce truncated but partially functional dystrophin to recapitulate a less severe Becker muscular dystrophy-like phenotype.^{3,4} A caveat associated with these treatments is that they exclusively target specific dystrophin mutations and therefore are suited to a minority of all DMD patients. Thus, identifying therapies that can be applied to all individuals with DMD regardless of their unique mutation is of the utmost importance.

Chronic stimulation of AMPK in skeletal muscle is an appealing therapeutic strategy for DMD because it abates the dystrophic phenotype in pre-clinical studies independent of dystrophin modulation, and thus would be applicable to all patients regardless of their specific gene mutation. Repeated exposure to pharmacological AMPK activators, such as 5-aminoimidazole-4-carboxamide ribonucleoside (AICAR), metformin, and resveratrol, shifts skeletal muscle towards a slower, more oxidative profile that displays a heightened resistance to the DMD myopathy.^{5–10} This attenuation of the dystrophic phenotype can be partially attributed to the upregulation of utrophin protein, an endogenously expressed functional homolog of dystrophin that is more abundant in slow, oxidative muscle fibers as compared to their faster, more glycolytic counterparts. Furthermore, beneficial AMPK-induced adaptations in dystrophic muscle include corrective alterations to the compromised autophagy program,^{11,12} as well as enhanced muscle stem cell (MuSC) biology and muscle regeneration.^{8,13} However, the translational impact of pharmacological AMPK activation on mitigating the dystrophic pathology in the DMD clinic has thus far been hindered due, in part, to significant

limitations associated with the compounds tested in the pre-clinical context.^{5–9,12,14–17} For example, chronic AICAR treatment causes lactic acidosis and hepatomegaly,¹⁸ while metformin and resveratrol are not particularly potent in attenuating the disease phenotype in DMD muscle.^{6,19,20} In contrast, a series of next-generation, orally-bioactive AMPK agonists have recently been identified to evoke high levels of kinase activation in the skeletal muscle of several pre-clinical models of metabolic dysfunction.^{21–26} Some of these small molecules were also validated and well-tolerated in metabolic disease patient cohorts.^{26–28} However, these new generation AMPK compounds have yet to be evaluated in the context of muscular dystrophy. Examining the acute responses to these novel AMPK agonists is important, as the results may broaden the applicability of these clinically relevant AMPK activators and potentially expand the current landscape for treatments available for all DMD mutations. Thus, the purpose of this study was to examine the effects of acute pharmacological AMPK activation with a next-generation, orally-bioavailable agonist on intracellular signaling and gene expression in dystrophic muscle. We hypothesized that treating mdx mice with a single dose of MK-8722 (MK) would stimulate AMPK and downstream signaling indicative of the slow, oxidative phenotype, induce corrective autophagic gene expression and signaling, and promote beneficial alterations in MuSC biology.

2 | MATERIALS AND METHODS

2.1 | Animals and experimental design

Ten-week-old dystrophic C57BL/10ScSn-DMD^{mdx}/J.mdx (mdx) and healthy C57BL/10SnJ wild-type (WT) animals were acquired from Jackson laboratory (mdx: 001801; WT: 000666). Animals were gavaged with MK [5 mpk; 1 mg/mL^{21,22,29}], or a Vehicle (Veh) solution composed of 0.25% methylcellulose, 5% polysorbate 80, and 0.02% sodium lauryl sulfate in deionized water. MK was obtained via a Material Transfer Agreement with Merck & Co. Oral gavages were performed between 6:00 and 10:00. Following gavage, all animals were left in individual cages and were provided food and water ad libitum. WT and mdx animals were euthanized via cervical dislocation 3, 6, and 12 h post gavage. tibialis anterior (TA), gastrocnemius (GAST), and

diaphragm (DIA) muscles were harvested at the prescribed timepoint and immediately flash-frozen in liquid nitrogen while the solues (SOL) and extensor digitorum longus (EDL) muscles were mounted in optimum cutting temperature (OCT; Thermo Fisher Scientific; Waltham, MA, USA) compound and frozen in isopentane cooled in liquid nitrogen. All tissues were stored at -80°C until analysis.

2.2 | Whole muscle protein extraction

Frozen TA or DIA muscles were mechanically homogenized with stainless steel lysing beads and TissueLyser (Qiagen, Hilden, NRW, Germany). Samples were suspended in RIPA buffer (R0278, Sigma-Aldrich S. Louis, MO, USA) supplemented with Complete Mini Protease Inhibitor Cocktail (05892970001, Sigma-Aldrich) and PhosSTOP Phosphatase Inhibitor Cocktail (04906837001, Sigma-Aldrich). Samples were then sonicated with a Branson Ultrasonics Sonifier (SFX150; Thermo Fisher Scientific) for $5 \times 2\text{ s}$ at 70% power. Supernatants were collected after samples were spun for 10 min at 14000g and tested with a bicinchoninic assay to determine protein concentrations. Samples were then diluted to equal concentrations ($1.5\ \mu\text{g}/\mu\text{L}$) mixed with 4x loading buffer and ddH_2O .

2.3 | Skeletal muscle nuclei fractionation

Nuclear fractions were isolated as previously described.³⁰ Briefly, whole GAST muscle were homogenized in STM buffer (250 mM Sucrose, 50 mM Tris-HCl pH 7.4, 5 mM MgCl_2 , protease and phosphatase inhibitor cocktails) with scissors and manually homogenized utilizing a Teflon pestle for 2 min. Samples were then centrifuged at 800g for 15 min. The pellet was resuspended in STM buffer and spun twice to wash the nuclear pellet. The remaining pellet was then resuspended in NET buffer (20 mM HEPES pH 7.9, 1.5 mM MgCl_2 , 0.5 M NaCl, 0.2 mM EDTA, 20% glycerol, 1% Triton-X-100, protease and phosphatase inhibitors), sonicated, and spun at 9000g for 30 min to produce the nuclear fraction. Protein concentrations were determined with a bicinchoninic assay. Myonuclear-enriched samples were then diluted to equal concentrations ($1.5\ \mu\text{g}/\mu\text{L}$) mixed with 4x loading buffer and ddH_2O .

2.4 | Immunoblotting

To assess muscle protein content, standard Western blotting techniques were applied. $15\ \mu\text{g}$ of prepared sample was loaded into a 7.5% polyacrylamide gel and separated by size using SDS-PAGE. Subsequently, proteins were transferred

onto a nitrocellulose membrane and then stained with Ponceau S (Sigma-Aldrich). Membranes were then incubated with 5% BSA in TBST for 60 min at room temperature. Primary antibodies were incubated at 4°C overnight with mild agitation. We employed antibodies against Thr172-phosphorylated AMPK (pAMPK^{Thr172}; 1:1000; 2535S; Cell Signaling, Danvers, MA, USA), AMPK (1:1000; 2532S; Cell Signaling), Ser212-phosphorylated acetyl-CoA carboxylase (pACC^{Ser212}; 1:1000; 3661S; Cell Signaling), ACC (1:1000; 3676S; Cell Signaling), Utrophin (1:1000; NCL-DRP2; Leica Biosystems, Concord, ON, Canada), microtubule-associated protein 1A/1B-light chain 3 (LC3; 1:1000; 4108S; Cell Signaling), sequestosome-1 (p62; 1:1000; P0067; Sigma-Aldrich), Ser555-phosphorylated unc-51-like autophagy activating kinase (pULK1^{Ser555}; 1:1000; 5869S; Cell Signaling), Ser757-phosphorylated ULK1 (pULK1^{Ser757}; 1:1000; 6888S; Cell Signaling), ULK1 (1:1000; 8054S; Cell Signaling), Ser235/236-phosphorylated S6 (pS6^{Ser235/236}; 1:1000; 2211S; Cell Signaling), S6 (1:1000; 2217S; Cell Signaling, Danvers), Ser473-phosphorylated protein kinase B (pAKT^{Ser473}; 1:1000; 9271S; Cell Signaling), AKT (1:1000; 4691S; Cell Signaling), Histone H3 (1:11000; ab18521; Abcam, Cambridge, UK) and glyceraldehyde 3-phosphate dehydrogenase (GAPDH; 1:11000; PA1-987; Thermo Fisher Scientific) antibodies were also utilized to evaluate the purity of the myonuclear sample preparations. On the following day, membranes were washed in TBST $3 \times 5\text{ min}$ and incubated with the appropriate horseradish peroxidase-linked secondaries (1:5000; 7074S/7076S; Cell Signaling) for 60 min. Blots were then washed with TBST, followed by visualization with enhanced chemiluminescence on the ChemiDoc MP Imaging System (Bio-Rad Laboratories, Inc., Hercules, CA, USA). Densitometry analysis was performed using Image Lab (Bio-Rad Laboratories). All blots were normalized to the ponceau and standardized to a pooled control on each gel.

2.5 | Immunofluorescence microscopy

EDL and SOL muscles stored in OCT compound were cut into $10\ \mu\text{m}$ thick sections at -20°C on a cryostat (Leica Biosystems), collected on Superfrost Plus Gold slides, and stored at -80°C . Sections from each experimental group were mounted on the same slide to ensure accurate comparisons. To determine the subcellular localization of peroxisome proliferator-activated receptor γ coactivator-1 α (PGC-1 α), we immunolabeled the nuclear and sarcolemma components as previously described.³¹ In brief, tissues were fixed with 4% paraformaldehyde for 10 min, washed with PBS/Tween20, and then blocked with 10% goat serum in 1% bovine serum albumin (BSA) for 60 min. Sections were then probed for PGC-1 α (1:1000; AB3242; EMD Millipore, Darmstadt, HE, Germany)

overnight at 4°C. The following day, samples were incubated in Alexa594-conjugated secondary (1:500; A11037; Thermo Fisher Scientific) for 120 min at room temperature. Laminin (1:500; L0663; Sigma-Aldrich) was then applied for 120 min at room temperature, followed by a fluorescent-conjugated goat anti-rat secondary antibody (1:500; 112-605-167; Jackson ImmunoResearch). Slides were then incubated with 4',6-diamidino-2-phenylindole dihydrochloride (DAPI; 1:10 000; D1306; Thermo Fisher Scientific) to reveal nuclei, respectively. After slides were washed and dried, a coverslip was mounted with a fluorescence mounting medium (DAKO, S3023, Agilent Technologies, Santa Clara, CA, USA).

To locate the subcellular localization of utrophin, muscle sections were blocked with a mouse-on-mouse (MOM) blocking reagent (BMK-2202, Vector Laboratories; Burlington, ON, Canada) in a 10% goat serum solution for 60 min. Samples were then probed for utrophin (1:100; NCL-DRP2; Leica Biosystems) for 120 min and revealed with the MOM biotinylated anti-mouse reagent and streptavidin as per manufacturer's instructions. Laminin (1:500; L0663; Sigma-Aldrich) was applied for 120 min at room temperature, followed by a fluorescent-conjugated secondary antibody (1:500; 112-605-167; Jackson ImmunoResearch). A fluorescent-conjugated α BTX (1:500; 13422; Thermo Fisher Scientific) was used to demark synaptic regions. After washing, the slides were mounted with Prolong Gold (P366930; Thermo Fisher Scientific).

To identify the cellular presence of transcription factor EB (TFEB), 10 μ M muscle sections were blocked with 10% goat serum solution for 60 min. Slides were then incubated with TFEB (1:50; sc-166736, Santa Cruz; Dallas, TX) in 1% BSA overnight at 4°C. On the subsequent day, sections were incubated in Alexa594-conjugated secondary (1:500; A11037; Thermo Fisher Scientific) for 120 min at room temperature. Slides were then incubated with laminin (1:500; L0663; Sigma-Aldrich) for 120 min at room temperature, followed by a fluorescent-conjugated goat anti-rat secondary antibody (1:500; 112-605-167; Jackson ImmunoResearch) to demark the sarcolemma. DAPI (1:10 000; D1306; Thermo Fisher Scientific) was then applied to reveal nuclei. After washing, the slides were mounted with Prolong Gold (Thermo Fisher Scientific).

To reveal satellite cell number and activation, muscle sections were immunolabeled as previously described.³² In brief, slides were blocked with a MOM blocking reagent (BMK-2202, Vector Laboratories) in a 2% BSA, 5% fetal bovine serum, 0.2% Triton X and 0.1% sodium azide solution for 60 min. Slides were then probed for paired box 7 (Pax7; 1:2; Developmental Studies Hybridoma Bank, Iowa City, IA) in MOM diluent reagent for 120 min, subjected to the MOM biotinylated anti-mouse reagent for 10 min and the fluorescent-conjugated streptavidin for 60 min. Sections

were then blocked in 10% goat serum and probed for myoblast determination protein 1 (MyoD; 1:500; C-20; Santa Cruz) overnight at 4°C. On the following day, Alexa488-conjugated goat anti-rabbit antibody (1:500; A11008; Thermo Fisher Scientific) was applied for 60 min at room temperature. Laminin (1:500; L0663; Sigma-Aldrich) was applied for 120 min at room temperature, followed by a fluorescent-conjugated goat anti-rat secondary antibody (1:500; 112-605-167; Jackson ImmunoResearch). DAPI was then applied to reveal nuclei. Slides were mounted with Prolong Gold (Thermo Fisher Scientific).

All immunolabeled muscle sections were imaged with the Nikon Eclipse *Ti* microscope, equipped with a high resolution photometric CoolSNAP HQ2 fluorescent camera and a 20 \times objective lens. The images were taken and analyzed using the Nikon NIS elements AR 3.2 software. Representative images were captured by confocal microscopy (60 \times , 1.4 NA oil emersion; Nikon Instruments, Mississauga, Ontario, Canada).

Myonuclear protein localization was evaluated as previously described.³¹ In brief, regions of interest spanning 40% of the total cross-sectional area of the muscle sample and devoid of fiber necrosis were identified and then a binary threshold was generated with the DAPI staining and applied to the protein of interest (PGC-1 α and TFEB) channel to determine binary sum intensity within nuclei, while the remaining intensities were considered cytosolic. To quantify MuSC activation and quiescence, MuSCs were first classified by nuclei that both were: (1) positive with Pax7 staining; and (2) at the periphery of the muscle fiber within the laminin staining. Activated MuSCs were then determined by the criteria above with the co-expression of Pax7 and MyoD, whereas quiescent MuSCs were indicated by the absence of MyoD. MuSC analyses were performed using an average of >200 fibers/muscle section.

To distinguish the expression of extrasynaptic and synaptic utrophin expression, we generated fluorescence intensity profile line scans with Nikon NIS elements AR 3.2 software, as done previously when assessing protein localization at synaptic regions.^{33,34} The lines were drawn to intersect the synaptic and extrasynaptic regions on the sarcolemma of α BTX-positive myofibers. A 5-pixel line width was used to average intensities at each point along the line to reduce signal noise. Fluorescence intensity along the lines were plotted as a function of distance.

2.6 | RNA isolation, reverse transcription, and real-time quantitative PCR

Total RNA was isolated from TA muscles. One milliliter of TRIzol reagent (15596018, Thermo Fisher Scientific)

was used to homogenize all muscle samples in Lysing D matrix tubes (MP Biomedicals; Santa Ana, CA, USA) with the FastPrep-24 Tissue and Cell Homogenizer (MP Biomedicals) for 40 s at a speed of 6.0 m/s. Homogenized muscles were mixed in 200 μ L of chloroform (Thermo Fisher Scientific) and shaken vigorously for 15 s, then centrifuged at 12000g for 10 min. The upper aqueous layer (RNA) was purified by the Total RNA Omega Bio-Tek kit (CA101319-242, VWR International; Radnor, PA, USA). The concentration and purity of the RNA were determined using the NanoDrop 1000 Spectrophotometer (Thermo Fisher Scientific). RNA samples were then reverse-transcribed into cDNA using a high-capacity cDNA reverse transcription kit (4368814; Thermo Fisher Scientific). All qPCR assays were run in triplicate 6 μ L reactions containing GoTaq qPCR Master Mix (A6002; Promega; Madison, WI, USA). qPCR primers utilized were as follows: *Rps11*: F – CGTGACGAACATGAAGATGC, R – GCACATTGAA TCGCACAGTC; *Pparg1a*: F – AGTGGTGTAGCGACCA AT, R – GGGCAATCCGCTTCATCCA; *Utrn*: F – CCGGA GCTAAACACCACTGT, R – ATTCAGCTGAGCGAGCAT GT; *Nrf1*: F – ATCCGAAAGAGACAGCAGACA, R – TGGAGGGTGAGATGCAGAGTA; *Ulk1*: F – GCTCCGG TGACTTACAAAGCTG, R – GCTGACTCCAAGCCAAAG CA; *Map1lc3*: F – CACTGCTCTGTCTTGTGTAGGTTG, R – CACTGCTCTGTCTTGTGTAGGTTG; *Gabra1*: F – CA TCGTGGAGAAGGTCCTA, R – ATACAGCTGGCCCA TGGTAG; *Sqstm1*: F – CCCAGTGTCTTGGCATTCTT, R – A GGGAAAGCAGAGGAAGCTC; *Nrf2*: F – TTCTTTCAGC AGCATCTCTCCAC, R – ACAGCCTTCAATAGTCCCG TCCAG; *Bnip3*: F – TTCCACTAGCACCTTCTGATGA, R – GAACACCGCATTACAGAACAA; *Pax7*: F – TTGGG GAACACTCCGCTGTGC, R – CAGGGCTTGGGAAGGG TTGGC; *MyoD*: F – TCTGGAGCCCTCTGGCACC, R – CG GGAAGGGGAGAGTGGGG; *MyoG*: F – GGAATTCG AGGCATATTATGA, R – TCACATAAGGCTAACACCCAG. Data were analyzed using the comparative CT method.³⁵ Ribosomal protein S11 (*Rps11*) was used as the normalizing gene since it did not differ between experimental groups (data not shown).

2.7 | Statistics

Preliminary one-way analysis of variance (ANOVA) tests indicated that there was no difference in muscle AMPK and ACC phosphorylation status between WT Veh cohorts at the different timepoints post-MK treatment, so they were collapsed into a single WT Veh group. The same transformation was performed for the mdx Veh group. One-way ANOVA and Tukey's post hoc test was then employed to compare means across all experimental groups. The statistical tests were performed with Prism GraphPad and on

the raw data prior to any conversion to fold differences displayed in some graphical summaries. Significance was accepted at $p < .05$. Data are presented as mean \pm SEM.

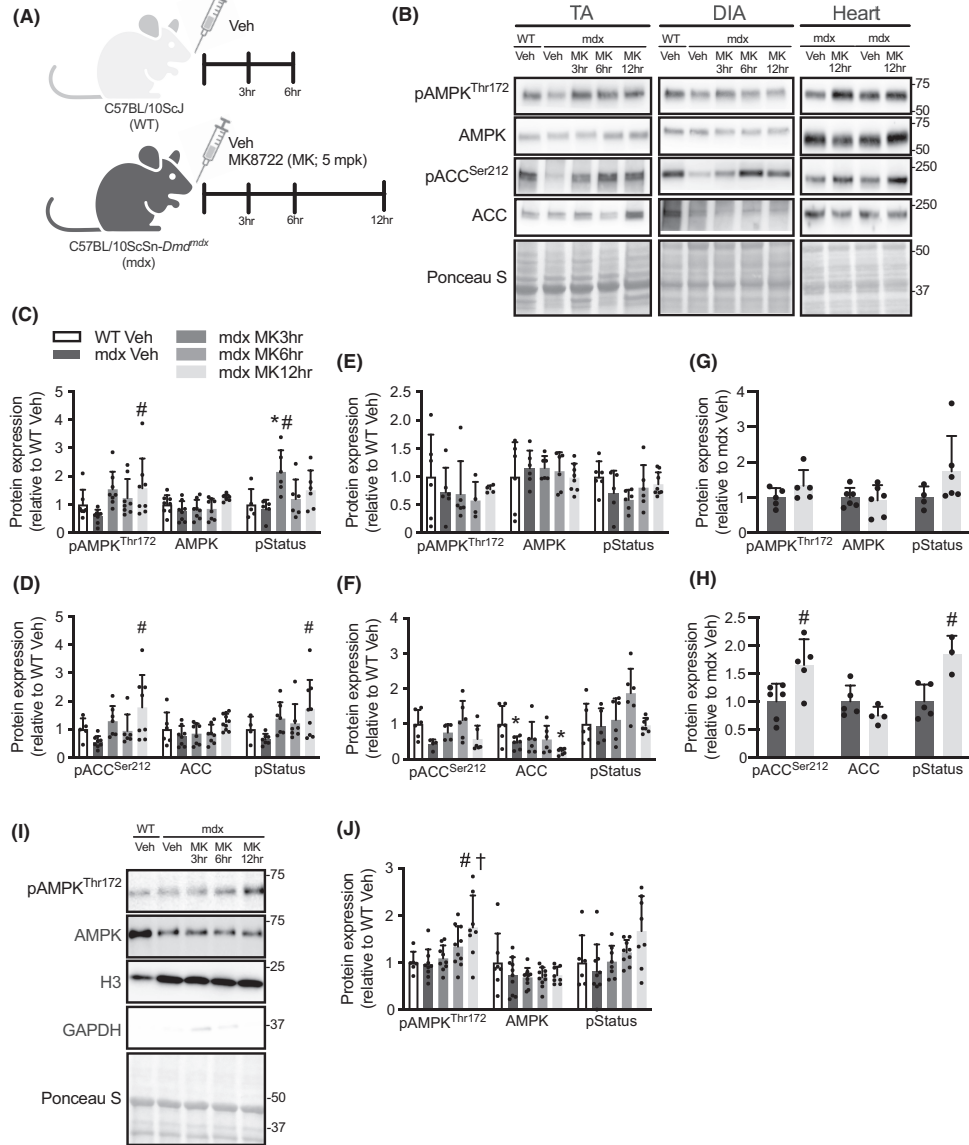
3 | RESULTS

3.1 | A single dose of MK evokes AMPK activation in dystrophic skeletal muscle

To evaluate the efficacy of a new class of orally-bioavailable and specific pharmacological agonists to acutely stimulate AMPK signaling in dystrophic skeletal muscle, we administered a single dose of MK (5 mpk) via oral gavage to mdx animals (Figure 1A). mdx mice were euthanized 3-, 6-, and 12-h post-treatment, while a cohort of age-matched WT and mdx mice were treated with the Veh solution to serve as control groups. Tissues from the Veh groups were collected 3- or 6-h post-gavage. A significant main effect of MK was observed on pAMPK^{Thr172} levels in the TA muscles of dystrophic mice (Figure 1B,C). Relative to the Veh-treated mdx controls, pAMPK^{Thr172} tended to be higher ($p = .06$) in the mdx MK6hr group and was significantly elevated (+170%) in mdx MK12hr animals. An acute dose of MK did not alter total AMPK content. AMPK phosphorylation status (i.e., pAMPK^{Thr172}/AMPK) was significantly greater in the mdx MK6hr group compared to the WT and mdx Veh groups. Downstream pACC^{Ser212} was significantly higher (+230%) in the mdx MK12hr group relative to mdx Veh animals (Figure 1B,D). ACC phosphorylation status in the mdx MK12hr animals was significantly elevated by 2.7-fold compared to their Veh counterparts.

We next evaluated the impact of MK in mdx mice by assessing AMPK signaling in clinically relevant muscle including the DIA and heart. pAMPK^{Thr172}, total AMPK, and AMPK phosphorylation status in the DIA were similar across all experimental groups (Figure 1B,E). pACC^{Ser212} and ACC phosphorylation status were trending higher ($p = .07$ and $p = .06$, respectively) in the mdx MK6hr group when compared to the mdx Veh animals (Figure 1B,F). Total ACC content was significantly lower (–66%) in the DIA muscles of dystrophic animals relative to WT mice and were not affected by MK. pAMPK^{Thr172}, total AMPK, and AMPK phosphorylation status were similar between cardiac muscles of Veh-treated and MK-treated mdx animals (Figure 1B,G), whereas pACC^{Ser212} and ACC phosphorylation status were 75% higher ($p < .05$) in the MK12hr-treated mice relative their Veh counterparts (Figure 1B,H). Total cardiac ACC content was similar between Veh- and MK-treated mdx animals.

Recent work investigating the subcellular localization of AMPK suggests that nuclear AMPK controls transcriptional



regulators of skeletal muscle plasticity.^{36,37} To evaluate whether this phenomenon is evident in the dystrophic context, we measured the presence of myonuclear AMPK in the GAST muscles of Veh-treated WT mice and Veh- and MK-treated mdx animals. The purity of our nuclear samples was confirmed by probing for histone H3 and GAPDH

protein content. The mdx MK12hr group demonstrated a 75% elevation ($p < .05$) in nuclear pAMPK^{Thr172} expression relative to their Veh-treated counterparts (Figure 1I,J). Nuclear AMPK phosphorylation status was trending higher ($p = .08$) in the mdx MK12hr mice compared to the mdx Veh animals. Total nuclear AMPK was similar across all groups.

FIGURE 1 MK-8722 (MK) elicits AMP-activated protein kinase (AMPK) activity in dystrophic skeletal muscles. (A) 10-week-old, male C57BL/19ScSn-Dmd^{mdx} (mdx) animals were orally gavaged a single dose of Veh or MK (5 mpk) solution. Dystrophic animals were euthanized 3- (mdx 3 hr), 6- (mdx 6 hr), or 12-h (mdx 12 hr) post-gavage, while healthy Veh-treated wild-type mice (C57BL/10ScJ.WT; WT Veh) served as controls. (B) Representative Western blots of threonine 172 (Thr172)-phosphorylated AMPK (pAMPK^{Thr172}), total AMPK, serine 212 (Ser212)-phosphorylated acetyl-CoA carboxylase (pACC^{Ser212}), and total ACC in the tibialis anterior (TA), diaphragm (DIA), and cardiac muscles of vehicle (Veh)-treated wild-type (WT) mice and Veh- or MK-8722 (MK)-treated mdx animals. Ponceau S staining is shown below to indicate equal loading between samples. Protein ladder markers at right are expressed as kDa. Graphical summaries of AMPK (C, E, G) and ACC (D, F, H) phosphorylation and total levels, as well as phosphorylation status (i.e., the phosphorylated form of the protein relative to its total amount within the same sample; pStatus) in the TA (C, D), DIA (E, F), and heart (G, H) muscles. (I) Typical Western blots of pAMPK^{Thr172}, AMPK, histone H3 (H3), and glyceraldehyde 3-phosphate dehydrogenase (GAPDH) in myonuclei isolated from gastrocnemius muscles of Veh-treated WT mice and Veh- or MK-treated mdx animals. (J) Graphical summary of nuclear pAMPK^{Thr172}, AMPK, and nuclear AMPK pStatus is depicted. Values are displayed as a fold difference relative to the WT Veh group. Graphical summaries show individual data (points), as well as group means (bars) with standard deviation (SD) of the means. * $p < .05$ versus WT Veh; # $p < .05$ versus mdx Veh; † $p < .05$ versus mdx 3 hr. $n = 8-10$.

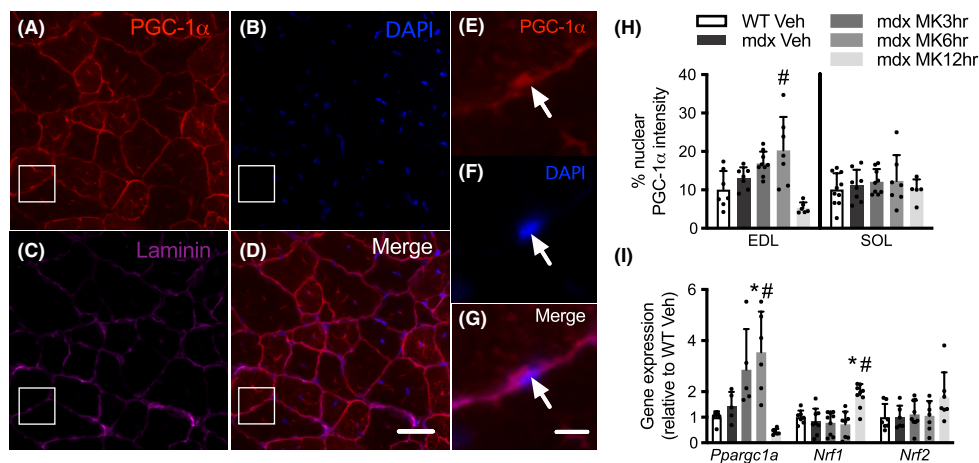


FIGURE 2 Acute MK-induced AMPK activation drives the myonuclear accumulation of peroxisome proliferator-activated receptor γ coactivator-1 α (PGC-1 α) in a fiber type-specific manner and evokes a slower, more oxidative gene program in dystrophic muscle. Confocal immunofluorescence images of PGC-1 α subcellular localization in the extensor digitorum longus (EDL) muscles of mdx animals (A–G). PGC-1 α (red; panels A and E), 4',6-diamidino-2-phenylindole (DAPI, blue; panels B and F) to denote nuclei, while laminin (purple; panel C) outlines the sarcolemma. D, Merged image displays the overlay of the three channels. Larger images (E–G) of the inset box in panels A–D demonstrate a PGC-1 α -positive myonucleus, indicated by the white arrow. Scale bars in panels D and G represent 25 μ m and 10 μ m, respectively. (H) Graphical summary of myonuclear PGC-1 α localization in the EDL and soleus (SOL) muscles from the five experimental groups. (I) Graphical summary of *Pparg1a*, nuclear respiratory factor-1 (*Nrf1*), and *Nrf2* mRNA expression. Graphical summaries show individual data (points) and group means (bars) with SDs. * $p < .05$ versus WT Veh; # $p < .05$ versus mdx Veh. $n = 8-10$.

3.2 | Acute MK administration elicits molecular signaling towards a slower, more oxidative muscle phenotype in mdx mice

Chronic AMPK stimulation with AICAR, resveratrol, or metformin elicits some beneficial alterations in the skeletal muscle of preclinical models of DMD.^{8,17,20,38} These include adaptations such as the induction of a slower, more oxidative muscle phenotype, normalization of the

autophagy program, and altered MuSC biology. Thus, we investigated the impact of acute MK exposure on upstream signals driving the slow, oxidative myogenic program. To this end, we first examined the subcellular localization of the transcriptional coactivator PGC-1 α , a master regulator of neuromuscular phenotype determination, maintenance, and remodeling, in the fast, glycolytic EDL and the slower, and more oxidative SOL muscles. A main effect of MK on myonuclear PGC-1 α accumulation (i.e., % nuclear PGC-1 α intensity) was revealed in the

EDL, but not the SOL muscle (Figure 2A–H). Specifically, myonuclear PGC-1 α localization was 55% greater ($p < .05$) in the EDL muscles of mdx MK6hr animals relative to the mdx Veh controls. We next utilized PGC-1 α (*Ppargc1a*) and nuclear respiratory factor 1 (*Nrf1*) transcript expression as additional measures to further confirm the elevation of PGC-1 α activity.^{31,39} *Ppargc1a* mRNA expression in the TA muscle was significantly higher (+150%) in the mdx MK6hr group relative to the WT and mdx Veh groups (Figure 2I). *Nrf1* mRNA was also significantly elevated (+120%) in the mdx MK12hr group compared to the Veh-treated WT and mdx animals. MK did not influence *Nrf2* [also known as GA-binding protein (GABP)] mRNA expression.

Another AMPK-induced adaption in DMD mice is the upregulation of utrophin protein, which has been shown to mitigate the dystrophic phenotype.³⁸ Immunoblotting analyses revealed a significant elevation in utrophin protein content in the TA muscles of mdx MK12hr animals relative to the Veh-treated WT and mdx groups (Figure 3A,B). We did not observe an effect of MK on *Utrn* mRNA levels (Figure 3C). Given the MK-induced effects of utrophin protein, we sought to investigate the extrasynaptic, sarcolemmal localization of utrophin in EDL muscles from WT Veh, mdx Veh, and mdx MK12hr groups. We observed typical features of utrophin distribution in WT Veh mice (Figure 3, row D), including an accumulation of the protein at the neuromuscular junction (NMJ), as well as the compensatory upregulation of extrasynaptic utrophin in mdx Veh animals (Figure 3, row E). Consistent with our immunoblotting analyses, we detected an overall amplification of utrophin content (Figure 3, row F) along with a specific expansion of extrasynaptic utrophin protein expression along the sarcolemma of mdx MK12hr animals relative to their mdx Veh counterparts (Figure 3G–J).

3.3 | Pharmacological AMPK activation induces autophagic signaling in dystrophic muscle

AMPK activation stimulates autophagy and attenuates the dystrophy pathology in mdx animals.^{12,38} Here, we sought to investigate upstream signaling pathways that induce autophagy with MK-mediated AMPK agonism. AMPK-specific phosphorylation of pULK1^{Ser555}, as well as its phosphorylation status, were significantly elevated (+250–435%) in the mdx MK12hr group relative to mdx Veh controls (Figure 4A,B). Conversely, despite being 3–3.8-fold higher ($p > .05$) in mdx Veh versus WT Veh, the expression and phosphorylation status of mammalian target of rapamycin (mTOR)-targeted pULK1^{Ser757} was similar between mdx MK12hr and WT Veh animals (Figure 4A,C).

The phosphorylation status of mTOR downstream targets, pS6^{Ser235/236}; (Figure 4A,D) and Thr37/46-phosphorylated Eukaryotic translation initiation factor 4E-binding protein 1 (data not shown), were higher (+340% and +30%, respectively; $p < .05$) in the Veh-treated mdx animals compared to their healthy counterparts. pS6^{Ser235/236} phosphorylation status was similar between MK-treated groups and WT Veh controls. The expression and phosphorylation status of pAkt^{Ser473} were not impacted by MK, however, total Akt was significantly higher (+44%) in the MK12hr group relative to the healthy and dystrophic Veh control groups (Figure 4A,E).

We next evaluated downstream markers of autophagy signaling, including LC3 ratios and p62 protein expression, as well as TFEB myonuclear localization and autophagy gene expression. A main effect of MK treatment was observed in LC3II/LC3I ratio and p62 protein expression (Figure 4F–H). Specifically, the LC3II/LC3I ratio was 45% higher ($p < .05$) in the TA muscles of mdx MK12hr animals relative to the mdx Veh group. p62 expression in MK-treated mdx animals (3-, 6-, and 12-hrs post-gavage) was 1.8-fold higher ($p < .05$) compared to their Veh counterparts. Next, we sought to investigate the effects of AMPK stimulation on the myonuclear localization of TFEB in dystrophic EDL and SOL muscles. The percentage of nuclear TFEB intensity was 210% and 70% higher ($p < .05$) in the EDL of the mdx MK6hr group relative to the WT Veh and mdx Veh controls, respectively (Figure 4I–P). Myonuclear TFEB intensity in SOL muscles was significantly higher (+2.3-fold) in the mdx MK6hr group compared to their healthy Veh-treated counterparts. Consistent with these findings, MK treatment significantly elevated several TFEB-targeted and autophagy-related genes,⁴⁰ including *Map1lc3* (+130%), gamma-aminobutyric acid receptor-associated protein-like 1 (*Gabra1*; +290%), *Ulk1* (+230%), *Sqstm1* (+70%), and BCL2 interacting protein 3 (*Bnip3*; +140%), in the TA muscles of mdx MK12hr animals when compared to their Veh-treated controls (Figure 4Q).

3.4 | Acute AMPK activation alters myogenic regulatory gene expression and MuSC biology in dystrophic muscle

Cycles of degeneration and regeneration are a well-characterized phenotype observed in DMD muscle. We questioned whether acute pharmacological AMPK activation with MK would modulate MuSC biology in mdx animals. Similar to previous studies,^{41,42} we observed higher ($p = .13$) whole muscle *Pax7* mRNA expression in TA muscles of mdx animals relative to their healthy controls (Figure 5A). This disparity was reduced to 1.2-fold between the mdx MK6hr group versus WT Veh mice. *MyoD*

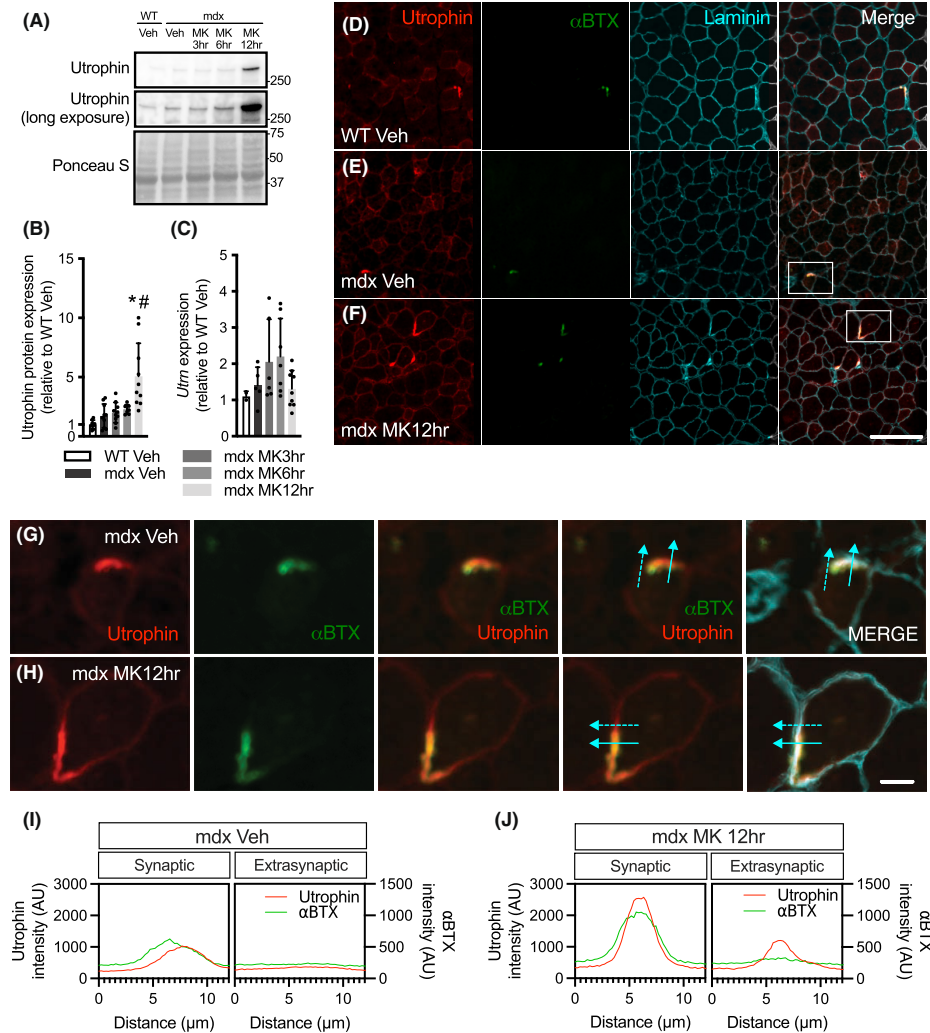


FIGURE 3 Acute MK dosing enhances utrophin protein expression in dystrophic skeletal muscle. (A) Typical Western blots of utrophin (regular and long exposures) in the TA muscles of all experimental groups. Ponceau S staining indicates equal loading between samples. Protein ladder markers at right are expressed as kDa. (B) Graphical summary of utrophin protein data. (C) Graphical summary of *Utrn* mRNA expression in the TA muscle of Veh-treated WT mice and Veh- or MK-treated mdx animals. Values are displayed as a fold difference relative to the WT Veh group. (D–F) Representative immunofluorescence images of utrophin (red) in the EDL muscles of WT Veh (row D), mdx Veh (row E), and mdx MK12hr (row F) animals. α -bungarotoxin (α BTX; Green) indicates AChRs at the neuromuscular junction, while laminin (cyan) outlines the sarcolemma. The Merge column displays the overlay of the three channels for each group. (G, H) Magnified images from the inset boxes in the Merge column of rows E and F depict synaptic and extrasynaptic utrophin expression in mdx Veh- or mdx MK12hr animals. Fluorescent intensity markers intersect the synaptic (solid cyan arrow) and extrasynaptic (dotted cyan arrow) utrophin-positive regions along the sarcolemma. Graphical summaries of the fluorescence intensity of synaptic and extrasynaptic utrophin in the mdx Veh (I) and mdx MK12hr (J) groups. Scale bars in rows G and H represent 100 μ m and 10 μ m, respectively. Graphical summaries show individual data (points) and group means (bars) with SDs. * $p < .05$ versus WT Veh; # $p < .05$ versus mdx Veh. $n = 8-10$.

transcript content was higher ($p > .05 < .1$) in all mdx groups compared to their WT counterparts (Figure 5B). Myogenin (*MyoG*) mRNA levels were significantly higher (+7.2-fold) in mdx Veh animals versus WT Veh mice (Figure 5C). A single dose of MK resulted in the reduction ($p < .05$) of *MyoG* transcripts 3- and 6-hrs post-gavage in dystrophic muscle, which returned to baseline levels in the mdx MK12hr group. To further investigate the influence of acute MK-evoked AMPK stimulation on MuSC biology, we utilized an immunofluorescence-based strategy to identify quiescent and activated satellite cells (Figure 5D–K). EDL muscles from MK-treated mdx animals (3-, 6-, and 12-hrs post-gavage) displayed a greater ($p < .05$) number of quiescent MuSCs (i.e., Pax7⁺/MyoD⁻ myonuclei) relative to WT and mdx Veh groups (Figure 5L). Quiescent MuSC content in SOL muscles were similar between all experimental groups. As reported previously,⁴³ a significantly higher (+100-fold) amount of differentiated MuSCs (Pax7⁻/MyoD⁺) was observed in the EDL and SOL muscles of Veh-treated mdx animals in comparison to their healthy WT controls (Figure 5M). MK treatment did not impact the number of differentiated cells (i.e., Pax7⁻/MyoD⁺) in the dystrophic EDL or SOL muscles. Activated satellite cell content (i.e., Pax7⁺/MyoD⁺) in the EDL and SOL muscles from mdx Veh, MK3hr and MK6hr animals were 4.6-fold higher than the WT controls (Figure 5N). Activated satellite cell content in the EDL and SOL muscles of the mdx MK12hr group were similar as compared to the WT Veh animals.

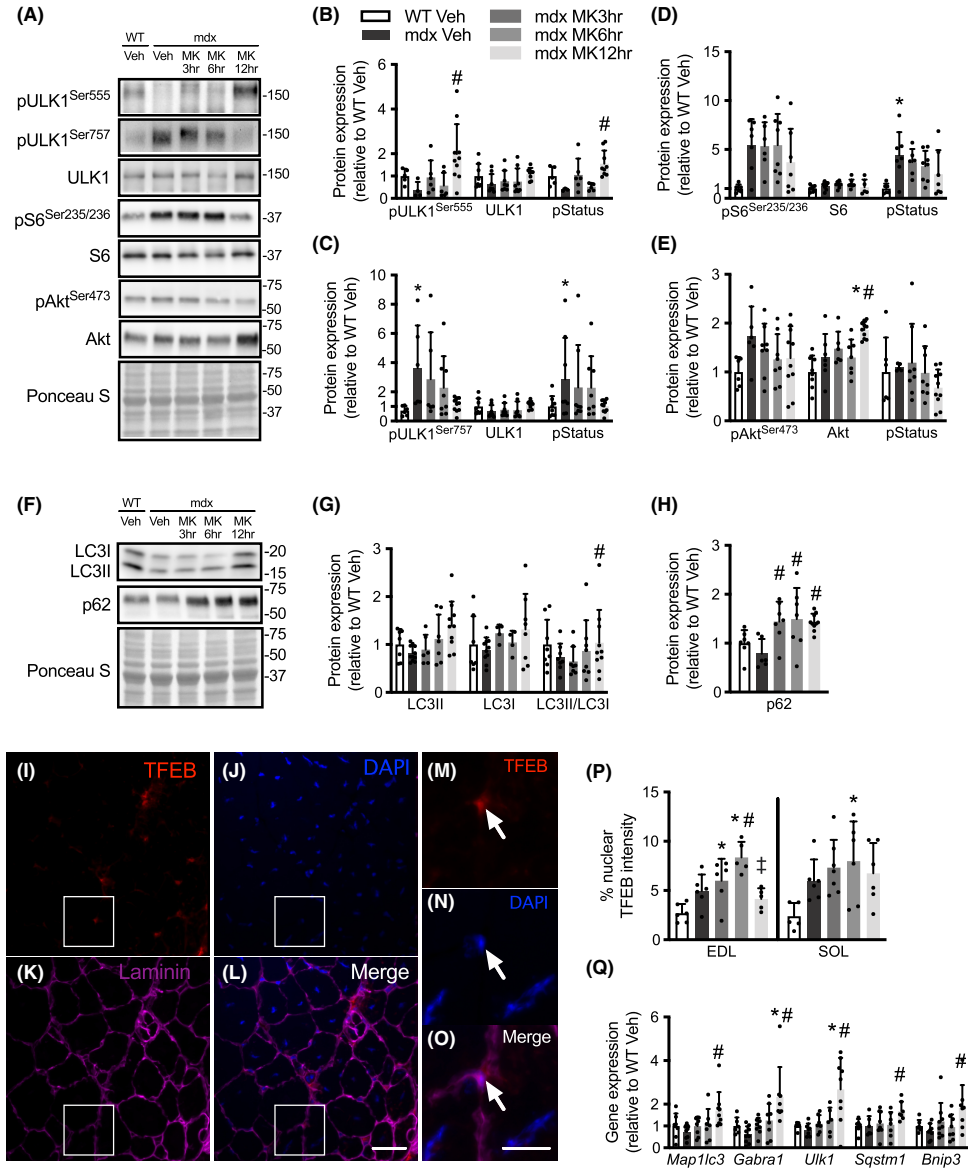
4 | DISCUSSION

The first series of studies examining the potential therapeutic effects of AMPK activation in mdx mice employed

the pharmacological tool AICAR,^{5,12,44} as well as supra-physiological doses of metformin, and resveratrol.^{6,15} Collectively, this proof-of-principle work revealed that the kinase can be effectively targeted in dystrophic muscle and that chronic AMPK stimulation evokes beneficial adaptations that mitigate the pathology. The purpose of the current investigation was to elucidate the efficacy of a next-generation small molecule compound to stimulate AMPK and its downstream network in dystrophic skeletal muscle. Our data demonstrate that a single dose of MK elicits several AMPK signaling cascades in the muscle of mdx mice that are associated with a mitigation of the dystrophic pathology. Specifically, MK triggered alterations indicative of the more disease resistant slow, oxidative phenotype, including AMPK and PGC-1 α myonuclear translocation and activation, as well as the induction of extrasynaptic utrophin protein. These responses occurred parallel with indicators of augmented autophagy downstream of AMPK, such as mTOR and ULK1 signaling, as well as elevations in the expression of key autophagy genes, including *Map1lc3*, *Gabra1*, and *Sqstm1*, and TFEB myonuclear accumulation. Lastly, we observed that acute MK-induced AMPK activation transiently normalizes the expression of myogenic regulatory factors such as MyoG, as well as amends MyoD⁺ MuSC content within the context of dystrophin-deficient muscle damage. Altogether, our results demonstrate that a single dose of MK elicits AMPK activity and the resultant stimulation of a broad downstream signaling and gene expression program in dystrophic skeletal muscle indicative of a more disease-resistant phenotype. This suggests that next-generation AMPK activation may be an effective and practical mutation-agnostic therapeutic platform for DMD.

MK is a novel compound that is part of a group of new generation, orally-bioactive AMPK activators.⁴⁵ MK

FIGURE 4 The effects of MK on autophagy signaling pathways in mdx muscle. (A) Representative Western blots of Serine 555 (Ser555)- and Ser757-phosphorylated unc-51-like autophagy activating kinase 1 (pULK1^{Ser555}, pULK1^{Ser757}), total ULK1 protein, Ser235/236-phosphorylated ribosomal protein 6 kinase (pS6^{Ser235/236}), total S6, Ser473-phosphorylated protein kinase B (pAkt^{Ser473}), and total Akt levels in the TA muscles of Veh-treated WT mice and Veh- or MK-treated mdx animals. Ponceau S staining is shown below to indicate equal loading between samples. Protein ladder markers at right are expressed as kDa. Graphical summaries of ULK1 (B, C), S6 (D), and Akt (E) data are shown. (F) Typical Western blots of cytosolic microtubule-associated protein 1A/1B-light chain 3 (i.e. LC3I), membrane bound LC3 (i.e. LC3II), and sequestosome-1 (p62) in the TA muscles of all experimental groups. Ponceau S staining is shown below to indicate equal loading between samples. Protein ladder markers at right are expressed as kDa. Graphical summaries of LC3II, LC3I, LC3I: LC3II ratios (G), as well as p62 protein expression (H). (I–O) Immunofluorescence images of transcription factor EB (TFEB, red; panels I and M) in dystrophic EDL muscle. DAPI (blue; panels J and N) denotes nuclei, while laminin (purple; panel K) outlines the sarcolemma. The merged images (panels L and O) display the overlay of the three channels. Larger images (M–O) of the inset boxes in panels I–L demonstrate a TFEB-positive myonucleus within myofibers, as indicated by white arrows. Scale bars in panels L and O represent 25 μ m and 10 μ m, respectively. (P) Graphical summary of myonuclear TFEB localization in the EDL and SOL muscles from the five experimental groups. (Q) LC3 (*Map1lc3*), GABA receptor-associated protein-like 1 (*Gabra1*), *Ulk1*, p62 (*Sqstm1*), and BCL2/adenovirus E1B 19 kDa protein-interacting protein 3 (*Bnip3*) mRNA expression in the TA muscles of WT Veh, mdx Veh, mdx MK3hr, mdx MK6hr, and mdx MK12hr animals. Values are displayed as a fold difference relative to the WT Veh group. Graphical summaries show individual data (points) and group means (bars) with SDs. * $p < .05$ versus WT Veh; [#] $p < .05$ versus mdx Veh. [†] $p < .05$ versus mdx Veh. $n = 8–10$.



directly binds to AMPK at its allosteric drug and metabolite site, which controls allosteric activation and prevents dephosphorylation of the kinase. Relative to other AMPK-activating molecules, such as AICAR and metformin, MK elicits greater kinase activity with high specificity in

several cell types.^{21,46} Furthermore, previous work from our laboratory, and others, demonstrates that a single dose of MK evokes targeted AMPK stimulation in the skeletal muscle of healthy mice in vivo.^{21,22,29,47} Chronic, daily MK administration to diabetic rodents also induces AMPK and

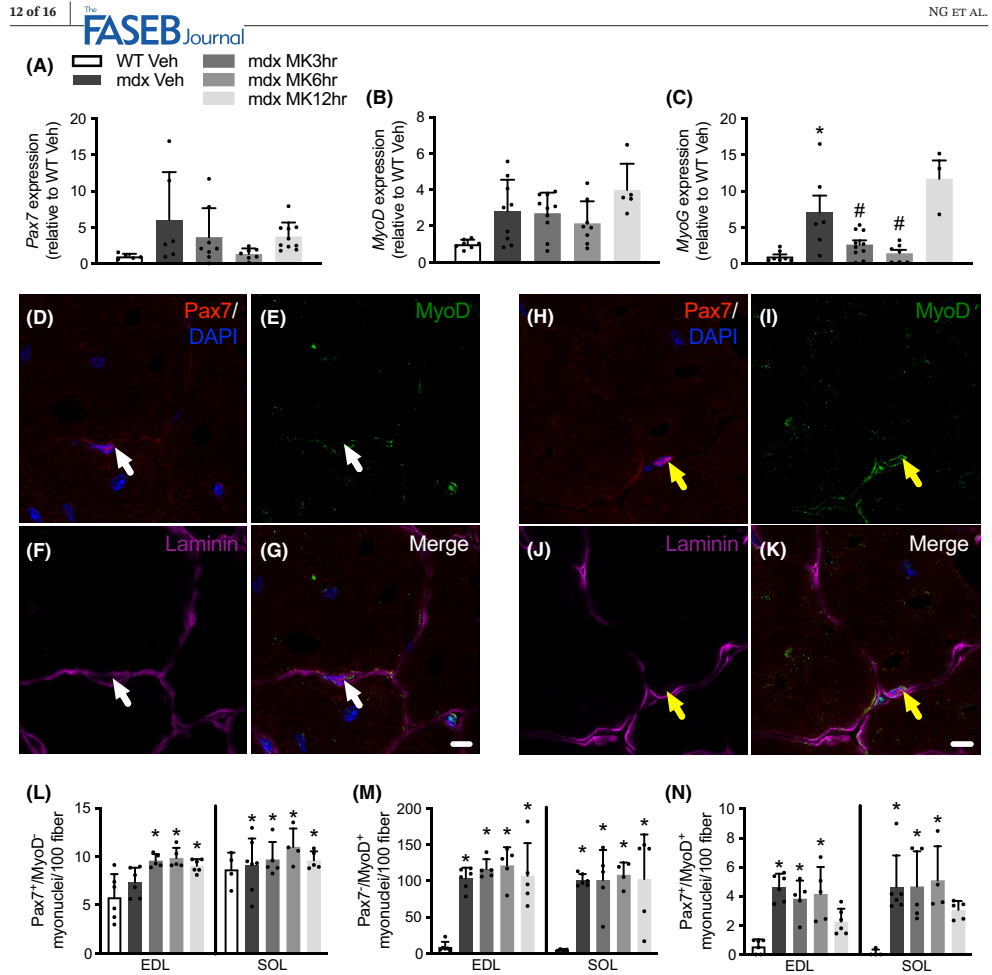


FIGURE 5 Effects of acute MK-evoked AMPK stimulation on myogenic regulatory factor expression and satellite cell biology in dystrophic muscle. Paired box 7 (*Pax7*; A), myogenic determination protein (*MyoD*; B), and myogenin (*MyoG*; C) mRNA expression in the TA muscles of Veh-treated WT mice and Veh- or MK-treated mdx animals. Data are expressed relative to the WT Veh group, represented by the dotted line. Representative immunofluorescence images of Pax7, MyoD, DAPI, and laminin in dystrophic EDL muscle (D–K). Pax7 and DAPI (red and blue, respectively; panels D, H), MyoD (green; panels E, I), and laminin (purple; panels F, J) are shown. Merged images of all channels are also shown (panels G, K). White arrows depict Pax7⁺/MyoD⁻ myonuclei in panels D–G, whereas yellow arrows indicate Pax7⁺/MyoD⁺ nuclei in panels H–K. Scale bars represent 10 μm. Graphical summaries of the number of Pax7⁺/MyoD⁻ myonuclei (L), Pax7⁺/MyoD⁺ myonuclei (M), and Pax7⁺/MyoD⁺ myonuclei (N) in the EDL and SOL muscles of WT Veh, mdx Veh, mdx MK3hr, mdx MK6hr, and mdx MK12hr animals. Graphical summaries show individual data (points) and group means (bars) with SDs. **p* < .05 versus WT Veh; #*p* < .05 versus mdx Veh. *n* = 8–10.

downstream outcomes such as decreased plasma glucose, reduced kidney fibrosis, and enhanced renal function.^{21,48} However, MK has not been examined in the dystrophic context. It therefore seemed reasonable to investigate the efficacy of MK at stimulating AMPK and its network in

dystrophic muscle. We observed an MK-induced elevation in several proximal metrics of AMPK activity in limb muscles of mdx animals, including AMPK and ACC phosphorylation status, as well as myonuclear pAMPK^{Thr172} levels. While the importance of nuclear-localized AMPK

content has not yet been fully elucidated, its potential role in the myonuclear compartment likely includes targeting of transcriptional regulators important for skeletal muscle plasticity, such as forkhead box O3a, histone deacetylases 4/5, and p300.³⁶ Our data also demonstrate strong trends for increased pACC^{Ser212} ($p = .07$) and ACC phosphorylation status ($p = .06$) in the DIA muscle, as well as significantly elevated pACC phosphorylation in the heart, of MK treated mdx mice, which suggests potential for MK efficacy in the context of severe myopathy of DMD patients. Our cardiac data should be interpreted with caution however, since chronic MK treatment has caused a reversible cardiac hypertrophy in diabetic rodents,²¹ a potentially undesirable phenotype in DMD. Thus, our initial findings demonstrate that the novel pan-AMPK agonist MK was effective at increasing AMPK activity in several dystrophic muscles. The long-term impact of MK administration on AMPK in dystrophic animals is beyond the scope of this study, however it is reasonable to hypothesize that chronic dosing would stimulate the kinase in muscle daily, analogous to habitual AMPK activation via exercise.⁴⁹

We next sought to determine if MK provokes downstream AMPK signaling germane to the dystrophic pathology. We detected in fast, glycolytic muscles a rise in myonuclear PGC-1 α translocation, increased *Ppargc1a* and *Nrf1* mRNA, and elevated utrophin protein expression in the MK-treated mdx animals. These alterations are indicative of a shift towards a slower, and more oxidative phenotype, which endows muscles with a heightened level of protection against DMD.^{38,50} The MK-induced myonuclear accumulation of PGC-1 α and increased *Ppargc1a* transcript levels strongly suggest augmented PGC-1 α activity,⁵¹ which is further supported by the subsequent increase in the PGC-1 α transcriptional target *Nrf1*.^{52,53} Our data also demonstrate a robust MK-evoked elevation in utrophin protein along with evidence of enhanced extrasynaptic utrophin expression in the absence of significant changes in *Utrn* transcript levels. These findings suggest that MK may regulate utrophin protein expression via post-transcriptional mechanisms likely at the 5' untranslated region (UTR) of *Utrn* mRNA.^{54,55} Similar findings have been reported with pravastatin treatment, which augmented utrophin protein content by recruiting eukaryotic elongation factor 1A2 to the utrophin 5' UTR.⁵⁶ Unfortunately, AMPK activity was not investigated in that recent study. However, statins, including pravastatin, evoke AMPK activation in skeletal muscle,^{57,58} which further supports the idea of AMPK-mediated pathways for utrophin upregulation.^{5,50} Collectively, our results demonstrate that a single dose of MK elicits the slow, oxidative gene program in the skeletal muscle of mdx animals via integration of transcriptional and post-transcriptional mechanisms.

We show that a single dose of MK can stimulate extensive autophagy signaling, including AMPK-specific pro-autophagic phosphorylation, as well as promote expression of the autophagy gene program in dystrophic muscle. In particular, MK conferred AMPK-mediated ULK1 regulation at the Ser555 mark, as well as reduced S6^{Ser235/236} phosphorylation status and tended to decrease mTOR-specific pULK1^{Ser757}, the latter two indicative of lower mTOR activity. These findings strongly suggest that MK targets ULK1 directly via AMPK and indirectly through the AMPK/mTOR/ULK1 signaling axis.^{59,60} Additionally, we observed elevations of autophagosome markers such as the LC3II/I ratio and p62 protein expression, as well as a rise in autophagy-related genes, including *Map1lc3*, *Gabra1*, and *Sqstm1*, in MK-treated mdx animals. Moreover, MK administration resulted in the myonuclear accumulation of the master regulator of autophagy gene expression, TFEB, which preceded the rise of autophagy-related genes. Together, these data assert that the autophagy program is initiated in dystrophic muscle following a single dose of MK. In non-dystrophic mice a single dose of exercise also evokes AMPK and significant autophagic programming in skeletal muscle.^{53,61} Interestingly, Muise and colleagues directly compared a single bout of exercise to a single dose of MK and observed similar transcriptional responses for autophagic genes in healthy skeletal muscle.²² Work from other laboratories have previously uncovered the effects of chronic AMPK activation on autophagy in skeletal muscle^{62,63} and associated beneficial outcomes in mdx animals.^{12,64,65} It is reasonable to speculate that repeated doses of this next-generation AMPK activator would also elicit autophagic adaptations accompanied by signs of mitigated muscular dystrophy.

Genetic and habitual pharmacological AMPK stimulation augment muscle regeneration in otherwise healthy animals.^{66–69} These chronic, AMPK-evoked benefits also enhance myogenic differentiation and myofiber repair in DMD models.^{8,13} Here, we sought to elucidate the acute cellular events that underpin these AMPK-mediated alterations in dystrophic mice. We report that a single dose of MK transiently reduces skeletal muscle *MyoG* transcript levels, a metric of early differentiation, as well as decreases the number of activated (i.e., Pax7⁺/MyoD⁺) MuSCs in the muscle of mdx animals. Although we are the first to document the rapid effects of acute AMPK agonism on MuSC biology in dystrophic mice, similar findings on muscle differentiation have been reported in mice subjected to a short-term (i.e., 48 h) cardiotoxin-induced regeneration timecourse and dosed with metformin.⁷⁰ Our data, indicating an altered myogenic program evoked by a single dose of MK, seem inconsistent with the chronic adaptations of genetic and pharmacological AMPK stimulation on

muscle regeneration in healthy and mdx animals.^{8,13,66–68} Nevertheless, our findings suggest that a transitory suppression of *MyoG* mRNA expression and activated MuSC abundance elicited by a single MK dose may contribute to the benefits of chronic, pharmacological AMPK agonism in dystrophic muscle. The mechanism by which this occurs is unknown, however we postulate these adaptations may be associated with the normalization of ectopic myogenic regulatory factor expression such as MyoD and myomaker, since high levels of these proteins induce a dystrophic phenotype.^{71,72} To answer this question more satisfactorily, it will be important to document the impact of AMPK activation on MuSC expression and function in the dystrophic and muscle repair/regeneration contexts using a comprehensive timecourse of acute and chronic dosing.

In summary, our study reveals that a single dose of MK elicits AMPK activation in the skeletal muscle of mdx mice and evokes several downstream signaling pathways and a gene expression signature that promote a disease-resilient phenotype in DMD. Our current experimental design does not allow us to conclude any long-term adaptations, including potentially adverse outcomes in the dystrophic context that may be realized from chronic MK treatment. Notably, although MK treatment in diabetic rodents provoked a reversible cardiac hypertrophy that was not associated with functional sequelae,²¹ an enlarged heart could exacerbate cardiovascular dysfunction in DMD. Future work should prioritize testing of chronic administration of next-generation AMPK activators in dystrophic animals to further examine their safety and therapeutic efficacy.

AUTHOR CONTRIBUTIONS

Sean Y. Ng and Vladimir Ljubcic conceived and designed the research; Sean Y. Ng, Andrew I. Mikhail, Stephanie R. Mattina, Alexander Manta, and Ian J. Diffey acquired and analyzed the data; and Sean Y. Ng and Vladimir Ljubcic interpreted the data. All authors approved the final manuscript.

ACKNOWLEDGMENTS

This work was supported by the Canadian Institutes of Health Research, the Canada Research Chairs program, Muscular Dystrophy Canada, and the Ontario Ministry of Economic Development, Job Creation and Trade (MEDJCT). SYN and SRM are Natural Sciences and Engineering Research Council of Canada postgraduate scholars. AIM is funded by an Ontario Graduate Scholarship. VL is the Canada Research Chair (Tier 2) in Neuromuscular Plasticity in Health and Disease and is a MEDJCT Early Researcher. All funding organizations did not have a role in the design, interpretation, or writing of this paper.

DISCLOSURES

The authors declare no competing interests.

DATA AVAILABILITY STATEMENT

The data that support the findings of this study are available on request from the corresponding author.

ORCID

Vladimir Ljubcic  <https://orcid.org/0000-0002-4592-4093>

REFERENCES

- Emery AEH. Population frequencies of inherited neuromuscular diseases—a world survey. *Neuromuscul Disord*. 1991;1:19-29.
- Birnkrant DJ, Bushby K, Bann CM, et al. Diagnosis and management of Duchenne muscular dystrophy, part 1: diagnosis, and neuromuscular, rehabilitation, endocrine, and gastrointestinal and nutritional management. *Lancet Neurol*. 2018;17:251-267.
- Verhaart IEC, Aartsma-Rus A. Therapeutic developments for Duchenne muscular dystrophy. *Nat Rev Neurol*. 2019;15:373-386.
- Himič V, Davies KE. Evaluating the potential of novel genetic approaches for the treatment of Duchenne muscular dystrophy. *Eur J Hum Genet*. 2021;29(29):1369-1376.
- Ljubcic V, Miura P, Burt M, et al. Chronic AMPK activation evokes the slow, oxidative myogenic program and triggers beneficial adaptations in mdx mouse skeletal muscle. *Hum Mol Genet*. 2011;20:3478-3493.
- Ljubcic V, Jasmin BJ. Metformin increases peroxisome proliferator-activated receptor γ Co-activator-1 α and utrophin a expression in dystrophic skeletal muscle. *Muscle Nerve*. 2015;52:139-142.
- Ljubcic V, Burt M, Lunde JA, Jasmin BJ. Resveratrol induces expression of the slow, oxidative phenotype in mdx mouse muscle together with enhanced activity of the SIRT1-PGC-1 axis. *AJP Cell Physiol*. 2014;307:C66-C82.
- Dong X, Hui T, Chen J, et al. Metformin increases sarcolemma integrity and ameliorates neuromuscular deficits in a murine model of Duchenne muscular dystrophy. *Front Physiol*. 2021;12:606.
- Gordon BS, Delgado Díaz DC, Kostek MC. Resveratrol decreases inflammation and increases utrophin gene expression in the mdx mouse model of duchenne muscular dystrophy. *Clin Nutr*. 2013;32:104-111.
- Al-Rewashdy H, Ljubcic V, Lin W, Renaud JM, Jasmin BJ. Utrophin a is essential in mediating the functional adaptations of mdx mouse muscle following chronic AMPK activation. *Hum Mol Genet*. 2015;24:1243-1255.
- Hulmi JJ, Oliveira BM, Silvennoinen M, et al. Exercise restores decreased physical activity levels and increases markers of autophagy and oxidative capacity in myostatin/activin-blocked mdx mice. *AJP Endocrinol Metab*. 2013;305:E171-E182.
- Pauly M, Daussin F, Burelle Y, et al. AMPK activation stimulates autophagy and ameliorates muscular dystrophy in the mdx mouse diaphragm. *Am J Pathol*. 2012;181:583-592.
- Juban G, Saclier M, Yacoub-Youssef H, et al. AMPK activation regulates LTBP4-dependent TGF- β 1 secretion by pro-inflammatory macrophages and controls fibrosis in Duchenne muscular dystrophy. *Cell Rep*. 2018;25:2163-2176.e6.

14. Péladeau C, Ahmed A, Amirouche A, et al. Combinatorial therapeutic activation with heparin and AICAR stimulates additive effects on utrophin expression in dystrophic muscles. *Hum Mol Genet.* 2016;25:24-43.
15. Hori YS, Kuno A, Hosoda R, et al. Resveratrol ameliorates muscular pathology in the dystrophic mdx mouse, a model for Duchenne muscular dystrophy. *Clin Nutr.* 2011;338:784-794.
16. Kuno A, Hosoda R, Sebori R, et al. Resveratrol ameliorates mitochondrial disturbance and improves cardiac pathophysiology of dystrophin-deficient mdx mice. *Sci Rep.* 2018;8:15555.
17. Mantuano P, Sanarica F, Conte E, et al. Effect of a long-term treatment with metformin in dystrophic mdx mice: a reconsideration of its potential clinical interest in Duchenne muscular dystrophy. *Biochem Pharmacol.* 2018;154:89-103.
18. Goodyear LJ. The exercise pill—too good to be true? *N Engl J Med.* 2008;359:1842-1844.
19. Hafner P, Bonati U, Klein A, et al. Effect of combination l-citrulline and metformin treatment on motor function in patients with Duchenne muscular dystrophy: a randomized clinical trial. *JAMA Netw Open.* 2019;2:e1914171.
20. Ljubicic V, Burt M, Jasmin BJ. The therapeutic potential of skeletal muscle plasticity in Duchenne muscular dystrophy: phenotypic modifiers as pharmacologic targets. *FASEB J.* 2014;28:548-568.
21. Myers RW, Guan H-P, Ehrhart J, et al. Systemic pan-AMPK activator MK-8722 improves glucose homeostasis but induces cardiac hypertrophy. *Science.* 2017;357:507-511.
22. Muise ES, Guan H-P, Liu J, et al. Pharmacological AMPK activation induces transcriptional responses congruent to exercise in skeletal and cardiac muscle, adipose tissues and liver. *PLoS One.* 2019;14:e0211568.
23. Gluais-Dagorn P, Foretz M, Steinberg GR, et al. Direct AMPK activation corrects NASH in rodents through metabolic effects and direct action on inflammation and fibrogenesis. *Hepatology Commun.* 2022;6:101-119.
24. Stephan Y, Souille M, Larcheveque M, et al. Both short-and long-term treatment with the direct AMP kinase activator PXL770 improves cardiac function in ZSF-1 rats. *Eur Heart J.* 2021;42:1050.
25. Kokorinos EC, Delmore J, Reyes AR, Wojtaszewski JFP, Cameron KO, Correspondence RAM. Activation of skeletal muscle AMPK promotes glucose disposal and glucose lowering in non-human primates and mice PF-739 treatment increases PGC1 α transcription and mitochondrial content in muscle. *Cell Metab.* 2017;25:1147-1159.e10.
26. Steneberg P, Lindahl E, Dahl U, et al. PAN-AMPK activator O304 improves glucose homeostasis and microvascular perfusion in mice and type 2 diabetes patients. *JCI Insight.* 2018;3:e99114.
27. Fouqueray P, Bolze S, Dubourg J, et al. Pharmacodynamic effects of direct AMP kinase activation in humans with insulin resistance and non-alcoholic fatty liver disease: a phase 1b study. *Cell Reports Med.* 2021;2:100474.
28. Cusi K, Alkhoury N, Harrison SA, et al. Efficacy and safety of PXL770, a direct AMP kinase activator, for the treatment of non-alcoholic fatty liver disease (STAMP-NAFLD): a randomised, double-blind, placebo-controlled, phase 2a study. *Lancet Gastroenterol Hepatol.* 2021;6:889-902.
29. Stouth DW, Van Lieshout TL, Ng SY, et al. CARM1 regulates AMPK signaling in skeletal muscle. *iScience.* 2020;23:101755.
30. Dimauro I, Pearson T, Caporossi D, Jackson MJ. A simple protocol for the subcellular fractionation of skeletal muscle cells and tissue. *BMC Res Notes.* 2012;5:1-5.
31. Ng SY, Mikhail A, Ljubicic V. Mechanisms of exercise-induced survival motor neuron expression in the skeletal muscle of spinal muscular atrophy-like mice. *J Physiol.* 2019;597:4757-4778.
32. Joannis S, Nederveen JP, Baker JM, Snijders T, Iacono C, Parise G. Exercise conditioning in old mice improves skeletal muscle regeneration. *FASEB J.* 2016;30:3256-3268.
33. Osseni A, Ravel-Chapuis A, Thomas J-L, Gache V, Schaeffer L, Jasmin BJ. HDAC6 regulates microtubule stability and clustering of AChRs at neuromuscular junctions. *J Cell Biol.* 2020;219:e201901099.
34. Mallik B, Dwivedi MK, Mushtaq Z, Kumari M, Verma PK, Kumar V. Regulation of neuromuscular junction organization by Rab 2 and its effector ICA69 in drosophila. *Dev.* 2017;144:2032-2044.
35. Schmittgen TD, Livak KJ. Analyzing real-time PCR data by the comparative CT method. *Nat Protoc.* 2008;3:1101-1108.
36. Trefts E, Shaw RJ. AMPK: restoring metabolic homeostasis over space and time. *Mol Cell.* 2021;81:3677-3690.
37. Schmitt DL, Curtis SD, Lyons AC, et al. Spatial regulation of AMPK signaling revealed by a sensitive kinase activity reporter. *Nat Commun.* 2022;13(13):1-12.
38. Dial AG, Ng SY, Manta A, Ljubicic V. The role of AMPK in neuromuscular biology and disease. *Trends Endocrinol Metab.* 2018;29:300-312.
39. Scarpulla RC. Metabolic control of mitochondrial biogenesis through the PGC-1 family regulatory network. *Biochim Biophys Acta-Mol Cell Res.* 2011;1813:1269-1278.
40. Palmieri M, Impey S, Kang H, et al. Characterization of the CLEAR network reveals an integrated control of cellular clearance pathways. *Hum Mol Genet.* 2011;20:3852-3866.
41. Yamane A, Akutsu S, Diekwisch TGH, Matsuda R. Satellite cells and utrophin are not directly correlated with the degree of skeletal muscle damage in mdx mice. *Am J Physiol Cell Physiol.* 2005;289:42-48.
42. Iannotti FA, Pagano E, Guardiola O, et al. Genetic and pharmacological regulation of the endocannabinoid CB1 receptor in duchenne muscular dystrophy. *Nat Commun.* 2018;9:3950.
43. Jin Y, Murakami N, Saito Y, Goto YI, Koishi K, Nonaka I. Expression of Myo D and myogenin in dystrophic mice, mdx and dy, during regeneration. *Acta Neuropathol.* 2000;99:619-627.
44. Ljubicic V, Khogali S, Renaud J-M, Jasmin BJ. Chronic AMPK stimulation attenuates adaptive signaling in dystrophic skeletal muscle. *AJP Cell Physiol.* 2012;302:C110-C121.
45. Steinberg GR, Carling D. AMP-activated protein kinase: the current landscape for drug development. *Nat Rev Drug Discov.* 2019;18(7):527-551. doi:10.1038/s41573-019-0019-2
46. Feng D, Biftu T, Romero FA, et al. Discovery of MK-8722: a systemic, direct pan-activator of AMP-activated protein kinase. *ACS Med Chem Lett.* 2018;9(1):39-44. doi:10.1021/acsmchemlett.7b00417
47. Rhein P, Desjardins EM, Rong P, et al. Compound- and fiber type-selective requirement of AMPK γ 3 for insulin-independent glucose uptake in skeletal muscle. *Mol Metab.* 2021;51:101228.
48. Zhou X, Muise ES, Haimbach R, et al. Pan-AMPK activation improves renal function in a rat model of progressive diabetic nephropathy. *J Pharmacol Exp Ther.* 2019;371:45-55.

49. Egan B, Zierath JR. Exercise metabolism and the molecular regulation of skeletal muscle adaptation. *Cell Metab.* 2013;17:162-184.
50. Ljubicic V, Jasmin BJ. AMP-activated protein kinase at the nexus of therapeutic skeletal muscle plasticity in Duchenne muscular dystrophy. *Trends Mol Med.* 2013;19:614-624.
51. Handschin C, Kobayashi YM, Chin S, Seale P, Campbell KP, Spiegelman BM. PGC-1 α regulates the neuromuscular junction program and ameliorates Duchenne muscular dystrophy. *Genes Dev.* 2007;21:770-783.
52. Ljubicic V, Joseph AM, Saleem A, et al. Transcriptional and post-transcriptional regulation of mitochondrial biogenesis in skeletal muscle: effects of exercise and aging. *Biochim Biophys Acta-Gen Subj.* 2010;1800:223-234.
53. Hood DA, Memme JM, Oliveira AN, Triolo M. Maintenance of skeletal muscle mitochondria in health, exercise, and aging. *Annu Rev Physiol.* 2019;81:19-41.
54. Miura P, Thompson J, Chakkalakal JV, Holcik M, Jasmin BJ. The utrophin a 5'-untranslated region confers internal ribosome entry site-mediated translational control during regeneration of skeletal muscle fibers. *J Biol Chem.* 2005;280:32997-33005.
55. Miura P, Coriati A, Bélanger G, et al. The utrophin a 5'-UTR drives cap-independent translation exclusively in skeletal muscles of transgenic mice and interacts with eEF1A2. *Hum Mol Genet.* 2010;19:1211-1220.
56. Péladeau C, Adam N, Bronicki LM, et al. Identification of therapeutics that target eEF1A2 and upregulate utrophin A translation in dystrophic muscles. *Nat Commun.* 2020;11:1990.
57. Dehnavi S, Kiani A, Sadeghi M, et al. Targeting AMPK by statins: a potential therapeutic approach. *Drugs.* 2021;81:923-933.
58. Izumi Y, Shiota M, Kusakabe H, et al. Pravastatin accelerates ischemia-induced angiogenesis through AMP-activated protein kinase. *Hypertens Res.* 2009;32:675-679.
59. Kim J, Kundu M, Viollet B, Guan KL. AMPK and mTOR regulate autophagy through direct phosphorylation of Ulk 1. *Nat Cell Biol.* 2011;13:132-141.
60. Egan DF, Shackelford DB, Mihaylova MM, et al. Phosphorylation of ULK1 (hATG1) by AMP-activated protein kinase connects energy sensing to mitophagy. *Science (80-).* 2011;331:456-461.
61. Spaulding HR, Yan Z. AMPK and the adaptation to exercise. *Annu Rev Physiol.* 2022;84:209-227.
62. Sanchez AMJ, Csibi A, Raibon A, et al. AMPK promotes skeletal muscle autophagy through activation of forkhead fox O3a and interaction with Ulk 1. *J Cell Biochem.* 2012;113:695-710.
63. Laker RC, Drake JC, Wilson RJ, et al. Ampk phosphorylation of Ulk 1 is required for targeting of mitochondria to lysosomes in exercise-induced mitophagy. *Nat Commun.* 2017;8:548.
64. De Palma C, Morisi F, Cheli S, et al. Autophagy as a new therapeutic target in Duchenne muscular dystrophy. *Cell Death Dis.* 2012;5:e1363.
65. Fiacco E, Castagnetti F, Bianconi V, et al. Autophagy regulates satellite cell ability to regenerate normal and dystrophic muscles. *Cell Death Differ.* 2016;23:1839-1849.
66. Mounier R, Thérét M, Arnold L, et al. AMPK α 1 regulates macrophage skewing at the time of resolution of inflammation during skeletal muscle regeneration. *Cell Metab.* 2013;18:251-264.
67. McArthur S, Juban G, Gobetti T, et al. Annexin A1 drives macrophage skewing to accelerate muscle regeneration through AMPK activation. *J Clin Invest.* 2020;130:1156-1167.
68. Theret M, Gsaier L, Schaffer B, et al. AMPK α 1-LDH pathway regulates muscle stem cell self-renewal by controlling metabolic homeostasis. *EMBO J.* 2017;36:1946-1962.
69. Yousuf Y, Datu A, Barnes B, Amini-Nik S, Jeschke MG. Metformin alleviates muscle wasting post-thermal injury by increasing Pax 7-positive muscle progenitor cells. *Stem Cell Res Ther.* 2020;11:1-14.
70. Pavlidou T, Marinkovic M, Rosina M, et al. Metformin delays satellite cell activation and maintains quiescence. *Stem Cells Int.* 2019;2019:1-19.
71. Boyer JG, Huo J, Han S, et al. Depletion of skeletal muscle satellite cells attenuates pathology in muscular dystrophy. *Nat Commun.* 2022;13(13):1-10.
72. Petranj MJ, Song T, Sadayappan S, Millay DP. Myocyte-derived Myomaker expression is required for regenerative fusion but exacerbates membrane instability in dystrophic myofibers. *JCI Insight.* 2020;5(9):e136095.

How to cite this article: Ng SY, Mikhail AI, Mattina SR, Manta A, Diffey IJ, Ljubicic V. Acute, next-generation AMPK activation initiates a disease-resistant gene expression program in dystrophic skeletal muscle. *The FASEB Journal.* 2023;37:e22863. doi:[10.1096/fj.202201846RR](https://doi.org/10.1096/fj.202201846RR)

CHAPTER 4:

Orally bioavailable pan-AMPK activator MK-8722 attenuates the dystrophic phenotype in D2.mdx animals

Title: Orally bioavailable pan-AMPK activator MK-8722 attenuates the dystrophic phenotype in D2.mdx animals

Authors: Sean Y Ng¹, Aislin K Osborne¹, Andrew I Mikhail¹, Irena A. Rebalka², Sophie I Hamstra^{3,4}, Shahzeb K Khan¹, Beverly V Yap¹, Val A. Fajardo^{3,4}, Gregory R Steinberg^{5,6,7}, Thomas J. Hawke², Vladimir Ljubcic^{1*}

Affiliations:

¹Department of Kinesiology, McMaster University, 1280 Main St. W., Hamilton, ON, Canada L8S 4L8.

²Department of Pathology and Molecular Medicine, McMaster University, Hamilton, ON, L8S 4L8, Canada

³Department of Kinesiology, Brock University, St. Catharines, ON, 1812 Sir Isaac Brock Way, St. Catharines, ON L2S 3A1

⁴Center for Bone and Muscle Health, Brock University, St. Catharines, ON, 1812 Sir Isaac Brock Way, St. Catharines, ON L2S 3A1

⁵Centre for Metabolism, Obesity and Diabetes Research, McMaster University, 1280 Main St. W., Hamilton, ON, Canada L8N 3Z5.

⁶Division of Endocrinology and Metabolism, Department of Medicine, McMaster University, 1280 Main St. W., Hamilton, ON, Canada L8N 3Z5.

⁷ Department of Biochemistry and Biomedical Sciences, McMaster University, 1280 Main St. W., Hamilton, ON, Canada L8N 3Z5.

*Corresponding author. Email: ljubicic@mcmaster.ca

Abstract:

Duchenne Muscular Dystrophy (DMD) is a devastating genetic disorder characterized by progressive muscle wasting and weakness, for which current gene-based therapies have not yet yielded a cure. AMP-activated protein kinase (AMPK) is a metabolic signaling protein that regulates several cellular pathways implicated in DMD pathogenesis; however, a safe and efficacious AMPK agonist has yet to be identified for the treatment of DMD. Herein, we demonstrate that the pan-AMPK agonist, MK-8722 (MK), effectively restores mitochondrial features and attenuates muscle fibrosis in dystrophic muscle, significantly contributing to the recovery of muscle function. These data suggest that the

chronic activation of AMPK mitigates symptoms of DMD and implicates this new class of AMPK activators as a potential therapeutic option for muscular dystrophy.

INTRODUCTION

Duchenne muscular dystrophy (DMD) is a X-linked recessive disorder, constituting the most prevalent congenital neuromuscular ailment that affects approximately 1 in 5,000 live male births (1, 2). DMD is caused by mutations within the *DMD* gene that prevent the production of the encoded protein product, dystrophin. The absence of this structural protein results in the dissociation of its larger oligomeric complex and results in the progressive loss of muscle mass and function (3, 4). While many management strategies exist, most patients do not survive to their forties, due to cardiac and/or respiratory failure. Several exon-skipping-based therapies and gene therapies have secured FDA approval, and will undoubtedly enhance the overall well-being and longevity of a considerable population affected by the disorder (5). It is imperative, however, to acknowledge that the majority of these therapies (i.e., Amondys 45, Exondys 51, Vyondys 53, Sarepta Therapeutics) solely target specific dystrophin mutations and do not encompass the extensive genetic heterogeneity prevalent in muscular dystrophy cases. Furthermore, emerging adenosine associated virus-based therapies have been shown to evoke adverse immune responses due to gene delivery vector and enclosed transgene (6). Consequently, it becomes paramount to prioritize the development of therapeutic approaches that can effectively address the needs of all individuals affected by DMD, regardless of the specific genetic mutation they harbor, while being safe and tolerable.

The repeated activation of AMP-activated protein kinase (AMPK) in skeletal muscle presents an attractive therapeutic approach for DMD due to its ability to ameliorate the dystrophic characteristics, irrespective of dystrophin modulation (7). As such, this strategy holds potential applicability to all DMD patients, regardless of the specific gene mutation they carry. Preliminary studies validating this concept have revealed that pharmacological AMPK activators can induce a transition of skeletal muscle towards a slower and more oxidative phenotype, resulting in enhanced resistance to the DMD myopathy (8–10). The attenuation of the dystrophic phenotype has also been attributed to the upregulation of the dystrophin homolog, utrophin (7, 8, 11), in addition to corrective adjustments to the compromised autophagy program (12, 13), enhanced muscle regeneration (14, 15), and reduced fibrosis (15, 16). These diverse cellular effects of AMPK present an attractive integrative approach to address the myriad of complications present in dystrophic muscle.

The practical implementation of pharmacological AMPK induction to alleviate dystrophic pathology in the clinical setting for DMD has faced obstacles, partially due to lack of potency and off-target cell effects associated with the compounds (8–11, 13, 17–19). Recently, a new series of orally-bioactive AMPK agonists has been identified, which demonstrated potent kinase activation in the skeletal muscle of various pre-clinical models of metabolic dysfunction (20–25) and exhibited good tolerability in patient cohorts with metabolic diseases (25–27). We have previously evaluated the immediate responses to one of these novel agonists, MK-8722 (MK), in the mdx mouse model, which unveiled notable enhancements in disease-mitigating mechanisms within dystrophic muscle (28). However,

whether the sustained administration of MK can yield beneficial effects on dystrophic pathology in skeletal muscle has yet to be ascertained. Therefore, we sought explore the impact of chronic MK treatment on the function and phenotype of dystrophic skeletal muscle, as well as provide a comprehensive analysis of the cellular and molecular adaptations that may accompany.

RESULTS

MK evokes AMPK and downstream signaling in D2.mdx animals.

To better resemble the dystrophic phenotype that is characterized in DMD patients, we utilized the D2.mdx animals, a more severe and clinically relevant murine model (29). First, we administered a single dose of MK (5 mpk) via oral gavage to D2.mdx animals and collected their tibialis anterior (TA) muscles 1-, 3-, and 12 h post-gavage to confirm the agonist effects in the skeletal muscles of D2.mdx animals (Fig. S1A). Immunoblotting analyses revealed that the phosphorylation status (Phospho-status) of AMPK was similar across all timepoints following MK treatment (Fig. S1B, C). Acetyl-CoA carboxylase (ACC) phospho-status (pACC^{Ser212}/ACC expression) was 120-150% higher in the 1- and 3 h post-gavage groups when compared to their Vehicle (Veh)-treated counterparts. Furthermore, the levels of ACC phospho-status 12 hr post treatment were similar to the Veh-treated animals. Together these data provide evidence of a transient MK-mediated effect on AMPK in dystrophic muscle.

Subsequently, we assessed AMPK-targeted transcripts in the TA muscles of Veh- and MK-treated animals at the 3-hour mark, with the aim of capturing early transcriptional

responses. We observed a 60% increase in *Ppargc1a* transcript in MK-treated D2.mdx animals when compared to their Veh-treated controls. Autophagy-related transcripts, including *Map1lc3a*, *Sqstm1*, *Ulk1*, and *Gabarapl1* (Fig. S1D), as well as myogenic regulatory transcript expression, such as *Pax7*, *Myf5*, *Myod*, and *Myog* (Fig. S1E), were similar between Veh- and MK-treated animals. Notably, we observed a 25-50% reduction in the expression of inflammation- and fibrosis-related transcripts (*Cd68*, *Lgal3*, *Ctgf*, and *Colla*) in the TA muscles of MK-treated animals when compared to their healthy WT counterparts (Fig. 1F).

The effects of chronic MK administration on tissue morphology.

To evaluate the therapeutic potential of chronic MK treatment in DMD, a Veh or MK (5 mpk) solution was administered daily for a duration of seven weeks. (Fig. 1A). The treated D2.mdx animals were further divided into two groups: sedentary (D2.mdx Veh, D2.mdx MK) and EX (D2.mdx EX, D2.mdx MK+EX) cohorts. D2.mdx animals exhibited a significantly lower (-7.6%) body weight and a higher (+5.0%) body fat composition compared to their healthy WT counterparts (Table 1). The relative mass of the triceps, quadriceps (QUAD), TA, and gastrocnemius (GAST) muscles from the D2.mdx animals were significantly reduced (-15-20%) when compared to their age-matched healthy controls. No discernible effects of MK treatment or EX on muscle mass were observed in the dystrophic animals. Cardiac mass did not differ significantly ($P > 0.05$) between genotypes, and neither MK treatment nor EX demonstrated any influence on heart mass. Liver mass remained consistent across all experimental groups following seven weeks of MK treatment, irrespective of physical activity.

Impact of MK treatment and EX on cardiac morphology and function in D2.mdx animals.

Consistent with our macroscopic observations, the predicted left ventricular (LV) cardiac mass was found to be similar ($P > 0.05$) across all experimental groups. Morphological metrics of the LV, including relative wall thickness, end-diastolic volume, and end-stroke volume, were comparable ($P > 0.05$) among Veh- or MK-treated D2.mdx animals (Table 2). Likewise, cardiac functional measures such as fractional shortening, ejection fraction, cardiac output, ejection time, and myocardial performance index displayed no significant differences ($P > 0.05$) between the experimental groups (Table 3), indicating no detrimental effects of MK or physical activity at this stage of disease. Additional analyses of the LV mitral valve were conducted to detect potential diastolic dysfunction previously reported in DMD animals (30, 31) and patients (32). Peak mitral E- and A-wave velocity were significantly lower (-25-35%) in the D2.mdx animals compared to their WT controls (Table 4). Notably, the MK-treated D2.mdx animals exhibited a 50% increase in peak mitral E-wave velocity relative to their Veh-treated D2.mdx littermates and was comparable ($P > 0.05$) to the healthy WT controls. Nonetheless, the collective findings indicate that neither MK treatment nor EX exacerbates the cardiac phenotype in presymptomatic D2.mdx animals.

Effects of MK treatment and EX on in vivo muscle strength and motor function metrics in D2.mdx animals.

As expected, D2.mdx animals displayed evident muscular weakness during our battery of in vivo functional tests. Dystrophic animals exhibited a 75% reduction ($P < 0.05$)

in inverted cage hang time, a 25% lower ($P < 0.05$) maximum grip strength force, a 100% higher ($P < 0.05$) grip strength fatigue, and a 46% decrease ($P < 0.05$) in EX duration compared to their WT counterparts (Fig. 1B-F). Following 6 weeks of intervention, D2.mdx MK+EX animals demonstrated a substantial 75% improvement ($P < 0.05$) in inverted cage hang time relative to their Veh-treated counterparts (Fig. 1B). Importantly, no discernible effect of MK treatment or EX was observed on maximum all limb grip strength force in the D2.mdx animals (Fig. 1C). However, the fatigue index of MK-treated D2.mdx animals was lower (-34%) compared to the sedentary Veh-treated D2.mdx animals and similar ($P > 0.05$) to their healthy WT controls, suggesting that MK improved the resistance to muscle fatigue. Lastly, a notable 32% increase ($P = 0.06$) in EX duration time was observed in the MK-treated D2.mdx animals compared to the Veh-treated D2.mdx mice (Fig. 1E, F).

The results of our motor performance and behavior testing indicated a significant impairment in dystrophic animals compared to the healthy WT mice. Rotarod testing showed a substantial 60% reduction in motor performance in dystrophic animals relative to the healthy WT animals (Fig. 2G). Analysis of open field behavior revealed a 35% reduction ($P < 0.05$) in the distance traveled by D2.mdx mice (Fig. 2H). Rotarod measures and open field metrics were similar ($P < 0.05$) between Veh- or MK-treated D2.mdx animals, suggesting that there were no improvements with chronic MK treatment or physical activity. Additional motor function outcomes, such as falls and reach testing (33), were similar ($P > 0.05$) between all D2.mdx groups (Data not shown).

Effects of MK treatment and EX on ex vivo muscle function metrics in D2.mdx animals.

To evaluate the gold standard of muscle force production, we performed a series of *ex vivo* muscle function tests to evaluate muscle twitch kinetics, force frequency relationships, and eccentric-induced force drop in Veh-treated or MK-treated D2.mdx animals. As expected, muscle twitch metrics were significantly altered in EDL muscles of the D2.mdx animals compared to their WT controls (Table 5). Specifically, the EDL muscles of D2.mdx animals exhibited a reduction in max twitch force (-62%), max rate of force development (-66%), and max rate of relaxation (-77%), along with a 250% increase in half relaxation rate. MK or EX interventions did not impact twitch. The half relaxation time was 30% lower in the MK-treated D2.mdx animals relative to their Veh treated counterparts. Max twitch force, as well as max rates of force development and relation, were similar ($P > 0.05$) between all D2.mdx animals.

Similar to previous reports (34, 35), the electrical stimulated muscle force produced in the EDL muscles of all D2.mdx animals were 50% lower compared to their age-matched WT counterparts. Sedentary MK-treated animals demonstrated a higher (+30%) absolute and greater (+10%) relative peak force production when compared to their Veh-treated controls (Fig. 2A, B, C). Our preliminary evaluation of NMJ morphology, revealed enlarged postsynapses in the epitrochleoanconeus (ETA) muscles of MK-treated mice. D2.mdx EX and D2.mdx MK+EX animals exhibited perforated pretzel-like shape NMJs resembling the healthy neuromuscular phenotype in WT animals. These observations

suggest that repeated MK treatment may enhance the stability of the NMJ, potentially contributing to the enhanced force production displayed in the MK-treated animals.

Following the force frequency protocol, an eccentric-induced muscle damage procedure was performed to evaluate the susceptibility to contractile damage in the EDL muscles. Dystrophic animals demonstrated a 50% reduction ($P < 0.05$) in force whereas a typical 30% drop was observed in the healthy control group (Fig. 2D, E). MK treatment or EX did not significantly impact the degree of force loss in dystrophic animals, as the percentage of force drop was similar ($P > 0.05$) among all dystrophic animals.

The effects of repeated MK treatment on the expression and localization of the utrophin associated protein complex

Contrary to previous reports with dystrophic animals, we did not observe a significant difference in utrophin expression between the WT and D2.mdx animals (Fig 3A, B). This diminished difference may be attributed to the reduced myogenic capacity observed in dystrophic muscle, as utrophin expression is known to be highly expressed in regenerating muscle fibers (36–38). Nonetheless, our study revealed a significant increase (+70%) in utrophin expression in the TA muscles of MK-treated D2.mdx animals compared to those treated with the Veh (Fig. 3A, B). Notably, the D2.mdx EX and D2.mdx MK+EX groups displayed utrophin expression levels akin to their Veh-treated controls (Fig. 3A, C). Similarly, the expression of utrophin-associated proteins, such as γ -sarcoglycan (γ SG) and β -dystroglycan (β DG), were trending ($P = 0.1$) 10-15% greater in MK-treated and EX animals when compared to their Veh-treated counterparts, and similar ($P > 0.05$) to their healthy WT controls (Fig. 3A, C). To further confirm this finding, immunolabeling of γ SG

and β DG was conducted to visualize the localization of the membrane proteins in the GAST and plantaris (G&P) muscles (Fig. 3H, I).

Next, we performed immunofluorescence experiments to reveal muscle fiber types and synaptic and extrasynaptic utrophin in serially cyrosectioned G&P muscles from all experimental groups. The combination of these techniques distinguishes regions enriched with slow oxidative (SO) muscle fibers (Fig 3D) and predominantly faster and more glycolytic areas (FG; Fig 3E), which permits the evaluation of AMPK-mediated fiber-type specific differences with utrophin expression. Consistent with previous observations (39), we demonstrate an apparent increase in utrophin expression along the sarcolemma of the SO regions compared to the FG areas of G&P muscles of dystrophic animals (Fig. 3D, E). Our initial assessment suggests that utrophin expression within the SO regions of the G&P muscles are similar among all experimental groups (Fig 3D). Variations between the groups became more apparent within the FG areas of G&P muscles. Specifically, we observed elevated levels of utrophin expression along the sarcolemma in the FG muscle fibers of Veh-treated D2.mdx animals relative to their healthy WT controls (Fig. 3C-D). Interestingly, this intensification of staining appeared to be more pronounced in the MK-treated D2.mdx animals, particularly within the synaptic and extrasynaptic regions of the sarcolemma (Fig. 3F-G).

Chronic effects of MK on mitochondrial content and function in dystrophic skeletal muscle.

Given previous reports of AMPK-mediated mitochondrial adaptations in dystrophic muscle, we sought to evaluate the effects of MK on mitochondrial respiration in the

severely affected QUAD muscle. High-resolution respiratory analysis using Oroboros-O2K revealed a significant 50-55% decrease in complex I (CI)-linked state III respiration, as well as a 55% lower ($P < 0.05$) CI+CII-linked respiration (Fig 4A, B) in sedentary Veh-treated D2.mdx animals compared to their healthy WT controls. Dystrophic animals receiving MK, EX, or MK+EX exhibited a remarkable increase (+80-125%, $P < 0.05$) in CI-linked state III respiration (Fig. 4A). Similarly, CI+CII-linked state 3 respiration was 95% elevated ($P < 0.05$) in D2.mdx animals that receiving MK, but not EX or MK+EX (Fig. 4B). Simultaneous measurement of reactive oxygen species (ROS) production revealed an elevated (+200%, $P < 0.05$) CI-linked state II ROS production. Interestingly, MK treatment resulted in a marked 70% reduction ($P < 0.05$) in CI-linked state II ROS production (Fig. 4C). EX alone or the combination of MK+EX did not significantly affect ROS production in dystrophic muscle. Collectively, these data demonstrate a significant decline in mitochondrial content and respiration in dystrophic animals that can be ameliorated with repeated MK treatment.

To compliment these findings, we evaluated mitochondrial content with immunoblotting experiments. As anticipated, the QUAD muscles of D2.mdx animals exhibited a substantial decrease (-20-45%) in mitochondrial content compared to their healthy WT controls (Fig. 4D, E). Remarkably, the expression levels of mitochondrial CI, CII, CIII, CIV, and CV were also significantly increased (+5-45%) by MK treatment, physical activity, and the combination of both, reaching levels comparable to the healthy control condition. The expression of peroxisome proliferator-activated receptor γ coactivator-1 α (PGC-1 α), a key regulator of mitochondrial biogenesis, was reduced (-50%)

in the D2.mdx Veh group, compared to the WT animals (Fig. 4D, F). The mitochondrial fusion marker optic atrophy 1 (OPA1) protein was 25% lower ($P < 0.05$) in the D2.mdx Veh group, while mitofusin 2 (MFN2) expression was remarkably higher (+190%), when compared to their healthy counterparts (Fig 4D, G). Indicators of mitochondrial fission, including the phospho-status of DRP^{Ser616} (Ser⁶¹⁶-phosphorylated dynamin-related protein 1 relative to total DRP expression) and the expression of fission1 (FIS) protein were 30-40% higher in the dystrophic animals compared to their WT controls (Fig. 4D, H), suggesting an imbalance favoring fission in the dystrophic condition. Interestingly, the expression of PINK, a protein involved in mitophagy, was consistently lower (-45-60%) in all dystrophic animals, suggesting a potential disruption in the clearance of damaged mitochondria (Fig. 4D, I). Despite the absence of discernible effects of MK, EX, or MK+EX in D2.mdx animals, our previous assertions (40) regarding the impact of DMD on mitochondrial balance and dynamics are further supported by these findings.

The effects of MK and EX on skeletal muscle fibrosis in D2.mdx animals.

Since a dose of MK elicited reductions in inflammatory and fibrosis-related genes, we were prompted to delve deeper into investigating the chronic effects of MK treatment on fibrosis in dystrophic muscle. Masson trichrome staining was performed to visualize extracellular matrix (ECM) deposition and fibrotic areas in the G&P muscles of dystrophic animals. Consistent with previous reports (29, 36, 41), the D2.mdx Veh animals exhibited an extensive, blue-stained collagen fibers throughout the G&P muscles (Fig. 5A, a), indicating a high level of ECM deposition and fibrosis (+15-25%) relative to their healthy controls (Fig, 5E, F). D2.mdx animals that received MK treatment, EX, or the combination

of both revealed lower ECM deposition (Fig 5E). Furthermore, the percentage of collagen-stained area was 15% lower in the GAST muscles of MK-treated and EX D2.mdx animals (Fig, 5F, G).

To compliment these data, we sought to elucidate the molecular mechanisms underlying the observed effects of MK treatment on muscle fibrosis in DMD. To this end, we evaluated the protein expression levels of key fibrosis signaling molecules, including platelet-derived growth factor receptor (PDGFR), transforming growth factor- β (TGF- β), and mothers against decapentaplegic homolog (SMAD). Our immunoblotting analyses revealed that that Veh-treated D2.mdx animals exhibited a significantly higher (+200-300%) level of PDGFR and TGF- β protein expression in the TA muscles compared to their healthy WT counterparts (Fig 5H-J). Additionally, SMAD phospho-status was also elevated (+75%, $P < 0.05$) in the Veh-treated group (Fig. 6K). In contrast, the D2.mdx MK, D2.mdx Ex, and D2.mdx MK+EX showed a significant decrease (-45-55%) in PDGFR protein expression compared to the Veh-treated animals. However, TGF- β protein expression was similar ($P > 0.05$) between the Veh- and MK-treated dystrophic animals. Furthermore, the MK-treated group exhibited a strong trend to a 30% reduction ($P = 0.06$) in SMAD phospho-status (Fig. 5K), suggesting that MK treatment may suppress downstream TGF- β signaling and mitigate fibrosis development.

DISCUSSION

Our previous work has established that a single dose of MK elicits AMPK activation and downstream signaling cascades in the skeletal muscle of mdx animals. In this current

study, we have further extended our inquiry to assess the effects of both acute and chronic MK administration in D2.mdx animals. The repeated dosing of MK in D2.mdx animals led to significant improvements in limb muscle function and force production, accompanied by a notable reduction in muscle fatiguability. The MK-treated animals also exhibited elevated membrane localization and expression of utrophin, along with the utrophin-associated proteins, γ SG and β DG. Furthermore, these pharmacological adaptations coincided with enhancements on mitochondrial respiration and content in the QUAD muscles of D2.mdx animals. Lastly, acute MK dosing led to the downregulation of inflammatory and fibrotic gene programs, consistent with the overall reduction in fibrosis and PDGFR expression observed in the skeletal muscles of chronically MK-treated D2.mdx animals. The data collectively demonstrate that the novel AMPK activator can endow a disease-resistant phenotype in DMD muscle, implicating MK as a potential therapy for the treatment of DMD.

Early AMPK enhancers, such as metformin, resveratrol, and 5-aminoimidazole-4-carboxamide-1- β -D-ribofuranoside (AICAR), have faced challenges in their translation to the neuromuscular clinic due to limited potency in skeletal muscle (10, 42) and adverse effects on the liver (43). The emergence of pan-AMPK activators, exemplified by MK, addresses potency concerns as they stimulate all AMPK isoforms, including those exclusive to skeletal muscle (20, 44). However, the daily administration of MK has been associated with hypertrophic cardiomyopathy, likely due to prolonged AMPK activation in cardiac cells (20, 21). Considering this potential deleterious impact on dystrophic hearts, we investigated the chronic effects of MK in this tissue. Following a 7-week daily treatment

regimen with MK, D2.mdx animals did not manifest cardiac hypertrophy or dysfunction, while concurrently, showing no instances of liver hepatomegaly. Interestingly, our previous findings have demonstrated that mdx mouse exhibit a sustained and prolonged AMPK activation in response to MK treatment (28), whereas the current data reveals a transient MK-induced AMPK stimulation in the skeletal muscles of D2.mdx animals. This disparity in catalytic duration between the models highlights the potential influence of disease severity on the pharmacodynamics of AMPK agonists. This is not surprising as variations in drug absorption, linked to gastrointestinal complications in late-stage DMD patients (2), likely explain the divergent pharmacokinetics between healthy and dystrophic phenotypes. Future research should assess whether the absence of adverse effects persist during the late stages of DMD, specifically during the symptomatic stage of cardiomyopathy.

In the current study, we demonstrate that the repeated MK treatment, EX, and the combination of both, preserve mitochondrial respiration in the skeletal muscles of D2.mdx animals. This adaptive response in the mitochondria coincides with a notable increase in mitochondrial content, as evidenced by elevated levels of mitochondrial CI-CV subunits and the acute induction of the *Ppargcal* transcript. In a previous study, Pauly and colleagues (13) demonstrated that repeated AICAR treatment failed to elicit any improvement in oxidative function within the diaphragm muscle. The observed discrepancies could be attributed to the inherent differences in fiber types between the muscles under investigation (diaphragm, slow oxidative fiber type; QUAD, mixed fiber type). In fact, prior research has established that fast glycolytic fibers exhibit greater plasticity in response to AMPK agonists in DMD muscle (39). Taken together, these

compelling findings strongly support the notion that repeated MK treatment leads to enhanced mitochondrial health in dystrophic muscle. To advance our comprehension of AMPK-mediated mitochondrial adaptations in DMD muscle, current research endeavors aim to conduct a more comprehensive assessment of the mitochondrial ultrastructure. This pursuit is prompted by the observed collection of mitochondrial fission and fusion markers, which suggest a pro-fission state in dystrophic muscle, a characteristic we have previously postulated (40) and now aim to substantiate further in ongoing investigations.

A hallmark characteristic of dystrophic muscle is the fragmentation and instability of the NMJ, which results in impaired neuromuscular transmission and function (45, 46). Given that recurrent pharmacological AMPK activation has previously been shown to improve the neuromuscular transmission, muscle force production, and motor function in dystrophic animals (8, 47), it was reasonable to speculate that D2.mdx animals treated with MK would present improvements in neuromuscular function. The current study provides experimental evidence to support this claim. First, the data demonstrate that the increased muscle fatigability caused by dystrophin deficiency can be ameliorated with repeated MK dosing. Second, improvements in muscle force production were observed in MK-treated D2.mdx animals. Third, NMJ of MK-treated animals adopted a larger and more complex morphology when compared to their Veh controls. This outcome is important because effective neurotransmission relies on the optimal arrangement of the pre- and postsynapse at the NMJ (48, 49). Fourthly, chronic administration of MK increased UAPC expression in the predominantly fast glycolytic TA and GAST muscles of D2.mdx animals. Consistent with previous reports in the mdx model (8, 50), these phenotypic changes were more

prominent in faster, more glycolytic muscle fibers. Together, these data from in vivo and ex vivo experiments implicate that MK treatment enhances neuromuscular transmission in dystrophic animals.

The pathogenesis of fibrosis and fatty infiltration in DMD muscle involves dysregulated elevation of immune cells, MuSC, FAP, and other cellular constituents within the regenerative niche. Seminal contributions from the Chazaud laboratory have highlighted the crucial role of AMPK in this niche, uncovering the its multifaceted impact on muscle inflammation, regeneration, and repair (15, 51–55). Specifically, Juban and colleagues (15) revealed that AMPK activation exert reduces the release of endogenous TGF- β through an LTBP4-dependent mechanism and instigates an anti-inflammatory and anti-fibrotic phenotype in *mdx* mice. Given that the D2.mdx model that features a *LTBP4* polymorphism and hyperactive TGF- β signaling (29, 41), we evaluated whether MK could exert antifibrotic effects in this more severe model of DMD. The data indicate that MK reduced inflammation- and fibrosis-related genes, as well as reduced in fibrosis upon chronic treatment in the skeletal muscle of D2.mdx animals. Moreover, the dystrophic muscle displayed a reduction FAP content following MK treatment and reveal strong trends ($p=0.07$) on the reduction of pSMAD^{Ser423} in MK-treated animals. Current work in the laboratory aims to further detail the origin of TGF- β , as the primary source of the fibrotic molecule has been reported to be macrophages (15). Nonetheless, the presented data reveal an anti-fibrotic effect of MK on dystrophic skeletal muscle. These findings are not surprising as allosteric AMPK activators have demonstrated similar findings other tissues such as in the kidney and liver (22, 56, 57). Future research should investigate whether

stimulating AMPK activity, in conjunction with other current FDA-approved treatments, can yield synergistic benefits.

In summary, the initial findings demonstrate that the repeated administration of MK leads to notable enhancements in muscle function and reduced muscle fatiguability, with no detrimental effects observed on cardiac function. Additionally, MK treatment induces increased membrane localization and expression of utrophin and associated proteins, while also displaying promising potential in ameliorating neuromuscular function and morphology. Moreover, MK exhibits significant enhancements in mitochondrial respiration and content, alongside its capacity to downregulate inflammation and fibrosis-related genes, resulting in decreased fibrosis and reduced FAP content in dystrophic muscle. These characteristics provide compelling evidence supporting MK as a potential therapeutic agent for treatment, presenting disease-resistant benefits to all DMD patients without notable adverse side effects.

MATERIALS AND METHODS

Animal experiments

To investigate the acute effects of MK, five-week-old male D2.mdx animals were given a dose of MK to confirm the agonistic effects on AMPK activity. MK-treated animals were euthanized via cervical dislocation 1-, 3-, or 12 hours post-gavage. Tissues from Veh-treated D2.mdx animals were also collected during the timepoints and pooled to serve as a control group. TA muscles were rapidly dissected and promptly flash frozen in liquid N₂ to preserve protein phosphorylation signals.

Five-week-old male D2.mdx animals were orally gavaged a Veh or MK solution daily for a duration of seven weeks. The treated D2.mdx animals were further divided into two groups: sedentary (D2.mdx Veh, D2.mdx MK) and exercised (D2.mdx EX, D2.mdx MK+EX) cohorts. EX animals were subjected to a low-moderately intense protocol (8m/min for 30 mins) three times per week (Monday, Wednesday and Friday) as previously described (58). DBA/2J (Wild-type, WT) animals treated with a Veh solution served as a healthy control group. All treatments and exercise sessions were conducted between the hours of 0900 - 1200hrs. After six weeks of treatment, the animals underwent a series of *in vivo* muscle function tests and echocardiography. At the end of the seventh week of treatment, the animals were euthanized, and their muscles were promptly processed for *ex vivo* muscle force measurements, and high-resolution respirometry. Additional skeletal muscles and tissues were dissected, weighed, and embedded in OCT compound or flash frozen in liquid N₂.

Skeletal muscle protein extraction

Muscle tissue or cell extracts were prepared for immunoblotting following the established protocol (28). Briefly, the samples were suspended in RIPA buffer (Sigma-Aldrich, R0278) supplemented with Complete Mini Protease Inhibitor Cocktail (Sigma-Aldrich, 05892970001) and PhosSTOP Phosphatase Inhibitor Cocktail (Sigma-Aldrich, 4906845001). To facilitate homogenization, muscle preparations were mechanically processed using the TissueLyser (Qiagen) and sonication with the Branson Ultrasonics Sonifier (Thermo Fisher Scientific, SFX150). After centrifugation at 14,000g, the cell debris was eliminated, and the resulting supernatants were collected for further analysis.

Immunoblotting

All protein samples underwent bicinchoninic assay (Thermo Fisher Scientific, PI23225) to determine their protein concentrations. Muscle homogenates were subsequently diluted to equal concentrations (2 µg/µl), mixed with 4x loading buffer and ddH₂O. Prepared samples of 10-20 µg were loaded onto 4-15% gradient polyacrylamide gels and subjected to electrophoresis. Following electrophoresis, the proteins were transferred onto a nitrocellulose membrane and stained with Ponceau S (Sigma-Aldrich, P7170) to ensure consistent loading amounts. Afterward, the membranes were blocked using a 5% bovine serum albumin (BSA) solution, and then incubated overnight with appropriately diluted primary antibodies at 4°C with gentle agitation. The following antibodies were used at a 1:1,000 dilution in 5% BSA solution: pAMPK^{Thr172} (Cell Signaling, 2535S), AMPK (Cell Signaling, 2532), pACC^{Ser212} (Cell Signaling, 3661S), ACC (Cell Signaling, 3676S), OXPHOS (Abcam, ab110413), PGC-1α (EMD Millipore, AB3242), OPA1 (Abcam, ab42364), MFN2 (Cell Signaling, D1E9), pDRP^{Ser637} (Cell Signaling, 4867), pDRP^{Ser616} (Cell Signaling, 3455), DRP (Cell Signaling, 8570), FIS (Proteintech, 10956-1-AP), PINK (Novus Biological, BC100-494), Utrophin (Leica Biosystems, NCL-DRP2), γSG (Leica Biosystems, G-SARC-CE), βDG (Developmental Studies Hybridoma Bank, MANDAG2-7D11), PDGFR (Cell Signaling, D1E1E), TGF-β (Abcam, ab9758), pSMAD^{Ser423} (Abcam, ab52903), and SMAD (Abcam, ab40854). On the following day, the membranes were washed and then incubated with the appropriate horseradish peroxidase-linked secondary antibodies (1:10,000, Cell Signaling, 7074S/7076S). After additional washing with TBST, the blots were visualized using

enhanced chemiluminescence on the ChemiDoc MP Imaging System (Bio-Rad Laboratories). Densitometry analysis was performed using Image Lab (Bio-Rad Laboratories). All blots were normalized to Ponceau S staining and standardized to a pooled control on each gel.

Gene expression analysis

The TRIzol reagent (Thermo Fisher Scientific, 15596018) was utilized to homogenize all skeletal muscle samples using Lysing D matrix tubes (MP Biomedicals, 6913-050) with the FastPrep-24 Tissue and Cell Homogenizer (MP Biomedicals). Following homogenization, the samples were mixed with chloroform, vigorously shaken, and then subjected to centrifugation at 12,000g, following the manufacturer's guidelines. The upper aqueous layer, containing RNA, was purified using the total RNA Omega Bio-Tek kit (VWR International, R6834-02). The concentration and purity of the RNA were assessed using the NanoDrop 1000 Spectrophotometer (Thermo Fisher Scientific). To proceed with cDNA synthesis, the RNA samples were appropriately diluted and then reverse-transcribed using the high-capacity cDNA reverse transcription kit (Thermo Fisher Scientific, 4368814), following the provided manufacturer's instructions.

All qPCR assays were run with 2 µg of cDNA in triplicate reactions containing GoTaq qPCR Master Mix (Promega, A6002). Data were analysed using the comparative CT method (59). Ribosomal protein S11 (*Rps11*) was used as the normalizing gene since it did not differ between all experimental groups (data not shown). qPCR primers (Sigma-Aldrich) used were as follows: *Rps11*: F – CGTGACGAACATGAAGATGC, R – GCACATTGAA TCGCACAGTC; *Pparg1a*: : F – AGTGGTGTAGCGACCAAT, R –

GGGCAATCCGTCTTCATCCA; *Map1lc3*: F – CACTGCTCTGTCTTGTGTAGGTTG,
R – CACTGCTCTGTCTTGTGTAGGTTG; *Sqstm1*: F –
CCCAGTGTCTTGGCATTCTT, R – A GGGAAAGCAGAGGAAGCTC; *Ulk1*: F –
GCTCCGG TGACTIONACAAAGCTG, R – GCTGACTCCAAGCCAAAG CA; *Gabra1*: F –
– CA TCGTGGAGAAGGCTCCTA, R – ATACAGCTGGCCCATGGTAG; *Pax7*: F –
TTGGGGAACACTCCGCTGTGC, R – CAGGGCTTGGGAAGGGTTGGC; *Myf5*: F –
TGAAGGATGGACATGACGGAC, R – TTGTGTGCTCCGAAGGCTGCT; *MyoD*: F –
TCTGGAGCCCTCCTGGCACC, R – CGGGAAGGGGGAGAGTGGGG; *MyoG*: F –
GGAATTCGAGGCATATTATGA, R – TCACATAAGGCTAACACCCAG; *Ctgf*: F –
AGCTGGGAGAACTGTGTACG, R – GCCAAATGTGTCTTCCAGTC; *Colla1*: F –
ATGTTTCAGCTTTGTGGACCT, R – CAGCTGACTTCAGGGATGT; *Cd68*: F -
CCAATTCAGGGTGGAAAGAAA, R - GAGAGAGACAGGTGGGGATG, *Lgal3*: F –
CAACCATCGGATGAAGAACC, R – TTCCCACTCCTAAGGCACAC.

In vivo function testing

All-limb grip strength and muscle fatiguability was measured with a grid-grip dynamometer (Columbus Instruments). Grip strength measurements and analyses were adapted from the Treat-NMD SOP: DMD_M.2.2.001. In brief, the mice underwent a series of seven sets, each consisting of three successive pulls. Between these series, the mice were allowed to rest in their home cage for 2 mins. The maximum grip strength was determined by averaging the highest three successive pull attempts, which were typically from the first attempt. To account for variations in body weight, the grip strength was normalized. To

calculate the fatigue, the difference between the maximum grip strength and the minimum grip strength was divided by the maximum grip strength.

The four-limb cage hanging test was modified from the Treat-NMD SOP: DMD_M.2.1.005. In this experiment, animals were carefully positioned on a grid and then inverted at a height of approximately 30cm above soft bedding. Each mouse underwent the test three times, with a 5-min rest period between attempts. To determine the holding impulse, we multiplied the total hold time by the recorded body weight on the day of testing.

Rotarod testing was conducted based on previous methods (60). In brief, mice were given a 48-hour acclimatization period to the rotarod before the actual testing day. During the testing, the animals were positioned on the rotarod, and the time and speed at which they experienced failure were recorded. The rotarod protocol involved an initial speed of 5 rpm, which was gradually accelerated at a rate of 0.1 rpm/sec. Each animal underwent the test three times, and the trial with the longest performance duration was selected for subsequent statistical analysis.

Ambulatory activity was assessed utilizing the open-field Opto-Varimex-5 Auto-Track in accordance with the Treat-NMD protocol: DMD_M.2.1.002. To ensure familiarity with the surroundings, the animals were acclimatized for 5 mins in the arena 24 hours before the actual testing. Subsequently, the mice were gently placed in the center of the open field arena and allowed to explore undisturbed for a duration of 10 mins in a quiet environment. Data collection and analyses were performed with the Opto-Varimex-5 Auto-Track analysis suite.

Exercise performance was evaluated using a progressive exercise-to-exhaustion protocol, following established procedures (Treat-NMD protocol - DMD_M2.1.003). Prior to testing, all animals were accustomed to the motor-driven rodent treadmill (Columbus Instruments, Columbus, OH) for at least 5 days. The testing day was scheduled one week before tissue collection to prevent any potential confounding effects of acute exercise on other analyses. During the testing, animals underwent a progressive exercise protocol, beginning at 5m/min with a gradual increase of 1m/min² at a 0° incline. Exercise exhaustion was defined as the inability to continue running for 10 seconds, despite the lack of response to repeated nudges. To ensure unbiased evaluation, animal testing was conducted by a blinded evaluator.

Echocardiogram

Transthoracic echocardiographic analysis (Prospect T1, Scintica) was performed four - five days prior to tissue collection to evaluate cardiac morphology and function in all chronically treated animals. Animals were sedated to physiologically relevant heart rate ranges (350-450 bpm) during measurement. Sedated animals were placed on a heated stage to maintain a body temperature of 37°C during all measurements. Cardiac morphology and functional measures (Diastolic LV posterior wall thickness, LV mass, EDV, ejection fraction and stroke volume) were determined from M-mode images of the LV short axis at the level of the papillary muscle. Fractional shortening (FS) was calculated as $(LVDd - LVDs)/LVDd \times 100$. Stroke volume was estimated as left ventricular diastolic volume - left ventricular systolic volume. Ejection fraction was estimated as $SV/\text{left ventricular diastolic volume}$. Cardiac output was estimated as $SV \times \text{heart rate}$. Diastolic function (Isovolumic

relaxation time, IVRT; E and A wave mechanics; and myocardial performance index) was assessed by visualizing the blood flow through the mitral valve in a 4-chamber apical view using color doppler. All data analysis was performed using the Prospect T1 analysis suite.

Ex vivo muscle force testing

Experiments involving ex vivo muscle functional testing were conducted using a whole-mouse test system (model 1300A, Aurora Scientific Inc., Aurora, ON, Canada). The EDL muscle was rapidly dissected and secured with silk at the proximal and distal tendons. Subsequently, the prepared EDL muscle was then connected to a stationary lever arm hook and a force transducer (model 809x, Aurora Scientific) submerged in a pre-oxygenated Ringer's solution bath (120 mM NaCl, 4.7 mM KCl, 2.5 mM CaCl₂, 1.2 mM KH₂PO₄, 1.2 mM MgSO₄, 25 mM HEPES, 5.5 mM glucose). To ensure optimal force production, the EDL muscle was properly aligned and allowed to rest for 10 mins before stimulation. The optimal stimulation voltage and muscle length were determined based on previously described methods [38,39].

Twitch contractions were performed to ascertain maximum twitch force, time to peak tension (TPT), maximum rates of force production ($+dF/dt$) and relaxation ($-dF/dt$), and half relaxation time ($1/2$ RT). The force-frequency curve was then established by subjecting the muscle to a 1-second stimulation every 30 seconds, starting at 10 Hz and incrementally increasing the stimulation frequency by 10 Hz until reaching a maximum of 140 Hz. Following the force-frequency protocol, an eccentric contraction (EC) damage protocol was applied, involving 10 ECs administered at 2-min intervals. Each EC was induced by applying a 700 ms train duration of supramaximal 10 V, 0.3 ms square pulses

at 200 Hz, with a 10% lengthening at a velocity of 0.5 Le/s during the last 200 ms. The force just before the eccentric contraction was recorded to determine the relative force drop. The preceding isometric force was recorded to determine the relative force drop. All data were collected and analysed via the Dynamic Muscle Control and Analysis Software (version 615A, Aurora Scientific Inc.). Following muscle stimulation, EDL muscles were removed, embedded in OCT compound and frozen for subsequent analyses.

Whole-mount muscle preparation, immunofluorescence, and confocal microscopy

The immunohistochemical labeling of the pre- and postsynaptic components was adapted from previous methods (61). The whole ETA muscles were carefully dissected in oxygenated Ringer's Solution (110 mM NaCl, 5 mM KCl, 1 mM MgCl₂, 25 mM NaHCO₃, 2 mM CaCl₂, 11 mM glucose, 0.3mM glutamic acid, 0.4 mM glutamine, 5 mM BES (N,N-Bis(2-hydroxyethyl)-2-aminoethanesulfonic acid sodium salt, 0.036 mM choline chloride, and 4.34 x 10⁻⁷ mM cocarboxylase) and pinned in a Sylgard coated 10 mm Petri dish. The dissected muscles were then pinned in a Sylgard-coated 10 mm Petri Dish. To fix the muscles, they were treated with 4% PFA at room temperature for 10 mins and subsequently permeabilized with cold methanol at -20 °C for 6 mins. To block nonspecific labeling, the muscles were incubated with 10% normal goat serum in PBS containing 0.1% Triton X-100 for 60 mins at room temperature. Motoneuron axons were labeled using anti-neurofilament M (anti-neurofilament M, 1:50, Developmental Studies Hybridoma Bank, 2H3), and nerve terminals were labeled with anti-synaptic vesicular protein 2 (mouse IgG1 anti-synaptic vesicular protein 2, 1:100; Developmental Studies Hybridoma Bank) overnight at 4 °C. On the following day, the muscles were incubated

with secondary antibodies, specifically goat anti-mouse IgG Alexa-594 (1:500, Jackson ImmunoResearch Laboratories) for 60 mins. Postsynaptic acetylcholine receptors were labeled with Alexa-488-conjugated- α -bungarotoxin (1:500, Invitrogen) for 60 mins. All antibody incubations were carried out in PBS containing 0.1% Triton X-100 and 2% normal goat serum at room temperature. After each step, the muscles were rinsed three times in PBS containing 0.01% Triton X-100 for 5 mins each. Finally, the samples were mounted in Prolong Gold antifade reagent (Invitrogen), and images were captured using confocal microscopy (X60, 1.4 NA oil immersion; Nikon Instruments, Mississauga, Ontario, Canada).

Preparation of permeabilized fiber bundles

Following cervical dislocation of the mouse, the QUAD muscle was rapidly dissected and placed in an ice-cold Biopsy Preservation Solution (BIOPS) buffer (50 mM K-MES, 7.23 mM K₂EGTA, 2.77 mM CaK₂EGTA, 20 mM imidazole, 20 mM taurine, 5.7 mM ATP, 14.3 mM phosphocreatine, and 6.56 mM MgCl₂, pH of 7.1). The immersed muscle was further dissected to clear connective tissue and fat and then portioned into smaller muscle bundles. Fiber bundles were separated and placed in a BIOPS containing saponin (Sigma-Aldrich, S7900) and 2,4-dinitrochlorobenzene (CDNB; 35 μ M) at 4°C for 30 mins. After the permeabilization step, the muscle fibers were washed in Buffer Z (105 mM K-MES, 30 mM KCl, 10 mM KH₂PO₄, 5 mM MgCl₂, 1 mM EGTA, 5 mg/mL BSA, pH 7.4) at 4 °C for 15 mins.

Mitochondrial respiration and H₂O₂ emission measurement

High-resolution respirometry was conducted using the Oxygraph-2k system (Oroboros Instruments, Innsbruck, Austria) at a temperature of 37 °C, while maintaining [O₂] at approximately 250–400 µM. Prior to introducing 2 mL of Buffer Z, horseradish peroxidase (4 U/mL), superoxide dismutase (30 U/mL), and Amplex Red (10 µM), the chambers were volume and air calibrated. To calibrate the fluorometric sensor, five titrations of 0.1 µM H₂O₂ were serially added. Once the permeabilized muscle sample (2 - 3 mg) was added, the system was allowed to equilibrate until the O₂ slope traces reached a steady-state. The experiment proceeded with the addition of pyruvate (5 mM) and malate (2 mM), followed by ADP (5 mM), glutamate (5 mM), Cyto C (10 mM), and succinate (10 mM). During the experiment, Amplex-Red-derived fluorescence was measured simultaneously with O₂ consumption using the O2k-Fluo LED2-Module (Oroboros Instruments). To account for variations in muscle size, values were normalized based on the wet muscle weights. Data collection and analysis were performed using DatLab (V.7.4, Oroboros Instruments).

Immunofluorescent labeling of muscle fiber type

The determination of skeletal muscle fiber types followed a previously established method (62). GAST muscles were sectioned into 10 µm thick slices at -20°C using a cryostat from Leica Biosystems. These sections were collected on Superfrost Plus Gold slides (Thermo Fisher Scientific, 22-035813) and stored at -80°C until staining. To begin the staining process, the slides were blocked with a solution of 10% goat serum in 1% BSA for 60 mins at room temperature. Next, the sections were incubated with a primary antibody cocktail containing 10% goat serum and specific antibodies: myosin heavy chain I (MHCI,

1:50, DSHB, BA-F8), MHCIIa (1:600, DSHB, SC-71), MHCIIb (1:100, DSHB, BF-F3), and laminin (1:500, Sigma-Aldrich, L0663) for 120 mins. After multiple washes with PBS, a secondary antibody cocktail consisting of Alexa Fluor 350 IgG2b, Alexa Fluor 488 IgG1, Alexa Fluor 555 IgM (all from Invitrogen), and 647-conjugated anti-rat (1:500, Jackson ImmunoResearch, 112-605-167) was applied for 60 mins. Following additional washing steps, the slides were air dried and mounted using Prolong Gold (Thermo Fisher Scientific, P366930). Immunolabelled muscle sections were then captured using a 20x Plan Fluor 0.5 NA objective from Nikon Instruments and a widefield photometric camera (Accu-Scope). To establish muscle fiber typing, the complete muscle section was scanned and marked to identify regions enriched with slow oxidative muscle fibers, as well as areas that predominantly consisted of fast glycolytic fibers.

Subcellular localization of utrophin, γ SG, and β DG

Determination of utrophin localization and expression was previously described. In brief, 10 μ m muscle sections were blocked with a mouse-on-mouse (MOM) blocking reagent (Vector Laboratories, BMK-2202) in a 10% goat serum solution for 60 mins. Following this, the samples were probed with utrophin (1:100; Leica Biosystems, NCL-DRP2) for 120 mins and visualized using the MOM biotinylated anti-mouse reagent and streptavidin. Laminin (1:500, Sigma-Aldrich, L0663) was then applied for 120 mins at room temperature, followed by a fluorescent-conjugated rat secondary antibody (1:500, Jackson ImmunoResearch, 112-605-167). To mark synaptic regions, a fluorescent-conjugated α BTX (1:500, Thermo Fisher Scientific, 13422) was used. After washing, the slides were mounted with Prolong Gold (Thermo Fisher Scientific, P366930).

To investigate the localization and expression of utrophin-associated proteins, γ SG and β DG, 10 μ m muscle sections were subjected to blocking with a 10% goat serum solution for 60 mins. Subsequently, the slides were incubated with primary antibodies specific to γ SG (1:100, Leica Biosystems, G-SARC-CE) or β DG (1:100, Developmental Studies Hybridoma Bank, MANDAG2-7D11) in 1% BSA overnight at 4°C. On the following day, the respective secondary antibodies (goat anti-mouse IgG2b, Invitrogen; goat anti-mouse IgG1, Invitrogen) were applied for 1 hour at room temperature. After PBS washes, Laminin (1:500, Sigma-Aldrich, L0663) was applied for 120 mins at room temperature, followed by a fluorescent-conjugated rat secondary antibody (1:500, Jackson ImmunoResearch, 112-605-167). After washing, the slides were mounted using Prolong Gold (Thermo Fisher Scientific).

Muscle histology

Masson's Trichrome stain was used to assess collagen content in muscle cross-sections following the manufacturer's instructions (Sigma Aldrich, HT15). In summary, 10 μ m sections were fixed in 4% PFA for 3 hrs, then incubated in Bouin's solution (Sigma Aldrich, HT10132) overnight at room temperature. Slides were rinsed in water, treated with Weigert's iron hematoxylin for 5 mins, washed again, and exposed to Biebrich scarlet acid fuchsin for 15 mins. Afterward, slides were rinsed in water, subjected to phosphomolybdic-phosphotungstic acid solution (3x3 mins) and incubated in aniline blue for 5 mins, followed by a water dip. Slides were then differentiated with 1% glacial acetic acid for 2 mins. Finally, the slides underwent graded ethanol washes and were coverslipped with Permount media (Thermo Fisher Scientific, SP15500). Stained muscles were

scanned using a 10x Plan Fluor 0.3 NA objective and a DS-Fi3 camera (Nikon Instruments). The endomysium fibrotic deposition and collagen-stained areas (stained blue) were determined by manually thresholding and selecting the positive regions. endomysium fibrosis was defined by fibrosis within the endomysium spaces as previously described (63). All analyses were conducted using Nikon NIS Elements AR 3.2 software, and the assessments were performed in a blinded fashion.

Statistical analyses

For the chronic experiments, a one-way analysis of variance (ANOVA) and Tukey post-hoc tests were performed to examine the differences among groups. Running survival data from these animals were evaluated using the Log-rank test to identify any significant differences. In the acute MK experiment, one-way ANOVA and Tukey post-hoc tests were again utilized to identify significant differences. To determine significant changes on gene expression in the acute experiment, an unpaired t-test was employed. GraphPad Prism software (V9.1.1) was used for statistical analysis. All individual points are displayed. Data are expressed as mean \pm standard error of mean. Statistical significance was accepted at $P < 0.05$.

References and Notes:

1. Emery, A.E.H. (1991) Population frequencies of inherited neuromuscular diseases-A world survey. *Neuromuscul. Disord.*, **1**, 19–29.
2. Birnkrant, D.J., Bushby, K., Bann, C.M., Apkon, S.D., Blackwell, A., Brumbaugh, D., Case, L.E., Clemens, P.R., Hadjiyannakis, S., Pandya, S., *et al.* (2018) Diagnosis and management of Duchenne muscular dystrophy, part 1: diagnosis, and neuromuscular, rehabilitation, endocrine, and gastrointestinal and nutritional management. *Lancet Neurol.*, **17**, 251–267.
3. Duan, D., Goemans, N., Takeda, S., Mercuri, E. and Aartsma-Rus, A. (2021) Duchenne muscular dystrophy. *Nat. Rev. Dis. Prim.*, **7**, 1–19.
4. Birnkrant, D.J., Bello, L., Butterfield, R.J., Carter, J.C., Cripe, L.H., Cripe, T.P., Mckim, D.A., Nandi, D. and Pegoraro, E. Cardiorespiratory management of Duchenne muscular dystrophy: emerging therapies, neuromuscular genetics, and new clinical challenges.
5. Wilton-Clark, H. and Yokota, T. (2022) Biological and genetic therapies for the treatment of Duchenne muscular dystrophy. <https://doi.org/10.1080/14712598.2022.2150543>, **23**, 49–59.
6. Kumar, S.R.P., Duan, D. and Herzog, R.W. (2023) Immune Responses to Muscle-Directed Adeno-Associated Viral Gene Transfer in Clinical Studies. <https://home.liebertpub.com/hum>, **34**, 365–371.
7. Ljubcic, V. and Jasmin, B.J. (2013) AMP-activated protein kinase at the nexus of therapeutic skeletal muscle plasticity in Duchenne muscular dystrophy. *Trends Mol. Med.*, **19**, 614–624.
8. Ljubcic, V., Miura, P., Burt, M., Boudreault, L., Khogali, S., Lunde, J.A., Renaud, J.M. and Jasmin, B.J. (2011) Chronic AMPK activation evokes the slow, oxidative myogenic program and triggers beneficial adaptations in mdx mouse skeletal muscle. *Hum. Mol. Genet.*, **20**, 3478–3493.
9. Ljubcic, V. and Jasmin, B.J. (2015) Metformin increases peroxisome proliferator-activated receptor γ Co-activator-1 α and utrophin a expression in dystrophic skeletal muscle. *Muscle Nerve*, **52**, 139–142.
10. Ljubcic, V., Burt, M., Lunde, J.A. and Jasmin, B.J. (2014) Resveratrol induces expression of the slow, oxidative phenotype in mdx mouse muscle together with enhanced activity of the SIRT1-PGC-1 axis. *AJP Cell Physiol.*, **307**, C66–C82.
11. Péladeau, C., Ahmed, A., Amirouche, A., Crawford Parks, T.E., Bronicki, L.M., Ljubcic, V., Renaud, J.M. and Jasmin, B.J. (2016) Combinatorial therapeutic activation with heparin and AICAR stimulates additive effects on utrophin A expression in dystrophic muscles. *Hum. Mol. Genet.*, **25**, 24–43.
12. Hulmi, J.J., Oliveira, B.M., Silvennoinen, M., Hoogaars, W.M.H., Pasternack, A., Kainulainen, H. and Ritvos, O. (2013) Exercise restores decreased physical activity levels and increases markers of autophagy and oxidative capacity in myostatin/activin-blocked mdx mice. *AJP Endocrinol. Metab.*, **305**, E171–E182.
13. Pauly, M., Daussin, F., Burelle, Y., Li, T., Godin, R., Fauconnier, J., Koechlin-Ramonatxo, C., Hugon, G., Lacampagne, A., Coisy-Quivy, M., *et al.* (2012) AMPK activation stimulates autophagy and ameliorates muscular dystrophy in the mdx

- mouse diaphragm. *Am. J. Pathol.*, **181**, 583–592.
14. Dong,X., Hui,T., Chen,J., Yu,Z., Ren,D., Zou,S., Wang,S., Fei,E., Jiao,H. and Lai,X. (2021) Metformin Increases Sarcolemma Integrity and Ameliorates Neuromuscular Deficits in a Murine Model of Duchenne Muscular Dystrophy. *Front. Physiol.*, **0**, 606.
 15. Juban,G., Saclier,M., Yacoub-Youssef,H., Kernou,A., Arnold,L., Boisson,C., Ben Larbi,S., Magnan,M., Cuvellier,S., Th eret,M., *et al.* (2018) AMPK Activation Regulates LTBP4-Dependent TGF- 1 Secretion by Pro-inflammatory Macrophages and Controls Fibrosis in Duchenne Muscular Dystrophy. *Cell Rep.*, **25**, 2163-2176.e6.
 16. Jahnke,V.E., Van Der Meulen,J.H., Johnston,H.K., Ghimbovski,S., Partridge,T., Hoffman,E.P. and Nagaraju,K. (2012) Metabolic remodeling agents show beneficial effects in the dystrophin-deficient mdx mouse model. *Skelet. Muscle*, **2**, 1–11.
 17. Yusuke S. Hori, Atsushi Kuno, Ryusuke Hosoda, Masaya Tanno, Tetsuji Miura, Kazuaki Shimamoto, and Y.H. (2011) Resveratrol Ameliorates Muscular Pathology in the Dystrophic mdx Mouse, a Model for Duchenne Muscular Dystrophy. *Clin. Nutr.*, **338**, 784–794.
 18. Kuno,A., Hosoda,R., Sebori,R., Hayashi,T., Sakuragi,H., Tanabe,M. and Horio,Y. (2018) Resveratrol Ameliorates Mitophagy Disturbance and Improves Cardiac Pathophysiology of Dystrophin-deficient mdx Mice. *Sci. Rep.*, **8**, 15555.
 19. Gordon,B.S., Delgado Diaz,D.C. and Kostek,M.C. (2013) Resveratrol decreases inflammation and increases utrophin gene expression in the mdx mouse model of duchenne muscular dystrophy. *Clin. Nutr.*, **32**, 104–111.
 20. Myers,R.W., Guan,H.-P., Ehrhart,J., Petrov,A., Prahallada,S., Tozzo,E., Yang,X., Kurtz,M.M., Trujillo,M., Gonzalez Trotter,D., *et al.* (2017) Systemic pan-AMPK activator MK-8722 improves glucose homeostasis but induces cardiac hypertrophy. *Science*, **357**, 507–511.
 21. Muise,E.S., Guan,H.-P., Liu,J., Nawrocki,A.R., Yang,X., Wang,C., Rodr iguez,C.G., Zhou,D., Gorski,J.N., Kurtz,M.M., *et al.* (2019) Pharmacological AMPK activation induces transcriptional responses congruent to exercise in skeletal and cardiac muscle, adipose tissues and liver. *PLoS One*, **14**, e0211568.
 22. Gluais-Dagorn,P., Foretz,M., Steinberg,G.R., Batchuluun,B., Zawistowska-Deniziak,A., Lambooj,J.M., Guigas,B., Carling,D., Monternier,P.A., Moller,D.E., *et al.* (2022) Direct AMPK Activation Corrects NASH in Rodents Through Metabolic Effects and Direct Action on Inflammation and Fibrogenesis. *Hepatol. Commun.*, **6**, 101–119.
 23. Stephan,Y., Souille,M., Larcheveque,M., Gluais-Dagorn,P., Hallakou-Bozec,S., Nicol,L. and Mulder,P. (2021) Both short-and long-term treatment with the direct AMP kinase activator PXL770 improves cardiac function in ZSF-1 rats. *Eur. Heart J.*, **42**.
 24. Cokorinos,E.C., Delmore,J., Reyes,A.R., Wojtaszewski,J.F.P., Cameron,K.O. and Correspondence,R.A.M. (2017) Activation of Skeletal Muscle AMPK Promotes Glucose Disposal and Glucose Lowering in Non-human Primates and Mice PF-739 treatment increases PGC1a transcription and mitochondrial content in muscle. *Cell Metab.*, **25**, 1147-1159.e10.
 25. Steneberg,P., Lindahl,E., Dahl,U., Lidh,E., Straseviciene,J., Backlund,F.,

- Kjellkvist,E., Berggren,E., Lundberg,I., Bergqvist,I., *et al.* (2018) PAN-AMPK activator O304 improves glucose homeostasis and microvascular perfusion in mice and type 2 diabetes patients. *JCI Insight*, **3**.
26. Fouqueray,P., Bolze,S., Dubourg,J., Gluais-Dagorn,P., Moller,D.E., Correspondence,K.C., Hallakou-Bozec,S., Theurey,P., Grouin,J.-M., Mence Chevalier,C., *et al.* (2021) Pharmacodynamic effects of direct AMP kinase activation in humans with insulin resistance and non-alcoholic fatty liver disease: A phase 1b study. *Cell Reports Med.*, **2**, 100474.
27. Cusi,K., Alkhoury,N., Harrison,S.A., Fouqueray,P., Moller,D.E., Hallakou-Bozec,S., Bolze,S., Grouin,J.M., Jeannin Megnien,S., Dubourg,J., *et al.* (2021) Efficacy and safety of PXL770, a direct AMP kinase activator, for the treatment of non-alcoholic fatty liver disease (STAMP-NAFLD): a randomised, double-blind, placebo-controlled, phase 2a study. *Lancet Gastroenterol. Hepatol.*, **6**, 889–902.
28. Ng,S.Y., Mikhail,A.I., Mattina,S.R., Manta,A., Diffey,I.J. and Ljubicic,V. (2023) Acute, next-generation AMPK activation initiates a disease-resistant gene expression program in dystrophic skeletal muscle. *FASEB J*, **37**, e22863.
29. van Putten,M., Putker,K., Overzier,M., Adamzek,W.A., Pasteuning-Vuhman,S., Plomp,J.J. and Aartsma-Rus,A. (2019) Natural disease history of the D2 -mdx mouse model for Duchenne muscular dystrophy. *FASEB J.*, **33**, 8110–8124.
30. Adamo,C.M., Dai,D.F., Percival,J.M., Minami,E., Willis,M.S., Patrucco,E., Froehner,S.C. and Beavo,J.A. (2010) Sildenafil reverses cardiac dysfunction in the mdx mouse model of Duchenne muscular dystrophy. *Proc. Natl. Acad. Sci. U. S. A.*, **107**, 19079–19083.
31. Yu,L., Zhang,X., Yang,Y., Li,D., Tang,K., Zhao,Z., He,W., Wang,C., Sahoo,N., Converso-Baran,K., *et al.* (2020) Small-molecule activation of lysosomal TRP channels ameliorates Duchenne muscular dystrophy in mouse models. *Sci. Adv.*, **6**.
32. Markham,L.W., Michelfelder,E.C., Border,W.L., Khoury,P.R., Spicer,R.L., Wong,B.L., Benson,D.W. and Cripe,L.H. (2006) Abnormalities of Diastolic Function Precede Dilated Cardiomyopathy Associated with Duchenne Muscular Dystrophy. *J. Am. Soc. Echocardiogr.*, **19**, 865–871.
33. Van Putten,M., Raymackers,J.-M., Dorchies,O. and Carlson,G. The use of hanging wire tests to monitor muscle strength and condition over time SOP (ID) Number.
34. Hammers,D.W., Hart,C.C., Matheny,M.K., Wright,L.A., Armellini,M., Barton,E.R. and Sweeney,H.L. (2020) The D2.mdx mouse as a preclinical model of the skeletal muscle pathology associated with Duchenne muscular dystrophy. *Sci. Rep.*, **10**, 1–12.
35. Hughes,M.C., Ramos,S. V., Turnbull,P.C., Rebalka,I.A., Cao,A., Monaco,C.M.F., Varah,N.E., Edgett,B.A., Huber,J.S., Tadi,P., *et al.* (2019) Early myopathy in Duchenne muscular dystrophy is associated with elevated mitochondrial H₂O₂ emission during impaired oxidative phosphorylation. *J. Cachexia. Sarcopenia Muscle*, **10**, 643–661.
36. Mázala,D.A.G., Novak,J.S., Hogarth,M.W., Nearing,M., Adusumalli,P., Tully,C.B., Habib,N.F., Gordish-Dressman,H., Chen,Y.W., Jaiswal,J.K., *et al.* (2020) TGF- β -driven muscle degeneration and failed regeneration underlie disease onset in a DMD mouse model. *JCI Insight*, **5**.

37. Kennedy, T.L. and Dugdale, H.F. (2023) Cardiac and Skeletal Muscle Pathology in the D2/mdx Mouse Model and Caveats Associated with the Quantification of Utrophin. *Methods Mol. Biol.*, **2587**, 55–66.
38. Helliwell, T.R., Nguyen thi, M., Morris, G.E. and Davies, K.E. (1992) The dystrophin-related protein, utrophin, is expressed on the sarcolemma of regenerating human skeletal muscle fibres in dystrophies and inflammatory myopathies. *Neuromuscul. Disord.*, **2**, 177–184.
39. Ljubicic, V., Miura, P., Burt, M., Boudreault, L., Khogali, S., Lunde, J.A., Renaud, J.M. and Jasmin, B.J. (2011) Chronic AMPK activation evokes the slow, oxidative myogenic program and triggers beneficial adaptations in mdx mouse skeletal muscle. *Hum. Mol. Genet.*, **20**, 3478–3493.
40. Mikhail, A.I., Ng, S.Y., Mattina, S.R. and Ljubicic, V. (2023) AMPK is mitochondrial medicine for neuromuscular disorders. *Trends Mol. Med.*, **In press**.
41. Coley, W.D., Bogdanik, L., Vila, M.C., Yu, Q., Van Der Meulen, J.H., Rayavarapu, S., Novak, J.S., Nearing, M., Quinn, J.L., Saunders, A., *et al.* (2016) Effect of genetic background on the dystrophic phenotype in mdx mice. *Hum. Mol. Genet.*, **25**, 130–145.
42. Hafner, P., Bonati, U., Klein, A., Rubino, D., Gocheva, V., Schmidt, S., Schroeder, J., Bernert, G., Laugel, V., Steinlin, M., *et al.* (2019) Effect of Combination l-Citrulline and Metformin Treatment on Motor Function in Patients With Duchenne Muscular Dystrophy: A Randomized Clinical Trial. *JAMA Netw. open*, **2**, e1914171.
43. Goodyear, L.J. (2008) The exercise pill - Too good to be true? *N. Engl. J. Med.*, **359**, 1842–1844.
44. Feng, D., Biftu, T., Romero, F.A., Kekec, A., Dropinski, J., Kassick, A., Xu, S., Kurtz, M.M., Gollapudi, A., Shao, Q., *et al.* (2017) Discovery of MK-8722: A Systemic, Direct Pan-Activator of AMP-Activated Protein Kinase. [10.1021/acsmchemlett.7b00417](https://doi.org/10.1021/acsmchemlett.7b00417).
45. Ng, S.Y. and Ljubicic, V. (2020) Recent insights into neuromuscular junction biology in Duchenne muscular dystrophy: Impacts, challenges, and opportunities. *EBioMedicine*, **61**, 103032.
46. Pratt, S.J.P., Shah, S.B., Ward, C.W., Inacio, M.P., Stains, J.P. and Lovering, R.M. (2013) Effects of in vivo injury on the neuromuscular junction in healthy and dystrophic muscles. *J. Physiol.*, **591**, 559–570.
47. Dong, X., Hui, T., Chen, J., Yu, Z., Ren, D., Zou, S., Wang, S., Fei, E., Jiao, H. and Lai, X. (2021) Metformin Increases Sarcolemma Integrity and Ameliorates Neuromuscular Deficits in a Murine Model of Duchenne Muscular Dystrophy. *Front. Physiol.*, **12**, 606.
48. Lovering, R.M., Iyer, S.R. and Edwards, B. (2020) Alterations of neuromuscular junctions in Duchenne muscular dystrophy. *Neurosci. Lett.*, [10.1016/j.neulet.2020.135304](https://doi.org/10.1016/j.neulet.2020.135304).
49. van der Pijl, E.M., van Putten, M., Niks, E.H., Verschuuren, J.J.G.M., Aartsma-Rus, A. and Plomp, J.J. (2016) Characterization of neuromuscular synapse function abnormalities in multiple Duchenne muscular dystrophy mouse models. *Eur. J. Neurosci.*, **43**, 1623–1635.

50. Ljubcic,V., Khogali,S., Renaud,J.-M. and Jasmin,B.J. (2012) Chronic AMPK stimulation attenuates adaptive signaling in dystrophic skeletal muscle. *AJP Cell Physiol.*, **302**, C110–C121.
51. Theret,M., Gsaier,L., Schaffer,B., Juban,G., Ben Larbi,S., Weiss-Gayet,M., Bultot,L., Collodet,C., Foretz,M., Desplanches,D., *et al.* (2017) AMPK α 1-LDH pathway regulates muscle stem cell self-renewal by controlling metabolic homeostasis. *EMBO J.*, **36**, 1946–1962.
52. Mounier,R., Théret,M., Arnold,L., Cuvellier,S., Bultot,L., Göransson,O., Sanz,N., Ferry,A., Sakamoto,K., Foretz,M., *et al.* (2013) AMPK α 1 regulates macrophage skewing at the time of resolution of inflammation during skeletal muscle regeneration. *Cell Metab.*, **18**, 251–264.
53. Fu,X., Zhu,M., Zhang,S., Foretz,M., Viollet,B. and Du,M. (2016) Obesity impairs skeletal muscle regeneration through inhibition of AMPK. *Diabetes*, **65**, 188–200.
54. Fu,X., Zhao,J.-X., Zhu,M.-J., Foretz,M., Viollet,B., Dodson,M. V and Du,M. (2013) AMP-Activated Protein Kinase α 1 but Not α 2 Catalytic Subunit Potentiates Myogenin Expression and Myogenesis. *Mol. Cell. Biol.*, **33**, 4517–4525.
55. Liu,X., Zhao,L., Gao,Y., Chen,Y., Tian,Q., Son,J.S., Chae,S.A., de Avila,J.M., Zhu,M.J. and Du,M. (2023) AMP-activated protein kinase inhibition in fibro-adipogenic progenitors impairs muscle regeneration and increases fibrosis. *J. Cachexia. Sarcopenia Muscle*, **14**, 479–492.
56. Zhang,J., Muise,E.S., Han,S., Kutchukian,P.S., Costet,P., Zhu,Y., Kan,Y., Zhou,H., Shah,V., Huang,Y., *et al.* (2020) Molecular Profiling Reveals a Common Metabolic Signature of Tissue Fibrosis. *Cell Reports Med.*, **1**, 100056.
57. Zhou,X., Muise,E.S., Haimbach,R., Sebat,I.K., Zhu,Y., Liu,F., Souza,S.C., Kan,Y., Pinto,S., Kelley,D.E., *et al.* (2019) Pan-AMPK activation improves renal function in a rat model of progressive diabetic nephropathy. *J. Pharmacol. Exp. Ther.*, **371**, 45–55.
58. Zelikovich,A.S., Quattrocchi,M., Salamone,I.M., Kuntz,N.L. and McNally,E.M. (2019) Moderate exercise improves function and increases adiponectin in the mdx mouse model of muscular dystrophy. *Sci. Rep.*, **9**, 1–10.
59. Schmittgen,T.D. and Livak,K.J. (2008) Analyzing real-time PCR data by the comparative CT method. *Nat. Protoc.*, **3**, 1101–1108.
60. Aartsma-Rus,A. and van Putten,M. (2014) Assessing functional performance in the mdx mouse model. *J. Vis. Exp.*, 10.3791/51303.
61. Villarroel-Campos,D., Schiavo,G. and Sleigh,J.N. (2022) Dissection, in vivo imaging and analysis of the mouse epitrochleoanconeus muscle. *J. Anat.*, **241**, 1108–1119.
62. Bloemberg,D. and Quadriatero,J. (2012) Rapid determination of myosin heavy chain expression in rat, mouse, and human skeletal muscle using multicolor immunofluorescence analysis. *PLoS One*, **7**.
63. Desguerre, I., Mayer, M., Leturcq, F., Barbet, J. P., Gherardi, R. K., & Christov, C. (2009). Endomysial fibrosis in Duchenne muscular dystrophy: a marker of poor outcome associated with macrophage alternative activation. *Journal of Neuropathology & Experimental Neurology*, *68*(7), 762-773.

Acknowledgments:

The authors extend our appreciation to Todd Prior and the rest of the Integrative Neuromuscular Biology Laboratory and the Exercise Metabolism Research Group.

Funding:

Canadian Institutes of Health Research (CIHR) Project Grant #408289 (VL)

Muscular Dystrophy Canada Translational Seed Science Grant #681362 (VL)

CIHR Tier 2 Canada Research Chair Grant #232338 (VL)

Ontario Ministry of Economic Development, Job Creation and Trade Early Researcher Grant #ER17-13-087 (VL)

Natural Sciences and Engineering Research Council of Canada Scholarship (SYN, SRM)

Ontario Graduate Scholarship (AIM)

Figures:

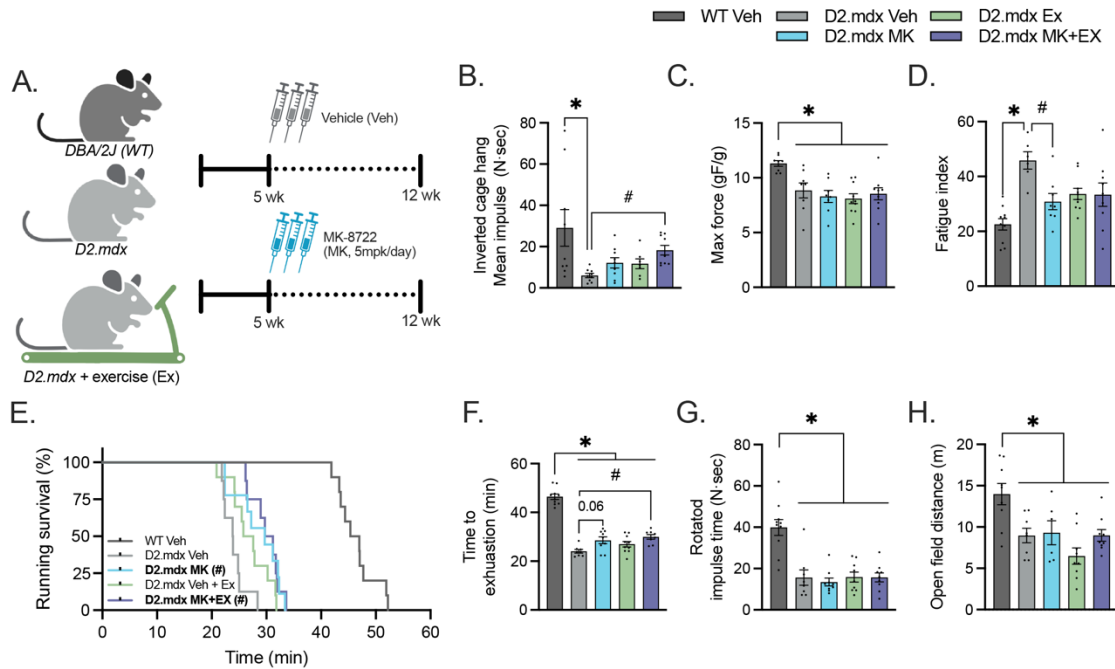


Fig 1. In vivo muscle function metrics in D2.mdx animals treated with MK-8722 (MK). (A) Five-week-old D2.mdx animals were treated with a vehicle (Veh) or MK solution on a daily basis for 7 weeks. Animals were divided into sedentary or physically active (EX) groups for the treatment period. Physically active animals were subjected to a moderately intense (8m/min for 30min) exercise session three times per week. In vivo muscle function testing was conducted after six weeks of treatment, and animals were euthanized the following week. Graphical summaries of key muscle function metrics including inverted cage hang impulse (B), maximum all-limb grip strength (C), and fatigue index [% difference between first and last all-limb grip strength measurement, (D)] in Veh-treated wild-type (WT) and Veh- and MK-treated D2.mdx animals. (E) Kaplan-Meier analysis comparing the maximum distance traveled by Veh-treated WT and Veh- or MK-treated D2.mdx animals during the exercise tolerance test. (F) Duration until exhaustion during exercise to fatigue on a motorized exercise treadmill was recorded and compared among all experimental groups. Graphical summaries of (G) rotarod impulse time and (H) open field distance in all experimental groups were generated to evaluate motor coordination and exploration behavior. Graphical summaries display individual data points and group means (bars) with standard error of the means (SEM). n = 8–10. Statistical significance was denoted as *, p < 0.05 versus WT Veh and #, p < 0.05 versus mdx Veh.

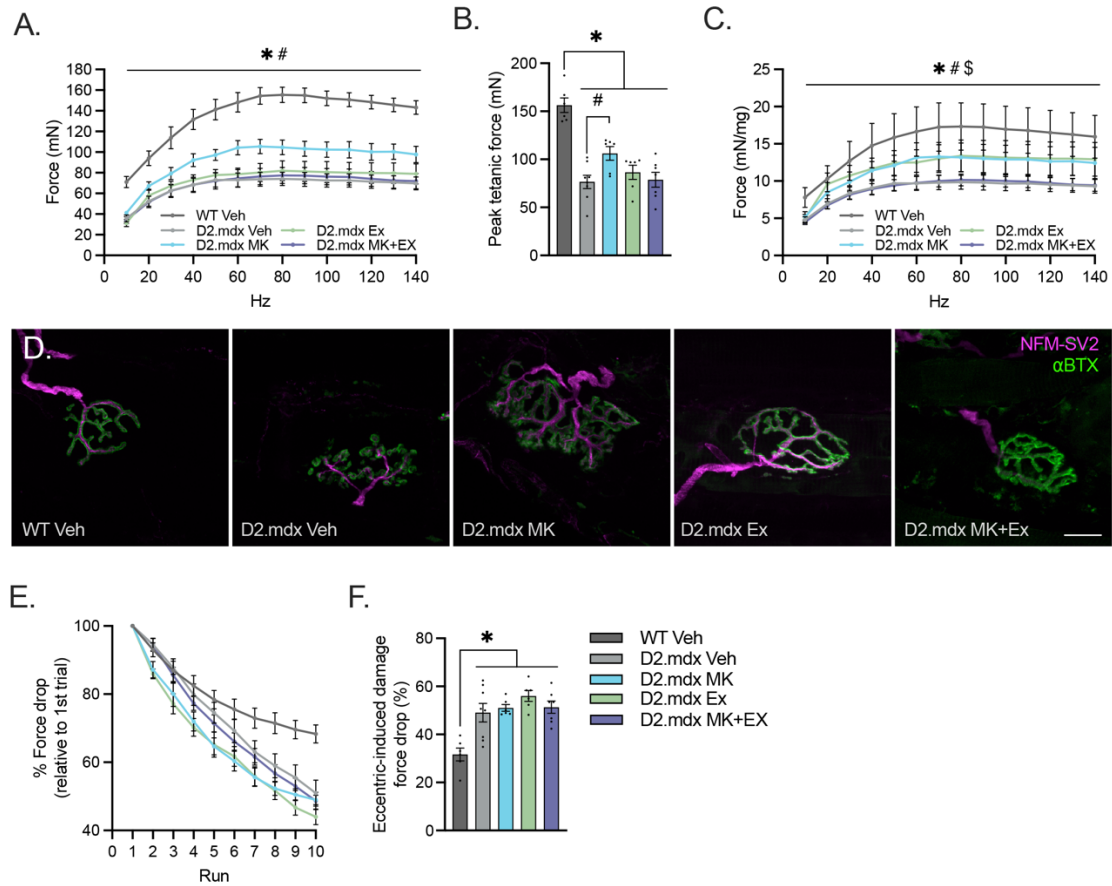


Fig 2. Ex vivo muscle function metrics in D2.mdx animals treated with MK. (A) Force-frequency curves of the extensor digitorum longus (EDL) muscles were assessed in Veh- and MK-treated D2.mdx animals, as well as Veh-treated WT animals. (B) Peak tetanic force production in the EDL muscles in all experimental groups. (C) Force-frequency curves of the EDL muscles in all experimental groups were expressed relative to the stimulated EDL weight. (D) Maximal force development of the EDL muscles was expressed as a percentage of the initial contraction during ten electrically stimulated eccentric contractions ex vivo. (E) Graphical summary illustrating the relative force drop in the EDL muscles of all experimental groups. (F) Representative confocal images of the neuromuscular junction (NMJ) images in the epitrochleoanconeus muscle of all experimental groups. Neurofilament M + synaptic vesicle 2 (NFM+SV2, magenta) highlights the presynaptic component, while α-bungarotoxin (αBTX, green) indicates the postsynapse. Scale bar represents 20 μm. n = 8–10. Statistical significance was denoted as *, p < 0.05 versus WT Veh (comparison with Veh-treated wild-type) and #, p < 0.05 versus mdx Veh (comparison with Veh-treated D2.mdx animals). Graphical summaries display individual data points and group means (bars) with SEM. Statistical significance for the force frequency and force drop data is denoted as *, p < 0.05 WT Veh versus D2.mdx Veh (main effect of genotype); #, p < 0.05 D2.mdx Veh versus D2.mdx MK (main effect of MK); and \$, p < 0.05 D2.mdx Veh versus D2.mdx EX (main effect of exercise).

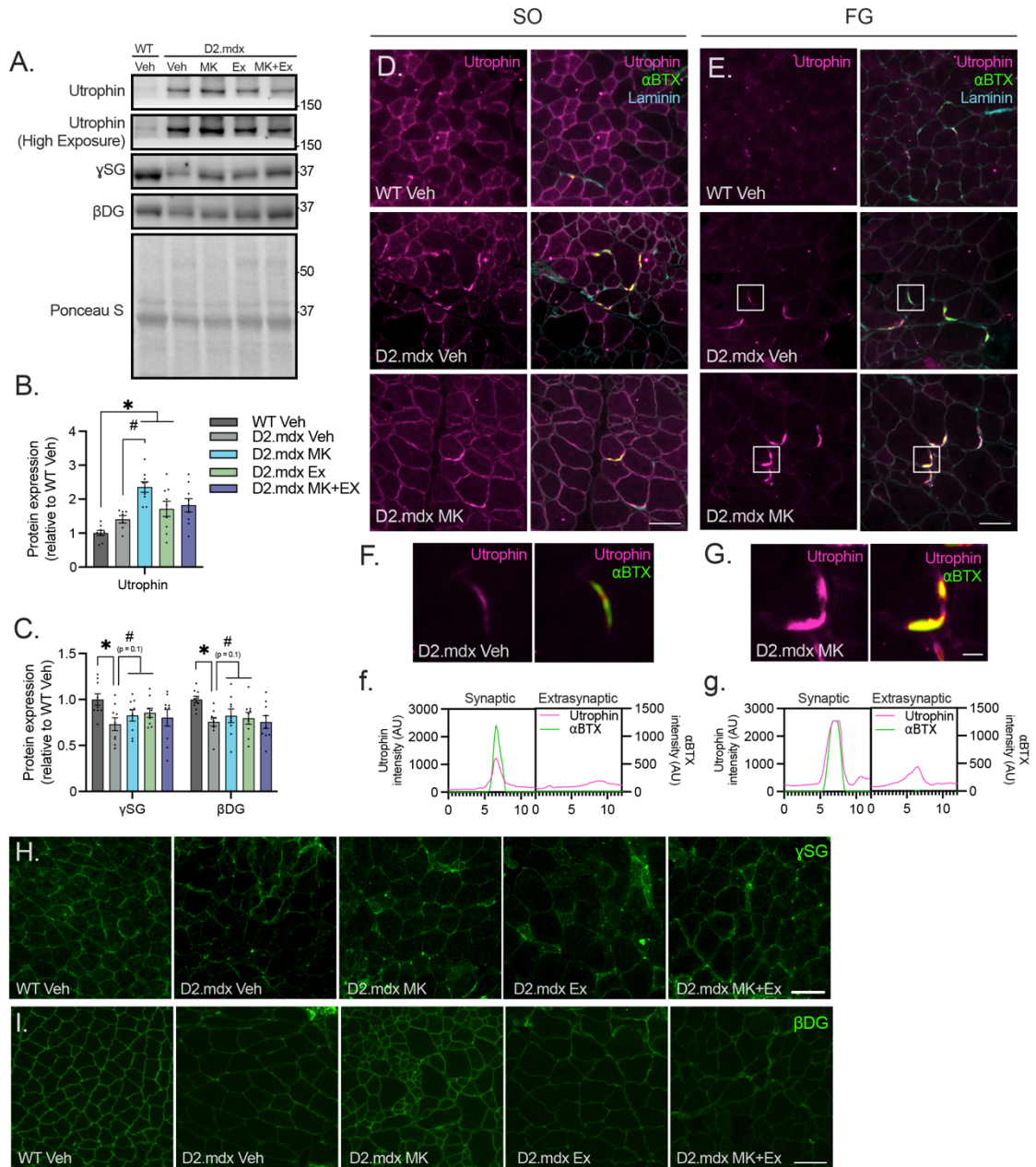


Figure 3. Enhanced utrophin expression in dystrophic skeletal muscle with MK treatment. (A) Typical Western blots of utrophin, γ -sarcoglycan (γ SG), and β -dystroglycan (β DG) in the TA muscles of Veh-treated WT mice and Veh- or MK-treated D2.mdx mice. Ponceau S staining is shown below as a loading control. Protein ladder markers on the right are denoted in kDa. B-C) Graphical summaries illustrating the protein expression levels of utrophin (B), as well as β DG and γ SG (C) in the tibialis anterior (TA) muscles all experimental groups. (D) Representative immunofluorescence images depicting utrophin (magenta) in the slow oxidative regions of the gastrocnemius and plantaris (G&P) muscles of Veh-treated WT and D2.mdx mice and MK-treated D2.mdx mice. (E) Additional images of the faster, more glycolytic regions of the GSP complex are also shown. The postsynaptic compartment of the neuromuscular junction is demarked by α -bungarotoxin (α BTX; green), while laminin (cyan) outlines the sarcolemma. Magnified images from the

white inset boxes in panels E highlight synaptic and extrasynaptic utrophin expression in the fast glycolytic regions of the G&P muscles from the D2.mdx Veh (**F**) and D2.mdx MK (**G**) groups. Fluorescent intensity markers intersect the synaptic (solid cyan arrow) and extrasynaptic (dotted cyan arrow) utrophin-positive regions along the sarcolemma. (**f-g**) Graphical summaries of fluorescence intensity quantification for synaptic and extrasynaptic utrophin in the D2.mdx Veh and D2.mdx MK groups. Scale bars in Panels C and D represent 100 μm , whereas the scale bars in E and F represent 10 μm , respectively. Immunoblotting data are presented as fold differences relative to the WT Veh group. (**H-I**) Representative immunofluorescence images of γSG and βDG in the fast glycolytic regions of the GSP complex from all experimental groups. Graphical summaries display individual data points and group means (bars) with SEM. $n = 8-10$. Statistical significance was denoted as *, $p < 0.05$ versus WT Veh and #, $p < 0.05$ versus mdx Veh.

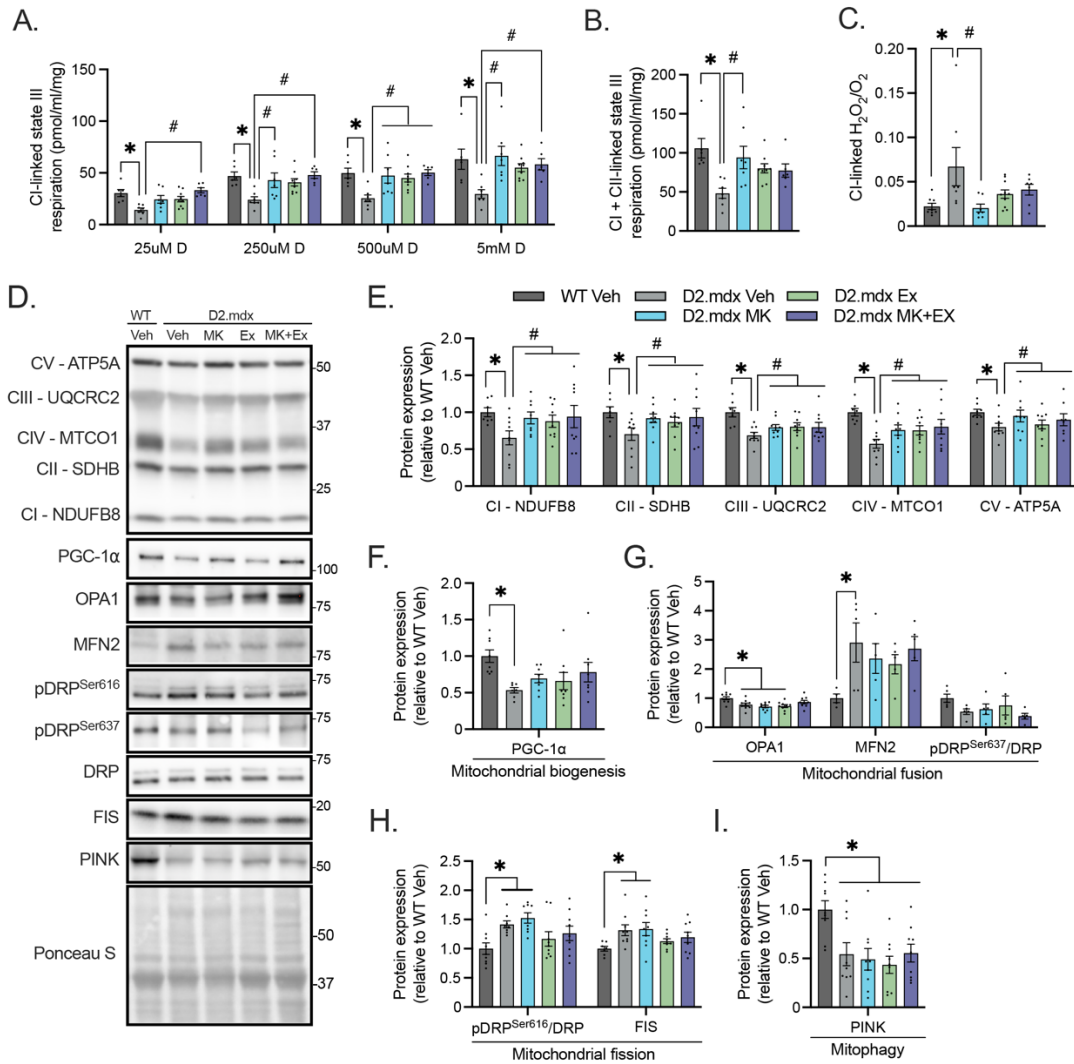


Fig 4. MK treatment and physical activity increases mitochondrial respiration and content in skeletal muscle of D2.mdx animals. Graphical summaries of Complex I (CI)-linked state III respiration (**A**) and CI and CII-linked state III respiration (**B**) in the quadriceps muscles of Veh-treated WT and Veh- or MK-treated D2.mdx animals. CI-linked state III respiration was assessed at various [ADP] levels: physiological (25 μ M), submaximal (250 μ M, 500 μ M), and supraphysiological (5 mM). (**C**) CI-linked state II reactive oxygen species production in the quadriceps muscles of Veh-treated WT and Veh- or MK-treated D2.mdx animals. (**D**) Representative Western blots depicting mitochondrial protein complexes (CI-CV), peroxisome proliferator-activated receptor γ coactivator-1 α (PGC-1 α), optic atrophy protein 1 (OPA1), mitofusin-2 (MFN2), Ser⁶¹⁶-phosphorylated dynamin-related protein 1 (pDRP^{Ser616}), Ser⁶³⁷-phosphorylated DRP (pDRP^{Ser637}), DRP, mitochondrial fission 1 (FIS), and PTEN-induced kinase (PINK) in the TA muscles of Veh-treated WT and Veh- or MK-treated D2.mdx animals. A representative Ponceau S stain is shown below as a loading control. Protein ladder markers on the right are denoted in kilodaltons (kDa). Graphical summaries of protein markers related to mitochondrial protein markers (**E**), mitochondrial biogenesis (**F**), fusion (**G**), fission (**H**), and mitophagy (**I**) in Veh-treated WT and Veh- or MK-treated D2.mdx animals. Immunoblotting data are presented as fold differences relative to the WT Veh group. Graphical summaries display individual data points and group means (bars) with SEM. n = 8–10. Statistical significance was denoted as *, p < 0.05 versus WT Veh and #, p < 0.05 versus mdx Veh.

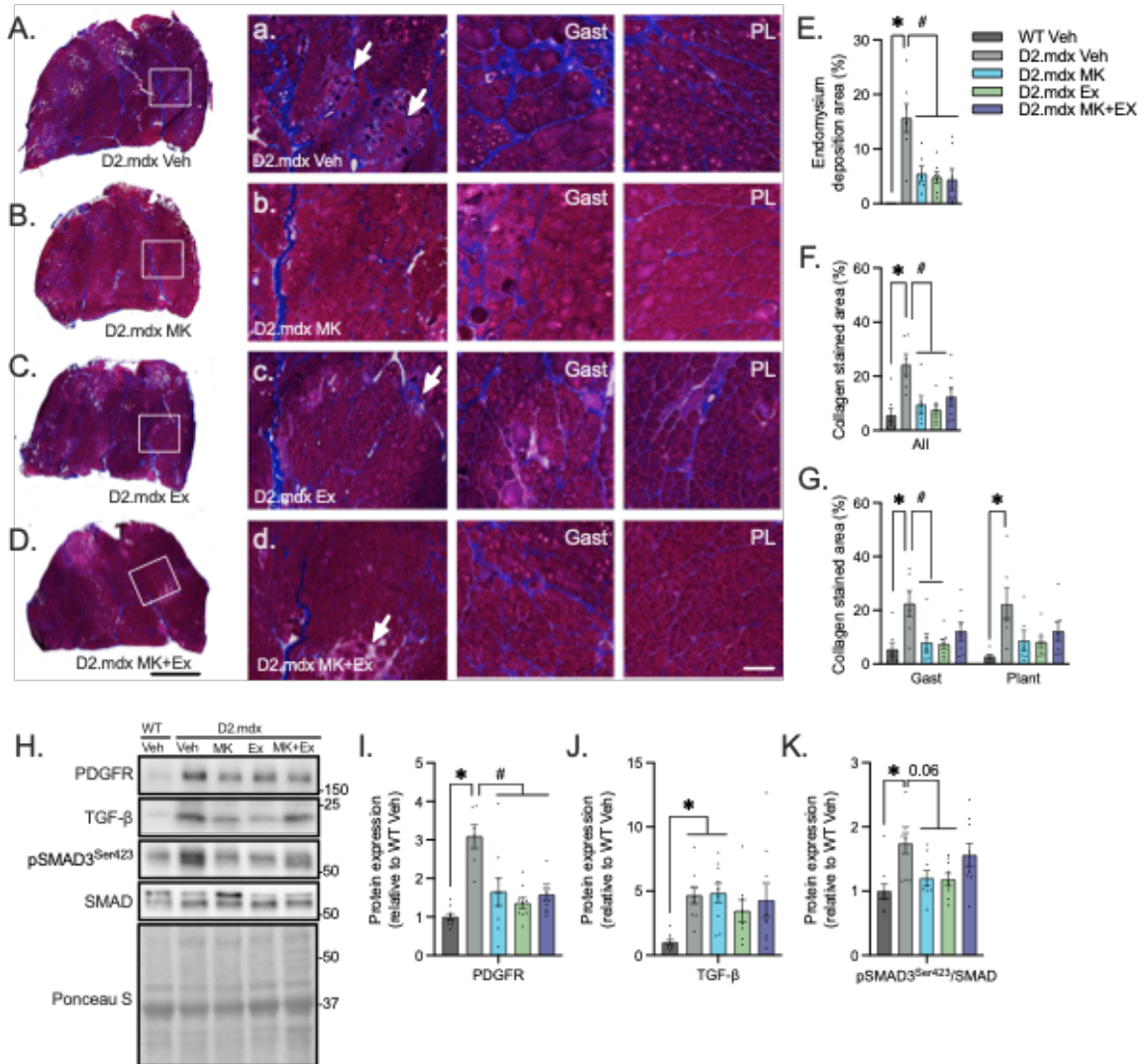
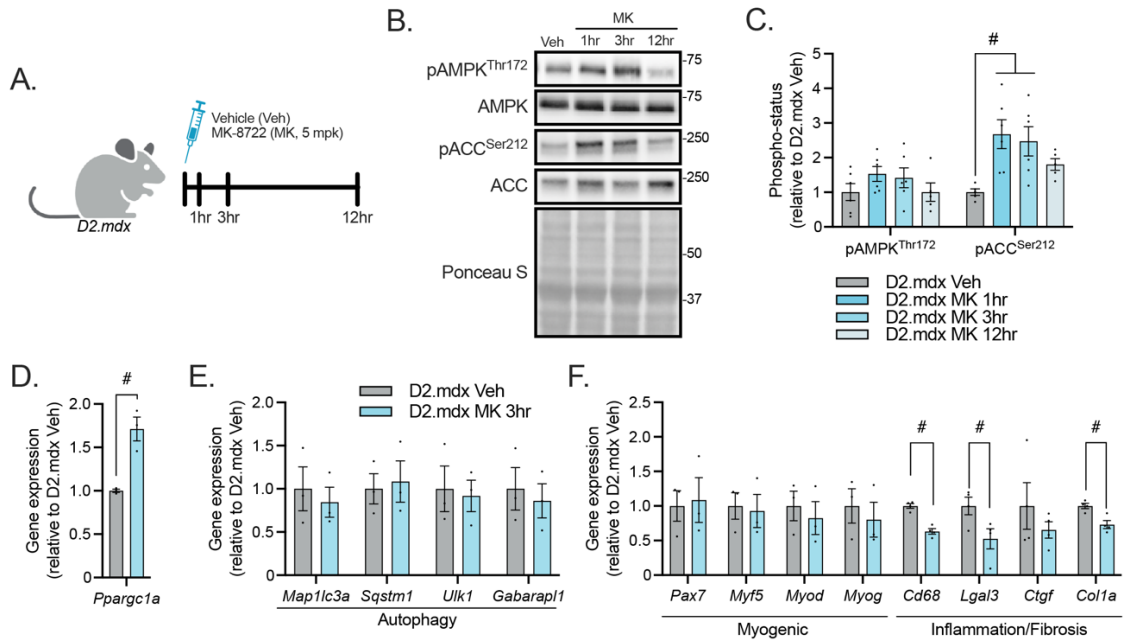


Fig 5. Effects of repeated MK treatment on skeletal muscle fibrosis in D2.mdx animals. (A-D) Representative Masson's trichrome stain images of the gastrocnemius (GAST) and plantaris (PL) complex in D2.mdx Veh (A), D2.mdx MK (B), D2.mdx EX (C), and D2.mdx MK+EX (D) mice. (Rows a-d) Enlarged images from the white inset boxes highlight ECM deposition (indicated by the white arrows), regions of the GAST and PL muscles in Veh- or MK-treated D2.mdx animals. (E-G) Graphical summaries of endomysium fibrosis (E) and collagen-stained area (F) in the entire section (E), as well as in the collagen-positive areas in GAST and PL muscles (G). (H) Representative Western blots of platelet-derived growth factor receptor (PDGFR), transforming growth factor- β (TGF- β), and Ser⁴²³-phosphorylated mothers against decapentaplegic homolog (pSMAD3^{Ser423}) and SMAD protein expression in the TA muscles of Veh-treated WT mice and Veh- or MK-treated D2.mdx mice. Ponceau S staining is shown below as a loading control. Protein ladder markers on the right are denoted in kDa. Graphical summaries illustrating the protein expression levels of PDGFR (I), TGF- β (J), and pSMAD3^{Ser423}/SMAD (K) in all experimental groups. Immunoblotting data are presented as fold differences relative to the WT Veh group. Graphical summaries display individual data points and group means (bars) with SEM. n = 8–10. Statistical significance was denoted as *, p < 0.05 versus WT Veh and #, p < 0.05 versus mdx Veh.



Supplementary Fig 1: The acute effects of MK dosing on AMPK and downstream signaling in dystrophic skeletal muscle. (A) 5-week-old, male D2.mdx animals were orally gavaged a single dose of vehicle (Veh) or MK solution. Following treatment, MK-treated animals were euthanized 1- (D2.mdx MK 1hr), 3- (D2.mdx MK 3hr), or 12 hours (D2.mdx MK 12hr) post-gavage. Veh-treated animals were euthanized at the same timepoints and pooled to serve as a control group (D2.mdx Veh). (B) Representative Western blots of threonine 172 (Thr¹⁷²)-phosphorylated AMPK (pAMPK^{Thr172}), total AMPK, serine 212 (Ser²¹²)-phosphorylated acetyl-CoA carboxylase (pACC^{Ser212}), and total ACC in the TA muscles of Veh- and MK-treated D2.mdx animals. Ponceau S staining is down below to indicate even sample loading. Protein ladders are expressed as kDa at the right. (C) Graphical summary of phosphorylation status (i.e., the phosphorylated form of the protein relative to its total amount within the same sample; Phospho-status) of AMPK and ACC in the TA muscles of Veh- or MK-treated mice. Graphical summaries display individual data points and group means (bars) with SEM. n = 3–6. Statistical significance was denoted as #, p < 0.05 versus mdx Veh (comparison with Veh-treated D2.mdx animals).

Tables:

Table 1: Effects of chronic MK-8722 (MK), exercise (EX), or MK+EX on tissue morphology in *D2.mdx* mice

	Tri/BM (mg/g)	Quad/BM (mg/g)	EDL/BM (mg/g)	SOL/BM (mg/g)	TA/BM (mg/g)	GAST/BM (mg/g)	Heart/BM (mg/g)	Liver/BM (mg/g)
<i>WT</i>	4.18 ± 0.13	7.02 ± 0.24	0.31 ± 0.02	0.19 ± 0.01	1.79 ± 0.16	5.51 ± 0.12	5.99 ± 0.54	49.37 ± 4.15
<i>D2.mdx</i> Veh	3.30 ± 0.22*	5.55 ± 0.17*	0.28 ± 0.02	0.23 ± 0.01*	1.44 ± 0.04	4.58 ± 0.14*	6.04 ± 0.27	64.38 ± 3.25
<i>D2.mdx</i> MK	3.01 ± 0.16*	5.53 ± 0.21*	0.27 ± 0.01	0.24 ± 0.01*	1.40 ± 0.06*	4.42 ± 0.18*	5.87 ± 0.44	58.70 ± 11.80
<i>D2.mdx</i> Ex	3.34 ± 0.20*	5.35 ± 0.10*	0.27 ± 0.01	0.25 ± 0.01*	1.40 ± 0.10*	4.61 ± 0.16*	5.89 ± 0.31	58.43 ± 9.71
<i>D2.mdx</i> MK+EX	3.18 ± 0.14*	5.59 ± 0.17*	0.24 ± 0.01*	0.26 ± 0.01*#	1.48 ± 0.05	4.61 ± 0.18*	6.08 ± 0.34	63.26 ± 5.45

Values are the mean +/- SEM (n = 8-9/Group). WT, Wild-type; Veh, Vehicle; MK, MK-8722; Ex, Exercise; Tri, Triceps weight; BM, Body mass; Quad, Quadriceps weight; EDL, Extensor digitorum longus weight; SOL, soleus weight; TA, Tibialis anterior weight; GAST, Gastrocnemius weight. *, P < 0.05 vs WT Veh; #, P < 0.05 vs *mdx* Veh.

Table 2: Effects of chronic MK, EX, or MK+EX on cardiac morphology

	RWT (mm)	EDV (µL)	ESV (µL)	SV (µL)
<i>WT</i>	0.91 ± 0.10	69.16 ± 4.48	23.08 ± 2.27	42.56 ± 3.76
<i>D2.mdx</i> Veh	1.29 ± 0.15	64.91 ± 7.16	23.28 ± 3.71	43.62 ± 3.73
<i>D2.mdx</i> MK	1.33 ± 0.16	66.71 ± 7.11	28.24 ± 4.21	38.47 ± 3.39
<i>D2.mdx</i> Ex	1.2 ± 0.14	66.58 ± 6.54	28.24 ± 4.13	38.34 ± 2.86
<i>D2.mdx</i> MK+EX	1.64 ± 0.21	64.67 ± 7.27	22.71 ± 5.72	41.97 ± 2.68

Values are the mean +/- SEM (n = 8-9/Group). RWT, relative wall thickness; EDV, end diastolic volume; ESV, end systolic volume; SV, stroke volume.

Table 3: Effects of chronic MK, EX, or MK+EX on cardiac function

	FS (%)	EF (%)	CO (mL/min)	ET (ms)	MPI
<i>WT</i> Veh	27.59 ± 2.55	53.45 ± 3.89	14.42 ± 1.38	56.14 ± 3.59	0.61 ± 0.04
<i>D2.mdx</i> Veh	35.56 ± 0.94	68.4 ± 2.99	14.81 ± 0.96	58.02 ± 1.72	0.58 ± 0.04
<i>D2.mdx</i> MK	34.23 ± 0.9	63.72 ± 1.24	21.77 ± 4.03	56.14 ± 1.69	0.55 ± 0.02
<i>D2.mdx</i> Ex	30.75 ± 1.72	58.69 ± 2.6	20.22 ± 4.37	55.53 ± 1.86	0.62 ± 0.04
<i>D2.mdx</i> MK+Ex	38.65 ± 3.27	68.5 ± 4.42	20.59 ± 3.28	50.51 ± 2.04	0.6 ± 0.02

Values are the mean +/- SEM (n = 8-9/Group). FS, fractional shortening; EF, ejection fraction; CO, cardiac output; ET, ejection time; MPI, myocardial performance index.

Table 4: Effects of chronic MK, EX, or MK+EX on mitral valve function

	Peak E wave velocity (mm/min)	Peak A wave velocity (mm/min)	A wave acceleration time (ms)	E wave deceleration time (ms)	E/A ratio
<i>WT</i> Veh	611.62 ± 37.6	375.65 ± 35.4	40.62 ± 7.33	33.01 ± 1.83	1.68 ± 0.14
<i>D2.mdx</i> Veh	400.12 ± 28.6*	279.1 ± 27.51*	27.88 ± 3.76	34.67 ± 3.81	1.58 ± 0.08
<i>D2.mdx</i> MK	605.72 ± 40.45#	345.4 ± 23.64	45.53 ± 3.35#	38.63 ± 3.3	1.78 ± 0.11
<i>D2.mdx</i> Ex	440.44 ± 31.85*	277.13 ± 24.84	28.27 ± 3.99	35.67 ± 1.75	1.67 ± 0.1
<i>D2.mdx</i> MK+EX	447.15 ± 28.88*	300.77 ± 19.93	34.98 ± 4.28	28.87 ± 2.65	1.51 ± 0.08

Values are the mean +/- SEM (n = 8-9/Group). E/A (Peak E wave velocity/Peak A wave velocity).

Table 5: Effects of chronic MK, Ex, or MK+EX on extensor digitorum longus (EDL) twitch kinetics

	Max twitch (mN)	TPT (ms)	+dF/dt (N/cm²/s)	½ RT (ms)	-dF/dt (N/cm²/s)
<i>WT</i> Veh	67.57 ± 1.25	375.65 ± 35.4	1297.17 ± 65.89	18.29 ± 0.43	1297.173 ± 65.89*
<i>D2.mdx</i> Veh	25.02 ± 0.78*	279.1 ± 27.51	287.40 ± 8.67*	63.84 ± 0.63*	287.39 ± 8.67*
<i>D2.mdx</i> MK	27.73 ± 0.67*	345.4 ± 23.64	376.64 ± 13.15	44.12 ± 2.14*#	376.64 ± 13.15*
<i>D2.mdx</i> Ex	14.97 ± 0.60*#	277.13 ± 24.84	238.82 ± 16.77*	54.76 ± 2.77*	238.82 ± 16.77*
<i>D2.mdx</i> MK + EX	20.846 ± 1.02*	300.77 ± 19.93	273.37 ± 12.39*	53.93 ± 2.11*	273.36 ± 12.39*

Values are the mean +/- SEM (n = 8-9/Group). TPT, time to peak tension; +dF/dt, maximal rate of force development; ½ RT, half relaxation time; -dF/dt, maximal rate of relaxation; T ½ W, twitch half-width (i.e., time from half rise to half relaxation). *, P < 0.05 vs. WT Veh #, P < 0.05 vs. *D2.mdx* Veh.

CHAPTER 5:
INTEGRATED DISCUSSION

5.1 - Introduction

The NMJ is a specialized synapse that enables precise and reliable communication between motor neurons and muscle fibers. Perturbations in molecular factors governing NMJ plasticity have been linked to the gradual breakdown of the synapse, resulting in neurotransmission failure and subsequent loss of motor function, common features that are present with aging, neurodegenerative diseases, and NMDs. Therefore, understanding the factors responsible for NMJ maintenance and remodeling provides potential therapeutic target for research. This dissertation aimed to evaluate the role of AMPK in neuromuscular biology concerning both health and disease. In Study 1, we employed transgenic, pharmacologic, and physiological methods to manipulate AMPK expression and function, with the goal of assessing its impact on the NMJ phenotype and gene expression. Our findings underscored the crucial role of AMPK in maintaining the NMJ and orchestrating the transcriptional processes that support synapse function. These results then prompted us to explore the potential therapeutic applications of AMPK in the context of the most prevalent congenital NMD, DMD. In Study 2, we analyzed the acute responses to the potent pan-AMPK activator, MK, successfully demonstrating pharmacological induction of AMPK and downstream signaling that was indicative of a disease-resistant phenotype in dystrophic muscle. Building upon these findings, Study 3 delved into investigating the chronic effects of AMPK activation in the D2.mdx mouse model. Here, MK caused noteworthy improvements in mitochondrial health, reductions in muscle fibrosis, and upregulation of utrophin protein, culminating in enhanced muscle function and resistance

to fatigue. In the subsequent sections, we will expand on these primary findings, relating them to prior research, and offering future considerations for warranted investigations.

5.2 AMPK as a nexus signaling molecule affecting the NMJ

AMPK represents a pleiotropic signaling molecule with an extensive array of downstream substrates, numbering in the hundreds (1, 2). These targeted proteins frequently govern intricate signaling cascades, thereby regulating acute metabolic processes, and endowing chronic adaptations. The significance of this kinase has been extensively highlighted through investigations employing gain-of-function and loss-of-function AMPK experimental models (3–7). The existing data from studies 1, 2, and 3 elucidate a novel regulatory role of AMPK on NMJ biology, encompassing both normal and pathological muscle conditions. This regulatory role likely hinges on AMPK-regulated processes such as autophagy, mitochondrial turnover, and regeneration, as these mechanisms have been implicated in the maintenance of the NMJ (8–11). By extension, the cells which support these processes may also be important for the regulation of the NMJ.

5.2.1 Regulatory impact of AMPK on cellular pathways relevant to the NMJ

AMPK-regulated processes have been extensively implicated in their potential contribution to age-associated NMJ dysfunction (8–11). Notably, AMPK plays a pivotal role in regulating various aspects of mitochondrial biology, encompassing biogenesis, mitophagy, and dynamics (12, 13). The significance of mitochondria in the maintenance and remodeling of the NMJ is well-established (14–16). The pronounced abundance of these energetic organelles within the pre- and postsynaptic compartments of the NMJ

strongly implies their involvement in NMJ functionality. This notion gains further support from observations in patients with mitochondrial diseases, typically characterized by compromised mitochondrial function and impaired NMJ morphology and function (13–15). Additionally, mitochondrial defects have been identified in various NMDs, such as DMD, amyotrophic lateral sclerosis (ALS), and spinal muscular atrophy (SMA), often preceding the symptomatic stages of these conditions (16, 17). Within the context of Study 1, skeletal muscles deficient in AMPK display compromised mitochondrial respiration and altered morphology, along with a notable reduction in exercise tolerability and muscle force production (18–20). The characteristics in these animals also suggest a significant role of mitochondria in contributing to NMJ fragmentation. To gain more precise insights into the effects of AMPK, it is imperative for future research to prioritize the investigation of conditional AMPK knockout (KO) models, such as the recently reported tamoxifen-inducible AMPK α 1 α 2 KO model (5, 7). Utilizing these refined models will enable a more targeted and specific understanding of the intricate interplay between AMPK and mitochondrial dynamics in the context of NMJ function and related neuromuscular pathologies.

The involvement of AMPK in initiating the autophagy process has been extensively documented, and this activation occurs through interactions with various autophagy-related proteins, including ULK1, mTOR, and TFEB (12, 21). The significance of autophagy in the context of the NMJ is exemplified by a study conducted by Carnio et al. (8). Here, the authors demonstrated that transgenic inhibition of autophagy led to the elimination of AChR, coincident with a denervated muscle phenotype. Moreover, autophagosomes

containing AChR subunits have been identified within the synaptic space (22–24), indicative of the degradation and recycling of these AChR units. Myopathies such as Danon’s disease, myotonic dystrophy, and DMD, are characterized by dysfunctional autophagy, as well as dysmorphic NMJs (25, 26). Intriguingly, research has revealed that restoring or enhancing the autophagy program can ameliorate the abnormal NMJ phenotype in dystrophic muscle (24). In the context of the current thesis, transgenic AMPK $\beta 1\beta 2$ muscle-specific knockout animals exhibit defective autophagy and impaired muscle force production (18). As such, there is a plausible association between AMPK, disturbances in autophagy, and neuromuscular dysfunction. Together, these findings underscore the significance of AMPK-mediated autophagy in the maintenance of NMJ integrity.

5.2.2 - Influence of AMPK on cell-specific alterations and implications for the neuromuscular synapse

Physiological AMPK activation via exercise or caloric restriction remodel the neuromuscular synapse (9, 27–29). Moreover, animal models presenting fragmented NMJs resulting from aging (9, 27, 28, 30, 31), dystrophy (16, 32), or neurodegenerative disorders (33–35), prolonged pharmacological stimulation of AMPK has been found to preserve synaptic morphology and function. However, these studies did not account experimentally for the contributions of the systemic activation of AMPK at the neuromuscular synapse. To gain additional insight on MK, we treated cultured muscle cells with MK to model targeted skeletal muscle-specific AMPK gain-of-function and investigated the role of the kinase on a neural AChR (Study 1). Our findings indicate that AMPK induces AChR clustering in C2C12 cells to a comparable extent as the canonical neurotrophic factors. Prior in vitro

studies have demonstrated that indirect AMPK activators like metformin and resveratrol do not exert any influence on AChR clustering (27). This discrepancy with our data may be attributed to the superior magnitude and specificity of AMPK stimulation achieved with MK in comparison to other compounds (36, 37). Additionally, we observed that agrin and Wnt did not elicit AMPK phosphorylation or activity, suggesting that their neurotrophic effects are AMPK-independent (Study 1). These findings imply that AMPK agonists may exhibit additive or synergistic effects in conjunction with other NMJ-targeted approaches to evoke synapse remodeling.

It is essential to note that the MK-induced NMJ adaptations observed in dystrophic muscle *in vivo* (Study 3) may also be influenced by AMPK activation in neuronal cells, as well as other NMJ-supporting cell type (Figure 1). Direct evidence for these alternative cellular adaptations are shown in studies which pharmacologically stimulate the kinase in these specific cell types. For instance, resveratrol- and AICAR-mediated AMPK stimulation has been shown to increase neurite outgrowth and mitochondrial biogenesis in Neuro2a neuroblastoma cells (38). The pharmacological induction of AMPK has been shown to influence perisynaptic glia cell function and myelin gene expression, which collectively function to support the NMJ (39). Lastly, Liu et al. (40, 41) revealed the consequences of conditional KO of MuSC on the regenerative capacity of NMJ and highlighted the crucial involvement of MuSC in the remodeling process of NMJ. This observation assumes relevance due to the established evidence indicating that pharmacological stimulation of AMPK augments the metabolic profile towards a state that

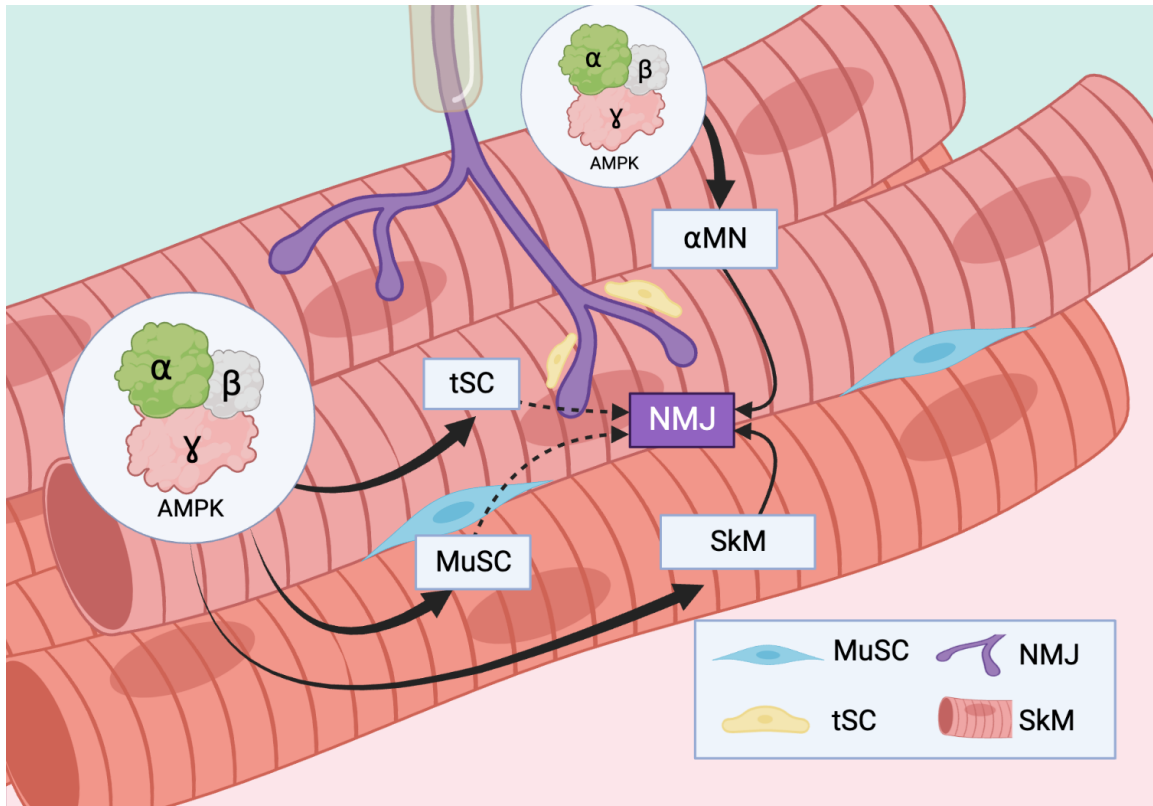


Fig 1. The role of AMPK in regulating the NMJ niche. The NMJ comprises an α -motoneuron (α MN), the innervated muscle fiber (SkM), and the terminal Schwann cell (tSC). The modulation of AMPK activity in α MN or SkM can alter the morphology and function of the NMJ. The tSC plays a crucial supportive role for the NMJ, essential for optimal functioning, however the role of AMPK in this cell type is undefined. Additionally, muscle stem cells (MuSC) are implicated in NMJ remodeling, and whether AMPK influences the NMJ through these cells remains to be investigated. Solid lines indicate established links between the groups, while dotted lines represent potential interactions resulting from AMPK-mediated changes at the NMJ.

favors MuSC quiescence (42, 43). Together these studies shed light on additional avenues beyond skeletal muscle, through which AMPK exerts regulatory influence on the neuromuscular synapse.

5.3 Proposed AMPK-mediated mechanisms affecting synapse maintenance

Acute stimulation of AMPK in skeletal muscle has been shown to play a significant role in activating gene programs involved in various metabolic pathways (44–46). In the present study, we shed light on the extent of AMPK-mediated transcriptional regulation at

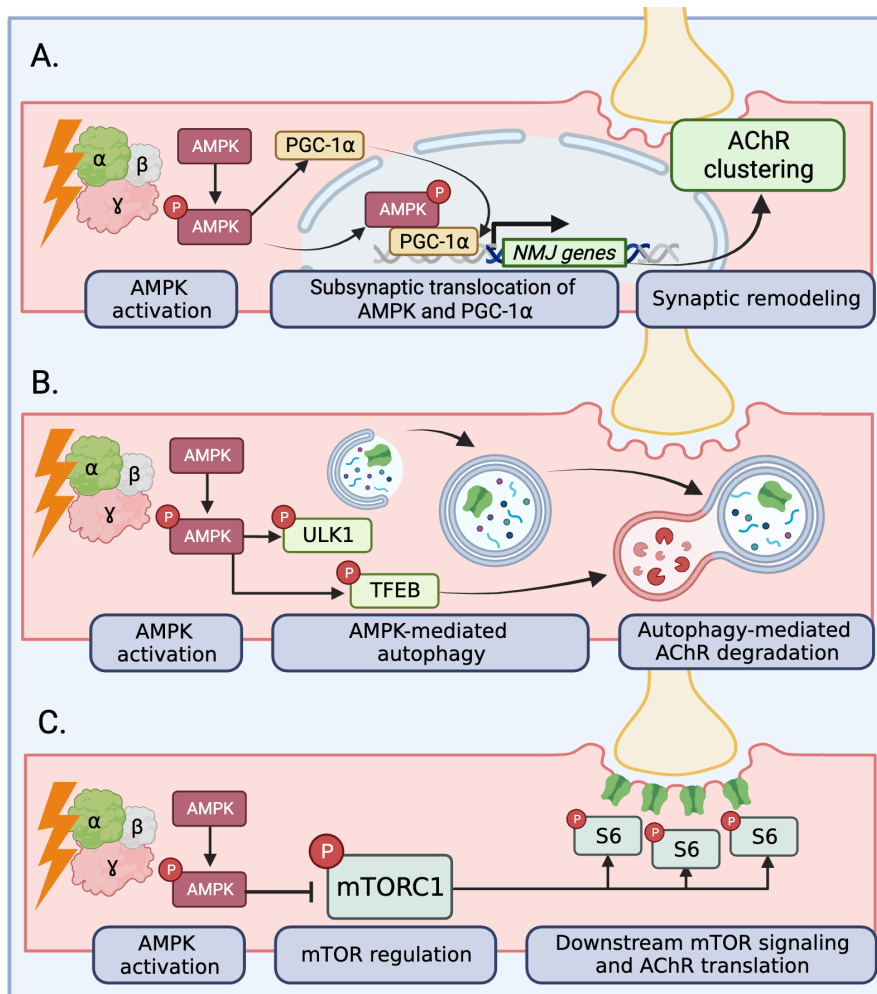


Fig 2. Proposed muscle mechanisms of AMPK-mediated NMJ plasticity. The maintenance of the NMJ during remodeling relies on the balance between the production and degradation of AChR (AChR turnover). We propose the following mechanisms through which AMPK may mediate NMJ plasticity: **(A)** AMPK activation and synaptic gene transcription: Upon AMPK activation, we hypothesize that the kinase promotes synaptic gene transcription through PGC-1 α within subsynaptic nuclei. **(B)** AMPK-mediated autophagy of AChR. AMPK is likely involved in autophagy regulation within the subsynaptic space, targeting AChR degradation. This process may be mediated through established autophagic regulators such as ULK1 and TFEB. **(C)** mTOR-mediated AChR translation at the postsynapse. AMPK may influence AChR translation at the postsynaptic site through mTOR signaling. The synaptic enrichment of mTOR targets, such as pS6, supports this hypothesis. Solid lines indicate established links between the proposed mechanisms and AMPK-mediated NMJ plasticity.

the NMJ (Figure 2A). Specifically, the data presented in Study 1 demonstrate a noteworthy increase in synaptic gene expression, including *Musk*, *Dok7*, and *Ppargal*, in response to pharmacological activation of AMPK. These MK-induced NMJ transcripts are under the control of an N-box promoter motif, which is regulated by a PGC-1 α /GABP complex (47).

Considering the well-established association between AMPK and PGC-1 α in skeletal muscle (44, 48), it is plausible to suggest that the induction of synaptic genes occurs through an AMPK/PGC-1 α /GABP signaling cascade. To bolster this claim, our investigation also revealed a rapid increase in postsynaptic pAMPK^{Thr172} and PGC-1 α following MK treatment, along with the concurrent accumulation of these molecules in fundamental (subsynaptic) nuclei. These events preceded the observed elevation in NMJ gene expression. It is worth noting that the nuclear localization of AMPK and PGC-1 α has been previously documented (49–51); however, these earlier studies focused on non-specific myonuclei and did not conduct mRNA analyses. It is essential to acknowledge that our current thesis did not delve into additional AMPK-inducible signaling pathways that may be related to neuromuscular plasticity, such as the Hippo/Yes-associated protein or Wnt/ β -catenin cascades (52, 53). Further exploration of downstream AMPK effects may unveil novel mechanisms through which this kinase coordinates activities at the neuromuscular synapse. Continued research in this direction holds the potential to provide valuable insights into the comprehensive regulatory network underlying neuromuscular function.

On balance, the postsynapse is regulated by the turnover (net rate of production relative to degradation) of the AChR (16, 53, 54). Emerging evidence suggests that signaling pathways involving the AMPK target, mTOR, play a modulatory role in AChR translation and degradation (29, 55, 56) (Figure 2C). Although mTOR has not been shown to localize to the NMJ directly, mTORC1 targets, such as eIF4E (57) and pS6^{Ser240} (29), have been found to be enriched at the NMJ in *Drosophila* larvae and mice, respectively. In Study 1, we have observed a significant reduction in the expression of pS6 in AMPK-

deficient muscle compared to their WT counterparts, suggesting a potential failure in translational processes that are essential to produce AChR. This finding aligns with earlier reports from studies involving mTOR activity depletion models, such as inducible mTOR knockout animals and repeated rapamycin-treatments, which have shown abnormalities in NMJ structure and function (56). It would be essential to conduct AChR turnover assays with dual postsynaptic labeling, an experiment that has not been performed in the AMPK- and mTOR-deficient muscle models. By doing so, we can better assess the impact of AMPK on the morphology and structure of the neuromuscular synapse through its influence on AChR translation.

AChR degradation is governed by the metabolic stability of AChR, a characteristic likely regulated by AMPK. Several studies have demonstrated that stimulating AMPK, via muscle contraction or pharmacological agents, enhances the metabolic stability of AChR receptors under denervated or dystrophic conditions (32, 59–60). Intriguingly, several AMPK motifs have been identified on various components of the DAPC/UAPC (61), which play a critical role in maintaining the stability of the NMJ (62, 63). Furthermore, recent work has shown that the Ser²⁹⁸ phosphorylation of utrophin enhances the mechanical stability of the protein (62), suggesting that posttranslational modifications of other UAPC proteins may also augment their mechanical properties. Consistent with this overarching hypothesis, the data in Studies 2 and 3 demonstrate that MK dosing can increase utrophin protein expression within the synaptic regions of the muscle. Together, these findings underscore the intricate relationship between AChR degradation and its metabolic stability, highlighting the potential significance of AMPK modulation in preserving NMJ integrity

(Figure 2B). Further investigation into these mechanisms could provide valuable insights into the generalizability of these therapeutic approaches.

5.3.1 AMPK drives favourable mitochondrial adaptations in preclinical models of DMD

In Study 2, notable findings were observed in fast, glycolytic muscles of the MK-treated mdx animals (Figure 3A). We observed a significant increase in the translocation of myonuclear PGC-1 α , accompanied by elevated levels of *Ppargc1a* and *Nrf1* mRNA, as well as enhanced utrophin protein expression. These observed changes collectively signify a transition towards a slower, more oxidative phenotype in the muscles, which confers heightened protection against DMD (26, 64). The observed myonuclear accumulation of PGC-1 α and the concurrent rise in *Ppargc1a* transcript levels strongly suggest an augmentation of PGC-1 α activity (65). This inference gains further support from the subsequent increase in *Nrf1*, a well-established transcriptional target of PGC-1 α (66, 67). These results imply that the administration of MK leads to enhanced PGC-1 α -mediated transcriptional regulation, which likely contributes to the observed shift in muscle phenotype towards a more oxidative state, known for its beneficial effects in ameliorating the progression of DMD.

Likewise, in Study 3, we observed that the repetitive administration of MK resulted in a significant enhancement of state III CI- and CI and CII-linked mitochondrial respiration in the skeletal muscles of D2.mdx animals. This adaptive response was accompanied by a conspicuous increase in mitochondrial content, as evidenced by elevated levels of mitochondrial CI-CV subunits. Notably, in a previous investigation conducted by Pauly et

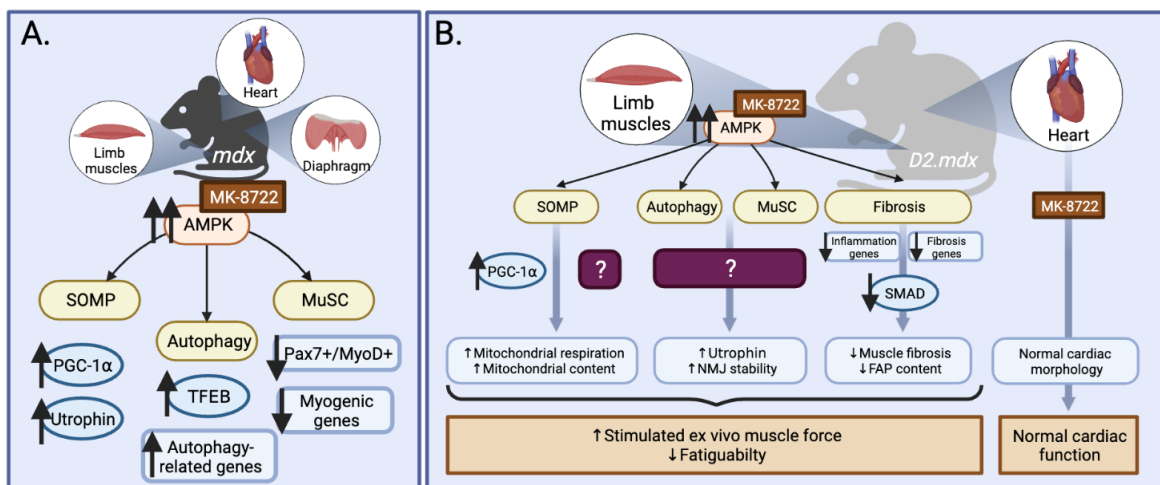


Fig 3. Acute responses and chronic adaptations from MK dosing in dystrophic animals. (A) Study 2: Acute effects of MK on skeletal muscles. In this study, we investigated the acute effects of MK treatment on various skeletal muscles, including the diaphragm and heart. Notably, MK evoked AMPK activation in limb muscles, leading to the induction of multiple AMPK signaling cascades. These included the upregulation of the slow oxidative muscle program, activation of autophagy processes, and normalization of muscle stem cell biology. **(B)** Chronic effects of MK in D2.mdx animals. In the subsequent study, we explored the chronic effects of repeated MK treatment in D2.mdx animals. Our preliminary findings revealed significant improvements in mitochondrial respiration and content, accompanied by elevated utrophin expression and enhanced NMJ stability. Moreover, we observed noteworthy reductions in inflammatory and fibrosis-related gene expression, as well as decreased SMAD signaling in the hind limb. These beneficial changes resulted in functional adaptations, including increased muscle force and reduced fatigability. Importantly, cardiac myopathy was not evident in these animals throughout the study. Solid lines indicate established links between the described effects of MK treatment in dystrophic animals.

al. (68), it was demonstrated that repeated AICAR treatment failed to induce any improvement in oxidative function within the diaphragm muscle. Between the two studies, the observed disparities on mitochondrial respiration findings could be attributed to inherent differences in fiber types present in the muscles being examined: with the diaphragm consisting of predominately slow oxidative fibers and the QUAD comprising a more glycolytic fiber type composition. In fact, earlier research has established that fast glycolytic fibers display a greater degree of plasticity in response to AMPK agonists in the context of DMD muscle (69, 70). Nevertheless, these findings provide robust support for

the proposition that repeated MK treatment fosters improved mitochondrial health in dystrophic muscle tissue.

5.3.2 AMPK controls autophagic signaling in DMD muscle

AMPK has been demonstrated to play multiple roles in autophagy, including the initiation of the process, enhancement of autophagosome formation, and promotion of lysosomal biogenesis (21, 71). Understanding the regulatory role of AMPK in autophagy is particularly crucial within the context of DMD, as dystrophic muscles exhibit impairments in each of these processes, both in preclinical models and in DMD patients (25, 68, 72). Moreover, it has been observed that chronic treatment with AICAR in mdx animals leads to significant improvements in autophagy-related processes and coincides with overall enhancements in muscle function (68). In Study 2, the administration of a single dose of MK, an AMPK agonist, elicited profound autophagy signaling in dystrophic muscle. This response included AMPK-specific pro-autophagic phosphorylation, increased expression of the autophagy gene program, and modulation of ULK1, a key regulator of autophagy, at the Ser⁵⁵⁵ mark. Additionally, the treatment with MK led to reduced phosphorylation of S6 at Ser^{235/236} and exhibited a tendency to decrease mTOR-specific phosphorylation of ULK1 at Ser⁷⁵⁷, both of which are recognized as indicators of diminished mTOR activity. Similarly, repeated acute dosing experiments with O304 revealed similar mTOR signalling events (Appendix B, Additional Data). These findings strongly suggest that the AMPK agonists, MK and O304, exert their effects on autophagy by directly targeting ULK1 via AMPK and indirectly through the AMPK/mTOR/ULK1 signaling axis in DMD muscle.

In dystrophic mice exposed acutely to MK and O304, there was a notable increase in the levels of autophagosome markers, such as the LC3II/I ratio and p62 protein expression (Study 2 and Appendix B). Furthermore, the expression of autophagy-related genes, including *Map1lc3*, *Gabra1*, and *Sqstm1*, was also found to be elevated in response to the AMPK agonists. The administration of MK also resulted in the myonuclear accumulation of TFEB, the master regulator of autophagy gene expression, which preceded the upregulation of autophagy-related genes. These collective findings strongly support the notion that the autophagy program is initiated in dystrophic muscle following a single dose of these novel AMPK activators.

5.4.3 AMPK targets muscle fibrosis and regeneration in dystrophic animals

The onset of fibrosis is a cellular consequence to the repeated chronic injury, activation of fibroblasts, and excessive collagen production. These processes are coordinated by resident immune cells, MuSC, FAP, and other cellular constituents within the regenerative niche. The data in Study 3 indicate that acute exposure to MK reduced inflammation- and fibrosis-related genes, as well as reduced in fibrosis upon chronic treatment in the skeletal muscle of D2.mdx animals. These findings are in line with previous contributions from the Chazaud laboratory that have highlighted the crucial role of AMPK on muscle inflammation, regeneration, and repair (43, 73–77). Specifically, Juban and colleagues (74) revealed that AMPK activation reduces the release of endogenous TGF- β through an LTBP4-dependent mechanism and instigates an anti-inflammatory and anti-fibrotic phenotype in *mdx* mice. Given that the D2.mdx model that features a *LTBP4* polymorphism and hyperactive TGF- β signaling (78, 79), it is tempting to hypothesize that

this is the primary mechanism by which MK exerts its anti-fibrotic effects. Corroborating these findings, data from Study 3 unveil a notable trend ($p=0.07$), indicating the reduction in the activity status of the downstream TGF- β signaling molecule, SMAD, in the skeletal muscles of D2.mdx animals following MK administration, substantiating the potential of MK as a therapeutic agent against fibrosis in DMD muscle. These findings are not surprising as allosteric AMPK activators have been demonstrated to attenuate tissue fibrosis in the kidney and liver (80–82).

In conjunction with the heightened activity of TGF- β , the excessive accumulation of FAP and the pathological deposition of the extracellular matrix have been postulated as potential contributors to the fibrotic manifestations observed in DMD muscle (83, 84). Consistent with this premise, our findings indicate a reduction in FAPs following chronic AMPK activation (Study 3). These observations align with the work of Saito et al. (85), which demonstrated that a two-week AICAR treatment in preclinical models of chronic inflammatory myopathies resulted in a decrease in FAP content. Additionally, this reduction was accompanied by the emergence of a senescent and apoptotic FAP phenotype, which was associated with enhanced muscle regeneration in dystrophic animals. Taken together, the alterations in fibrotic progenitors and muscle fibrosis in MK-treated D2mdx animals suggest a plausible role of senescence in FAP cells.

Upon muscle damage, macrophages play a crucial role in regulating the persistent inflammation at the site of injury and signaling neighboring cells within the regenerative niche. The resolution of this chronic inflammation in skeletal muscle has been shown to depend on AMPK activity (86, 87), which has proven beneficial in mitigating chronic

inflammatory in several myopathies, including DMD (73, 74, 85). In Study 3, we conducted experiments to investigate the effects of acute exposure to MK on the inflammatory gene profile that is characteristic of dystrophic muscle. Moreover, we have also examined the acute impact of O304 in D2.mdx animals and demonstrate a reduction in the inflammatory gene program (Appendix B). Previous research has reported on the anti-inflammatory effects of with direct AMPK activators, such as AICAR (74), salicylate (88), and A769662 (89), as well as other indirect AMPK activators (86). While the data presented in this thesis did not specifically explore the effects of MK or O304 on macrophages, it is reasonable to speculate that the observed suppression of inflammation genes is likely attributed to the actions of these immune cells. With this premise, it can be inferred that the activation of AMPK induced by MK may contribute to attenuating the inflammatory phenotype, thus offering an additional avenue that can promote muscle regeneration in dystrophic muscle.

5.4 Future considerations for AMPK activators

The investigation of AMPK activators as potential therapeutic agents for NMDs carries substantial significance within contemporary biomedical research. A comprehensive understanding of the pharmacokinetics, mechanisms, and potential combinatory therapies is imperative to fully unlock the therapeutic potential of AMPK activators in ameliorating the burden of NMDs. This exploration may bring forth a new era in precision medicine for addressing these debilitating conditions.

The duration and timing of AMPK activation have been postulated to hold a crucial role in AMPK-mediated adaptations. This significance is exemplified by a series of naturally occurring AMPK mutations in the *Prkag2* gene, which lead to a hypertrophic

cardiac phenotype detrimental to the heart's physiology (90–92). Likewise, chronic use of MK has been reported to contribute to hypertrophy and glycogen deposition in the hearts of healthy animals (36, 45). It is reasonable to suggest that mediating AMPK activation within a transient duration, akin to the patterns observed during exercise training, may mitigate these adverse effects on cardiac tissue (1). These observations underscore the importance of carefully considering the pharmacokinetic and pharmacodynamic profiles of both current and emerging AMPK agonists.

The diverse composition of AMPK across various cell types offers intriguing prospects for selectively stimulating specific cell populations. For instance, β 1-selective AMPK activators, exemplified by A769662 and PF-249, demonstrate the ability to target cell types that predominantly express this isoform, such as macrophages or hepatocytes in rodent models. However, it is noteworthy that there is currently a lack of available β 2-specific AMPK activators. Therefore, to activate β 2-containing AMPK complexes, which are predominantly found in muscle tissue, systemic pan-AMPK activators must be employed. The specificity of AMPK agonists in relation to distinct cell types has been elegantly demonstrated in previous research (93). Of particular interest, skeletal muscle cells possess the capacity to express γ 3-containing AMPK heterotrimers, an isoform not commonly found in most cell types. This observation raises the possibility of selectively activating AMPK in skeletal muscle if a γ 3-specific agonist were to be developed. Leveraging the isoform-specific activation of AMPK may provide a more targeted and effective treatment while minimizing off target effects. Together, the collection of evidence

emphasizes the importance of understanding the precise mechanism of action for AMPK agonist.

Combinatory therapies that incorporate AMPK agonists have emerged as a promising approach to enhance treatment efficacy for NMDs. Initial investigations exploring the effects of exercise in combination with AICAR treatment demonstrated negligible additive improvements in the metabolic profile of treated mdx muscle (94). However, recent studies have reported that the joint application of exercise and AICAR have revealed a synergistic effect, leading to significant advancements in muscle regeneration. This notable improvement has been attributed to the enhanced apoptosis and senescence of FAP cells in mdx mice (85), underscoring the distinct cellular responses induced by combinatory AMPK therapies. Following combination of MK administration and physical activity, specific alterations in the mitochondria and extracellular matrix manifest. However, it is noteworthy that certain molecular and cellular adaptations, such as utrophin expression and NMJ morphology, do not exhibit evident changes under these experimental conditions.

Of particular interest, previous research has suggested that the use of dual AMPK agonists may elicit a more robust stimulation of the kinase compared to the administration of each agonist individually. Consequently, this heightened activation has the potential to induce further metabolic adaptations (88, 95, 96). While speculative, this observation holds importance, as the combination of allosteric and indirect AMPK activators might lead to additive benefits like those observed with the combination of exercise previously mentioned. These findings underscore the potential of combinatory therapies involving

AMPK agonists as a promising avenue for enhancing treatment outcomes in specific aspects of NMDs. However, it is essential to acknowledge that further research is necessary to fully elucidate the underlying mechanisms and optimize the therapeutic approaches in this area. Continued investigation in this direction will contribute to the advancement of precision medicine and improved management of NMDs.

5.5 Limitations and future directions

The present dissertation offers valuable insights into the role of AMPK in neuromuscular biology within both health and disease contexts. In the second chapter of this study, we investigated the effects of transgenic or pharmacological manipulation of AMPK on the neuromuscular synapse. Our analysis revealed that these interventions exert significant changes on the NMJ through the transcriptional regulation of NMJ-related transcripts that play crucial roles in development and remodeling processes. Furthermore, we employed a publicly available web-tool, MetaMex, to examine a panel of NMJ genes in exercised human muscle samples (46). Our investigation led to the identification of two conserved gene targets, namely *Ppargc1a* and *Dok7*. These findings were corroborated by Muise and colleagues, who demonstrated that acute muscle contractions and exercise also induce alterations in synaptic transcripts (45). However, it is essential to acknowledge the limitations inherent in studying synaptic nuclei due to their specialized and limited nature. The muscle samples used in our rodent studies encompassed whole-muscle gene preparations, and the human muscle biopsies might not have consistently represented regions densely populated with postsynapses. Consequently, it is crucial to interpret the

results with caution, as they might either underestimate or overestimate the true transcriptional response of these synaptic transcripts.

To address this issue, future studies could utilize samples enriched with NMJs, such as employing laser microdissection techniques. Alternatively, novel genomic approaches like single-nuclei RNA sequencing could be employed to explore the transcriptional responses specific to NMJ nuclei. More recently, several research groups have applied these advanced techniques to characterize gene signatures in aged muscle (29, 97). Interestingly, the age-induced changes observed in these studies exhibit consistency with some transcripts identified in our Study 1 data (*Chrna1*, *Pparca1*, *Chrng*), while divergent changes also emerged (*Musk*, *Lrp4*, *Chrne*). These observations underscore the critical importance of considering the specialized nature of subsynaptic nuclei in interpreting research findings accurately. Therefore, by examining the acute responses to AMPK induction while taking these considerations into account, it is plausible that additional transcriptional targets relevant to neuromuscular biology may be realized.

In Study 2, we employed the mdx mouse model raised on a C57BL background to investigate the effects of MK-induced AMPK signaling in dystrophic muscle. Specifically, 10-week-old mdx animals were treated with MK, and various skeletal muscles, including the TA, DIA, GAST, EDL, SOL, and cardiac muscles, were utilized to assess AMPK signaling. It is important to acknowledge that the mdx mouse model represents a relatively less severe form of DMD, and the dystrophic phenotype is most evident in the diaphragm muscles at this timepoint. We were able to demonstrate MK-induced kinase activation in this muscle, however, due to the size of the muscle samples (~dissected <5 mg wet weight),

we could not comprehensively evaluate the downstream signaling in this clinically relevant muscle group. As a result, many of the interpretations made in Study 2 are inferred from the less severely affected distal limb muscle groups. To address this limitation, Study 3 focused on utilizing mdx animals on the DBA/2J background, which presents a more severe and persistent dystrophic phenotype in all skeletal muscles (78, 79). Our initial findings from this study indicate that MK can stimulate AMPK signaling in the affected TA muscles of D2.mdx animals. Continued analysis of additional muscle groups is ongoing to confirm the systemic effects of MK in this disease model.

Studies 1 and 2 utilize acute interventions to evaluate early transcriptional responses to AMPK activation. However, this approach is limited because it does not provide any data on the long-term adaptations on neuromuscular biology or adverse effects of targeted AMPK induction. This constitutes a major weakness in using an acute study design. Future work should build on previous studies that examined the AMPK-mediated neuromuscular adaptations in models which exhibit an impaired NMJ phenotype such as those observed in murine models of aging and NMDs (53). Notably, ongoing analyses in Study 3 aims to further address this issue by examining the chronic NMJ adaptations in response to repeated MK treatment in dystrophic animals.

5.6 Summary and main contributions of the dissertation

The plasticity of the NMJ is governed by a plethora of intracellular cues that is incompletely understood. Fundamentally, the NMJ relies on the coordinated interactions of its cellular components to establish and maintain its canonical role in neurotransmission. The phenotype of these cells is supported, or in some cases, thought to be driven by several

critical kinases, among which includes AMPK. The present dissertation dissects the regulatory role of AMPK at the NMJ in health and disease. In Study 1, we evaluated the necessity of skeletal muscle AMPK on NMJ biology during aging. We then determined whether the stimulation of the kinase could augment synaptic gene transcription with the intentions of later translating these findings in a compromised neuromuscular phenotype, such as DMD. In doing so, we revealed that AMPK plays a central role in regulating NMJ phenotype in young and aged animals. We then leveraged these findings to explore the therapeutic potential of AMPK in the context of the most prevalent congenital NMD, DMD. Study 2 validated the stimulatory effects of the allosteric pan-AMPK activator, MK, in the mdx mouse model. This is important as previous AMPK agonists have failed to translate to the clinic due to their lack of potency. Extending on this work, Study 3 evaluated the chronic adaptations following daily MK treatment in a pre-clinical model of DMD. We provide promising data revealing substantial improvements in mitochondrial health and neuromuscular function, as well as reductions in muscle fibrosis and fatigability. These findings collectively support the hypothesis that AMPK is a critical regulator of neuromuscular plasticity in health and disease. We also demonstrate that AMPK may be a viable therapeutic target worth pursuing for the treatment of muscular dystrophy. Further research is now needed fully elucidate the transcriptional and translational processes that underlie the neuromuscular adaptations mediated by AMPK. This will require a comprehensive investigation into the chronic alterations resulting from targeted AMPK stimulation, along with the use of sensitive approaches to discern synapse-specific changes.

5.7 References

1. Steinberg,G.R. and Carling,D. (2019) AMP-activated protein kinase: the current landscape for drug development. *Nat. Rev. Drug Discov.*, 10.1038/s41573-019-0019-2.
2. Steinberg,G.R. and Hardie,D.G. (2022) New insights into activation and function of the AMPK. *Nat. Rev. Mol. Cell Biol.* 2022 244, **24**, 255–272.
3. Kjøbsted,R., Hingst,J.R., Fentz,J., Foretz,M., Sanz,M.-N., Pehmøller,C., Shum,M., Marette,A., Mounier,R., Treebak,J.T., *et al.* (2018) AMPK in skeletal muscle function and metabolism. *FASEB J.*, **32**, 1741–1777.
4. O’Neill,H.M., Maarbjerg,S.J., Crane,J.D., Jeppesen,J., Jorgensen,S.B., Schertzer,J.D., Shyroka,O., Kiens,B., van Denderen,B.J., Tarnopolsky,M.A., *et al.* (2011) AMP-activated protein kinase (AMPK) 1 2 muscle null mice reveal an essential role for AMPK in maintaining mitochondrial content and glucose uptake during exercise. *Proc. Natl. Acad. Sci.*, **108**, 16092–16097.
5. Hingst,J., Rasmuss,;, Kjøbsted,R.;; Birk,J., Bratz,;; Jørgensen,N., Oldenburg,;; Larsen,M.R.;; Kido,K.;; Larsen,J., *et al.* Inducible deletion of skeletal muscle AMPK 1 reveals that AMPK is required for nucleotide balance but 2 dispensable for muscle glucose uptake and fat oxidation during exercise Inducible deletion of skeletal muscle AMPKa reveals that AMPK is required for nucleotide balance but dispensable for muscle glucose uptake and fat oxidation during exercise. 10.1016/j.molmet.2020.101028.
6. Cokorinos,E.C., Delmore,J., Reyes,A.R., Wojtaszewski,J.F.P., Cameron,K.O., *et al.* (2017) Activation of Skeletal Muscle AMPK Promotes Glucose Disposal and Glucose Lowering in Non-human Primates and Mice PF-739 treatment increases PGC1a transcription and mitochondrial content in muscle. *Cell Metab.*, **25**, 1147-1159.e10.
7. Rhein,P., Desjardins,E.M., Rong,P., Ahwazi,D., Bonhoure,N., Stolte,J., Santos,M.D., Ovens,A.J., Ehrlich,A.M., Sanchez Garcia,J.L., *et al.* (2021) Compound- and fiber type-selective requirement of AMPK γ 3 for insulin-independent glucose uptake in skeletal muscle. *Mol. Metab.*, **51**.
8. Carnio,S., LoVerso,F., Baraibar,M.A., Longa,E., Khan,M.M., Maffei,M., Reischl,M., Canepari,M., Loeffler,S., Kern,H., *et al.* (2014) Autophagy Impairment in Muscle Induces Neuromuscular Junction Degeneration and Precocious Aging. *Cell Rep.*, **8**, 1509–1521.
9. Taetzsch,T. and Valdez,G. (2018) NMJ maintenance and repair in aging. *Curr. Opin. Physiol.*, **4**, 57–64.
10. Gonzalez-Freire,M., de Cabo,R., Studenski,S.A. and Ferrucci,L. (2014) The neuromuscular junction: Aging at the crossroad between nerves and muscle. *Front. Aging Neurosci.*, **6**, 208.
11. Aare,S., Spendiff,S., Vuda,M., Elkrief,D., Perez,A., Wu,Q., Mayaki,D., Hussain,S.N.A., Hettwer,S. and Hepple,R.T. (2016) Failed reinnervation in aging skeletal muscle. *Skelet. Muscle*, **6**, 1–13.
12. Mikhail,A.I., Ng,S.Y., Mattina,S.R. and Ljubicic,V. (2023) AMPK is mitochondrial medicine for neuromuscular disorders. *Trends Mol. Med.*, **In press**.
13. Anagnostou,M.-E. and Hepple,R.T. cells Mitochondrial Mechanisms of

- Neuromuscular Junction Degeneration with Aging. 10.3390/cells9010197.
14. Anagnostou,M.-E., Burke,S.S., Konokhova,Y., Ferguson,C., Fenton,A., Kim,M.-J., Someya,S. and Hepple,R.T. (2019) Mitochondrial DNA Mutations Induce Neuromuscular Junction Degeneration. *FASEB J.*, **33**, 701.8-701.8.
 15. Braz,L.P., Ng,Y.S., Gorman,G.S., Schaefer,A.M., McFarland,R., Taylor,R.W., Turnbull,D.M. and Whittaker,R.G. (2021) Neuromuscular Junction Abnormalities in Mitochondrial Disease: An Observational Cohort Study. *Neurol. Clin. Pract.*, **11**, 97.
 16. Ng,S.Y. and Ljubivic,V. (2020) Recent insights into neuromuscular junction biology in Duchenne muscular dystrophy: Impacts, challenges, and opportunities. *EBioMedicine*, **61**, 103032.
 17. Ripolone,M., Ronchi,D., Violano,R., Vallejo,D., Fagiolari,G., Barca,E., Lucchini,V., Colombo,I., Villa,L., Berardinelli,A., *et al.* (2015) Impaired Muscle Mitochondrial Biogenesis and Myogenesis in Spinal Muscular Atrophy. *JAMA Neurol.*, **72**, 1–10.
 18. Bujak,A.L., Crane,J.D., Lally,J.S., Ford,R.J., Kang,S.J., Rebalka,I.A., Green,A.E., Kemp,B.E., Hawke,T.J., Schertzer,J.D., *et al.* (2015) AMPK activation of muscle autophagy prevents fasting-induced hypoglycemia and myopathy during aging. *Cell Metab.*, **21**, 883–890.
 19. Bujak,A.L., E Blümer,R.M., Marcinko,K., Fullerton,M.D., Kemp,B.E. and Steinberg,G.R. (2014) Reduced skeletal muscle AMPK and mitochondrial markers do not promote age-induced insulin resistance. *J Appl Physiol*, **117**, 171–179.
 20. Thomas,M.M., Wang,D.C., D’Souza,D.M., Krause,M.P., Layne,A.S., Criswell,D.S., O’Neill,H.M., Connor,M.K., Anderson,J.E., Kemp,B.E., *et al.* (2014) Muscle-specific AMPK β 1 β 2-null mice display a myopathy due to loss of capillary density in nonpostural muscles. *FASEB J.*, **28**, 2098–2107.
 21. Mihaylova,M.M. and Shaw,R.J. (2011) The AMPK signalling pathway coordinates cell growth, autophagy and metabolism. *Nat. Cell Biol.*, **13**, 1016–1023.
 22. Rudolf,R., Khan,M.M., Lustrino,D., Labeit,S., Kettelhut,Í.C. and Navegantes,L.C.C. (2013) Alterations of cAMP-dependent signaling in dystrophic skeletal muscle. *Front. Physiol.*, **4**, 290.
 23. Khan,M.M., Strack,S., Wild,F., Hanashima,A., Gasch,A., Brohm,K., Reischl,M., Carnio,S., Labeit,D., Sandri,M., *et al.* (2014) Role of autophagy, SQSTM1, SH3GLB1, and TRIM63 in the turnover of nicotinic acetylcholine receptors. *Autophagy*, **10**, 123–136.
 24. Rudolf,R., Khan,M.M., Labeit,S. and Deschenes,M.R. (2014) Degeneration of neuromuscular junction in age and dystrophy. *Front. Aging Neurosci.*, **6**, 99.
 25. Sandri,M., Coletto,L., Grumati,P. and Bonaldo,P. (2013) Misregulation of autophagy and protein degradation systems in myopathies and muscular dystrophies. *J. Cell Sci.*, **126**, 5325–5333.
 26. Dial,A.G., Ng,S.Y., Manta,A. and Ljubivic,V. (2018) The Role of AMPK in Neuromuscular Biology and Disease. *Trends Endocrinol. Metab.*, **29**, 300–312.
 27. Stockinger,J., Maxwell,N., Shapiro,D., DeCabo,R. and Valdez,G. (2017) Caloric Restriction Mimetics Slow Aging of Neuromuscular Synapses and Muscle Fibers. *J. Gerontol. A. Biol. Sci. Med. Sci.*, **73**, 21–28.
 28. Valdez,G., Tapia,J.C., Kang,H., Clemenson,G.D., Gage,F.H., Lichtman,J.W. and

- Sanes, J.R. (2010) Attenuation of age-related changes in mouse neuromuscular synapses by caloric restriction and exercise. *Proc. Natl. Acad. Sci. U. S. A.*, **107**, 14863–14868.
29. Ham, D.J., Börsch, A., Lin, S., Thürkauf, M., Weihrauch, M., Reinhard, J.R., Delezie, J., Battilana, F., Wang, X., Kaiser, M.S., *et al.* (2020) The neuromuscular junction is a focal point of mTORC1 signaling in sarcopenia. *Nat. Commun.*, **11**, 1–21.
 30. Samuel, M.A., Emanuela Voinescu, P., Lilley, B.N., de Cabo, R., Foretz, M., Viollet, B., Pawlyk, B., Sandberg, M.A., Vavvas, D.G. and Sanes, J.R. (2014) LKB1 and AMPK regulate synaptic remodeling in old age. *Nat. Publ. Gr.*, **17**.
 31. Andonian, M.H. and Fahim, M.A. (1988) Endurance exercise alters the morphology of fast- and slow-twitch rat neuromuscular junctions. *Int. J. Sports Med.*, **9**, 218–223.
 32. Dong, X., Hui, T., Chen, J., Yu, Z., Ren, D., Zou, S., Wang, S., Fei, E., Jiao, H. and Lai, X. (2021) Metformin Increases Sarcolemma Integrity and Ameliorates Neuromuscular Deficits in a Murine Model of Duchenne Muscular Dystrophy. *Front. Physiol.*, **0**, 606.
 33. Coughlan, K.S., Mitchem, M.R., Hogg, M.C. and Prehn, J.H.M. (2015) ‘Preconditioning’ with latrepirdine, an adenosine 5’-monophosphate-activated protein kinase activator, delays amyotrophic lateral sclerosis progression in SOD1G93A mice. *Neurobiol. Aging*, **36**, 1140–1150.
 34. Mancuso, R., del Valle, J., Modol, L., Martinez, A., Granado-Serrano, A.B., Ramirez-Núñez, O., Pallás, M., Portero-Otin, M., Osta, R. and Navarro, X. (2014) Resveratrol Improves Motoneuron Function and Extends Survival in SOD1G93A ALS Mice. *Neurotherapeutics*, **11**, 419–432.
 35. Cerveró, C., Montull, N., Tarabal, O., Piedrafita, L., Esquerda, J.E. and Calderó, J. (2016) Chronic Treatment with the AMPK Agonist AICAR Prevents Skeletal Muscle Pathology but Fails to Improve Clinical Outcome in a Mouse Model of Severe Spinal Muscular Atrophy. *Neurotherapeutics*, **13**, 198–216.
 36. Myers, R.W., Guan, H.-P., Ehrhart, J., Petrov, A., Prahallada, S., Tozzo, E., Yang, X., Kurtz, M.M., Trujillo, M., Gonzalez Trotter, D., *et al.* (2017) Systemic pan-AMPK activator MK-8722 improves glucose homeostasis but induces cardiac hypertrophy. *Science*, **357**, 507–511.
 37. Feng, D., Biftu, T., Romero, F.A., Kekec, A., Dropinski, J., Kassick, A., Xu, S., Kurtz, M.M., Gollapudi, A., Shao, Q., *et al.* (2017) Discovery of MK-8722: A Systemic, Direct Pan-Activator of AMP-Activated Protein Kinase. [10.1021/acsmchemlett.7b00417](https://doi.org/10.1021/acsmchemlett.7b00417).
 38. Dasgupta, B. and Milbrandt, J. (2007) Resveratrol stimulates AMP kinase activity in neurons. *Proc. Natl. Acad. Sci. U. S. A.*, **104**, 7217–7222.
 39. Liu, X., Peng, S., Zhao, Y., Zhao, T., Wang, M., Luo, L., Yang, Y. and Sun, C. (2017) AMPK Negatively Regulates Peripheral Myelination via Activation of c-Jun. *Mol. Neurobiol.*, **54**, 3554–3564.
 40. Liu, W., Wei-LaPierre, L., Klose, A., Dirksen, R.T. and Chakkalakal, J. V (2015) Inducible depletion of adult skeletal muscle stem cells impairs the regeneration of neuromuscular junctions. *Elife*, **4**.
 41. Liu, W., Klose, A., Forman, S., Paris, N.D., Wei-LaPierre, L., Cortés-Lopéz, M., Tan, A., Flaherty, M., Miura, P., Dirksen, R.T., *et al.* (2017) Loss of adult skeletal muscle stem

- cells drives age-related neuromuscular junction degeneration. *Elife*, **6**.
42. White, J.P., Billin, A.N., Campbell, M.E., Russell, A.J., Huffman, K.M. and Kraus, W.E. (2018) The AMPK/p27Kip1 Axis Regulates Autophagy/Apoptosis Decisions in Aged Skeletal Muscle Stem Cells. *Stem Cell Reports*, **11**, 425–439.
 43. Theret, M., Gsaier, L., Schaffer, B., Juban, G., Ben Larbi, S., Weiss-Gayet, M., Bultot, L., Collodet, C., Foretz, M., Desplanches, D., *et al.* (2017) AMPK α 1-LDH pathway regulates muscle stem cell self-renewal by controlling metabolic homeostasis. *EMBO J.*, **36**, 1946–1962.
 44. Kjøbsted, R., Hingst, J.R., Fentz, J., Foretz, M., Sanz, M.N., Pehmøller, C., Shum, M., Marette, A., Mounier, R., Treebak, J.T., *et al.* (2018) AMPK in skeletal muscle function and metabolism. *FASEB J.*, **32**, 1741–1777.
 45. Muise, E.S., Guan, H.-P., Liu, J., Nawrocki, A.R., Yang, X., Wang, C., Rodríguez, C.G., Zhou, D., Gorski, J.N., Kurtz, M.M., *et al.* (2019) Pharmacological AMPK activation induces transcriptional responses congruent to exercise in skeletal and cardiac muscle, adipose tissues and liver. *PLoS One*, **14**, e0211568.
 46. Pillon, N.J., Gabriel, B.M., Dollet, L., Smith, J.A.B., Sardón Puig, L., Botella, J., Bishop, D.J., Krook, A. and Zierath, J.R. (2020) Transcriptomic profiling of skeletal muscle adaptations to exercise and inactivity. *Nat. Commun. 2020 111*, **11**, 1–15.
 47. Handschin, C., Kobayashi, Y.M., Chin, S., Seale, P., Campbell, K.P. and Spiegelman, B.M. (2007) PGC-1 α regulates the neuromuscular junction program and ameliorates Duchenne muscular dystrophy. *Genes Dev.*, **21**, 770–783.
 48. Jäger, S.S., Handschin, C.C., St-Pierre, J.J. and Spiegelman, B.M. (2007) AMP-activated protein kinase (AMPK) action in skeletal muscle via direct phosphorylation of PGC-1 α . *Pnas*, **104**, 12017–12022.
 49. Schmitt, D.L., Curtis, S.D., Lyons, A.C., Zhang, J., Chen, M., He, C.Y., Mehta, S., Shaw, R.J. and Zhang, J. (2022) Spatial regulation of AMPK signaling revealed by a sensitive kinase activity reporter. *Nat. Commun. 2022 131*, **13**, 1–12.
 50. Trefts, E. and Shaw, R.J. (2021) AMPK: restoring metabolic homeostasis over space and time. *Mol. Cell*, **81**, 3677–3690.
 51. Little, J.P., Safdar, A., Cermak, N., Tarnopolsky, M.A. and Gibala, M.J. (2010) Acute endurance exercise increases the nuclear abundance of PGC-1 α in trained human skeletal muscle. *Am. J. Physiol. Regul. Integr. Comp. Physiol.*, **298**, R912-7.
 52. Belotti, E. and Schaeffer, L. (2020) Regulation of Gene expression at the neuromuscular Junction. *Neurosci. Lett.*, **735**, 135163.
 53. Li, L., Xiong, W.-C. and Mei, L. (2018) Neuromuscular Junction Formation, Aging, and Disorders. *Annu. Rev. Physiol.*, **80**, 159–188.
 54. Tintignac, L.A., Brenner, H.R. and Rüegg, M.A. (2015) Mechanisms regulating neuromuscular junction development and function and causes of muscle wasting. *Physiol. Rev.*, **95**, 809–852.
 55. Tang, H., Inoki, K., Brooks, S. V., Okazawa, H., Lee, M., Wang, J., Kim, M., Kennedy, C.L., Macpherson, P.C.D., Ji, X., *et al.* (2019) mTORC1 underlies age-related muscle fiber damage and loss by inducing oxidative stress and catabolism. *Aging Cell*, **18**, 1–20.
 56. Baraldo, M., Geremia, A., Pirazzini, M., Nogara, L., Solagna, F., Türk, C., Nolte, H.,

- Romanello,V., Megighian,A., Boncompagni,S., *et al.* (2020) Skeletal muscle mTORC1 regulates neuromuscular junction stability. *J. Cachexia. Sarcopenia Muscle*, **11**, 208–225.
57. Sigrist,S.J., Thiel,P.R., Reiff,D.F., Lachance,P.E.D., Lasko,P. and Schuster,C.M. (2000) Postsynaptic translation affects the efficacy and morphology of neuromuscular junctions. *Nat. 2000 4056790*, **405**, 1062–1065.
59. Brenner,H.R. and Rudin,W. (1989) On the effect of muscle activity on the end-plate membrane in denervated mouse muscle. *J. Physiol.*, **410**, 501–512.
60. Akaaboune,M., Culican,S.M., Turney,S.G. and Lichtman,J.W. Rapid and Reversible Effects of Activity on Acetylcholine Receptor Density at the Neuromuscular Junction in Vivo.
61. Hoffman,N.J., Parker,B.L., Chaudhuri,R., Fisher-Wellman,K.H., Kleinert,M., Humphrey,S.J., Yang,P., Holliday,M., Trefely,S., Fazakerley,D.J., *et al.* (2015) Global Phosphoproteomic Analysis of Human Skeletal Muscle Reveals a Network of Exercise-Regulated Kinases and AMPK Substrates. *Cell Metab.*, **22**, 922–935.
62. Ramirez,M.P., Rajaganapathy,S., Hagerty,A.R., Hua,C., Baxter,G.C., Vavra,J., Gordon,W.R., Muretta,J.M., Salapaka,M. V. and Ervasti,J.M. (2023) Phosphorylation alters the mechanical stiffness of a model fragment of the dystrophin homologue utrophin. *J. Biol. Chem.*, **299**, 102847.
63. Grady,R.M., Akaaboune,M., Cohen,A.L., Maimone,M.M., Lichtman,J.W. and Sanes,J.R. (2003) Tyrosine-phosphorylated and nonphosphorylated isoforms of α -dystrobrevin roles in skeletal muscle and its neuromuscular and myotendinous junctions. *J. Cell Biol.*, **160**, 741–752.
64. Ljubcic,V., Burt,M. and Jasmin,B.J. (2014) The therapeutic potential of skeletal muscle plasticity in Duchenne muscular dystrophy: Phenotypic modifiers as pharmacologic targets. *FASEB J.*, **28**, 548–568.
65. Scarpulla,R.C. (2011) Metabolic control of mitochondrial biogenesis through the PGC-1 family regulatory network ☆. *BBA - Mol. Cell Res.*, **1813**, 1269–1278.
66. Ljubcic,V., Joseph,A.M., Saleem,A., Ugucioni,G., Collu-Marchese,M., Lai,R.Y.J., Nguyen,L.M.D. and Hood,D.A. (2010) Transcriptional and post-transcriptional regulation of mitochondrial biogenesis in skeletal muscle: Effects of exercise and aging. *Biochim. Biophys. Acta - Gen. Subj.*, **1800**, 223–234.
67. Hood,D.A., Memme,J.M., Oliveira,A.N. and Triolo,M. (2019) Maintenance of Skeletal Muscle Mitochondria in Health, Exercise, and Aging. *Annu. Rev. Physiol.*, **81**, 19–41.
68. Pauly,M., Daussin,F., Burelle,Y., Li,T., Godin,R., Fauconnier,J., Koechlin-Ramonatxo,C., Hugon,G., Lacampagne,A., Coisy-Quivy,M., *et al.* (2012) AMPK activation stimulates autophagy and ameliorates muscular dystrophy in the mdx mouse diaphragm. *Am. J. Pathol.*, **181**, 583–592.
69. Ljubcic,V., Khogali,S., Renaud,J.-M. and Jasmin,B.J. (2012) Chronic AMPK stimulation attenuates adaptive signaling in dystrophic skeletal muscle. *AJP Cell Physiol.*, **302**, C110–C121.
70. Ljubcic,V., Miura,P., Burt,M., Boudreault,L., Khogali,S., Lunde,J.A., Renaud,J.M. and Jasmin,B.J. (2011) Chronic AMPK activation evokes the slow, oxidative

- myogenic program and triggers beneficial adaptations in mdx mouse skeletal muscle. *Hum. Mol. Genet.*, **20**, 3478–3493.
71. Herzig,S. and Shaw,R.J. (2018) AMPK: guardian of metabolism and mitochondrial homeostasis. [10.1038/nrm.2017.95](https://doi.org/10.1038/nrm.2017.95).
 72. De Palma,C., Morisi,F., Cheli,S., Pambianco,S., Cappello,V., Vezzoli,M., Rovere-Querini,P., Moggio,M., Ripolone,M., Francolini,M., *et al.* (2012) Autophagy as a new therapeutic target in Duchenne muscular dystrophy. *Cell Death Dis.*, **5**, e1363.
 73. Mounier,R., Th  ret,M., Arnold,L., Cuvellier,S., Bultot,L., G  ransson,O., Sanz,N., Ferry,A., Sakamoto,K., Foretz,M., *et al.* (2013) AMPK α 1 regulates macrophage skewing at the time of resolution of inflammation during skeletal muscle regeneration. *Cell Metab.*, **18**, 251–264.
 74. Juban,G., Saclier,M., Yacoub-Youssef,H., Kernou,A., Arnold,L., Boisson,C., Ben Larbi,S., Magnan,M., Cuvellier,S., Th  ret,M., *et al.* (2018) AMPK Activation Regulates LTBP4-Dependent TGF- β 1 Secretion by Pro-inflammatory Macrophages and Controls Fibrosis in Duchenne Muscular Dystrophy. *Cell Rep.*, **25**, 2163-2176.e6.
 75. Fu,X., Zhu,M., Zhang,S., Foretz,M., Viollet,B. and Du,M. (2016) Obesity impairs skeletal muscle regeneration through inhibition of AMPK. *Diabetes*, **65**, 188–200.
 76. Fu,X., Zhao,J.-X., Zhu,M.-J., Foretz,M., Viollet,B., Dodson,M. V and Du,M. (2013) AMP-Activated Protein Kinase α 1 but Not α 2 Catalytic Subunit Potentiates Myogenin Expression and Myogenesis. *Mol. Cell. Biol.*, **33**, 4517–4525.
 77. Liu,X., Zhao,L., Gao,Y., Chen,Y., Tian,Q., Son,J.S., Chae,S.A., de Avila,J.M., Zhu,M.J. and Du,M. (2023) AMP-activated protein kinase inhibition in fibro-adipogenic progenitors impairs muscle regeneration and increases fibrosis. *J. Cachexia. Sarcopenia Muscle*, **14**, 479–492.
 78. van Putten,M., Putker,K., Overzier,M., Adamzek,W.A., Pasteuning-Vuhman,S., Plomp,J.J. and Aartsma-Rus,A. (2019) Natural disease history of the D2 -mdx mouse model for Duchenne muscular dystrophy. *FASEB J.*, **33**, 8110–8124.
 79. Coley,W.D., Bogdanik,L., Vila,M.C., Yu,Q., Van Der Meulen,J.H., Rayavarapu,S., Novak,J.S., Nearing,M., Quinn,J.L., Saunders,A., *et al.* (2016) Effect of genetic background on the dystrophic phenotype in mdx mice. *Hum. Mol. Genet.*, **25**, 130–145.
 80. Zhang,J., Muise,E.S., Han,S., Kutchukian,P.S., Costet,P., Zhu,Y., Kan,Y., Zhou,H., Shah,V., Huang,Y., *et al.* (2020) Molecular Profiling Reveals a Common Metabolic Signature of Tissue Fibrosis. *Cell Reports Med.*, **1**, 100056.
 81. Gluais-Dagorn,P., Foretz,M., Steinberg,G.R., Batchuluun,B., Zawistowska-Deniziak,A., Lambooj,J.M., Guigas,B., Carling,D., Monternier,P.A., Moller,D.E., *et al.* (2022) Direct AMPK Activation Corrects NASH in Rodents Through Metabolic Effects and Direct Action on Inflammation and Fibrogenesis. *Hepatol. Commun.*, **6**, 101–119.
 82. Zhou,X., Muise,E.S., Haimbach,R., Sebhat,I.K., Zhu,Y., Liu,F., Souza,S.C., Kan,Y., Pinto,S., Kelley,D.E., *et al.* (2019) Pan-AMPK activation improves renal function in a rat model of progressive diabetic nephropathy. *J. Pharmacol. Exp. Ther.*, **371**, 45–55.
 83. Lemos,D.R., Babaeijandaghi,F., Low,M., Chang,C.K., Lee,S.T., Fiore,D.,

- Zhang,R.H., Natarajan,A., Nedospasov,S.A. and Rossi,F.M.V. (2015) Nilotinib reduces muscle fibrosis in chronic muscle injury by promoting TNF-mediated apoptosis of fibro/adipogenic progenitors. *Nat. Med.* 2015 217, **21**, 786–794.
84. Mázala,D.A.G., Novak,J.S., Hogarth,M.W., Nearing,M., Adusumalli,P., Tully,C.B., Habib,N.F., Gordish-Dressman,H., Chen,Y.W., Jaiswal,J.K., *et al.* (2020) TGF- β -driven muscle degeneration and failed regeneration underlie disease onset in a DMD mouse model. *JCI Insight*, **5**.
85. Saito,Y., Chikenji,T.S., Matsumura,T., Nakano,M. and Fujimiya,M. Exercise enhances skeletal muscle regeneration by promoting senescence in fibro-adipogenic progenitors. 10.1038/s41467-020-14734-x.
86. Steinberg,G.R. and Schertzer,J.D. (2014) AMPK promotes macrophage fatty acid oxidative metabolism to mitigate inflammation: implications for diabetes and cardiovascular disease. *Immunol. Cell Biol.*, **92**, 340–345.
87. Chazaud,B. (2020) Inflammation and Skeletal Muscle Regeneration: Leave It to the Macrophages! 10.1016/j.it.2020.04.006.
88. Fullerton,M.D., Ford,R.J., McGregor,C.P., LeBlond,N.D., Snider,S.A., Stypa,S.A., Day,E.A., Lhoták,Š., Schertzer,J.D., Austin,R.C., *et al.* (2015) Salicylate improves macrophage cholesterol homeostasis via activation of Ampk. *J. Lipid Res.*, **56**, 1025–1033.
89. Galic,S., Fullerton,M.D., Schertzer,J.D., Sikkema,S., Marcinko,K., Walkley,C.R., Izon,D., Honeyman,J., Chen,Z.P., Van Denderen,B.J., *et al.* (2011) Hematopoietic AMPK β 1 reduces mouse adipose tissue macrophage inflammation and insulin resistance in obesity. *J. Clin. Invest.*, **121**, 4903–4915.
90. Hu,D., Hu,D., Liu,L., Barr,D., Liu,Y., Balderrabano-Saucedo,N., Wang,B., Zhu,F., Xue,Y., Wu,S., *et al.* (2017) Identification, clinical manifestation and structural mechanisms of mutations in AMPK associated cardiac glycogen storage disease. *JSES Open Access*, **1**, 139–140.
91. Kim,M., Hunter,R.W., Garcia-Menendez,L., Gong,G., Yang,Y.Y., Kolwicz,S.C., Xu,J., Sakamoto,K., Wang,W. and Tian,R. (2014) Mutation in the γ 2-subunit of AMPK Stimulates Cardiomyocyte Proliferation and Hypertrophy Independent of Glycogen Storage. *Circ. Res.*, **114**, 966.
92. Calore,M. (2017) The PRKAG2 gene and hypertrophic cardiomyopathy: an energetically imbalanced relationship. 10.1152/ajpheart.00316.2017.
93. Cokorinos,E.C., Delmore,J., Reyes,A.R., Albuquerque,B., Kjøbsted,R., Jørgensen,N.O., Tran,J.L., Jatkar,A., Cialdea,K., Esquejo,R.M., *et al.* (2017) Activation of Skeletal Muscle AMPK Promotes Glucose Disposal and Glucose Lowering in Non-human Primates and Mice. *Cell Metab.*, **25**, 1147-1159.e10.
94. Bueno Júnior,C.R., Pantaleão,L.C., Voltarelli,V.A., Bozi,L.H.M., Brum,P.C. and Zatz,M. (2012) Combined Effect of AMPK/PPAR Agonists and Exercise Training in mdx Mice Functional Performance. *PLoS One*, **7**, e45699.
95. Bultot,L., Jensen,T.E., Lai,Y.C., Madsen,A.L.B., Collodet,C., Kviklyte,S., Deak,M., Yavari,A., Foretz,M., Ghaffari,S., *et al.* (2016) Benzimidazole derivative small-molecule 991 enhances AMPK activity and glucose uptake induced by AICAR or contraction in skeletal muscle. *Am. J. Physiol. - Endocrinol. Metab.*, **311**, E706–E719.

96. Ducommun,S., Ford,R.J., Bultot,L., Deak,M., Bertrand,L., Kemp,B.E., Steinberg,G.R. and Sakamoto,K. (2014) Enhanced activation of cellular AMPK by dual-small molecule treatment: AICAR and A769662. *Am. J. Physiol. - Endocrinol. Metab.*, **306**, 688–696.
97. Petrany,M.J., Song,T., Sadayappan,S. and Millay,D.P. (2020) Myocyte-derived Myomaker expression is required for regenerative fusion but exacerbates membrane instability in dystrophic myofibers. *JCI Insight*, **5**.

APPENDIX A:
Copyright Permissions

Creative Commons Legal Code

Attribution 4.0 International

Official translations of this license are available [in other languages](#).

Creative Commons Corporation (“Creative Commons”) is not a law firm and does not provide legal services or legal advice. Distribution of Creative Commons public licenses does not create a lawyer-client or other relationship. Creative Commons makes its licenses and related information available on an “as-is” basis. Creative Commons gives no warranties regarding its licenses, any material licensed under their terms and conditions, or any related information. Creative Commons disclaims all liability for damages resulting from their use to the fullest extent possible.

Using Creative Commons Public Licenses

Creative Commons public licenses provide a standard set of terms and conditions that creators and other rights holders may use to share original works of authorship and other material subject to copyright and certain other rights specified in the public license below. The following considerations are for informational purposes only, are not exhaustive, and do not form part of our licenses.

Considerations for licensors: Our public licenses are intended for use by those authorized to give the public permission to use material in ways otherwise restricted by copyright and certain other rights. Our licenses are irrevocable. Licensors should read and understand the terms and conditions of the license they choose before applying it. Licensors should also secure all rights necessary before applying our licenses so that the public can reuse the material as expected. Licensors should clearly mark any material not subject to the license. This includes other CC-licensed material, or material used under an exception or limitation to copyright.

Considerations for the public: By using one of our public licenses, a licensor grants the public permission to use the licensed material under specified terms and conditions. If the licensor’s permission is not necessary for any reason—for example, because of any applicable exception or limitation to copyright—then that use is not regulated by the license. Our licenses grant only permissions under copyright and certain other rights that a licensor has authority to grant. Use of the licensed material may still be restricted for other reasons, including because others have copyright or

other rights in the material. A licensor may make special requests, such as asking that all changes be marked or described. Although not required by our licenses, you are encouraged to respect those requests where reasonable.

Creative Commons Attribution 4.0 International Public License

By exercising the Licensed Rights (defined below), You accept and agree to be bound by the terms and conditions of this Creative Commons Attribution 4.0 International Public License ("Public License"). To the extent this Public License may be interpreted as a contract, You are granted the Licensed Rights in consideration of Your acceptance of these terms and conditions, and the Licensor grants You such rights in consideration of benefits the Licensor receives from making the Licensed Material available under these terms and conditions.

Section 1 – Definitions.

- a. **Adapted Material** means material subject to Copyright and Similar Rights that is derived from or based upon the Licensed Material and in which the Licensed Material is translated, altered, arranged, transformed, or otherwise modified in a manner requiring permission under the Copyright and Similar Rights held by the Licensor. For purposes of this Public License, where the Licensed Material is a musical work, performance, or sound recording, Adapted Material is always produced where the Licensed Material is synched in timed relation with a moving image.
- b. **Adapter's License** means the license You apply to Your Copyright and Similar Rights in Your contributions to Adapted Material in accordance with the terms and conditions of this Public License.
- c. **Copyright and Similar Rights** means copyright and/or similar rights closely related to copyright including, without limitation, performance, broadcast, sound recording, and Sui Generis Database Rights, without regard to how the rights are labeled or categorized. For purposes of this Public License, the rights specified in Section 2(b)(1)-(2) are not Copyright and Similar Rights.
- d. **Effective Technological Measures** means those measures that, in the absence of proper authority, may not be circumvented under laws fulfilling obligations under Article 11 of the WIPO Copyright Treaty adopted on December 20, 1996, and/or similar international agreements.
- e. **Exceptions and Limitations** means fair use, fair dealing, and/or any other exception or limitation to Copyright and Similar Rights that applies to Your use of the Licensed Material.
- f. **Licensed Material** means the artistic or literary work, database, or other material to which the Licensor applied this Public License.
- g. **Licensed Rights** means the rights granted to You subject to the terms and conditions of this Public License, which are limited to all Copyright and Similar Rights that apply to Your use of the Licensed Material and that the Licensor has authority to license.

- h. **Licensor** means the individual(s) or entity(ies) granting rights under this Public License.
- i. **Share** means to provide material to the public by any means or process that requires permission under the Licensed Rights, such as reproduction, public display, public performance, distribution, dissemination, communication, or importation, and to make material available to the public including in ways that members of the public may access the material from a place and at a time individually chosen by them.
- j. **Sui Generis Database Rights** means rights other than copyright resulting from Directive 96/9/EC of the European Parliament and of the Council of 11 March 1996 on the legal protection of databases, as amended and/or succeeded, as well as other essentially equivalent rights anywhere in the world.
- k. **You** means the individual or entity exercising the Licensed Rights under this Public License. **Your** has a corresponding meaning.

Section 2 – Scope.

- a. **License grant.**
 - 1. Subject to the terms and conditions of this Public License, the Licensor hereby grants You a worldwide, royalty-free, non-sublicensable, non-exclusive, irrevocable license to exercise the Licensed Rights in the Licensed Material to:
 - A. reproduce and Share the Licensed Material, in whole or in part; and
 - B. produce, reproduce, and Share Adapted Material.
 - 2. Exceptions and Limitations. For the avoidance of doubt, where Exceptions and Limitations apply to Your use, this Public License does not apply, and You do not need to comply with its terms and conditions.
 - 3. Term. The term of this Public License is specified in Section 6(a).
 - 4. Media and formats; technical modifications allowed. The Licensor authorizes You to exercise the Licensed Rights in all media and formats whether now known or hereafter created, and to make technical modifications necessary to do so. The Licensor waives and/or agrees not to assert any right or authority to forbid You from making technical modifications necessary to exercise the Licensed Rights, including technical modifications necessary to circumvent Effective Technological Measures. For purposes of this Public License, simply making modifications authorized by this Section 2(a)(4) never produces Adapted Material.
 - 5. Downstream recipients.
 - A. Offer from the Licensor – Licensed Material. Every recipient of the Licensed Material automatically receives an offer from the Licensor to exercise the Licensed Rights under the terms and conditions of this Public License.
 - B. No downstream restrictions. You may not offer or impose any additional or different terms or conditions on, or apply any Effective Technological Measures to, the Licensed Material if

doing so restricts exercise of the Licensed Rights by any recipient of the Licensed Material.

6. **No endorsement.** Nothing in this Public License constitutes or may be construed as permission to assert or imply that You are, or that Your use of the Licensed Material is, connected with, or sponsored, endorsed, or granted official status by, the Licensor or others designated to receive attribution as provided in Section 3(a)(1)(A)(i).

b. Other rights.

1. Moral rights, such as the right of integrity, are not licensed under this Public License, nor are publicity, privacy, and/or other similar personality rights; however, to the extent possible, the Licensor waives and/or agrees not to assert any such rights held by the Licensor to the limited extent necessary to allow You to exercise the Licensed Rights, but not otherwise.
2. Patent and trademark rights are not licensed under this Public License.
3. To the extent possible, the Licensor waives any right to collect royalties from You for the exercise of the Licensed Rights, whether directly or through a collecting society under any voluntary or waivable statutory or compulsory licensing scheme. In all other cases the Licensor expressly reserves any right to collect such royalties.

Section 3 – License Conditions.

Your exercise of the Licensed Rights is expressly made subject to the following conditions.

a. Attribution.

1. If You Share the Licensed Material (including in modified form), You must:
 - A. retain the following if it is supplied by the Licensor with the Licensed Material:
 - i. identification of the creator(s) of the Licensed Material and any others designated to receive attribution, in any reasonable manner requested by the Licensor (including by pseudonym if designated);
 - ii. a copyright notice;
 - iii. a notice that refers to this Public License;
 - iv. a notice that refers to the disclaimer of warranties;
 - v. a URI or hyperlink to the Licensed Material to the extent reasonably practicable;
 - B. indicate if You modified the Licensed Material and retain an indication of any previous modifications; and
 - C. indicate the Licensed Material is licensed under this Public License, and include the text of,

or the URI or hyperlink to, this Public License.

2. You may satisfy the conditions in Section 3(a)(1) in any reasonable manner based on the medium, means, and context in which You Share the Licensed Material. For example, it may be reasonable to satisfy the conditions by providing a URI or hyperlink to a resource that includes the required information.
3. If requested by the Licensor, You must remove any of the information required by Section 3(a)(1)(A) to the extent reasonably practicable.
4. If You Share Adapted Material You produce, the Adapter's License You apply must not prevent recipients of the Adapted Material from complying with this Public License.

Section 4 – Sui Generis Database Rights.

Where the Licensed Rights include Sui Generis Database Rights that apply to Your use of the Licensed Material:

- a. for the avoidance of doubt, Section 2(a)(1) grants You the right to extract, reuse, reproduce, and Share all or a substantial portion of the contents of the database;
- b. if You include all or a substantial portion of the database contents in a database in which You have Sui Generis Database Rights, then the database in which You have Sui Generis Database Rights (but not its individual contents) is Adapted Material; and
- c. You must comply with the conditions in Section 3(a) if You Share all or a substantial portion of the contents of the database.

For the avoidance of doubt, this Section 4 supplements and does not replace Your obligations under this Public License where the Licensed Rights include other Copyright and Similar Rights.

Section 5 – Disclaimer of Warranties and Limitation of Liability.

- a. **Unless otherwise separately undertaken by the Licensor, to the extent possible, the Licensor offers the Licensed Material as-is and as-available, and makes no representations or warranties of any kind concerning the Licensed Material, whether express, implied, statutory, or other. This includes, without limitation, warranties of title, merchantability, fitness for a particular purpose, non-infringement, absence of latent or other defects, accuracy, or the presence or absence of errors, whether or not known or discoverable. Where disclaimers of warranties are not allowed in full or in part, this disclaimer may not apply to You.**
- b. **To the extent possible, in no event will the Licensor be liable to You on any legal theory (including, without limitation, negligence) or otherwise for any direct, special, indirect,**

incidental, consequential, punitive, exemplary, or other losses, costs, expenses, or damages arising out of this Public License or use of the Licensed Material, even if the Licensor has been advised of the possibility of such losses, costs, expenses, or damages. Where a limitation of liability is not allowed in full or in part, this limitation may not apply to You.

- c. The disclaimer of warranties and limitation of liability provided above shall be interpreted in a manner that, to the extent possible, most closely approximates an absolute disclaimer and waiver of all liability.

Section 6 – Term and Termination.

- a. This Public License applies for the term of the Copyright and Similar Rights licensed here. However, if You fail to comply with this Public License, then Your rights under this Public License terminate automatically.
- b. Where Your right to use the Licensed Material has terminated under Section 6(a), it reinstates:
 - 1. automatically as of the date the violation is cured, provided it is cured within 30 days of Your discovery of the violation; or
 - 2. upon express reinstatement by the Licensor.For the avoidance of doubt, this Section 6(b) does not affect any right the Licensor may have to seek remedies for Your violations of this Public License.
- c. For the avoidance of doubt, the Licensor may also offer the Licensed Material under separate terms or conditions or stop distributing the Licensed Material at any time; however, doing so will not terminate this Public License.
- d. Sections 1, 5, 6, 7, and 8 survive termination of this Public License.

Section 7 – Other Terms and Conditions.

- a. The Licensor shall not be bound by any additional or different terms or conditions communicated by You unless expressly agreed.
- b. Any arrangements, understandings, or agreements regarding the Licensed Material not stated herein are separate from and independent of the terms and conditions of this Public License.

Section 8 – Interpretation.

- a. For the avoidance of doubt, this Public License does not, and shall not be interpreted to, reduce,

- limit, restrict, or impose conditions on any use of the Licensed Material that could lawfully be made without permission under this Public License.
- b. To the extent possible, if any provision of this Public License is deemed unenforceable, it shall be automatically reformed to the minimum extent necessary to make it enforceable. If the provision cannot be reformed, it shall be severed from this Public License without affecting the enforceability of the remaining terms and conditions.
 - c. No term or condition of this Public License will be waived and no failure to comply consented to unless expressly agreed to by the Licensor.
 - d. Nothing in this Public License constitutes or may be interpreted as a limitation upon, or waiver of, any privileges and immunities that apply to the Licensor or You, including from the legal processes of any jurisdiction or authority.

Creative Commons is not a party to its public licenses. Notwithstanding, Creative Commons may elect to apply one of its public licenses to material it publishes and in those instances will be considered the "Licensor." The text of the Creative Commons public licenses is dedicated to the public domain under the [CC0 Public Domain Dedication](#). Except for the limited purpose of indicating that material is shared under a Creative Commons public license or as otherwise permitted by the Creative Commons policies published at creativecommons.org/policies, Creative Commons does not authorize the use of the trademark "Creative Commons" or any other trademark or logo of Creative Commons without its prior written consent including, without limitation, in connection with any unauthorized modifications to any of its public licenses or any other arrangements, understandings, or agreements concerning use of licensed material. For the avoidance of doubt, this paragraph does not form part of the public licenses.

Creative Commons may be contacted at creativecommons.org.

Additional languages available: العربية, čeština, Dansk, Deutsch, Ελληνικά, Español, euskara, suomeksi, français, Frysk, hrvatski, Bahasa Indonesia, italiano, 日本語, 한국어, Lietuvių, latviski, te reo Māori, Nederlands, norsk, polski, português, română, русский, Slovenščina, svenska, Türkçe, українська, 中文, 華語. Please read the [FAQ](#) for more information about official translations.

JOHN WILEY AND SONS LICENSE
TERMS AND CONDITIONS

Jul 24, 2023

This Agreement between McMaster University -- Sean Ng ("You") and John Wiley and Sons ("John Wiley and Sons") consists of your license details and the terms and conditions provided by John Wiley and Sons and Copyright Clearance Center.

License Number 5595460944691

License date Jul 24, 2023

Licensed
Content
Publisher John Wiley and Sons

Licensed
Content
Publication THE FASEB JOURNAL

Licensed
Content Title Acute, next-generation AMPK activation initiates a disease-resistant gene expression program in dystrophic skeletal muscle

Licensed
Content Author Sean Y. Ng, Andrew I. Mikhail, Stephanie R. Mattina, et al

Licensed
Content Date Apr 5, 2023

Licensed
Content Volume 37

Licensed
Content Issue 5

Licensed Content Pages 16

Type of use Dissertation/Thesis

Requestor type Author of this Wiley article

Format Print and electronic

Portion Full article

Will you be translating? No

Title The Role of AMP-activated Protein Kinase in Neuromuscular Health and Disease

Institution name McMaster Univeristy

Expected presentation date Sep 2023

Requestor Location
McMaster University
100 Beddoe Drive Unit 110
Hamilton, ON L8P4Z2
Canada
Attn: McMaster University

Publisher Tax ID EU826007151

Total 0.00 CAD

Terms and Conditions

TERMS AND CONDITIONS

This copyrighted material is owned by or exclusively licensed to John Wiley & Sons, Inc. or one of its group companies (each a "Wiley Company") or handled on behalf of a society with which a Wiley Company has exclusive publishing rights in relation to a particular work (collectively "WILEY"). By clicking "accept" in connection with completing this licensing transaction, you agree that the following terms and conditions apply to this transaction (along with the billing and payment terms and conditions established by the Copyright Clearance Center Inc., ("CCC's Billing and Payment terms and conditions"), at the time that you opened your RightsLink account (these are available at any time at <http://myaccount.copyright.com>).

Terms and Conditions

- The materials you have requested permission to reproduce or reuse (the "Wiley Materials") are protected by copyright.
- You are hereby granted a personal, non-exclusive, non-sub licensable (on a stand-alone basis), non-transferable, worldwide, limited license to reproduce the Wiley Materials for the purpose specified in the licensing process. This license, **and any CONTENT (PDF or image file) purchased as part of your order**, is for a one-time use only and limited to any maximum distribution number specified in the license. The first instance of republication or reuse granted by this license must be completed within two years of the date of the grant of this license (although copies prepared before the end date may be distributed thereafter). The Wiley Materials shall not be used in any other manner or for any other purpose, beyond what is granted in the license. Permission is granted subject to an appropriate acknowledgement given to the author, title of the material/book/journal and the publisher. You shall also duplicate the copyright notice that appears in the Wiley publication in your use of the Wiley Material. Permission is also granted on the understanding that nowhere in the text is a previously published source acknowledged for all or part of this Wiley Material. Any third party content is expressly excluded from this permission.
- With respect to the Wiley Materials, all rights are reserved. Except as expressly granted by the terms of the license, no part of the Wiley Materials may be copied, modified, adapted (except for minor reformatting required by the new Publication), translated, reproduced, transferred or distributed, in any form or by any means, and no derivative works may be made based on the Wiley Materials without the prior permission of the respective copyright owner. **For STM Signatory Publishers clearing permission under the terms of the [STM Permissions Guidelines](#) only, the terms of the license are extended to include subsequent editions and for editions in other languages, provided such editions are for the work as a whole in situ and does not involve the separate exploitation of the permitted figures or extracts**, You may not alter, remove or suppress in any manner any copyright, trademark or other notices displayed by the Wiley Materials. You may not license, rent, sell, loan, lease, pledge, offer as security, transfer or assign the Wiley Materials on a stand-alone basis, or any of the rights granted to you hereunder to any other person.
- The Wiley Materials and all of the intellectual property rights therein shall at all times remain the exclusive property of John Wiley & Sons Inc, the Wiley Companies, or their respective licensors, and your interest therein is only that of having possession of and the right to reproduce the Wiley Materials pursuant to Section 2 herein during the

continuance of this Agreement. You agree that you own no right, title or interest in or to the Wiley Materials or any of the intellectual property rights therein. You shall have no rights hereunder other than the license as provided for above in Section 2. No right, license or interest to any trademark, trade name, service mark or other branding ("Marks") of WILEY or its licensors is granted hereunder, and you agree that you shall not assert any such right, license or interest with respect thereto

- NEITHER WILEY NOR ITS LICENSORS MAKES ANY WARRANTY OR REPRESENTATION OF ANY KIND TO YOU OR ANY THIRD PARTY, EXPRESS, IMPLIED OR STATUTORY, WITH RESPECT TO THE MATERIALS OR THE ACCURACY OF ANY INFORMATION CONTAINED IN THE MATERIALS, INCLUDING, WITHOUT LIMITATION, ANY IMPLIED WARRANTY OF MERCHANTABILITY, ACCURACY, SATISFACTORY QUALITY, FITNESS FOR A PARTICULAR PURPOSE, USABILITY, INTEGRATION OR NON-INFRINGEMENT AND ALL SUCH WARRANTIES ARE HEREBY EXCLUDED BY WILEY AND ITS LICENSORS AND WAIVED BY YOU.
- WILEY shall have the right to terminate this Agreement immediately upon breach of this Agreement by you.
- You shall indemnify, defend and hold harmless WILEY, its Licensors and their respective directors, officers, agents and employees, from and against any actual or threatened claims, demands, causes of action or proceedings arising from any breach of this Agreement by you.
- IN NO EVENT SHALL WILEY OR ITS LICENSORS BE LIABLE TO YOU OR ANY OTHER PARTY OR ANY OTHER PERSON OR ENTITY FOR ANY SPECIAL, CONSEQUENTIAL, INCIDENTAL, INDIRECT, EXEMPLARY OR PUNITIVE DAMAGES, HOWEVER CAUSED, ARISING OUT OF OR IN CONNECTION WITH THE DOWNLOADING, PROVISIONING, VIEWING OR USE OF THE MATERIALS REGARDLESS OF THE FORM OF ACTION, WHETHER FOR BREACH OF CONTRACT, BREACH OF WARRANTY, TORT, NEGLIGENCE, INFRINGEMENT OR OTHERWISE (INCLUDING, WITHOUT LIMITATION, DAMAGES BASED ON LOSS OF PROFITS, DATA, FILES, USE, BUSINESS OPPORTUNITY OR CLAIMS OF THIRD PARTIES), AND WHETHER OR NOT THE PARTY HAS BEEN ADVISED OF THE POSSIBILITY OF SUCH DAMAGES. THIS LIMITATION SHALL APPLY NOTWITHSTANDING ANY FAILURE OF ESSENTIAL PURPOSE OF ANY LIMITED REMEDY PROVIDED HEREIN.
- Should any provision of this Agreement be held by a court of competent jurisdiction to be illegal, invalid, or unenforceable, that provision shall be deemed amended to achieve as nearly as possible the same economic effect as the original provision, and the legality, validity and enforceability of the remaining provisions of this Agreement shall not be affected or impaired thereby.
- The failure of either party to enforce any term or condition of this Agreement shall not constitute a waiver of either party's right to enforce each and every term and condition of this Agreement. No breach under this agreement shall be deemed waived or

excused by either party unless such waiver or consent is in writing signed by the party granting such waiver or consent. The waiver by or consent of a party to a breach of any provision of this Agreement shall not operate or be construed as a waiver of or consent to any other or subsequent breach by such other party.

- This Agreement may not be assigned (including by operation of law or otherwise) by you without WILEY's prior written consent.
- Any fee required for this permission shall be non-refundable after thirty (30) days from receipt by the CCC.
- These terms and conditions together with CCC's Billing and Payment terms and conditions (which are incorporated herein) form the entire agreement between you and WILEY concerning this licensing transaction and (in the absence of fraud) supersedes all prior agreements and representations of the parties, oral or written. This Agreement may not be amended except in writing signed by both parties. This Agreement shall be binding upon and inure to the benefit of the parties' successors, legal representatives, and authorized assigns.
- In the event of any conflict between your obligations established by these terms and conditions and those established by CCC's Billing and Payment terms and conditions, these terms and conditions shall prevail.
- WILEY expressly reserves all rights not specifically granted in the combination of (i) the license details provided by you and accepted in the course of this licensing transaction, (ii) these terms and conditions and (iii) CCC's Billing and Payment terms and conditions.
- This Agreement will be void if the Type of Use, Format, Circulation, or Requestor Type was misrepresented during the licensing process.
- This Agreement shall be governed by and construed in accordance with the laws of the State of New York, USA, without regards to such state's conflict of law rules. Any legal action, suit or proceeding arising out of or relating to these Terms and Conditions or the breach thereof shall be instituted in a court of competent jurisdiction in New York County in the State of New York in the United States of America and each party hereby consents and submits to the personal jurisdiction of such court, waives any objection to venue in such court and consents to service of process by registered or certified mail, return receipt requested, at the last known address of such party.

WILEY OPEN ACCESS TERMS AND CONDITIONS

Wiley Publishes Open Access Articles in fully Open Access Journals and in Subscription journals offering Online Open. Although most of the fully Open Access journals publish open access articles under the terms of the Creative Commons Attribution (CC BY) License only, the subscription journals and a few of the Open Access Journals offer a choice of Creative Commons Licenses. The license type is clearly identified on the article.

The Creative Commons Attribution License

The [Creative Commons Attribution License \(CC-BY\)](#) allows users to copy, distribute and transmit an article, adapt the article and make commercial use of the article. The CC-BY license permits commercial and non-

Creative Commons Attribution Non-Commercial License

The [Creative Commons Attribution Non-Commercial \(CC-BY-NC\) License](#) permits use, distribution and reproduction in any medium, provided the original work is properly cited and is not used for commercial purposes.(see below)

Creative Commons Attribution-Non-Commercial-NoDerivs License

The [Creative Commons Attribution Non-Commercial-NoDerivs License](#) (CC-BY-NC-ND) permits use, distribution and reproduction in any medium, provided the original work is properly cited, is not used for commercial purposes and no modifications or adaptations are made. (see below)

Use by commercial "for-profit" organizations

Use of Wiley Open Access articles for commercial, promotional, or marketing purposes requires further explicit permission from Wiley and will be subject to a fee.

Further details can be found on Wiley Online Library
<http://olabout.wiley.com/WileyCDA/Section/id-410895.html>

Other Terms and Conditions:

v1.10 Last updated September 2015

Questions? customercare@copyright.com.

APPENDIX B:
ADDITIONAL DATA

Title: Chronic adaptations in response to repeated O304 treatment in D2.mdx animals

Authors: Sean Y Ng¹, Salah A Mohammed¹, Manshi Rana¹, Beverly Yap¹, Vladimir Ljubicic^{1*}

Affiliations:

¹Department of Kinesiology, McMaster University, 1280 Main St. W., Hamilton, ON, Canada L8S 4L8.

*Corresponding author. Email: ljubicic@mcmaster.ca

Figures:

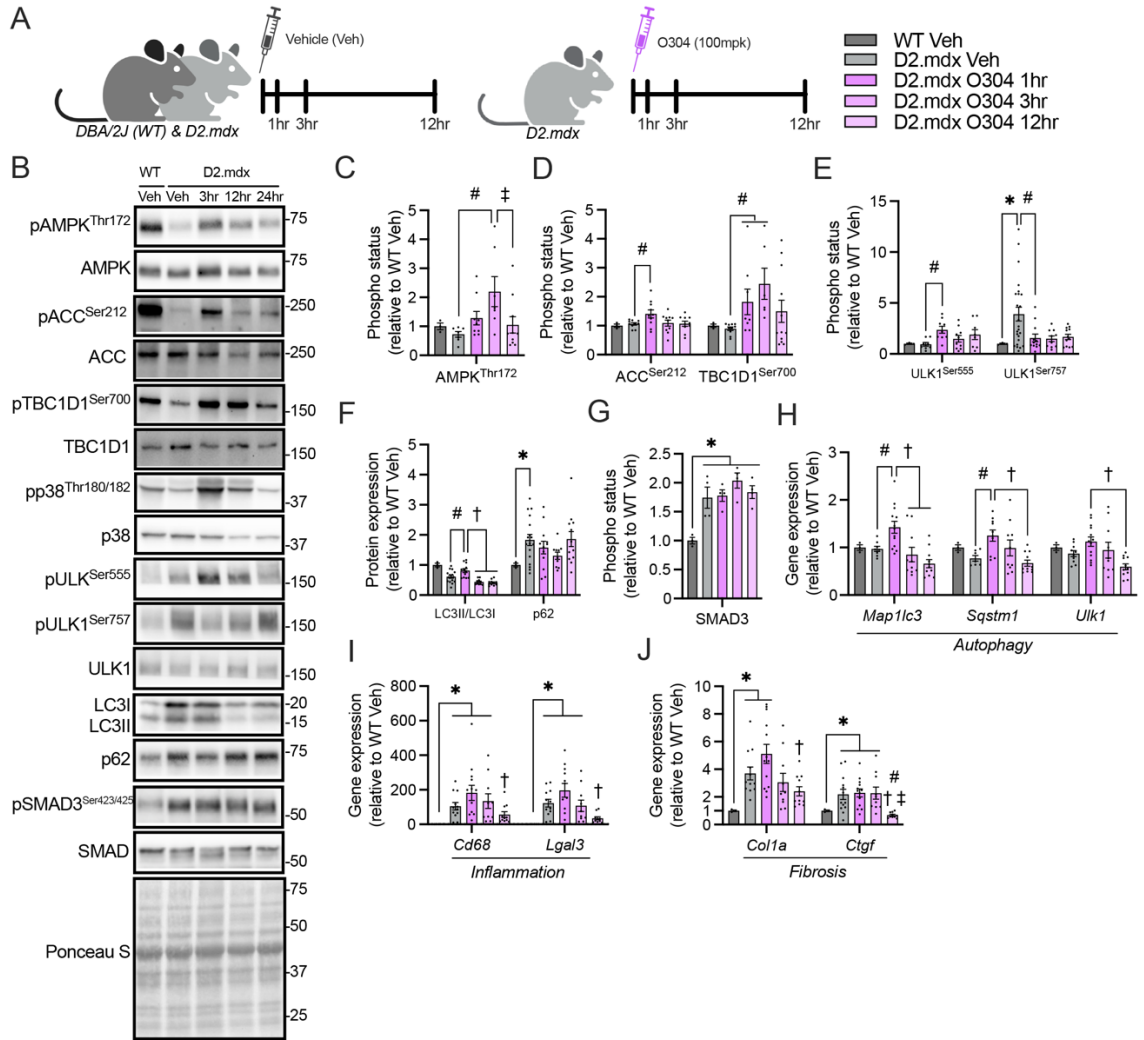


Fig AB1. The effects of a O304 dosing on AMP-activated protein kinase (AMPK) signaling in skeletal muscle of D2.mdx animals. (A) 5-week-old, male DBA/2J (WT) and D2.mdx animals were orally treated with a dose of vehicle (Veh) or O304 solution. Tibialis anterior (TA) muscles from Veh- and O304-treated D2.mdx mice were collected 1- (D2.mdx O304 1hr), 3- (D2.mdx O304 3hr), and 12 hours (D2.mdx O304 12hr) post-gavage. Veh-treated D2.mdx animals were pooled to serve as a control group. (B) Representative Western blots of threonine 172 (Thr¹⁷²)-phosphorylated AMPK (pAMPK^{Thr172}), total AMPK, serine 212 (Ser²¹²)-phosphorylated acetyl-CoA carboxylase (pACC^{Ser212}), total ACC, Ser⁷⁰⁰-phosphorylated TBC1 domain family member 1 (pTBC1D1^{Ser700}), TBC1D1, Thr^{180/182}-phosphorylated p38 mitogen-activated kinase (pp38^{Thr180/182}), p38, Ser⁵⁵⁵-phosphorylated unc-51-like autophagy activating kinase (pULK1^{Ser555}), Ser⁵⁵⁵-phosphorylated ULK1 (pULK1^{Ser757}), ULK1, microtubule-associated protein 1A/1B-light chain 3 (LC3), sequestosome-1 (p62), Ser⁴²³-phosphorylated mothers against decapentaplegic homolog (pSMAD^{Ser423/425}), and SMAD in the TA muscles of Veh- and O304-treated D2.mdx animals. Ponceau S staining is below to indicate even sample loading. Protein ladders are expressed as kDa at the right. (C-E) Graphical summaries of phosphorylation status (i.e., the phosphorylated form of the protein relative to its total amount within the same sample; Phospho-status) of AMPK (C), ACC and TBC1D1 (D), and ULK1 (E) in the TA muscles of Veh- or O304-treated mice. (F) Graphical summary of LC3II/LC3I and p62 protein expression in the TA

muscles of Veh- or O304-treated mice. **(G)** Graphical summary of SMAD3 Phospho-status in the TA muscles of Veh- or O304-treated mice. Graphical summaries of mRNA transcripts related to autophagy **(H)**, inflammation **(I)**, and fibrosis **(J)**. Graphical summaries display individual data points and group means (bars) with standard error of the mean (SEM). $n = 7-15$. Immunoblotting data are presented as fold differences relative to the WT Veh group. Statistical significance was denoted as: *, $p < 0.05$ versus WT Veh (comparison with Veh-treated wild-type); #, $p < 0.05$ versus D2.mdx Veh (comparison with Veh-treated D2.mdx animals); †, $p < 0.05$ versus D2.mdx O304 1hr (comparison with O304-treated D2.mdx animals); and ‡, $p < 0.05$ versus D2.mdx O304 3hr.

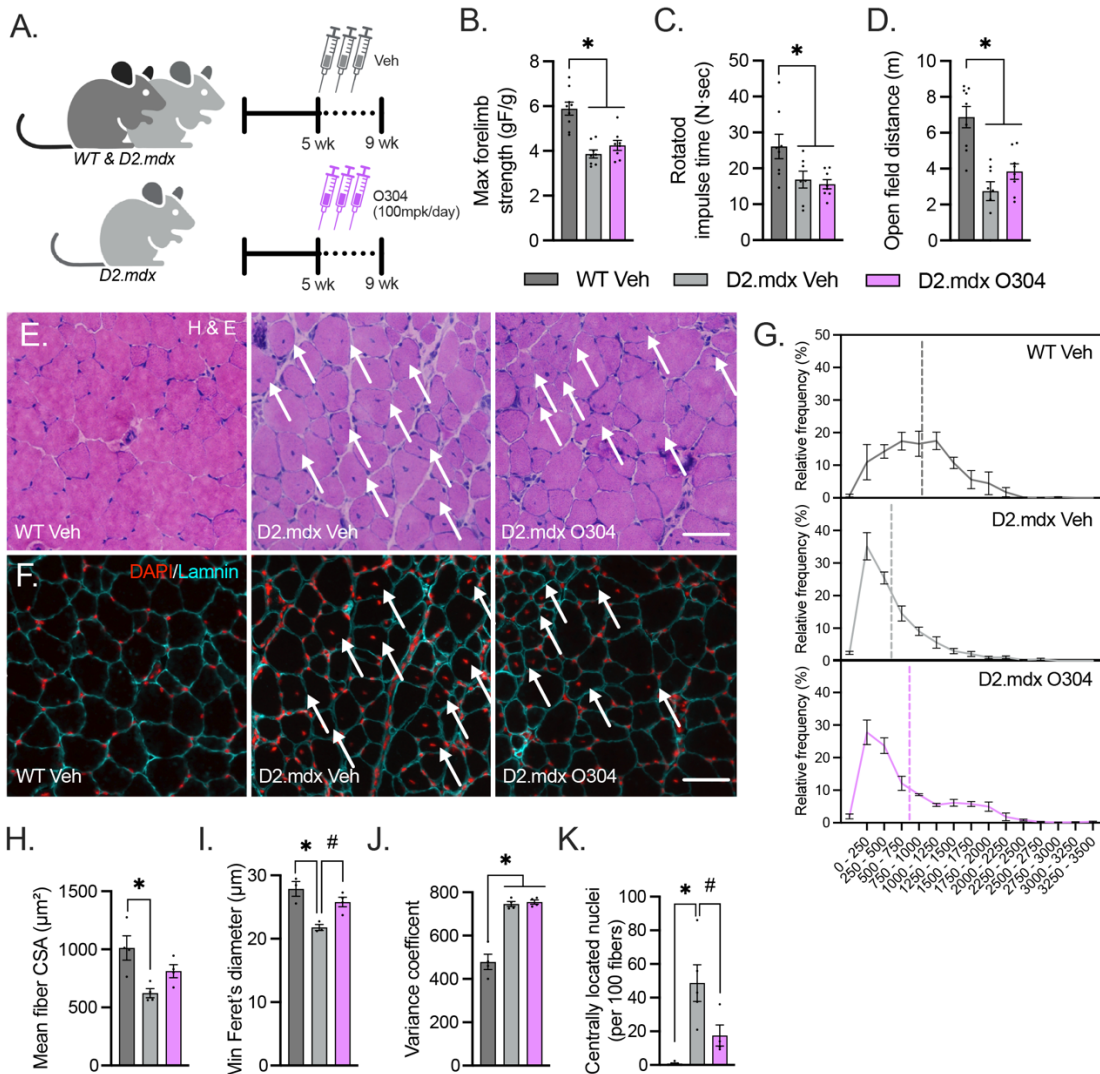


Fig AB2. The impact of repetitive O304 treatment on muscle function and morphology in D2.mdx animals. (A) Five-week-old D2.mdx animals received daily oral gavage with a vehicle or O304 solution for four weeks. Graphical summaries of muscle function metrics including maximum forelimb grip strength (B), rotarod impulse time (C), and open field distance (D) in Veh- and O304-treated animals. (E) Representative hematoxylin and eosin (H&E) images of extensor digitorum longus (EDL) muscles of Veh- and O304-treated animals. (F) Typical immunofluorescent (IF) images of 4',6-diamidino-2-phenylindole dihydrochloride (DAPI, Pseudo-colored red) denote nuclei, while laminin (cyan) demarks the sarcolemma. White arrows indicate centrally located nuclei. Scale bars represent 100 μM . (G) Relative frequency distribution of muscle fiber cross-sectional area (CSA) in the EDL muscles of all experimental groups. Dotted lines represent the mean fiber CSA of each experimental group. Graphical summary of mean fiber CSA (H), Minimum Feret's diameter (I), muscle fiber CSA variance (J) from EDL muscles of Veh-treated and O304-treated animals. (K) Summary of the total number of centrally located nuclei in the EDL muscles of all treated animals. Graphical summaries display individual data points and group means (bars) with SEM. Muscle function data, $n = 7-8$. Muscle fiber analysis, $n = 3-4$. Statistical significance was denoted as: *, $p < 0.05$ versus WT Veh; and #, $p < 0.05$ versus D2.mdx Veh.

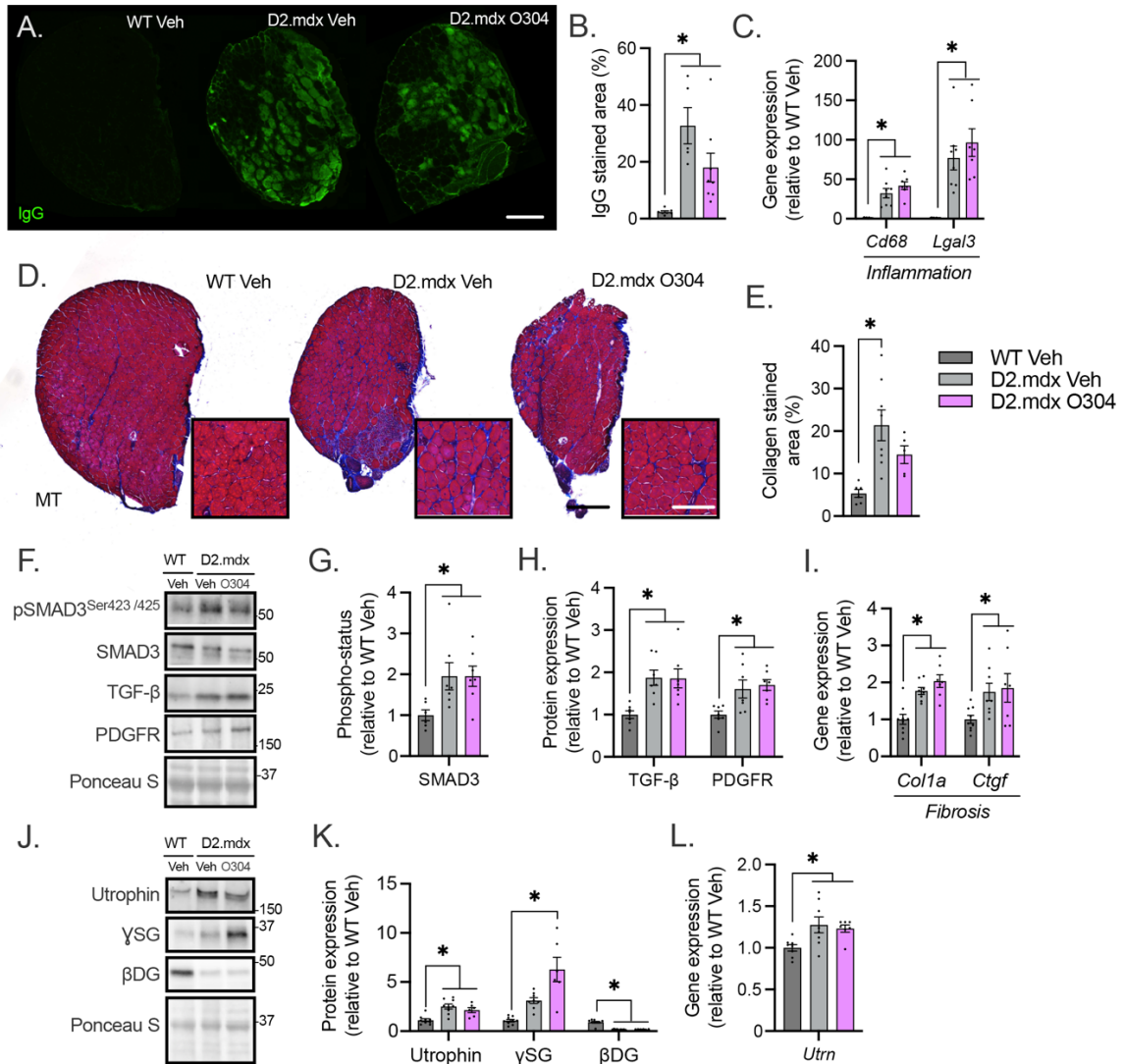


Fig AB3. Effects of repeated O304 treatment on skeletal muscle fibrosis in D2.mdx animals. (A) Representative images of IgG staining in the EDL muscles of Veh- and O304-treated mice. (B) Graphical summary of IgG-stained area expressed relative to total muscle CSA. (C) Inflammation-related transcripts in the TA muscles of Veh- and O304-treated animals. (D) Typical Masson's Trichrome (MT) stained images of the EDL muscle from all groups. Smaller inset squares represent a magnified region of the larger image. The black scale bar represents 300 μ M, while the white bar represents 100 μ M. (E) Graphical summary of the percentage of collagen-stained area relative to the muscle CSA. (F) Representative Western blots of pSMAD3^{Ser423/425}, SMAD3, transforming growth factor- β (TGF- β), platelet-derived growth factor receptor (PDGFR) in the TA muscles of all groups. Ponceau S staining is shown to indicate even sample loading. Protein ladders are expressed as kDa at the right. Graphical summaries of SMAD3 Phospho-status (G), as well as TGF- β and PDGFR protein expression (H). (I) Graphical summary of fibrosis-related genes expression in the TA muscles of all experimental animals. (J) Representative Western blots of Utrophin, γ -sarcoglycan (γ SG), and β -dystroglycan (β DG) in the TA muscles of Veh- and O304 treated animals. (K) Graphical summary of Utrophin, γ SG, and β DG protein expression. (L) Summary of *Utrn* gene expression in the TA muscles of all experimental animals. Immunoblotting and qPCR data are presented as fold differences relative to the WT Veh group. Graphical summaries display individual data points and group means (bars) with SEM. $n = 8-10$. Statistical significance was denoted as *, $p < 0.05$ versus WT Veh.

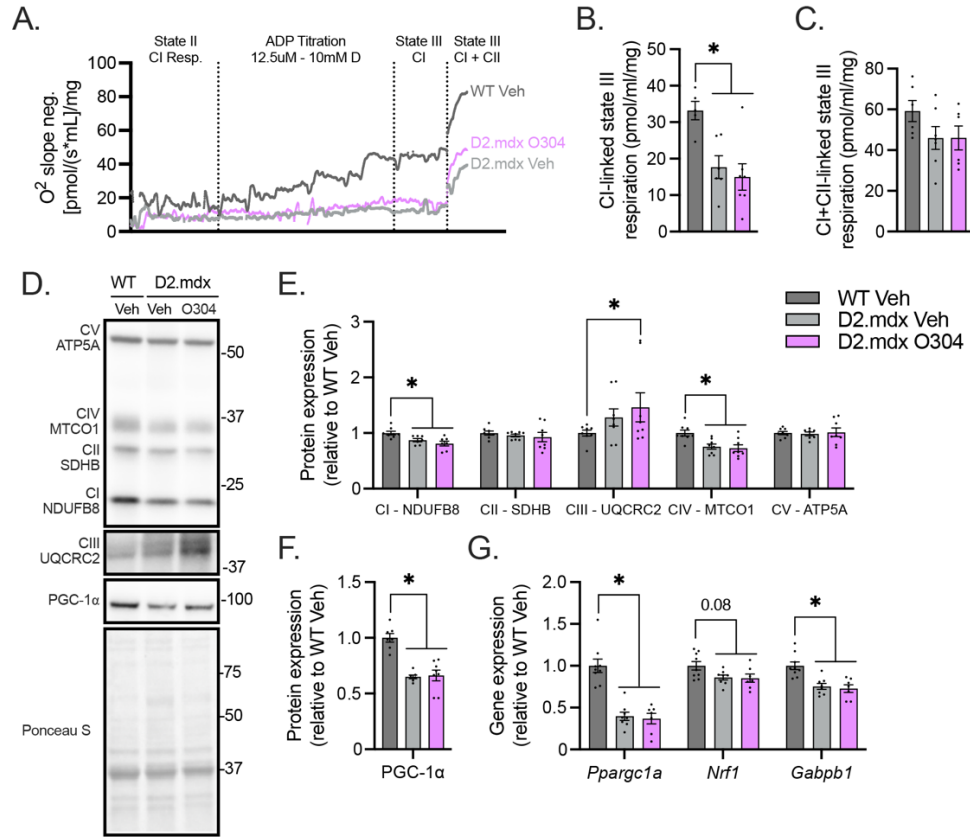


Fig AB4. The influence of chronic O304 dosing on mitochondrial respiration and content. (A) Real-time trace from a permeabilized quadriceps muscle from the WT Veh, D2.mdx Veh, and D2.mdx O304 groups. (B-C) Graphical summaries of complex I (CI)-linked state III respiration (B) and CI and CII-linked state III respiration (C) in the quadriceps muscles of Veh-treated WT and Veh- or MK-treated D2.mdx animals. (D) Representative Western blots depicting mitochondrial protein complexes (CI-CV), in the TA muscles of all treated animals. A representative Ponceau S stain is shown below. Protein ladder markers on the right are denoted in kDa. Graphical summaries of mitochondrial CI-CV (E) and PGC-1 α (F) protein expression. (G) Graphical summaries of *Ppargc1a*, *Nrf1*, and *Gabpb1* transcript expression in the TA muscles of all experimental animals. Immunoblotting and qPCR data are presented as fold differences relative to the WT Veh group. Graphical summaries display individual data points and group means (bars) with SEM. $n = 5-6$. Statistical significance was denoted as *, $p < 0.05$ versus WT Veh.

APPENDIX C:
OTHER CONTRIBUTIONS

OTHER CONTRIBUTIONS

During my Doctoral tenure, I made contributions to the following publications not included in my Dissertation:

12. Brown A, Parise G, Thomas ACQ, **Ng SY**, McGlory C, Phillips SM, Kumbhare D, Joannisse S. High responders to resistance training have low baseline ribosome content and a greater decrease than low responders following resistance training. Submitted to *Journal of Cellular Physiology*, July 19, 2023.
11. vanLieshout TL, Stouth DW, **Ng SY**, Manta A, Mattina SR, Ljubicic V. 2022. Sex-specific impact of CARM1 in skeletal muscle adaptations to exercise. Submitted to *Medicine and Science in Sports and Exercise*, June 20, 2023.
10. Stouth DW, vanLieshout TL, **Ng SY**, Mikhail AI, Webb EK, Ljubicic V. Skeletal muscle-specific CARM1 deletion attenuates autophagy flux to blunt fasting-induced atrophy. Submitted to *Autophagy*, February 7, 2023.
9. Webb EK, **Ng SY**, Mikhail AI, Stouth DW, vanLieshout TL, Syroid A, Ljubicic V. 2023. Impact of short-term, pharmacological CARM1 inhibition on skeletal muscle mass, function, and atrophy. *American journal of physiology. Endocrinology and metabolism*, 325(3), E252–E266.
8. Lim C, McKendry J, Giacomini T, McLeod J, **Ng SY**, Currier B, Coletta G, Phillips SM. 2023. Foretetrophin® supplementation prevented the rise in myostatin circulation level, but not disuse atrophy, in young men during single-leg immobilization: A randomized controlled trial. *Plos One*. 18(5): e0286222.
7. Mikhail AI, Manta A, **Ng SY**, Osborne AK, Mattina SR, Mackie MR, Ljubicic V. 2023. A single dose of exercise stimulates skeletal muscle mitochondrial plasticity in myotonic dystrophy type 1. *Acta Physiologica*. 237(4): e13943
6. Young LV, Wakelin G, Cameron AWR, Springer SSA, Ross JP, Wolters G, Murphy JP, Arseneault MG, **Ng SY**, Collao N, De Lisio M, Ljubicic V, Johnston AP. 2022. Muscle injury induces a transient senescence-like state that is required for myofiber growth and myonuclear accretion during muscle regeneration. *FASEB J*. 36(11):e22587.
5. vanLieshout TL, Stouth DW, Hartel NG, Vasam G, **Ng SY**, Webb EK, Rebalka IA, Mikhail A, Graham NA, Menzies KJ, Hawke TJ, Ljubicic V. 2022. The CARM1 transcriptome and arginine methylproteome mediate skeletal muscle integrative biology. *Molecular Metabolism*. 64:101555.

4. Mikhail AI, Nagy PL, Manta K, Rouse N, Manta A, **Ng SY**, Nagy MF, Smith P, Lu JQ, Nederveen JP, Ljubicic V, Tarnopolsky MA. 2022. Aerobic exercise elicits clinical adaptations in myotonic dystrophy type 1 patients independent of pathophysiological changes. *The Journal of Clinical Investigation*. 132(10): e156125.
3. Young LV, Morrison W, Campbell C., Moore EC, Arsenault MG, Dial AG, **Ng SY**, Bellissimo CA, Perry CG, Ljubicic V, Johnston AP. 2021. Loss of dystrophin expression in skeletal muscle is associated with senescence of macrophages and endothelial cells. *American Journal of Physiology-Cell Physiology*, 321(1).
2. Stouth DW, vanLieshout TL, **Ng SY**, Webb EK, Manta A, Moll Z, Ljubicic V. 2020. CARM1 regulates AMPK signaling in skeletal muscle. *iScience*, 23(11):101755.
1. **Ng SY**, Mikhail A, Ljubicic V. 2019. Mechanisms of exercise-induced survival motor neuron expression in the skeletal muscle of spinal muscular atrophy-like mice. *The Journal of Physiology*. 597(18): 4757-4778.